Biofunctionalization of UHMWPE fabric for ligament or tendon regeneration

Thesis Submitted to
The University of Sydney
School of Biomedical Engineering

For the degree of
Doctor of Philosophy
By

Sonia Binte Wahed

Declaration

I, Sonia Binte Wahed, confirm that this work does not contain any content used in my name to get another degree or diploma from a university or other educational institution. Additionally, I confirm that no portion of this work will ever be submitted in my name for a different degree or certificate at another university or academic institution without the University of Sydney's prior consent.

I now further certify that I am the author of the thesis. Every bit of assistance I've gotten with my research and thesis preparation has been acknowledged. I affirm that the thesis includes citations to all information sources and works cited.

All experiments related to material characterization and cells conducted on the biomaterials & tissue Engineering lab at the School of Biomedical Engineering in collaboration with Applied and Plasma Physics group at the School of Physics the University of Sydney, NSW 2006, Australia. Mechanical experiments conducted in mechanical engineering lab, AMME, USYD. I acknowledge the ACMM (for SEM), and Sydney Analytical (for XPS) for supporting image analysis and material characterization.

I give consent that this copy of my thesis may be loaned out and copied with the caveats of the Copyright Act of 1968 once it has been put in the university library.

Name of the student

Sonia Binte Wahed

28/02/2023

Authorship attribution statement

Chapter II of this thesis is published as “Wahed, S. B.; Dunstan, C. R.; Boughton, P. A.; Ruys, A. J.; Faisal, S. N.; Wahed, T. B.; Salahuddin, B.; Cheng, X.; Zhou, Y.; Wang, C. H.; et al. Functional Ultra-High Molecular Weight Polyethylene Composites for Ligament Reconstructions and Their Targeted Applications in the Restoration of the Anterior Cruciate Ligament. *Polymers (Basel).*, **2022**, *14* (11). https://doi.org/10.3390/polym14112189

Conceptualisation, original draft preparation, data curation, writing review & editing was done by Sonia Binte Wahed.

Name of the student

Sonia Binte Wahed

28/02/2023

The authorship attribution claims above are accurate, as I can attest as the candidate's supervisor for the candidature on which this thesis is founded.

Name of the supervisor

Prof. Colin Dunstan

28/02/2023

Supervisors

Primary supervisor:

Professor Colin Dunstan

Associate supervisors:

Professor Marcela Bilek

Dr Behnam Akhavan

Acknowledgments

I started my PhD in 2018, and since then went through ups and downs which I never expected. I had to change my supervisors several times to get the right path and guidance for me after the retirement of my primary supervisor Prof. Andrew Ruys. Due to those circumstances, I lost my 1 and half my year's study. During my PhD, I lost my both parents due to Covid infections. I never imagined that I could finish my study after this grief.

I want to thank Professor Colin Dunstan, whose guidance I sought when I started researching and writing my thesis. From the beginning to the end, your support and encouragement helped me get the confidence I needed to finish this thesis. He took me as a student during his retirement period and tried his best to help me throughout my difficult time.

I appreciate the advice and assistance I received from my co-mentors and co-supervisors, Professor Marcela Bilek, and Dr. Behnam Akhavan, Dr. Clara Tran, and Dr. Anna Waterhouse at every stage of the project.

I appreciate the time and work you put into guiding and advising me on my research. I also thank, Professor Hala Zreiqat, Dr. Zufu Lu, Dr. MD Musharraf Hossain and my colleague Dr, Stephanie Yee, Chloe Ann Martinez.

I would like to thank my previous supervisors Professor Andrew Ruys and Philip Boughton for sharing their knowledge and guidance in choosing my research topic.

I would like to thank Dr. Bonny Tsoi- lab manager of Biomedical Engineering, Dr. Hongjian Wang- lab manager of mechanical engineering lab, Dr. Ashalata- SEM training provider, Dr. Vijay-ACMM lab manager, Dr Julie Dechorgnat-lab manager LEES, Dr Ying Su-technical staff ACMM, Dr. Minh Huynh, Dr. Francesca Charlton-lab manager of level 3, CPC who provided me access and training to their facilities to conduct my experiments smoothly.

Finally, I want to thank my parents, husband, my dearest daughter. You have my sincere gratitude for all that you have done for me.

List of publications, presentations, and Awards

Publications:

1. Wahed, S. B.; Dunstan, C. R.; Boughton, P. A.; Ruys, A. J.; Faisal, S. N.; Wahed, T. B.; Salahuddin, B.; Cheng, X.; Zhou, Y.; Wang, C. H.; et al. Functional Ultra-High Molecular Weight Polyethylene Composites for Ligament Reconstructions and Their Targeted Applications in the Restoration of the Anterior Cruciate Ligament. *Polymers (Basel).*, **2022**, *14* (11). https://doi.org/10.3390/polym14112189

2. **In progress Sonia Binte Wahed**, Clara Tran, Marcela M.M Bilek, Behnam Akhavan*, Colin R. Dunstan*Biomimetic polyethylene fabrics as tissue engineering constructs for ligament and tendon regeneration

Conference:

1. The Sydney Musculoskeletal, Bone & Joint Health Alliance (SydMSK) 4th Annual virtual meeting, 2020.

Awards:

- University of Sydney Completion Stipend scholarship, 2022
- University of Sydney Paulette Isabel Jones Scholarships by Deputy Vice chancellor, 2021
- University of Sydney Postgraduate research support scheme Award 2020, 2021
- Research training program stipend scholarship, 2018

Abstract

Due to superior physical qualities, ultra-high molecular weight polyethylene has become a prominent biomaterial for ligament/tendon (L/T) implants. There has been interest in addressing UHMWPE's bio-inert shortcomings by using bioactive components like hydroxyapatite, either as composite fillers or as a surface coating. In this thesis, as an alternative strategy, we explored the application of Plasma Immersion Ion Implantation (PIII) as a surface treatment for UHMWPE to enhance bioactivity by altering its surface properties and to offer a practical method for covalently immobilizing biomolecules on the surfaces of UHMWPE fabric.

Chapter III focuses on fundamental knowledge of the physical and chemical properties of UHMWPE fabric surfaces after they have been treated with the PIII procedure. It describes the characterization of the surface properties of two different types of UHMWPE fabric.

Chapter IV reports on developing a synthetic ultra-high molecular weight polyethylene (UHMWPE) ligament graft to evaluate the mechanical properties before and after the PIII treatment. Immediate and long-term physiological loading was used to validate the mechanical performance of the synthetic ligament graft.

Chapter V focuses on the immobilization of collagen and fibronectin protein to investigate the covalent binding of proteins on the surface of UHMWPE fabric without any chemical linkers. Release dynamics of bovine serum albumin (BSA) proteins with or without PIII treatment were studied for ligament/tendon healing processes.

Chapter VI demonstrates in vitro biocompatibility of two different grades of UHMWPE fabric surfaces for ligament/tendon (L/T) cells and describes how the PIII treatment of UHMWPE surfaces impacts biocompatibility. The cell interactions with the bare PIII-modified UHMWPE surfaces in the absence of any protein functionalization are studied in this section using two easily obtainable and well-known cells, human fibroblasts (FB) and human adipose-derived stem cells (ADSC).

Chapter VII describes whether the biomolecules fibronectin, collagen type I, and Connective tissue growth factor (CTGF) can still function after becoming attached on the surface of UHMWPE fabric. It also describes whether the PIII treatment leads to better bioactivity results than passive binding without PIII by evaluating the effects of bound proteins on cell adhesion, proliferation, and differentiation.

Graphical Abstract

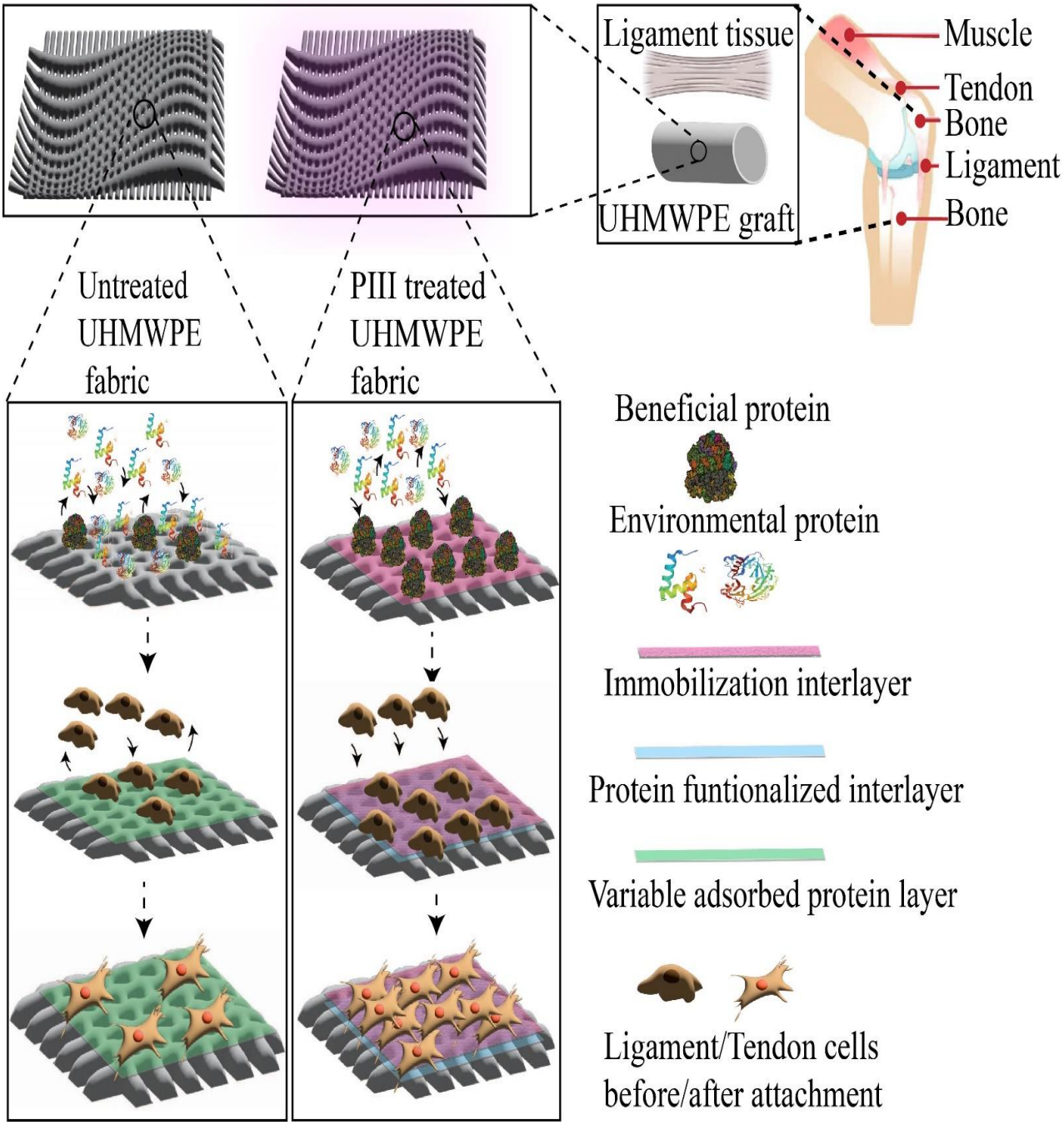

A diagrammatic representation of the initial stages of ligament/tendon tissue integration for non-functionalized and biomolecule-functionalized implants.

Table of contents

List of Figures

List of Tables

List of Abbreviations

- **ADSC**- Adipose derived stem cells
- **ALP -** Alkaline Phosphatase
- **AC**-Alternating current
- **BMP**-Bone morphogenic protein
- **BSA -** Bovine serum albumin
- **COL –** Collagen
- **CTGF-** Connective tissue growth factor
- **CAP-**Cold atmospheric plasma
- **DBD-** Dielectric barrier discharge
- **DMEM -** Dulbecco's Modified Eagle Medium
- **DMSO -** Dimethyl-sulfoxide
- **ECM -** Extracellular matrix
- **ECR-** Electron cyclotron resonance
- **ERD-** Elastic recoil detection
- **ESR-**Electron spin resonance
- **ELISA-**Enzyme linked immunosorbent assay
- **EPR-**Electron paramagnetic resonance
- **FB-**Fibroblast
- **FITC-** Fluorescein isothiocyanate
- **Fn-**Fibronectin
- **FDA -** Food and Drug Administration
- **HDPE-**High density polyethylene
- **HMDA-** Hexamethylenediamine

- **hPDLCs -**Human periodontal ligament fibroblast
- **HA -** Hydroxyapatite
- **HRP -** Horseradish - α-minimal essential medium
- **KLAD-** Kennedy ligament augmentation device
- **LPDE-**Low density polyethylene
- **MTT -** Methylthiazolyldiphenyl-tetrazolium bromide
- **α MEM** Adipose derived mesenchymal stem cells
- **MAPS- γ-**methacryloxypropyl trimethoxysilane
- **MWCN-**Multi wall carbon nanotubes
- **PMMA-** Polymethyl methacrylate
- **PFA –** Paraformaldehyde
- **PACVD-** Plasma-assisted chemical vapor deposition
- **PDA-**Polydopamine
- **RF-**Radiofrequency
- **SEM -** Scanning electron microscopy
- **SCX-**Scleraxis
- **SDS-**Sodium dodecyl sulfate
- **TNC-**Tenascin-C
- **TNMD-**Tenomodulin
- **UHMWPE –** Ultra high molecular weight polyethylene
- **VTMS-** Vinyl trimethoxy silane
- **VTEOS-** Vinyl triethoxysilane
- **XPS-**X- ray photoelectron spectroscopy

Chapter 1: Introduction

1.1 Introduction

Ligament and tendon are connective tissues with strong mechanical properties that stabilize a joint through fixation at either end [1]. Ligaments usually attach two bones together while tendons attach to muscle at one end and bone at the other. Together they prevent dislocation and restrain or enable movement of the joints. Injuries of the ligament/tendon are common in sports such as soccer, football, or downhill running [2–6], ranging from mild tears to more severe rupture in completely torn ligaments. As most of the ligament/tendon injuries don't heal themselves due to their avascular complex structure, autografts and allografts have been used to reconstruct the damaged tissue [7]. Autograft is the transplantation of tissue from a different location from the same individual while allograft tissue is from a donor. Autograft has been known for the fastest incorporation and healing; however, it has a high risk of inducing morbidity at the donor site. Although allograft can reduce this risk for patients, it has a higher failure rate and may transmit diseases from the donors [8].

Due to such significant drawbacks associated with allografts and autografts, synthetic ligament grafts are receiving particular attention for ligament/tendon reconstruction [9]. A synthetic ligament/tendon graft connecting the ends of two bones is made from a layered or tubular woven ligament with an extra-articular region, consisting of at least one bending region and one end region. Each area should be woven to provide support and flexibility in response to expected stresses [1]. Ligament/tendon grafts should have desirable properties such as strength and stiffness comparable to a natural ligament/tendon, minimal inflammation upon implantation into the body, and be degradable over time to facilitate tissue ingrowth [11].

Various biomaterials have been developed over the past few years as artificial ligaments such as poly -l-lactic acid (PLLA)polycarbonates, poly arylates, polycaprolactone, PDS, poly(diaxonane), PLGA, poly (lactic-co-glycolic acid), PLLA, poly (L-lactic acid) [12–15]. However, the selection of biomaterials for such regeneration is a major challenge due to the lack of biocompatibility of mechanically suitable materials that are capable of appropriately handling in vivo mechanical loadings [10]. Further, after a ligament/tendon rupture, the blood supply is disturbed, s hampering ligament/tendon regeneration [10].

In the last few decades, bioabsorbable and non-bioabsorbable biopolymers have been applied for use in orthopedic applications due to their high mechanical strength and biocompatibility compared to metals and ceramics [16]. Ultra-high molecular weight polyethylene (UHMWPE) is among the non-bioabsorbable polymers which are commonly used for joining replacement and other applications where sustained function is required. The market demand for medical-grade UHMWPE has increased tremendously from 60.9 kilotons (2015) to 204.8 kilotons (2024) according to a survey conducted by Grand view research [17]. The comprehensive use of UHMWPE in the medical field is due to its low wear volume, ultimate tensile strength, and low coefficient of friction [18]. However, despite all these advantages, its biocompatibility needs to be improved as this polymer is not easily linked to most biomolecules due to its hydrophobicity and the absence of functional groups for forming the bonds [19].

Various strategies have been investigated to resolve these problems and enhance the surface properties of UHMWPE including physical treatments and chemical treatments. Physical treatments such as gamma or electron beam radiation followed by chemical modification [20–22], conventional plasma treatments [23, 24], UV treatment [25], gamma irradiation [26], and corona discharging

[27] have been investigated. However, some of the treatments are accompanied by a decrease in bulk mechanical properties, such as toughness, tensile strength, fatigue performance and wear resistance[2].

Wet chemical-based methods have been described in the literature for creating covalent bonds of biomolecules to the substrates [28, 29]. Silane and polyethylene glycol (PEG) are the two most often utilized synthetic linker molecules in orthopedics for protein immobilization [30, 31]. Salinization of orthopedic substrates was first published in 1995 and has since become the most extensively used approach for protein immobilization. Alkyl silane linkers form an O-Si bond with hydroxylated substrates through a condensation reaction [32, 33].

Proteins have been immobilized by PEGylation of orthopedic substrates [33] using the substrate's pre-existing hydroxyl terminals to chemisorb the PEG molecules [34]. In place of unmodified PEG molecules, terminally modified PEG molecules have recently been employed. Protein immobilization by carbodiimide reactions using amine- (NH_2 – PEG-NH_2) and carboxyl- (COOH–PEG-NH_2) functionalized PEG has been investigated [35]. Although linker chemistry approaches only change the polymer surface without affecting the bulk properties, they involve a series of wet chemical reactions, which makes the process complex, producing additional chemical by-products, creating toxicity and solvent disposal issues [36].

Plasma immersion ion implantation (PIII) has been known as a surface modification technique for polymers to facilitate covalent bonds with biomolecules with very minimal impact on the bulk material. The ion bombardment from the PIII treatment creates a reservoir of long-lived reactive radicals embedded in sub-surface layers [36]. The PIII treatment has been shown to covalently

immobilize proteins and peptides on a wide range of natural and synthetic polymers without the use of multi-step wet chemistry [37, 38].

It has been shown that such surface-embedded radicals facilitate covalent attachment of bioactive molecules, including proteins and peptides, thereby endowing a biomimetic character to the material [37, 39–41]. The hydrophilic nature of the PIII-treated polymer surfaces enables the bioactive conformation of protein molecules to be preserved while being immobilized on the surface. These works suggest that the PIII technology holds great potential to bioengineer the surfaces of UHMWPE woven fabric used to create biomimetic constructs for ligament and tendon regeneration.

Here we demonstrate the capability of PIII treatment to create biomimetic UHMWPE woven fabric constructed through covalent attachment of cell signaling proteins such as collagen and fibronectin. A woven fabric form was selected due to its high surface area and mechanical properties as well as its suitability for implant design and fixation. The biomimetic fabrics were further used to investigate the attachment, growth, and activity of human primary fibroblast cells (FB) and adipose derived stem cells (ADSC) for synthetic ligament graft purposes.

The opportunity to construct designs for total ligament/tendon (L/T) replacements and implants is appealing when using UHMWPE fabric that had increased histocompatibility and was able to encourage the ingrowth of new ligament/tendon tissues.

In this research, a bioactive surface was created by the nitrogen-based Plasma immersion ion implantation (PIII) technique on UHMWPE fabric to construct a synthetic ligament implant. The purpose of this study was to determine whether new hybrid artificial ligaments could facilitate tendon-bone healing processes and accomplish "ligamentization" through in vitro study.

Firstly, characterization of two grades of untreated & PIII treated UHMWPE fabric was completed to understand their surface functional properties.

Secondly, a woven synthetic ligament/tendon graft prototype was created to study mechanical properties of synthetic UHMWPE ligament/tendon graft.

Thirdly, protein immobilization on untreated & PIII treated UHMWPE fabric was evaluated to check covalent bonding of proteins with the fabric surface. Immunofluorescence experiments were used to assess the surface's physical characteristics and test its capacity to bind proteins covalently.

Fourthly, the biocompatibility, and bioactivity of untreated and PIII modified UHMWPE fabric with attached Fibroblast (FB) and Adipose derived stem cells (ADSC) were evaluated.

Finally, primary human fibroblasts and ADSC cultured on untreated, PIII-treated, and protein-functionalized UHMWPE fabric were tested for adhesion, proliferation, and differentiation.

Chapter 2 : Literature Review

2.1 Introduction

The biomaterials used as biomedical implants are expected to be biocompatible i.e. they need to be non-toxic, non-inflammatory and should not cause any allergic reactions in the human body [3]. Moreover, the material must have an excellent combination of high strength and low Young's modulus closer to the implant to ensure longer service life and avoid implant loosening and revision surgery [4]. Ultra-high molecular weight polyethylene (UHMWPE) is distinguished by its high ultimate tensile strength, good biocompatibility, corrosion resistance, low water uptake, low coefficient of friction, and high abrasion resistance [5]. Such properties define UHMWPE's use in many development areas and in medicine and biology, including the manufacture of artificial joints and implants for orthopedic surgery. All knee replacements and 85% of hip replacements today use UHMWPE on their bearing surfaces, which represents over two million orthopedic implants per year [6, 7]. Two key factors decide the quantity and consistency of cell adherence to the implants: implant wettability (surface chemistry) and surface topography (surface roughness) [8, 9]. Currently, UHMWPE is commercially fabricated under several brand names: Polymin SK (BASF, Germany), Polystone M (Roechling, Germany), Tivar (Quadrant, Belgium), Tecafine PE10 (Ensinger, Germany), Okulen 2000 (SP-Plast, Finland), GUR (Tina, Solidurraz, Germany) and by various companies, such as Goodfellow (United Kingdom) and Braskem (Brazilian Chemicals) [10, 11].

In ACL and other ligament and tendon reconstructions, UHMWPE fiber is selected because of its having the most durable property known in the biomedical field [11–14]. In addition, it possesses excellent tensile strength, enough to support human load-bearing demands [15]. Despite these features, particular drawbacks have been noted, such as UHMWPE fibers being problematic to bond to

most materials due to their chemical inertness, and poor wear resistance[16]. Wear debris generated during joint motions, could cause osteolysis and implant displacement, contributing to the primary reason for joint revision[17].

UHMWPE fibers' appealing physical and mechanical qualities are related to their highly aligned crystalline microstructure polythene chains[18]. These days, gel-spinning processes are usually used to manufacture UHMWPE filaments. In this technique an oxygen-rich slim limit layer is created during turning of UHMWPE filaments, which is responsible for a decrease in the bond properties of strands[19]. As a result, eliminating oxygen-rich boundaries is required to maximize fiber adhesion to other materials through surface modification of UHMWPE. Multiple methods have been utilized to modify the surface biocompatibility and wear resistance of UHMWPE [20]. These modifications can be divided into two types: chemical and dry techniques. Chemical surface modifications conducted with oxidative acid etching [19], coating treatment [21, 22]and chemical grafting [23] of UHMWPE [24, 25]. Dry surface modification techniques include different types of plasma treatments, grafting, UV & gamma irradiation treatments[26–28]. Typically, molecular modification processes involve the insertion of oxygen-rich functional groups on the surface of UHMWPE fibers, which provide excellent chemical bonding sites. Additionally, the surface treatment would introduce imperfections or roughening, such as micro-pits, which act as mechanical anchor points, facilitating mechanical interlocking of the polymer matrix to fibers. Sometimes combined methods applied to improve interfacial adhesion of the materials[29]. Nano-reinforcement, such as carbon nanotubes (CNTs), nano clay, graphene, boron carbide, nano alumina (AL_2O_3),vitamin C, has recently been employed to change the polymer matrix to be used with fiber in order to create the best potential interfacial connection through resonance[30–33].

The improvement of its surface can modify its biological and tribological properties [34, 35]. Use of these materials can improve the surface hardness and abrasion resistance of the UHMWPE. Traditional ways of upgrading the wear performance of the UHMWPE include techniques such as gamma or electron beam radiation followed by thermal stabilization [36]. These techniques are accompanied by an increase in bulk mechanical properties, such as toughness, tensile strength, fatigue performance, and wear resistance [37].

Plasma treatment is currently another technologically successful and safe method (which does not need any corrosive reagents/solvents) for the surface modification of polymeric material. Properties can be improved by surface treatment of UHMWPE with argon plasma, cold atmospheric plasma (CAP), Dielectric barrier discharge (DBD) plasma, plasma-assisted chemical vapor deposition (PACVD) and plasma immersion ion implantation (PIII) methods followed by protein immobilization. To resolve the wear and to enhance the life of UHMWPE as implant, in recent years this field has witnessed numerous innovative methodologies such as biofunctionalization or high temperature melting of UHMWPE to enhance its toughness and strength. The modifications of surface of the material through plasma can improve its hydrophilicity, surface energy, wear resistance by introducing functional groups to the material which have been characterized by water contact angle, Fourier Transform Infrared (FTIR) and Scanning Electron Microscope (SEM)[38, 39].

The surface effective functionalization/modification/treatment of UHMWPE is very challenging in orthopedic applications such as ligament regeneration. In spite of the difficulties, several surface roughening, functionalization, and irradiation processing

technologies have been developed and applied in the recent past [40–43]. The basic research and direct industrial applications of such material improvement technologies is very significant as evidenced by the significant number of published literatures[44]. However, there is a lack of a comprehensive source for the research community to access information on the research methodology and techniques for material property enhancement and protection of wear of UHMWPE.

Therefore, the objective of this review is to provide an overview of recent developments and core challenges in the surface modification/functionalization/irradiation of UHMWPE and apply these findings to the case study of UHMWPE for ligament e.g., anterior cruciate ligament reconstruction. Fig 2.1 illustrates the overview of the surface treatments of UHMWPE and Table 2.1 summarizes the influence on surface properties of UHMWPE after surface treatments.

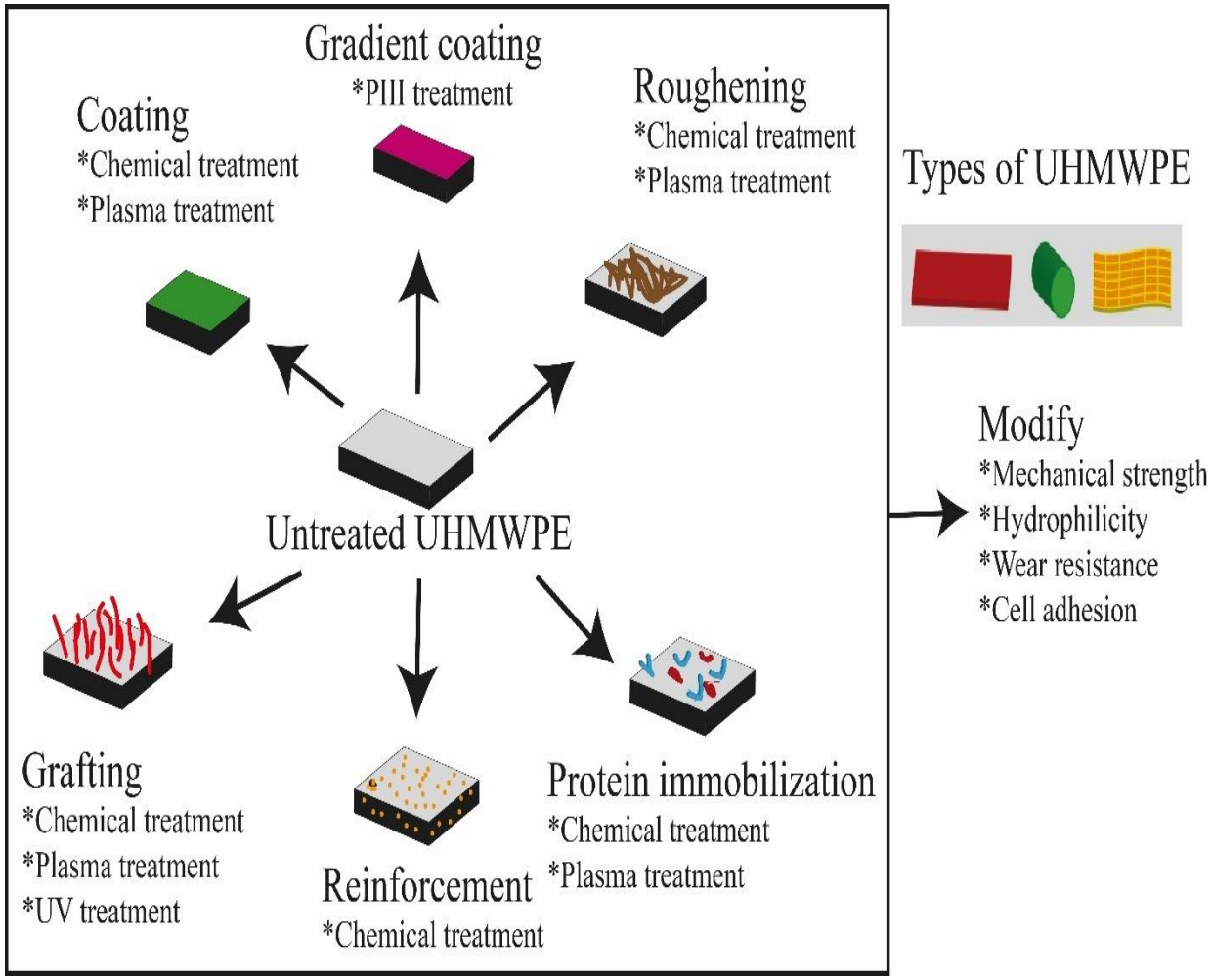

Figure 2. 1 Contrasting approaches for surface functionalization of UHMWPE.

Table 2.1 The influence on surface properties of UHMWPE after surface treatment.

Treatment	Parameters	Additional peaks found after treatment	Elemental analysis after oxidation on the surface (%)				Surface & Tribological properties	Mechanical properties	References
			C	O	N	Others			
Chemical	Chromic acid, hydrogen per oxide, potassium permanganate		89.6, 73.6, 91.6	9.6, 16.5, 6.6	-		Improvement in surface adhesion properties	Improvement in interfacial tensile strength	[19]
Chemical	Polydopamine, Ethylene glycol diglycidyl ether (EGDGE)						Water contact angle (WCA) decreased from 109° to 97°	67.5% improvement in mechanical strength	[45]
Chemical	Polydopamine (PDA), hexamethylene diamine (HMDA)	C-OH, -NH, C=C stretching	73.14, 74.39, 74.39	21.3, 18.65	5.13, 6.96			Shear strength 0.920 MPa	[46]
Chemical	Hyaluronic acid						WCA decreased from 80° to 50°, increased crystallinity	High wear resistance	[47]
Chemical	PEG-like coating	-OH stretch, C-O-C, C-OH	68.8	31.2	-			WCA decreased from 90.3° to 44.8°	[48]
Chemical	VTMS and SiO_2	Si-C, Si-O	40.39	35.38		24.23	WCA decreased from 123° to 43°, increased antifouling properties		[49]

Table 2.1 cont.									
Treatment	**Parameters**	**Additional peaks found after treatment**	**Elemental analysis after oxidation on the surface (%)**				**Surface & Tribological properties**	**Mechanical properties**	**References**
			C	**N**	**O**	**Others**			
Cold plasma	He and O_2 gas	C-C stretching, C-N, Hydrogenated amorphous C					Increased surface hydrophilicity and cell adhesion	High wear resistance	[50]
Cold plasma	H_2 and O_2 gas	CH vibrations, C-O stretching, C=O					WCA decreased from 102° to 43°, Improved cell adhesion property, Roughness increased from 588 nm to 687 nm		[51]
PACVD plasma	Air and Ar gas							Tear resistance, 40% increase in tensile strength	[27]
ECR plasma	H_2 and N_2 gas	C-O/C-OH, C-C, C=C, C=O	60	37	8		Increased surface roughness	Increased surface hardness and elastic modulus	[39]
ECR plasma	(N_2 + H_2) and O_2 gas	C-N, C-O Stretching, N-H bending, C=O Stretching					WCA decreased from 96° to 22°, improvement in surface cell adhesion		[38]

Table 2.1 Cont.

Treatment	Parameters	Additional peaks found after treatment	Elemental analysis after oxidation on the surface (%)				Surface & Tribological properties	Mechanical properties	References
			C	N	O	Others			
ECR plasma	Peroxides, acrylic acid, itaconic acid, collagen	C-O, -COOH, -NH, C-N							[52]
DBD + chitosan treatment	(Ar + O_2) gas & chitosan	C=O, -COO, C-O/C-N	93.15, 82.1, 74.0	5.8, 15.2, 2 .7	1.1, 2.7, 3.0		Surface adhesion increased by 72.2%, WCA decreased from 101° to 82°	Decreased tensile strength by 5.6%	[53]
DBD plasma	(He + Ar + air + N_2 + H_2) gas	C-C, C-C=O, O=C-O	88.3	6.3	6.9		WCA decreased from 95.2° to 70°		[54]
DBD plasma	Ar gas	C-H, -OH, C-C, C=O					WCA decreased from 91° to 67.4°		[35]
DBD plasma	Ar gas, Multi walled carbon nanotube	C-H stretching, C-C, O-H, C=O					Wear volume was reduced by 73.3%, surface roughness was reduced by 17%, hardness of the composite increased by 45%		[55]
Gamma	Thermal treatment + gamma dose							Toughness increased by 67%,	[56]
Gamma							Increased cross linking, wear rate 37%		[57]

Table 2.1 Cont.

Treatment	Parameters	Additional peaks found after treatment	Elemental analysis after oxidation on the surface (%)				Surface & Tribological properties	Mechanical properties	References
Gamma	UV + PEG grafting	C=C, C-Si, C=O					Crystallinity increased, resistance to protein adsorption increased		[58]
Gamma	Irradiation + Vitamin E						Reduced crystallinity, wear resistance		[59]
PIII treatment	Ar gas	C=C, –OH, COOH and COO–					WCA decreased from 80° to 28°		[60]
PIII treatment	N_2 + gas						A small decrease in WCA, surface roughness increased from 39 nm to 71 nm		[61]
PIII treatment	N_2 + gas + HRP protein		71.1	15.5	13.4		Roughness increased from 528° to 1130°, surface area increased from 101.9 nm to 15.6 nm		[62]
PIII treatment	N_2 + HRP + PVC	C=O, C-O, -OH					WCA decreased from 90° to 58°.		[63]

2.2 Background for the use of UHMWPE in orthopaedic implants

UHMWPE belongs to a subgroup of thermoplastic polyethylene (PE) that are obtained from monomers of ethylene by a polymerization reaction. It is composed of extremely long polyethylene chains which effectively transfer load and provide a polymer backbone by reinforcing intermolecular interactions [64]. The desired degree of polymerization of UHMWPE is dependent on its end applications, the degree of polymerization is observed in orthopedic applications within a range of 71,000–214,000 with a molecular weight ranging from 2 to 6 million g/mole [65, 66]. UHMWPE is a semicrystalline polymer, and its properties are strongly dependent on its microstructure [67].

The semicrystalline structure of UHMWPE consists of two phases known as crystalline and amorphous phases. Its properties are determined by the relations between amorphous and crystalline phases, such as binding molecules, crystallinity, degree of crosslinks and entanglements; and the crystallite positions [68]. The crystalline phase comprises lamellae consisting of strongly directed folded chains [69]. UHMWPE is also known as high modulus PE or high-performance PE because of its toughness and good impact strength. High density polyethylene (HDPE) has also been used for biomedical skeletal and orthopedic applications [70, 71].

It also has extraordinary properties such as nontoxicity, high resistance to corrosive chemicals, and wear strength that makes it reliable for orthopedic applications, but UHMWPE is more abrasion and wear resistant than HDPE. Several monomer units attach during polymerization based on metallocene catalysts to make UHMWPE stronger compared to HDPE.

Table 2.2 Physical properties of HDPE & UHMWPE [65]**.**

Property	HDPE	UHMWPE
Molecular weight ($\times 10^6$ g/mol)	0.05-0.25	3.5-7.5
Tensile ultimate strength (MPa)	22-31	39-48
Tensile ultimate elongation (%)	10-1200	350-525

In 1962, Sir John Charnley introduced UHMWPE ($-[CH_2-CH_2]_n-$) for biomedical use, and it was then applied as a joint surface load bearing material for hip and knee replacements. Hip and knee replacements are prosthetic joints that replace human joints affected by arthritis. The oxidation resistance of UHMWPE was improved by cross-linking, high-pressure crystallization, and introducing antioxidants.

UHMWPE can also be used as woven, knitted, or nonwoven sheets to provide three-dimensional structures for cell ingrowth. UHMWPE fabrics can be produced by a gel spinning technique that allows for the parallel orientation of the fibers resulting in a high modulus of elasticity and strength. The market demand for medical-grade UHMWPE has risen tremendously from 60.9 kilotons (2015) to a projected 204.8 kilotons in (2024), according to a survey conducted by Grand view research [72, 73]. Extensive use of UHMWPE in the medical field is due to its superior biocompatibility, chemical resistance, low wear volume, ultimate tensile strength, and low coefficient of friction.

2.3 Methodologies for surface modification of UHMWPE

In ACL reconstruction, UHMWPE can be used in fabric or fiber form but in other biomedical sectors, it can be used as a sheet, rod, or powder form. UHMWPE has been used for shoulder replacements, hip arthroplasty, ankle replacements, and other joint replacements due to its high performance with low friction coefficient, high abrasion resistance, great aging resistance, and

high impact strength properties. However, inertness and extreme hydrophobicity makes it inappropriate for its application in shoulder and joint replacements [74, 75]. Different methods to improve the surface properties of UHMWPE are described below:

2.3.1 Chemical treatment

Several types of materials such as acetic acid, sulfuric acid, and chromic acid have been used to modify the surface properties of UHMWPE [76]. Silverstein et al. [77] have explored surface treatments using chromic acid, potassium permanganate, and hydrogen peroxide to reduce the smoothness of the polymer surface. These etchants were used to remove the weak outer layer of the polymer. A rough and oxidized UHMWPE surface was formed, with increased surface tension and enhanced wetting[78] .The oxidized UHMWPE contains 6:1 combinations of ether and carbonyl bonds. Increased C and O components of untreated and treated UHMWPE are presented in table 2.3. [77]

Table 2.3 Elemental analysis of UHMWPE after oxidation on the surface[77]**.**

Samples	C (%)	O (%)
Untreated	74.2	21.9
Chromic acid	89.6	9.6
Potassium permanganate	73.6	16.5
Hydrogen peroxide	91.6	6.6

Firouzi et al. [79] investigated the mechanical and biological properties of UHMWPE after nylon coating. The results confirmed that nylon coating can increase toughness, maximum breaking

force, and creep time. Excellent mechanical strength and wear resistance with lower cytotoxicity can entitle UHMWPE for biomedical applications.

Sa.et al. [80] explained another surface modification of UHMWPE fiber using bioinspired polydopamine deposition and epoxy grafting to improve the surface activity and adhesion properties of the material. One of our studies investigated the wettability by water contact angle test and tribological performance single fiber pull out test, showing the change in contact angle for untreated and modified UHMWPE (Fig 2.2) and an increased interfacial strength of modified UHMWPE fibers than pure UHMWPE fiber (Fig 2.3) [45].

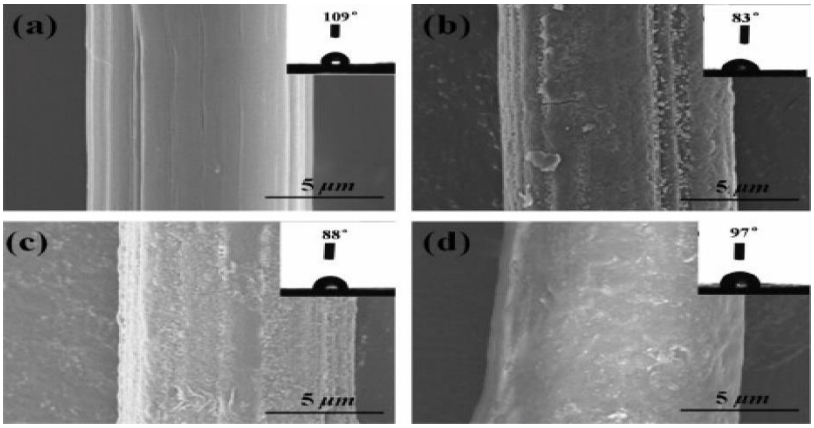

Figure 2. 2 SEM images for (a) Pristine UHMWPE fibers: (b) UHMWPE-PDA fibers; (c) UHMWPE-PDA-EDGE fibers; (d) UHMWPE-(PDA+EGDE) fibers; and micrographs of water contact angle test. Reprinted with permission from [45].

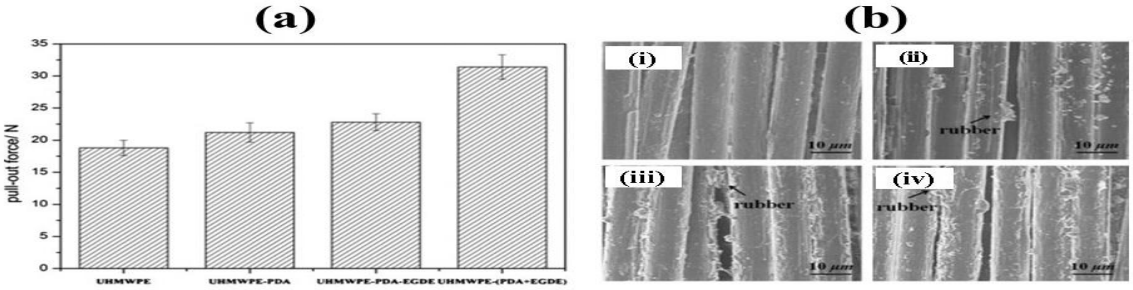

Figure 2. 3 (a) Pull out test of UHMWPE and modified fibers; (b) SEM images of untreated and treated UHMWPE; (i) UHMWPE fibers/rubber, (ii) UHMWPE–PDA fibers/ rubber, (iii) UHMWPE–PDA–EGDE fibers/rubber, and (iv) UHMWPE–(PDA+EGDE) fibers/rubber. Reprinted with permission from[45].

Similar work was carried out by J. Hu et al. [81] to improve the surface activity and adhesion property of UHMWPE fibers using polydopamine (PDA) and hexamethylenediamine (HMDA) . The findings showed that the surface of UHMWPE-PDA fibers and UHMWPE-PDA-HMDA fibers were much rougher than that of pure fibers with increased interfacial shear strength. It was observed that the reaction between primary and secondary amine groups of PDA and HMDA with epoxy groups of epoxy resins increased the interfacial adhesion between the UHMWPE-PDA-HMDA with epoxy resin (Fig 2.4) [46].

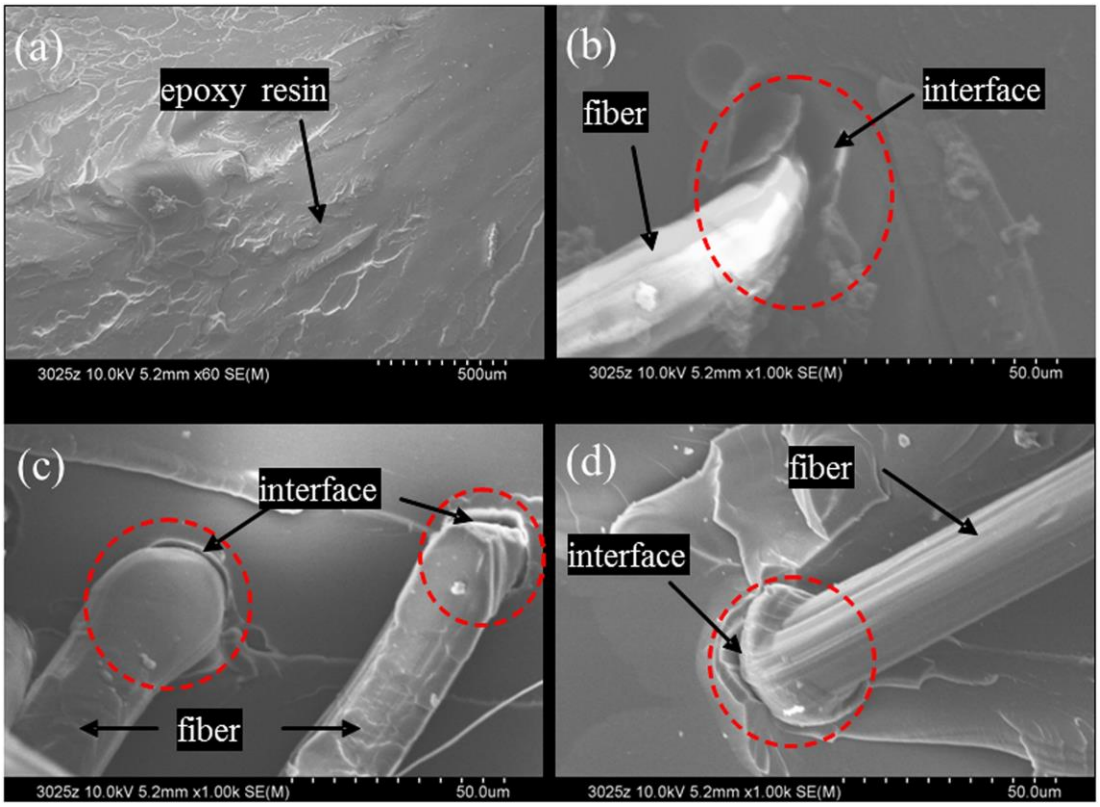

Figure 2. 4 Scanning electron microscopy of UHMWPE fibers with tensile fracture surface; (a) epoxy resin (b) UHMWPE-epoxy resin (c) UHMWPE-PDA-epoxy resin (d) UHMWPE-PDA-HMDA-epoxy resin Reprinted with permission from [46].

Incorporation of HA can increase tensile strength and hydrophilicity of UHMWPE material [82, 83]. James et al.[47] from Colorado State University developed a UHMWPE - hyaluronan (HA) micro composite where a small portion of HA was covalently bonded into a porous preform of UHMWPE to act as articular cartilage and joint replacement materials. It was claimed that UHMWPE is hydrophobic, while articular cartilage is hydrophilic containing chondrocytes and extracellular matrix with proteoglycans [84]. HA introduced a hydrophilic lubricous well hydrated surface on UHMWPE. The processing of UHMWPE–HA biomaterials involves molding techniques to make it fully dense. Sham control doesn't include the molding step. Wear resistance of different grades of UHMWPE-HA is shown in Fig 2.5(a). The UHMWPE-HA wear rate was slightly lower than both the UHMWPE convention and the sham control across the whole process [47].

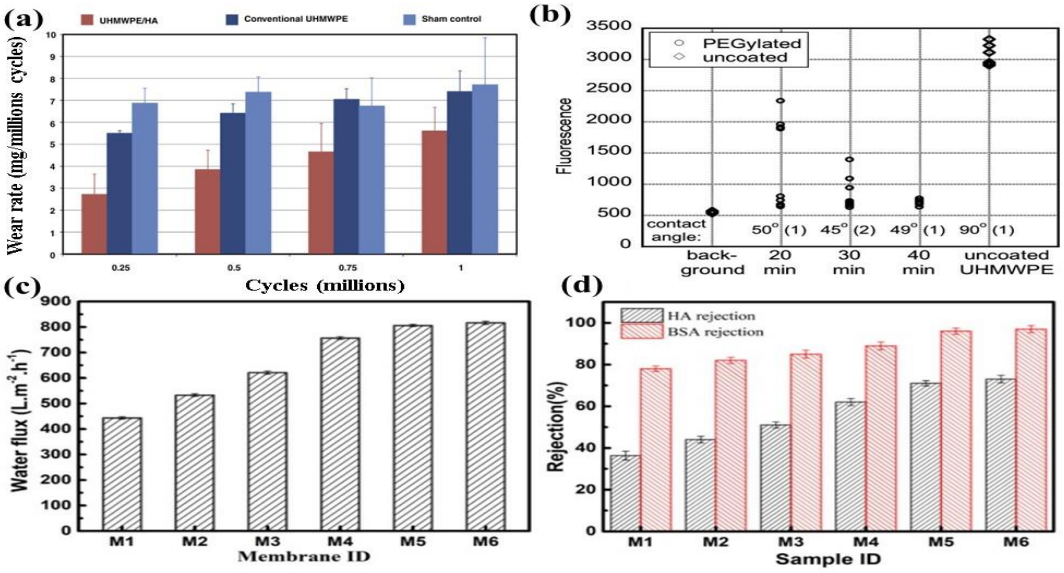

Figure 2. 5 (a) Wear rate comparison of conventional UHMWPE and UHMWPE-HA composite and control samples; (b) Water contact angle and protein adsorption resistance results of untreated and treated UHMWPE; Water flux and protein rejection of various membranes (c) Water flux and protein rejection of various membranes (d) HA and BSA rejection. Reprinted with permission from [47–49].

Kane et al. [48] have examined the tribological properties of PEG-like coatings on UHMWPE for total hip replacement. PEG- like hydrogel was covalently bonded to the surface of UHMWPE to improve its lubricity, wear resistance, and antithrombogenic properties. Surface of PEGylated UHMWPE shows higher resistance to protein adsorption compared to untreated UHMWPE and surface hydrophilicity does not have any impact on it (Fig 2.5(b)). Unlike UHMWPE particles, fragments of the PEG-like coating are less likely to induce an *in vivo* immune reaction.

Liu et al. introduced a hydrophilic inorganic vinyl trimethoxy silane (VTMS) and SiO_2 layer on UHMWPE to make the surface of UHMWPE more hydrophilic and to improve its antifouling properties. This hydrophilic layer will create a protective hydrated sheath by absorbing water and protecting the surface from unwanted contaminants. After the grafting, the water flux of UHMWPE increased from 452.2 $L \cdot m^{-2} \cdot h^{-1}$ to 532.7 $L \cdot m^{-2} \cdot h^{-1}$ as shown in Fig 2.5(c). On the other hand, HA and BSA rejection of the original UHMWPE was 36% and 78%, but after the treatment it increased to 42.3% and 82% as shown in Fig: 5(d).

2.3.2 Surface modification of UHMWPE by different plasma (DBD, PACVD, ECR, CAP, PIII) and gamma irradiation methods

Plasma modification is one of the most productive ways for the surface treatment of polymers as plasma treatment could selectively modify the physical and chemical properties of the surface of the polymers without affecting the original bulk characteristics of the polymer. This treatment can modify the surface of the substrate without changing the mechanical properties of the substrate [85].

Ionized precursor fragments are deposited on the substrate surface and result in the deposition of thin films on the substrate. Plasma treatments can provide the biocompatibility of the materials [86, 87] drug delivery devices [88, 89], biofilms [90, 91], next generation of nanobiointerfaces

[92], anti-corrosion coatings, and corrosion with enhanced tribological properties, and can improve antibacterial properties [93] Compared to other surface modification treatments, plasma surface modification offers shorter treatment time [88]. Plasma treatment is usually reliable, reproducible, non-line of sight, applicable to different sample geometries, as well as different materials such as metal, polymers, ceramics, and composites [94]. Plasma processing can provide sterile surfaces and can be adopted easily by industrial purposes. Plasma activation has been successfully done for the improvement of the wettability of the polymer surfaces [34,36]. Surface properties of the polymers can be modified by using energetic photons, ions, or electric beams or laser treatment. Surface modifications of UHMWPE bring changes to surface topography and wettability of the sample [96]. Different plasma techniques and gamma irradiation for surface modification of UHMWPE have been described below:

2.3.2.1 Cold atmospheric plasma (CAP)

The functionalization of UHMWPE with cold atmospheric pressure gas plasma results in improved wear performance without affecting the cytocompatibility of the material. This is an inexpensive method that has been used for modification of the surface properties of materials and can provide a sterile surface environment. The longevity of replacement joints and discs is an important factor in determining the success of implant materials. The antimicrobial properties of cold gas plasma allow simultaneous wear performance enhancement and material sterilization [97].

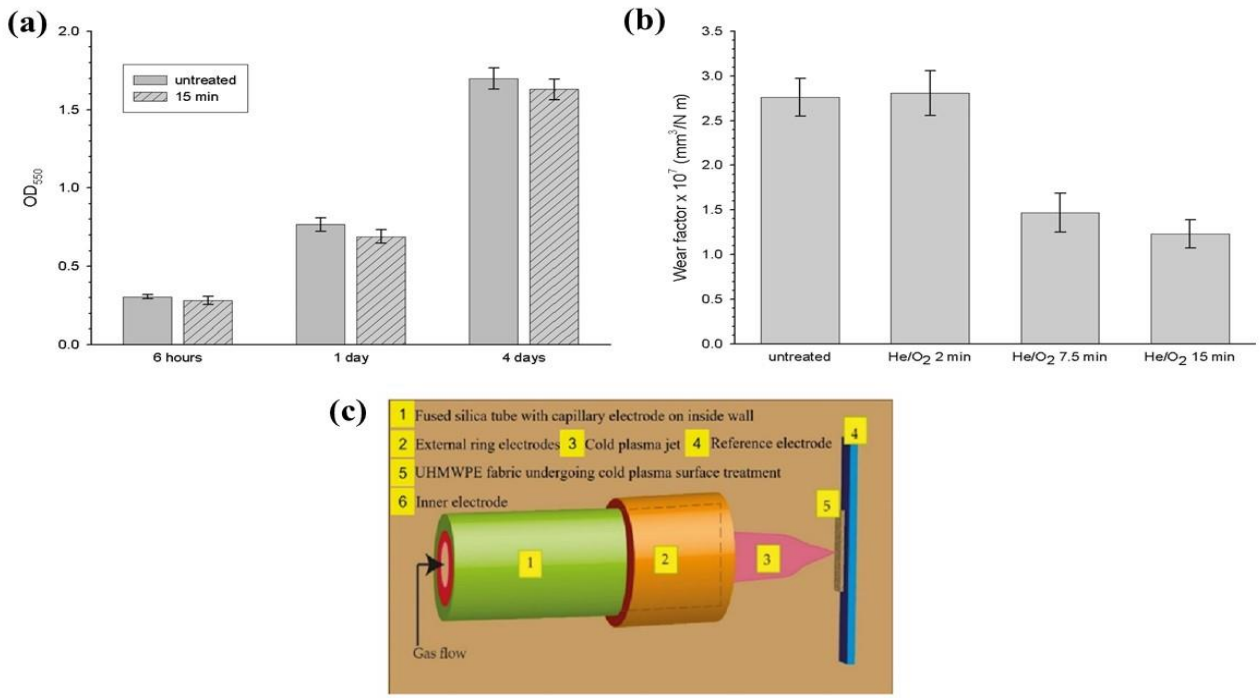

Figure 2. 6 (a) Wear factors of untreated and treated UHMWPE after cold plasma treatment. Reprinted with permission from [98]; (b) Osteoblast cell adhesion to untreated and cold plasma treated UHMWPE. Reprinted with permission from [98]; (c) a schematic diagram of Cold atmospheric plasma.

Perni et al. [98] have determined that cold atmospheric plasma functionalized materials show a greater level of cross-linking of the polyethylene chains. [98] In this treatment wear factors and cytotoxicity assessed by scratch resistance and 3-(4,5-dimethylthiazol-2-yl)-2,5-diphenyl-2H-tetrazolium bromide (MTT) assay. UHMWPE treated with He/O_2 at different time frames. Results in Fig 2.6 (a) showed that wear factors of sample treated for 7 min and 15 mins were almost same but half of the untreated UHMWPE. Fig 2.6 (b) showed the adhesion of osteoblast cells to UHMWPE increased over time but there was no significant difference between untreated and treated UHMWPE.

In another study, S.Van et al. [99] illustrated that the surface functionalization of UHMWPE through a cold plasma method in the absence of air, can provide enhanced adhesion forces, and improved hydrophilicity. Similar functionalization of UHMWPE is achieved by using cold

plasma where ionized gas produced from electrical discharge penetrates the material's surface at low pressure [51, 100]. Sterilization was achieved by the formation of reactive species, which inactivates the nucleophilic sites of microorganisms. Rodrigues et al.[101] found that UHMWPE treated with cold plasma can improve hydrophilicity, and influence cell adhesion properties which have been illustrated in Fig 2.7. Cell biocompatibility tested on three different types of treated samples (OP1-optimal points based on surface wettability, OP2 and UV). After 7 days incubation OP2 showed less cell adhesion compared to OP1 and UV. It has been confirmed from the results that hydrophobic surfaces favor cell adhesion properties more than plasma treated hydrophilic surfaces [101].

2.3.2.2 Plasma-assisted chemical vapor deposition (PACVD)

Among different plasma treatments, Struszczyk et al.[27] have implemented a plasma-assisted chemical vapor deposition (PACVD) method for modification of the surface of UHMWPE composites [102]. The PACVD system consisted of two aluminum electrodes; the charged surface was positioned between the electrodes. Two materials hexamethyldisiloxane (HMDSO) and tetradecafluorohexan to be deposited on the UHMWPE composite were injected into the gas mixture. The surface of composite UHMWPE was modified in a low-temperature plasma method with a radio frequency of 13.56 MHz as the generator in an argon and air-gas mixture.
The use of the PACVD method to deposit a polymer layer on composite of UHMWPE can improve the main functionalities of the composite and provide new functional properties [27, 70, 103]. Das et al.[104] introduced a new technique of biomolecule immobilization on UHMWPE substrate at different gas flow rates by using the PACVD technique. This technique showed that a significant number of biomolecules attached on DLN (Diamond like nanocomposite) coated

UHMWPE rather than untreated UHMWPE. The following table 2.4 shows adhesion strength of deposited DLN films on UHMWPE, the strength of adhesion was seen to slowly increase and then later decrease. Whole PACVD system shown in Fig 2.8(a).

Table 2.4 Adhesion properties of DLN films on UHMWPE substrate [104]**.**

Ar gas flow (ml/min)	LP (w)	Adhesion strength (MPa)	Load applied (N)
25	180	12	65.8
50	225	33	187.3
75	290	37	209.2
100	260	20	112.6
175	255	12	70.6

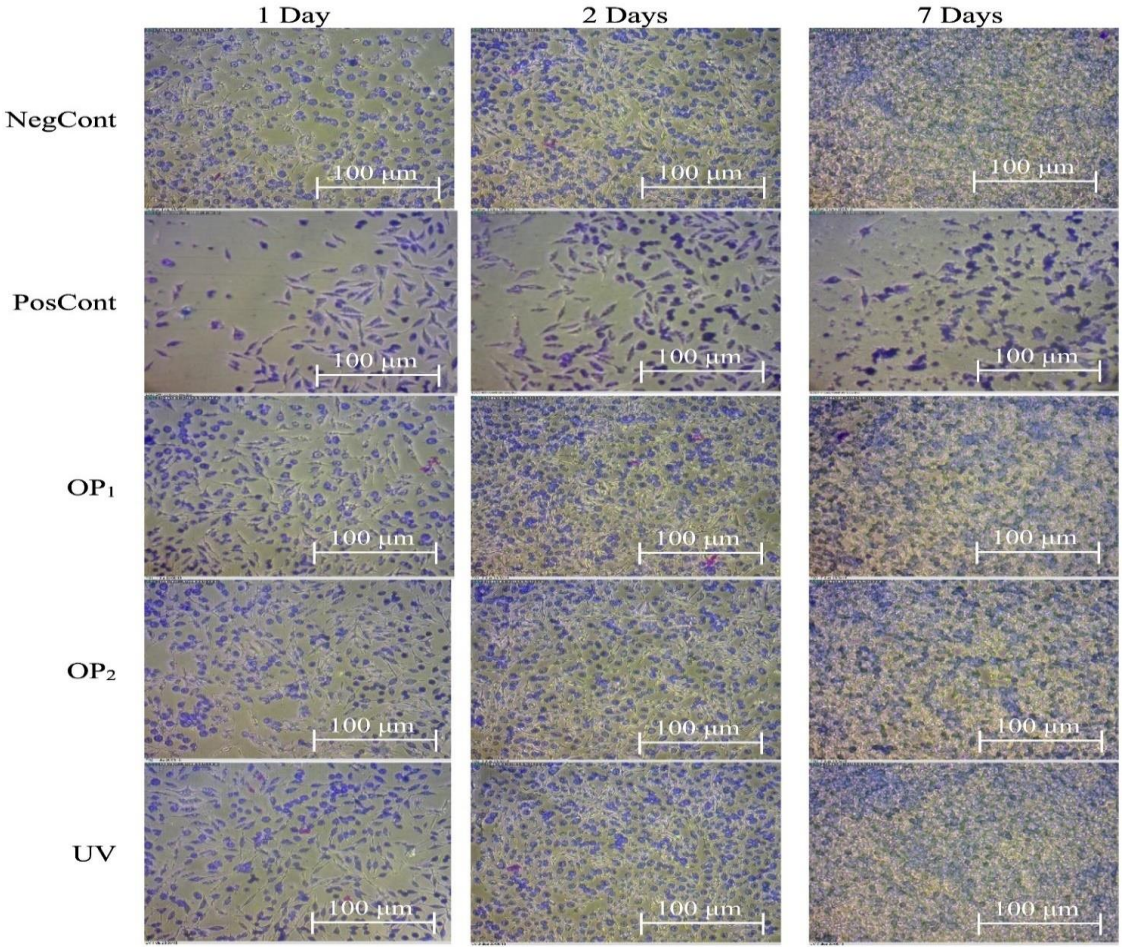

Figure 2. 7 L929 Cell attachment on untreated and treated UHMWPE. Reprinted with permission from [101].

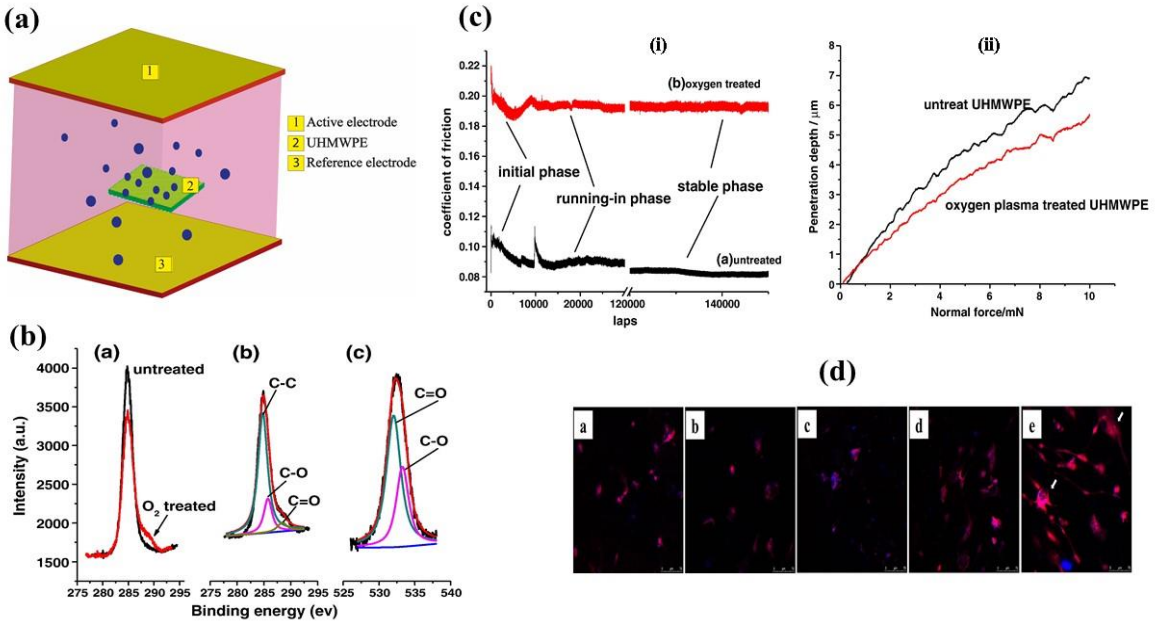

Figure 2. 8 (a) Plasma-assisted chemical vapor deposition (PACVD) coating of UHMWPE fabric; (b) Introduction of additional groups into UHMWPE before and after treatment. Reprinted with permission from [39];(c) (i) Friction Coefficient of friction of untreated and treated UHMWPE; (B) Scratch penetration vs load graph. Reprinted with permission from [39]; (d) Differentiation of PBMNCs to osteoclast. (a) untreated UHMWPE (b) HN-1 min (c) O_2-1 min and (d) HN-2 min do not display presence of osteoclasts, whereas (e) O_2-2 min displays the presence of multinucleated giant osteoclasts on its surface (indicated with arrows). Reprinted with permission from [38].

2.3.2.3 Electron cyclotron resonance (ECR) plasma

Another technique have been developed to etch the surface of materials using gas pressure and microwave power [105]. Liu et al. [39] have studied the surface and tribological properties of UHMWPE after ECR plasma treatment. It has been stated that ECR plasma can improve wettability, anti-scratch and tribological properties of UHMWPE through increased cross linking of UHMWPE molecular chains. Introduction of several additional functional polar groups (C–O/C–OH and C=O group) into the material made the surface of the material hydrophilic shown

in Fig 2.8(b). On the other hand, more cross linking enhanced the hardness, anti-scratch, and anti-friction properties of UHMWPE which are presented in Fig 2.8(c).

More et al. [38] presented a surface modification technique of UHMWPE with microwave-assisted electron cyclotron resonance (ECR) plasma for osteoblast and osteoclast differentiation. A microwave power of 150 W and 2.45 GHz was implanted through a quartz window into the ECR plasma chamber [106]. It has been determined that plasma treatment for 2 min increased surface roughness and reduced friction functional groups relative to untreated and 1 min plasma treated UHMWPE. This treatment plays a role in improving cell migration and facilitating the fusion of peripheral blood mononuclear cells (PBMNCs) to form osteoclasts which is shown in Fig 2.8(d).

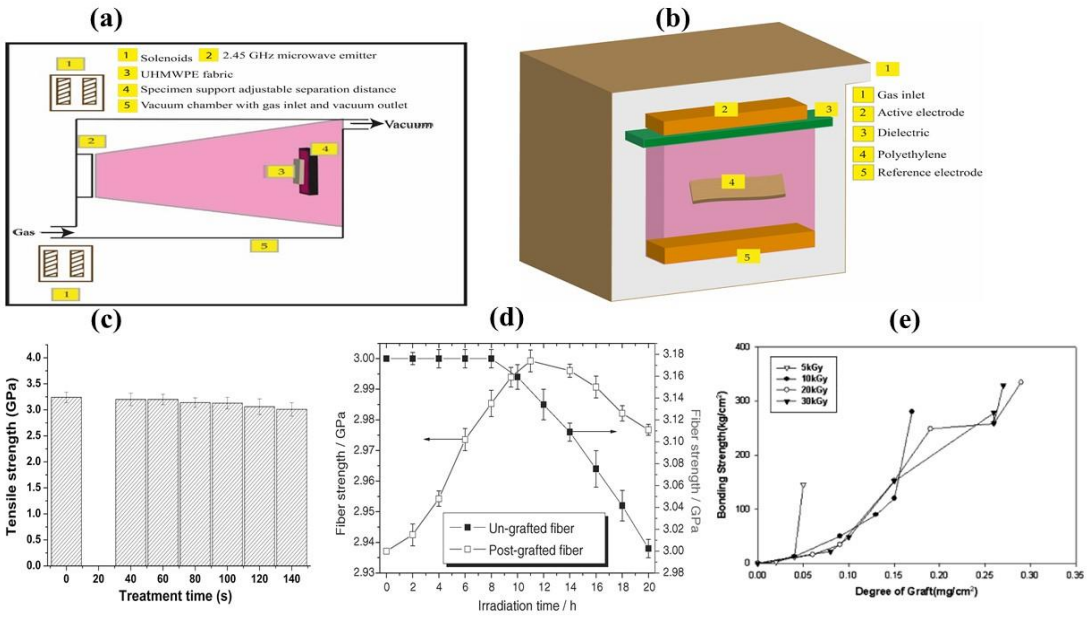

Figure 2. 9 (a) Plasma treatment of UHMWPE fabric in an electron-cyclotron resonance (ECR) plasma reactor system (b) Dielectric barrier discharge (DBD) plasma treatment of polyethylene fabric, (c) Impact of plasma treatment time on tensile strength of modified DBD-chitosan treatment UHMWPE fibers. Reprinted with permission from [53], (d) Tensile strength of untreated and UV treated UHMWPE. Reprinted with permission from [23], (e) The influence of degree of graft on tensile strength. Reprinted with permission from[57].

2.3.2.4 Dielectric barrier discharge (DBD) plasma

The Dielectric discharge barrier (DBD) is based on an alternating current (AC) discharge that produces plasma thermodynamic nonequilibrium at environmental pressure. Low temperature plasma treatments are suitable for temperature sensitive polymers. Plasma generated between two plane parallel aluminum electrodes. Electrodes were 200 cm long and the upper electrode was covered with the insulating quartz glass layer (10 mm thick). The gap width between quartz glass sheet insulating and ground electrode was 2 mm. The sample was placed between two electrodes and exposed to plasma at 200V, 50 Hz from main power supply. A schematic of the DBD plasma treated apparatus is shown in Fig 2.9 (b).

Ren et al. [53] developed a new combined technique of dielectric barrier discharge (DBD) plasma and chitosan coatings to functionalize the surface of UHMWPE. The plasma treated sample was immersed in 0.7% w/v concentration of chitosan solution and stirred for 10 h at the room temperature. Due to the plasma treatment hydroxyl, carbonyl, and carboxyl groups were introduced onto the surface of UHMWPE fiber surfaces and enhanced the wettability of the surfaces [107]. It was believed that the amino groups of chitosan could be covalently bound to the surfaces of plasma treated UHMWPE by carboxyl groups to form amide bonds and increased the strength [53]. Impact on plasma treatment on UHMWPE is shown in Fig 2.9(c).

R.Sa et al. [45] outlined two less time consuming surface modification methods to identify their effects on surface properties of UHMWPE fibers. Three different types of epoxy resins: neat DGEBA, poly-urethane-crosslinked DGEBA and BHHBP-DGEBA were examined as resin matrices for UHMWPE fiber-reinforced composites. Before each experiment, UHMWPE was cleaned in a polar and non-polar solvent and then dried in an oven at 60°C. UHMWPE was

plasma treated for four different times, and after the treatment, the fiber was exposed to the air. In the chemical method, the UHMWPE fiber was plasma treated for 10 minutes and then immersed in dodecyl benzyl sulfonic acid mixture in different weight ratios and temperatures. It was reported that both experiments increased the degree of interfacial contact between fibers and mechanical strength but plasma treated UHMWPE showed better mechanical strength than chemically treated UHMWPE [108].

Table 2.5 Mechanical strength comparison of untreated and treated UHMWPE [45]**.**

Samples	Amount of fibre (vol%)	Tensile strength MPa
Raw UHMWPE	34.6	526.7
DBD-UHMWPE	34.2	543.4
BHHBP-DGEBA-UHMWPE	34.5	537.3

2.3.2.5 Grafting on UHMWPE by gamma irradiation

Wang et al. established a surface modification technique by introducing acrylamide groups through high energy ultraviolet initiated grafting reactions, and thus, was able to increase the tensile strength of UHMWPE (Fig 2.9(d) [23]).

Diphenyl ketone was used as an initiator for absorbing energy and producing double-free radicals for the process. The process of grafting was carried out by several steps; (i) initiation (ii) propagation (iii) transfer & termination reactions [109]. Another similar surface modification was carried out on UHMWPE; the material was exposed to γ radiation for improving bonding strength to polymethyl methacrylate (PMMA) cement. Two types of irradiation methods were adopted for this study: pre-irradiation and syn-irradiation. The intensity was 5-30 kGy for pre irradiation and 1-3 kGy for syn irradiation. pre-irradiation introduced a small coating of PMMA on the surface of UHMWPE but higher bonding strength than syn-irradiation [57].

Hu et al. [110] studied a functionalization method for UHMWPE fabric by the radiation-induced graft polymerization reaction of γ-methacryloxypropyl trimethoxysilane (MAPS) and subsequent cohydrolysis of the graft chains (PMAPS) with tetra butyl titanate. Nanocrystalline titania films generated on UHMWPE to improve thermal properties and UV resistance [110].Gamma irradiated UHMWPE exhibited a smaller area of accumulated cracks when reciprocating the loading movement compared to virgin UHMWPE.

Tomita et al. [111] reported that, incorporation of blended vitamin E into UHMWPE can reduce the crack formation and flaking like destruction of pure UHMWPE [28]. Vitamin E (alpha tocopherol) blending can generate different microstructures on the surface and subsurface of the UHMWPE. Vitamin E blending reduced crystallinity which is beneficial for increasing mechanical strength [59]. Another study revealed that, cross linking and vitamin E stabilization influenced microbial adhesions on UHMWPE. The combination of vitamin E stabilization and crosslinking can give additional benefits in terms of microbial adhesion reduction [37, 112].

To reduce the inertness of UHMWPE, vinyl triethoxysilane (VTEOS) containing hydrolyzable alkoxyl groups was grafted in situ onto UHMWPE by air plasma treatment. The graft proficiency controlled by reaction conditions, including time, radiofrequency (RF) plasma power, and pressure in the reaction chamber. Incorporation of VTEOS into the UHMWPE enhanced wettability, high cell proliferation rate, and coarse structure without damaging the bulk structure of the material [113]. The functionalization of biomedical UHMWPE was achieved by plasma treatment, using atmospheric pressure plasma polymerization technology. The investigation done by Cools et al. demonstrates the effect of plasma polymerization treatment on UHMWPE. They have carried out the functionalization in the helium atmosphere at an ambient pressure to introduce methyl methacrylate into the PE samples to increase the adhesion between the polymer

and the PMMA bone cement. The introduction of functional groups on the PE helps to anchor the polymer film to the substrate [54]. A similar study for the functionalization of UHMWPE by Aziz et al.[114] explains the post-irradiation grafting and UV polymerization onto UHMWPE surface. In this method of polymerization, He (Helium) has been used for activation and as a carrier gas for post-irradiation and plasma polymerization process and it increased the bonding strength of the material presented in Fig 2.9(e). The treatment is based on nitrogen-containing polymer coating on UHMWPE samples by different plasma and UV based techniques at different conditions [114].

2.3.2.6 Plasma immersion ion implantation (PIII)

Plasma immersion ion implantation, commonly expressed as PIII or PI^3, is a unique plasma treatment technique initially developed as a revolutionary non-line of sight process. Instead of other conventional ion extraction methods, PIII works by placing a 3D shaped target in the ion acceleration scheme itself [115]. In this method, the target substrate is immersed in plasma, accelerated with high voltages, resulting in energetic ions being implanted from plasma to the substrate. Conrad et al. have developed the basic principles and applied them to treat specific 3D components and modified several materials using PIII[116]. Nowadays, PIII can be used to deposit a carbon-based coating on the substrate rather than as an ion bombardment surface treatment. This treatment is carried out by injecting carbon-containing gas into the plasma formed in a background gas, which is referred to as plasma immersion ion implantation and deposition (PIII & D) [117]. PIII treated diamond-like carbon films have been widely used in blood-contacting devices such as rotary blood pumps, artificial hearts, mechanical heart valves, and coronary stents [118].

In the biomedical field, one of the applications of PIII is to enhance the blood compatibility of materials [93]. Different structures and compositions of Ti-O films were synthesized by PIII treatment. The structural difference was carried out by changing the oxygen flow rate into the vacuum chamber of the PIII device. This oxygen content can change the structure of the material from amorphous to a mixed crystalline structure of anatase and rutile, and further becomes more rutile (stable form of TiO_2). Increasing oxygen content enhanced the adhesion of platelets to the material [119, 120].

Surface modification of UHMWPE by plasma immersion ion implantation with nitrogen gas, showed promising results for improving surface mechanical properties such as hardness and elastic modulus[121]. Due to the formation of cross-linked molecular microstructure, the surface of UHMWPE is expected to be predominantly modified. Weak secondary bonds of the untreated material were replaced by strong covalent bonds at the cross-linked points, therefore decreasing mobility of the molecular chain. As a result when subjected to applied force, modified UHMWPE showed higher hardness and wear resistance than the untreated UHMWPE [60].

Table 2.6 Coefficient of wear and friction [68].

Sample	Coefficient of wear (mm^3/Nm)	Coefficient of friction
UN	19.6 X 10-9	0.060–0.063
PE1	14.1 X 10-9	0.066–0.068
PE2	8.45 X 10-9	0.065–0.066
PE3	6.51 X 10-9	0.060–0.070

Chen et al. [70] have studied the surface modification of UHMWPE implanted by 80 keV N_2^+, $C_3H_8^+$, with a plasma density ranging from 1×10^{14} to 5×10^{15} ions/cm^2. Surface modification was carried out by Elastic recoil detection (ERD) and X-ray photoelectron spectroscopy (XPS). Table

2.7 illustrated the ERD results, detected the hydrogen deficient layer on the surface after the implantation, which increased polar groups and hydrophilicity of the material.

Table 2.7 Total surface energy, polar and dispersive components in PIII treated UHMWPE [123]**.**

Sample	Polar components(dyne/cm)	Dispersive components(dyne/cm)	Total surface energy(dyne/cm)
Untreated	18.7	39.5	58.2
PIII treated	50.7	22.1	72.8

Very recently a similar experiment was conducted by Rossi et al.[61] with different mechanism of using surface breakdown voltage to improve the resistance of surface flashover. After the surface treatment, its surface roughness increased from 39 nm to 71 nm which has been confirmed by the AFM surface measurement technique[61]. Table 2.8 provided various disadvantages of traditional parameters used for surface functionalization methods. Advantages and disadvantages of different plasma methods are provided in Table 2.9.

Table 2.8 Disadvantages of traditional parameters used for surface functionalization methods [124]**.**

Parameter	Effects
High temperature	Deteriorates the material [97]
High-intensity energy	Oxidizes the material, increases crystallinity, destroys the lifetime [125]
UV radiation	Oxidative degradation of the material can damage the material [22, 66]
Chemical reagent	Changes surface chemistry, the formation of toxic residues and by-products, including carcinogens [41]

Table 2.9 Advantages and disadvantages of different plasma methods [68, 126–129]**.**

Methods	Advantages	Disadvantages
DBD Plasma	• Atmospheric pressure • Less time required • High deposition rate	• Sample could be contaminated
PACVD plasma	• Low temperature • Unique chemical properties of deposited film • High solvent and corrosion resistance	• Time consuming • Unstable against ageing • Very thin layer of deposition
ECR plasma	• Low-pressure range • High degree of ionization • Provide sterile environment	• Non-uniform etches surface. • Sample could be contaminated
Cold Plasma	• Can provide sterile environment. • Low temperature • Suitable for porous structures • Uniform surface treatment	• Covers limited surface area. • Limited temperature range
PIII	• Large treatment area • High efficiency • Can treat 3D objects. • Batch processing capability • Small instrument footprint • Provide uniformity in treated surface	• Difficult to achieve accurate in situ dose monitoring

2.3.2.7 Nano reinforcement

The concept of synergy or synergistic effect has recently evolved in the effort to attain superior adhesion and attenuate matrix dominating qualities. The fiber surface is treated with a suitable functional group, either by adding virgin nano-reinforcements or functionalized nano-reinforcements, to achieve the synergistic effects. Due to the exceptional properties of nano reinforcements such as carbon nano tubes (CNT), nano clay, multi wall carbon nanotubes (MECNT), single wall carbon nanotubes (SWCNT) and carbon nano fibers have been frequently employed to modify the polymer matrix[7, 29, 130, 131].

Graphene nanoplatelets, CNTs are incorporated with UHMWPE to enhance its mechanical properties [132, 133]. Graphene is a flexible 2D carbon nanomaterial with a large specific surface area, with an ultimate tensile strength of 130 GPa. Blending of UHMWPE with graphene fillers can increase its wear resistance[134]. MWCNTs were integrated into an epoxy matrix reinforced by surface treated UHMWPE fiber to provide novel interfacial adhesion through resonance[135]. Both the UHMWPE fiber and MWCNTs were chemically treated with glycidyl methacrylate (GMA) and amino-thiol end radicals via free radical polymerization and click chemistry, respectively, to produce a high level of compatibility with epoxy matrix. LDPE/MWCNT and LDPE/MWCNT/UHMWPE self-reinforced fiber-composite were invented by M.A.A Seraji et al.[136]. To improve physical properties of UHMWPE. A novel nanocomposite coating of UHMWPE reinforced with nano clay and C nanotubes were developed to improve tribological properties of UHMWPE. These nanocomposite powder was deposited and fused onto the substrate which increased the melting temperature of the material[137].

Xin et al.[138] reported that Zeolitic imidazolate frameworks (ZIF8) were mixed with carbon nano fiber to act as a filler of UHMWPE by a facile liquid-phase chemical reaction. The results show that ZIF8-CNF can greatly increase UHMWPE crystallization and improve its thermal and mechanical properties. A surface porous UHMWPE composites were invented in the hot-pressing technique, where NaCl and graphene oxide (GO) were used to enhance its mechanical and tribological properties[139].

Most recently, UHMWPE is incorporated with 0.1 wt.% boron carbide by twin screw extrusion method @200 °C to improve its physical and mechanical performance[30]. The improved wear resistance of UHMWPE was discovered to be due to increased entanglement in amorphous and increased content of the interphase (better shear resistance), as well as the load-bearing effect of the particles[16].

A biocompatible UHMWPE/nano-Al_2O_3/Vitamin-C hybrid composites were developed by hot press technique for joint prosthesis. Vitamin C was employed as an antioxidant and Al_2O_3 was used as an anti-wear additive in UHMWPE[33]. Another biomimetic composite surface produced via Polydopamine (PDA) functionalized surface and then coated with Zinc oxide nanoparticles to improve interfacial adhesion properties of UHMWPE [140].

2.4 Biofunctionalization of UHMWPE by protein immobilization

Biomimetic materials for implants and microarray technology have been obstructed by the shortage of safe and simple methods to covalently combine bioactive molecules to the surface of a wide range of materials. Different types of wet chemical approaches are described in the literature for linking biomolecules to surfaces [141]. Puertas et al. have reported that the carboxyl group of polymers can be activated by carbodiimide chemistry [142]. N-hydroxysuccinimide

(NHS) or sulfo-NHS is also used to increase the coupling efficiency of materials [143]. Salinization and plasma functionalization have been used for pretreatment of surfaces for the generation of reactive sites for covalent coupling on polymer surfaces [144]. Biofunctionalization of the pure base material is carried out by the attachment of bioactive proteins to surfaces. Secure attachment is required sometimes because many applications may require the protein to remain stable under hostile environmental conditions such as in the flow of blood or during washing with strong detergents or buffers [145]. Additionally, The optimal device performance is dependent on dense surface coverage and long term retention of the proteins conformation [63]. Surface modification of polymer for protein attachment can be done in physical or chemical ways such as by attachment of linker molecules through active groups [146, 147] (UV treatment, plasma treatment [6, 148] and ion beam implantation [34, 121, 126, 149, 150]

2.4.1 Protein immobilization by chemical methods

Surface modification schemes are essential to functionalize the surface interfaces of materials. Serro et al.[24] examined the bio tribological properties of UHMWPE after incubation in bovine serum albumin (BSA) and sodium hyaluronate (NaHA) solution. Results showed that albumin was strongly adsorbed into UHMWPE, whereas NaHA adsorbed poorly. Fig 2.10(a) shows that surface becomes more hydrophilic after protein incubation. Atomic force microscopy (AFM) results confirmed the surface morphology of UHMWPE after three different treatments. BSA-incubated surface appeared as a globular structure and NaHA incubated surface exhibited a needle like structure, but combined protein incubated surfaces had a smaller size globular structure as shown in Fig 2.10(b) [24].

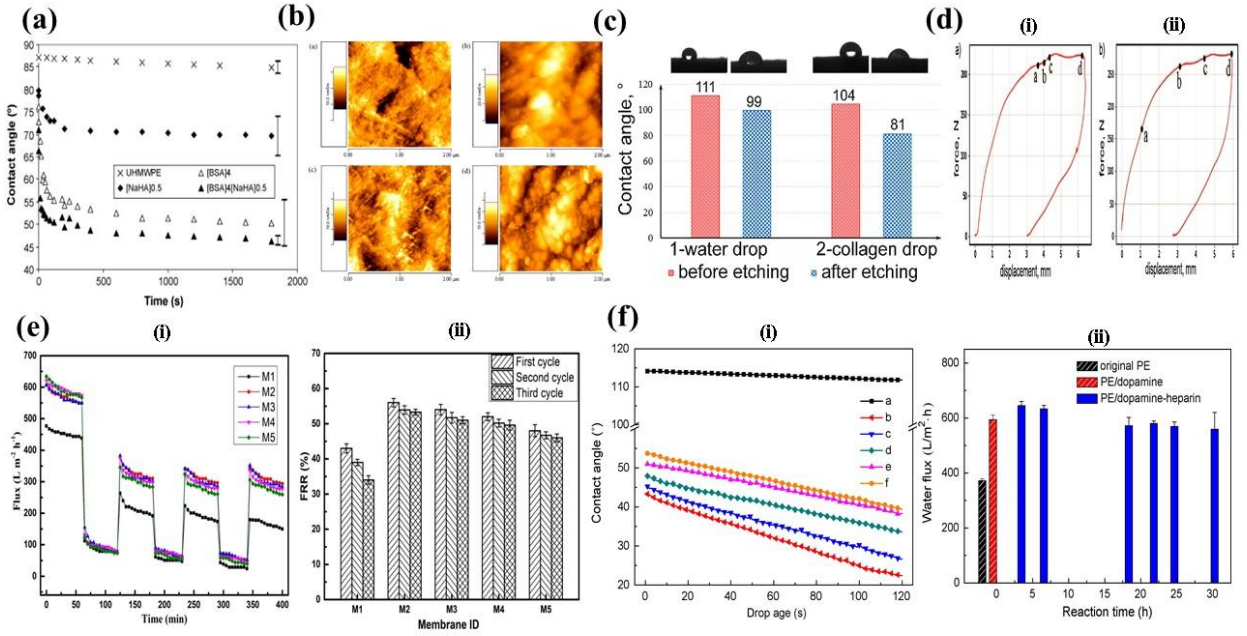

Figure 2. 10 (a) Water contact angle of UHMWPE before and after protein incubation. Reprinted with permission from [24]. (b) AFM images of UHMWPE with or without protein incubation; (a) Pure UHMWPE; (b) after incubation in BSA solution; (c) after incubation in NaHA solution; (d) after incubation in both solutions. Reprinted with permission from [24]. (c) Water contact angle of treated and untreated UHMWPE after surface treatment. Reprinted with permission from [151]. (d) The force-displacement curve of three-point bending test for (i) Freeze-dried collagen hybrid; (ii) Collagen-HAp hybrid. Reprinted with permission from [151]. (e) Antifouling properties of different membranes (M1, M2, M3, M4, and M5): (i) Variation of time-dependent flux over three periods with Bovine serum albumin (BSA) as a pollutant; (ii) Values of FRR with BSA as a pollutant. Reprinted with permission from [81]. (f) Contact angle vs drop age curve for the original and modified PE porous membranes (i) Untreated PE membrane; (ii) PE-polydopamine composite membrane; (c-f) PE/dopamine-heparin composite membrane; (b) Impact of heparin immobilization period for PE membranes on water flux. Reprinted with permission from [74].

Kan et al. [151] studied the influence of collagen and hydroxyapatite (HAp) in surface functionalization of UHMWPE. It was claimed that the water contact angle dropped from 111° to 81° after collagen and HA impregnation presented in Fig 2.10(c). Three-point bending test plotted in Fig 2.10(d) confirmed that the increased rigidity of UHMWPE-Collagen-HAp hybrid comes from the combined impregnated layer.

PDA has been cross-linked or coated on materials to modify the surface chemistry of materials [45]. Surface modification and protein immobilization on UHMWPE polymer were carried out by dopamine self-polymerization and Schiff base reaction [81]. The dopamine layer introduced hydrophilicity of the composite membrane, and mPEG-NH_2 modified the protein fouling resistance of the material. Fig 2.10 e (i) shows that the pure water flux of all PDA-modified composite membranes (M2, M3, M4, and M5) remained at approximately 310 (L m^{-2} h^{-1}) after three cyclic filtration tests, which was greater than that of the initial composite membrane. On the other hand, compared to the original membrane, the flux recovery ratio (FRR) values of the PDA-modified composite membranes (M2, M3, M4, and M5) were increased during all three cycles, but the FRR values of all five of these membranes were not reasonable (Fig 2.10 e (ii)).

In similar work conducted by Jiang et al. [22], UHMWPE was biofunctionalized for blood contacting biomedical applications with a polydopamine solution based on self-polymerization reactions. After polydopamine coating and heparin immobilization, the hydrophilicity of PE membranes was greatly enhanced [26]. Contact angle of PE decreased drastically after surface modification with polydopamine which increased hydrophilicity of the PE membrane as shown in Fig 2.10 f(i). Changes of water flux with retention time is presented in Fig 2.10 f (ii). After the dopamine coating, the water flux increases 1.6 times compared to that of the original PE. Surface heparinization significantly suppressed the adhesion of platelets and enhanced the anticoagulation ability of PE membranes is observed in Fig 2.11. Numerous platelets acted as adhesion, outspread, and aggregated on the surface of the original PE porous membrane. On the other hand, Dopamine deposition and heparin immobilization significantly reduced platelet adhesion, activation, and transformation.

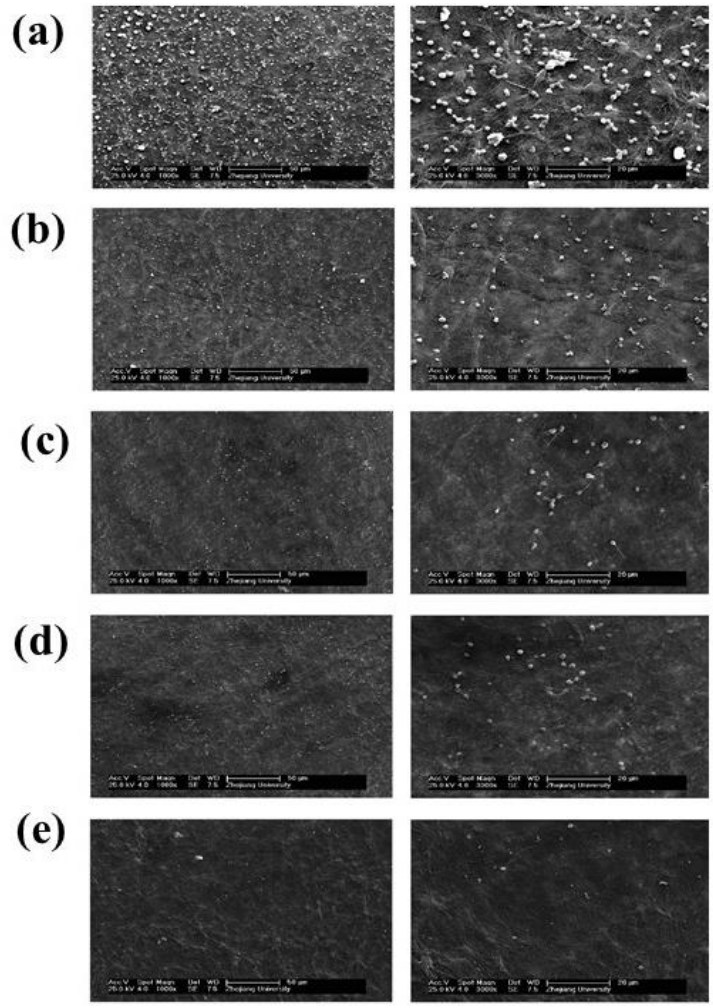

Figure 2. 11 Unmodified and modified PE porous membrane surface platelet morphology: (a) initial PE membrane, (b) PE / dopamine composite membrane, (c-d) PE / dopamine-heparin composite membrane, (c-e). Reprinted with permission from [74].

2.4.2 Protein immobilization by plasma methods

Radiation damage of polymers through UV treatment, plasma treatment, and ion beam implantation can provide protein binding on polymers by strong binding, especially covalent binding without specific linker groups.

Biofunctionalization of UHMWPE polymer was conducted by plasma treatment for adhesion improvement. A dielectric barrier discharge in Ar, He/O_2, He, N_2 or O_2 at atmospheric pressure

was used for the continuous plasma treatment of UHMWPE fibers [152]. In terms of studies related to the biomedical application of plasma-treated UHMWPE, Rodrigues et al. demonstrated that the surface treatment of UHMWPE by cold plasma technique has significant effects on the proliferation of cells and improved the inertness of UHMWPE surface to a level comparable to commercially available cell culture materials [101]. Widmer and Spencer treated UHMWPE with oxygen plasma to increase its hydrophilicity for getting faster and better protein adsorption [148].

A wide range of work has focused on improving the longevity of joint implants used in human bodies, as the biomedical implant contributes to wear debris when exposed to the actions of human blood serum triggering the release of wear particles. In some work, a dense boundary layer of Human serum albumin (HSA) proteins applied on PE surface to enhance boundary lubrication and reduce 50% of dynamic friction as well as reduction of static friction in hip implants [148].

The biofunctionalization of UHMWPE was derived from the detailed studies conducted by. Ho et al. explaining two methods for plasma treatment of an UHMWPE substrate. In this method of functionalization, Ar, and nitrogen PIII treatment with high electrical pulses was used to modify the surface of UHMWPE to provide improved hydrophilicity and interactions with proteins. The best performance was achieved by plasma immersion ion implantation using nitrogen gas [153]. Gan et al.[154, 155] reported that energetic ions extracted from inductively coupled nitrogen plasma was used to modify the surface properties of UHMWPE.

Biofunctionalization of UHMWPE was reported by Kondyurin et al., explaining the mechanism of covalently attached horseradish peroxide (HRP) on the surface of UHMWPE. The formation of the carbonized surface layer due to the oxidation of the ion damaged surface was claimed to

account for protein binding on UHMWPE [153]. Among various methods, ion beam implantation and its variant plasma immersion ion implantation has been used successfully for the covalent attachment of proteins on polymer surfaces [144]. Table 2.10 illustrated the influence on HRP immobilization after PIII treatment on UHMWPE.

Table 2.10 Surface property influence on HRP immobilization after PIII treatment on UHMWPE.

Sample	Roughness A°	Surface area (μm^2)	C (%)	N (%)	O (%)	Optical density @450nm from HRP activity
Untreated	528	101.9	94.9	Nil	5.1	0.45
PIII treated	1130	105.6	71.1	13.4	15.5	0.52

Another similar approach has been made to functionalize the surface of UHMWPE by PIII treatment to improve the wettability of the surface. HRP was immobilized on plasma-treated plasticized and unplasticized PVC and UHMWPE. PIII was conducted in nitrogen plasma with a radio frequency of 13.56 MHz at different time frames. Different types of low molecular weight additives (e.g., plasticizer, solvent, adsorbed molecules on the surface) have been utilized on the surface to facilitate the protein immobilization. Small molecular additives held the protein molecules and helped to attach the protein on to the surface of the polymer. But presence of plasticizer does not have an influence on protein attachment on UHMWPE [63]. Protein attachment on UHMWPE with or without additives are listed in Table 2.11.

Table 2.11 Protein attachment on UHMWPE with or without additives [63]**.**

Samples	HRP protein remains after wash (%)
Untreated	19
PIII treated	84
PIII treated + Plasticizer	62-72

Several studies have demonstrated that biological molecules contained in synovial fluid play a significant role in vivo friction and wear behavior [156]. Zolotarevova et al. [157] studied the interaction between plasma proteins and UHMWPE wear particles generated from hip periprosthetic granuloma tissues. It has been examined that UHMWPE itself is not responsible for macrophages activity. Several plasma proteins became denatured after binding with the particles and caused an accumulation of macrophages and other sensitive cells[157]. In another study done by Nicas et al. [158] reported that slow sliding speed is responsible for denaturization of protein and loss of their original structure; whereas at high sliding speed most of the protein kept their original structure and some formed aggregates. Friction behavior depends on type of protein and its concentration. Fig 2.12(a) illustrates the correlation among coefficient of friction, concentration of protein and sliding speed [158].

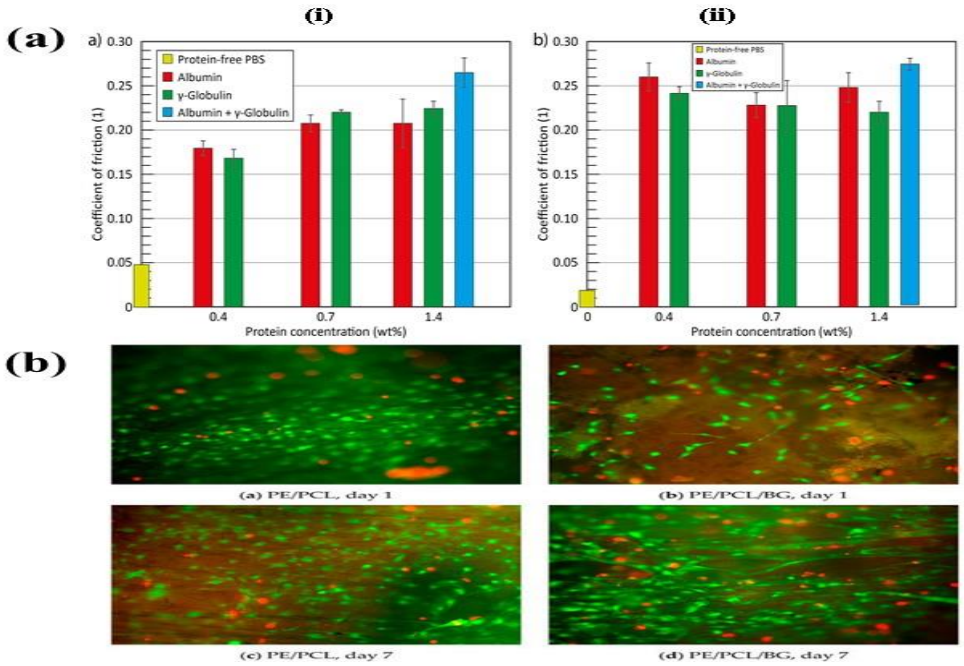

Figure 2. 12 (a) The bar graph represents the coefficient of friction vs protein concentration for all tested protein solutions at different sliding speed (i) 10 mm and (ii) 50 mm [109]. Reprinted with permission from [159]; (b) Live (green) and dead (red) cells on PE/PCL (a,c) and PE/PCL/BG composites (b,d) after one (a,b) and seven (c,d) days of culture [160].

2.5 Relationship between human ligament & UHMWPE

Ligaments are connective tissues with strong mechanical properties that can stretch a joint and become hooked at either end[161]. They attach two bones together, prevent dislocation and restrain movement of the joints. They differ in location, size, shape, and orientation. There are four different types of ligaments in the knee, such as: Medial Collateral Ligament (MCL), Lateral Collateral Ligament (LCL), Posterior Cruciate Ligament (PCL) & Anterior Cruciate Ligament (ACL)[162].

Table 2.12 Advantages and disadvantages of some common biomaterials

Biomaterial	**Advantages**	**Disadvantages**
Collagen [47, 163, 164]	Biocompatible, major component of native ACL.	Lacks mechanical strength, immunogenic
Hyaluronic acid [165]	Biocompatible ECM component; can be in sponge or hydrogel form.	Lacks mechanical strength.
Silk [166]	Good tensile strength.	Limited cell adhesion. Sericin coating is immunogenic.
Alginate [167]	Biocompatible, can encapsulate cells, can be in sponge or hydrogel form	Lacks mechanical strength.
Chitosan [168–170]	Biocompatible, chemically modifiable.	Limited cell adhesion and lacks mechanical strength.
PGA [171]	Common FDA-approved suture material.	Rapid degradation and loss of mechanical Strength, biologically inert. Acidic degradation By product.
PDS [172]	Common FDA-approved sutures material Easily manufactured into different forms.	Rapid loss of mechanical strength.

Table 2.12 continued		
Biomaterial	**Advantages**	**Disadvantages**
PLGA [173]	Degradation rate can be changed. Easily manufactured.	Biologically inert, Acidic degradation by-product.
PCL [174–176]	Common FDA approved suture material, easily manufactured.	Very slow degradation rate, biologically inert.
PLLA [171, 177, 178]	Slow degradation rate, better cell adhesion than PLA or PLGA. Easily manufactured.	Biologically inert, Acidic degradation by
PET [179]	Nondegradable, biocompatible, mechanically strong properties	Insufficient hydrophilicity and bioactivity
UHMWPE [67]	Mechanically strong, easily manufactured	Fragmentation of fabrics

2.5.1 Structure of anterior cruciate ligament (ACL)

The knee joint is complex which is composed of three separate joints: the tibiofemoral, patellofemoral, and the proximal tibiofibular joints[180]. The knee joint most referred to is the tibiofemoral joint. These knee joints are stabilized by several ligaments, including the anterior cruciate ligament (ACL), the posterior cruciate ligament (PCL), the medial collateral ligament (MCL), and the lateral collateral ligament (LCL). Ligaments are made of bands of collagenous connective tissue [181]. These paralleled collagen bundles are linked to each other by crosslinking [182]. Ligaments contain two-thirds water and one-third solid. Collagen is the major component of the ligament with 5 prominent collagen types: I, III, VI, XI, and XIV [183, 184]. The majority (90%) of the collagen in ligaments is type I which is responsible for its tensile strength. To maintain the mechanical and biological stability of ligaments, related organ systems, as well as the bone, play a vital role [185].

2.5.2 ACL injury & Selection of UHMWPE for ACL reconstruction

ACL injuries are common in sports such as football, soccer, or with uneven surfaces. ACL injury more commonly causes knee instability that further causes injury to other knee ligaments. Injuries of the ACL range from mild such as small tears to severe such as when the ligament is completely torn[162]. Allograft, autograft, and synthetic grafts have been used for ACL reconstruction. Due to the drawbacks of allografts and autografts, synthetic grafts may be a good choice for ACL reconstruction. The synthetic ligament graft is an artificial ligament device for joining the ends of two bones. Laflamme reported that the type of material and its particle size, are important factors regarding synthetic ligament graft selection [186]. UHMWPE fibers are commonly used in synthetic ligament implants due to their excellent tensile strength and elastic modulus. Mechanical properties of several materials used for ACL regeneration have been presented in the following table:

Table 2.13 Mechanical properties of materials for synthetic grafts compared to normal ACL [179, 187]**.**

Ligaments/grafts	**Ultimate tensile strength(N)**	**Stiffness(N/mm)**
Human ACL	1730	242
Human hamstring graft	3790	776
Human patellar tendon graft		685
Carbon fibres	660	230
Gore-Tex prosthesis	5300	322
Dacron	3631	420
Twisted silk matrix	2337	354

Table 2.13 continued		
Ligaments/grafts	**Ultimate tensile strength(N)**	**Stiffness(N/mm)**
Parallel silk matrix	1740	2214
KLAD	280	1500
Trevira	68.3	1866
Leeds-Keio	270	2000
Braided PLGA	907	
PLLA fiber	175	
UHMWPE fabric	52570	115

Table 2.14 illustrated different types of prostheses and materials used for ligament/tendon regeneration.

Table 2.14 Different types of prostheses and materials

Commercial name	**Manufacturer**	**Class**	**Materials**
Stryker	Stryker, Michigan, USA	Woven/Knitted	PET [188]
ABC Surgicraft	Surgicraft, Redditch, UK	Braided	PET/PET-C [189]
Gore-Tex	WL core & Associates, Arizona, USA	Braided	PTFE [190, 191]
Leeds-Keio	Neoligament Ltd, UK	Woven	PET [188]
LARS	Structural instruments and Devices, Arc-sur-Tille, France.	Loose/Knitted	PET [192]
Kennedy-LAD	3M, Minnesota, USA	Braided	Polypropylene [193, 194]
Proflex	Protek, France	Braided	PET [193]
Lygeron	Orthogroup, France	Woven	PET [195]

Table 2.14 continued.			
Commercial name	**Manufacturer**	**Class**	**Materials**
Ligastic	Orthomed, France	Knitted	PET [196]
Ligaid	Porth-Aid, France	Twisted	PAA [197]
Raschel	Cendis medical, France	Knitted	UHMWPE [198]
Braided PHP	Cendis Medical, France	Braided	UHMWPE [199]

Overen et al. reported [200] on thrombogenicity testing of UHMWPE compared to expanded polytetrafluoroethylene (ePTFE) and polyethylene terephthalate (PET) fibres for vascular applications. Hemobile is a method used to detect the damage of blood components and activation of platelets throughout the material/device. It is also used for testing vascularity of UHMWPE, ePTFE and PET fiber. Due to lower hemolysis and low activation of the inflammatory responses, UHMWPE showed better hemocompatibility than ePTFE and PET fibres [200].

Hunter et al. [194] reported on attachment, and proliferation of a variety of cell types on UHMWPE for orthopedic implantation. Cell multiplication was measured with a tritiated thymidine assay. Radioactively labelled thymidine (tritium) was used to measure lymphocyte proliferation by incorporation of 3H thymidine into the dividing cell's DNA. A component vinculin, a cell focal adhesion plaque, was labeled by indirect immunofluorescence to assess the attachment of cells [201]. Fibroblasts and osteoblasts cultured directly on UHMWPE were tested by determining the mean number of adhesion plaques using an image analysis system. Fibroblasts attached well on UHMWPE fabric. High tensile strength, bio-inertness, and fibroblast adhesion makes it appropriate for ACL reconstruction [202]. Several materials have

been developed that can be used for the reinforcement of matrix to modify the properties of UHMWPE, utilized for its application in ACL reconstruction.

Surface modification plays a major role in helping osteogenesis and bone anchorage of synthetic grafts [203]. Chitosan is a naturally derived polysaccharide that has been used for the modification of synthetic grafts [53]. Chitosan-hyaluronic is a composite that promotes new bone formation at the graft bone interface because of its porosity, biodegradability, biocompatibility, anti-infective activity, and ability to accelerate wound healing[204]. Vaquette et al. [205] reported that polystyrene sodium sulfonate as surface modification could improve the osteointegration of a synthetic graft [206].

Bioactive glass has been used for ligament graft modification due to its stimulation of angiogenic growth factors [119, 207] A composite of UHMWPE-PCL-Bioglass was developed as a synthetic graft by an electrospinning method. Bioglass was coated on UHMWPE by slurry dipping technique; melt derived glass particles were suspended in demineralized water to make a slurry with 5% w/v concentration, followed by 30 minutes agitation in magnetic stirrer. Fibroblast cells were seeded on a composite graft to examine cell adhesion. Cells adhering to UHMWPE composite were well flattened and more spread out compared to cells on pure UHMWPE. Excellent fibroblastic cell growth on composite UHMWPE-PCL-Bioglass synthetic graft is shown in Fig 2.12 (b) [160].

Bioactive glasses have unique compositional ranges of dense amorphous calcium sodium phosphosilicate (CSPS) that develop strong chemical bonds with the collagen of living tissues [208, 209]. The composition of 45S5 bioglass is 45% SiO_2, 24.5% CaO, 24.5% Na_2O, and 6% P_2O_5 [210]. Bioactive glasses dissolve slowly in a simulated body fluid (SBF) with some reactions taking place on the surface of the glass [204, 211–213]. These reactions include: (i)

Ions release due to the ion exchange between the solution and surface of the glass, but other components of the glass remain intact [214]; (ii) H^+ ions attack the silica network and as a result Si-O-Si bonds break down, and new Si-OH and Si $(OH)_4$ groups are formed at the surface of the glass; (iii) A soluble porous silica-rich layer forms on the surface of the glass due to condensation and re-polymerization; (iv) A calcium phosphate-rich layer forms on the Si-rich layer due to the migration of Ca^{2+} and $(PO_4)^{3-}$ ions; and (v) A polycrystalline apatite layer forms on the surface of the bioglass. Collagen fibres can attach to the surface of the bioactive glass. The transparent silica-rich layer induces precipitation of hydroxyapatite like (HCA) layer. Interactions between bioglass and collagen fibres occur and get stronger when HCA precipitation increases [215].

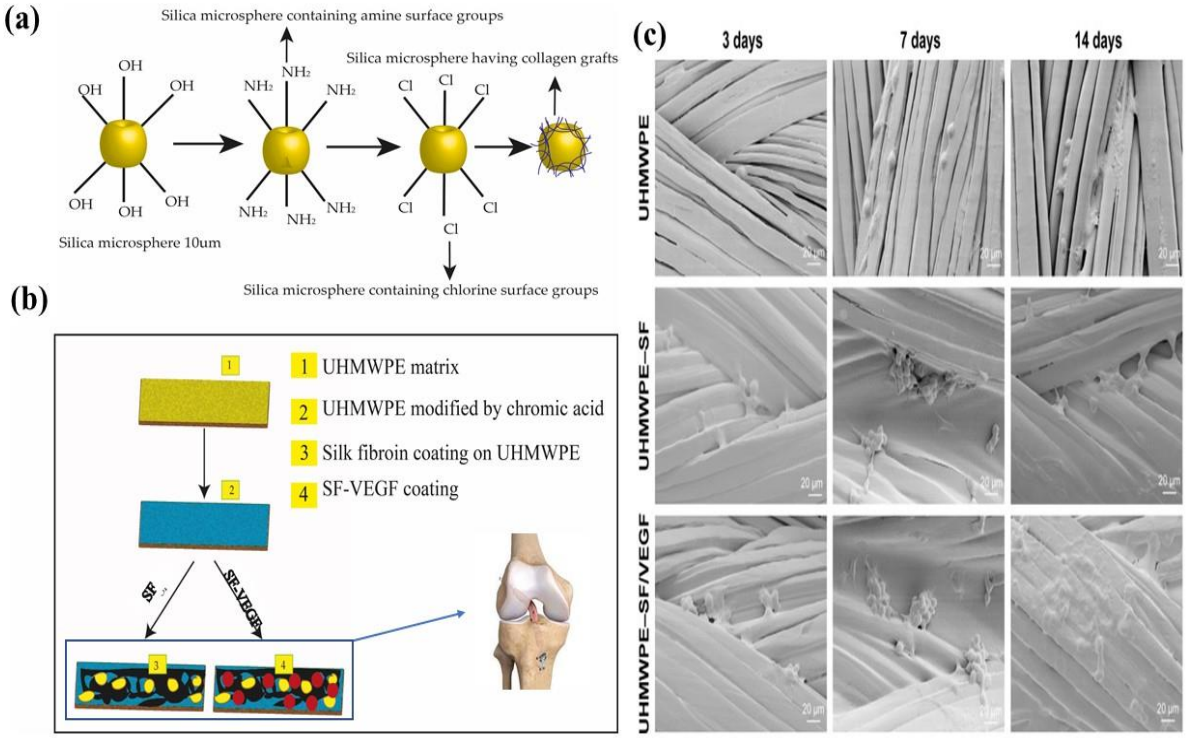

Figure 2. 13 (a) Bioactivity of bioglass;(b) Schematic preparation of SF/VEGF coating[42];(c) Morphology of different groups of UHMWPE[42].

Guidoin et al. [216] reported that a thick collagenous tissue partly penetrated the outer layers of the braided structure of UHMWPE prosthesis. This collagen penetration caused the expansion and separation of the multifilament yarns into individual fibres. However, while the knit fabric was encapsulated by thin collagenous tissue, there was no significant infiltration into the structure. Thus, a hollow braided structure was designed with a core of parallel poly(vinyl alcohol) (PVA) cord wrapped by a braided diamond structure of UHMWPE threads for better mechanical performance [173]. Bach et al. [40] have been invented a hydrogel fiber for ACL reconstruction, made from PVA hydrogel. Tensile strength was enhanced by incorporating UHMWPE fibres around the PVA cord.

Zhang et al. [175] reported that UHMWPE filament could be modified with Polycaprolactone for ligament and tendon regeneration[217]. Absorbable polycaprolactone PCL has attracted mainstream attention in recent years for the development of tendon/ligament repair materials due to its excellent performance attributes of degradation, high stability, non-toxicity, and bioresorbability [218]. Fibrous PCL has also been reported to be able to help cell growth [217].

Schmidt et al. reported that growth factors play an essential role in the stimulation of fibroblast division and ligament healing. Growth factors such as platelet-derived growth factor AA, platelet-derived growth factor-BB, basic fibroblast growth factor, insulin-like growth factor 1, and interleukin 1- alpha can enhance the proliferation of fibroblastic cells [219]. Growth factors can elicit specific biological responses such as proliferation, chemotaxis, matrix synthesis, and secretion of other growth factors, during wound healing.

Molloy et al. [220] investigated some of the recent research into the functions of five growth factors whose actions were better defined during tendon healing. Five growth factors are: Insulin-like growth factor I (IGF-I), Transforming growth factor β (TGF -β), Vascular endothelial growth factor (VEGF), Platelet-derived growth factor (PDGF), and Basic fibroblast growth factor (BFGF).

Table 2.15 A summary of the role of the seven growth factors during tendon and ligament healing.

Growth factor	The active site of growth factors	Role	Reference
PDGF AA	Proliferation, remodeling	Controls DNA and protein synthesis at the injured site, controls the expression of other growth factors.	[219]
PDGF BB	Proliferation, remodeling	Controls DNA and protein synthesis at the injured site, controls the expression of other growth factors.	[221]
IGF-1	Inflammation, proliferation	Supports the proliferation and migration of cells, triggers matrix production	[222]
TGFβ	Inflammation	Controls cell migration, proteinase expression, fibronectin-binding interaction, and stimulation of collagen production	[220]
VEGF	Proliferation, remodeling	Supports angiogenesis	[220]
bFGF	Proliferation, remodeling	Supports cellular migration, angiogenesis	[219]
IL1A	Proliferation induces pro-collagen type I and III synthesis.	Supports proliferation, and induction	[223]
BMP	Remodeling of impaired tissues	Supports angiogenesis	[224]
GDF	Proliferation	Supports in ligament/tendon formation	[224]
Elastin	Proliferation	Controls DNA and protein synthesis at the injured site	[225]
Heparin	Proliferation	Supports the release of growth factors	[226]
PRP (Platelet-rich plasma)		Increased cellular metabolic activity, reduced apoptotic rate, and stimulation of collagen production in the cells	[227]

Based on previous research studies, the biofunctionalization of UHMWPE was conducted by loading of VEGF (vascular endothelial growth factor) into UHMWPE followed by SF (Silk fibroin) coating for ACL reconstruction [42]. Firstly, UHMWPE fibres were treated with ethanol and chromic acid to remove impurities. Chromic acid introduced additional functional groups to the surface of the fibres and etched the amorphous regions of threads. Then the chromic acid-treated UHMWPE was immersed in either SF or VEGF/SF solution at 4° C for 12 hours. SF loading growth factor VEGF was used to achieve the sustained release and to improve the neovascularization. Fig 2.13(b) presented the whole procedure of the SF/VEGF coating and reconstruction model. Cell morphology of bone marrow mesenchymal stem cells (BMSCs) is shown in Fig: 13(c). Filopodia of BMSCs attached to the surface of bare UHMWPE were not visible until after 14 days of cultivation but it was noticed on the surface of UHMWPE–SF and the UHMWPE–SF/VEGF group after 7-day of culture [228].

2.5.3 Fixation of UHMWPE graft animal model for Ligament reconstruction

Several animal models of ACL reconstruction have been reported in different articles[229, 230]. According to these methods, an inhalation mask was used to administer 2 percent isoflurane in O_2 gas (1.5 liters/minute) to the animals. Procedures were carried out on a heating blanket in a sterile atmosphere. The animal was put in supine position on the surgical table. The selected knee section was sanitized before skin cuts were made. The Lateral parapatellar arthrotomy was utilized to uncover the knee joint of the animal. A notchplasty was performed to remove remnants of ligaments[231]. The bone tunnels were made using a 3.0 mm drill in the anatomic sites of the natural ACL in the femur and tibia. The UHMWPE grafts were threaded through the tunnels and knotted out of the femoral and tibial bone tunnels on both ends. The wound was

irrigated with sterile saline solution after the graft was permanently attached. Lastly, sutures were used to seal the capsular layers and skins [231].

2.6 Conclusion

While many polymers, metals, ceramics, and composite materials are in use as biomaterials, UHMWPE is one of the most important of the bioinert polymers used in the manufacture of medical implants. Problems associated with the use of UHMWPE as implants include wear debris and oxidative degradation due to the generation of free radicals when exposed to irradiation with gamma rays for grafting or sterilization.

To resolve the wear and to enhance the life of UHMWPE as implant, in recent years this field has witnessed numerous innovative methodologies such as biofunctionalization or high temperature melting of UHMWPE to enhance its toughness and strength. Sometimes one surface modification strategy is taken to solve a particular wear problem but may lead to a new problem and further strategies are required to eliminate that new problem. For example, occurrence of bioreactions of soft tissues are triggered by UHMWPE wear particles that can ultimately lead to aseptic loosening of hip implants. Therefore, high dose irradiation is used to highly cross-link UHMWPE which decreases the wear rate but initiates free radical formation that causes oxidative degradation in UHMWPE. To reduce or eliminate the free radical formation, annealing or post-irradiation technique is used. Despite this, there is a chance of increased incidence of rim fracture under impingement and adverse loading conditions due to the lowered fatigue strength of this material. Thus, an alternative method of vitamin E stabilization of UHMWPE is carried out to provide oxidation resistance without sacrificing the fatigue strength. Again, vitamin E has a capacity to act as a free radical scavenger during irradiation which can lower the crosslinking

efficiency of UHMWPE and limits the vitamin E concentration in the blend to less than 0.3 wt.%.

Surface modification can improve functional properties such as mechanical properties, resistance to wear, biocompatibility, cytocompatibility, wettability, and biomaterial surface properties. Chromic acid, and hydrogen peroxide can be used to reduce the smoothness of the surface and polydopamine can be used to add functional amine groups on the surface along with protein immobilization. Recently, much attention has been focused on plasma treatment for surface modification of UHMWPE. DBD plasma was introduced to modify the surface properties of material and then later PACVD, ECR, CAP, and PIII introduced a new era in surface modification compared to other surface functionalization methods. Plasma treatments can improve the hydrophilicity of materials, reduce the smoothness of the surface, and increase protein attachments through cross linking and covalent bonding.

It has been stated that different cellular functions such as adhesion, proliferation, and differentiation are influenced by surface energy, surface functionalization, and surface morphology. Among different plasma methods, plasma immersion ion implantation (PIII) is receiving attention due to the biofunctionalization of materials with complex shapes. In addition, it allows the use of protein immobilization. The surface functionalization of UHMWPE is quite straightforward, and surface treatments can be used to change only the surface properties without affecting the bulk properties of the material.

UV irradiation is the most common method used for cross linking of free radicals with the substrate. UV irradiation and grafting can modify the wear and mechanical properties of material. Adverse effect of oxidation can be improved by blending vitamin E with the substrate during the treatment.

UHMWPE is a unique material due to its high potential capacity for vascularization throughout the whole structure, which is considered a primary requirement of grafts and other biomedical prostheses. Ligament/tendon reconstruction is considered a promising research application area for UHMWPE. Owing to the extreme hydrophobicity of UHMWPE and its surface chemistry, which is very different from that of natural ligaments and tendons, modern ACL reconstructions do not enjoy the low friction and wear of the original ligaments. Chitosan-hyaluronic acid composite has been used for modification of UHMWPE graft. Bioglass and PCL coatings on UHMWPE show excellent results in fibroblastic cell adhesion assays and ligament regeneration. Several proteins and growth factors on the surface of UHMWPE showed significantly improved outcomes on ligament/tendon regeneration. The results described in the literature were related to the surface improvement of UHMWPE with protein adsorption making the surface bioactive for cell adhesion by displaying the signaling motifs of biological molecules. However, successful biofunctionalization depends on selection of the proper type and concentration of protein molecules to minimize inflammation, friction and wear related issues of UHMWPE implants. Surface functionalization of biomaterials for ligaments/tendons is needed to be further developed, with the potential for improved outcomes for patients.

2.7 Challenges & future perspectives

Many of these procedures have been proven successful in the laboratory by competent chemists, but that is not the case in manufacturing. The essential chemicals are potentially dangerous, costly, or currently unavailable in the large quantities required for manufacturing. The plasma treatment for polymer surface alteration has acquired an amazing consideration, attributable for its potential benefits in improvement of surface properties without influencing mass properties.

Yet, non-uniformity, instability, inhomogeneity, and transfer into hot plasma over long treatment periods remain challenges to some plasma treatment. The integration of the two or more modification methods revealed fascinating multi-functional characteristics, however due to the complex methodology and high cost, this strategy does not appear to be scalable.

Significant progress has been made in the field of functionalization of UHMWPE implants for ligament/tendon regeneration. Biological functionalization of orthopedic surfaces is a well-studied field with a lot of opportunities for advancement. The adaptation of current biomolecule immobilization techniques is the challenge for the next generation of research in this subject. Among different plasma treatments, plasma immersion ion implantation showed promising results due to its ability to enable the covalent binding of biomolecules to all the exposed surfaces of UHMWPE. A better understanding of surface chemistry of UHMWPE with proteins needed for more innovative biomolecule selection and design, resulting in more effective multifunctional interfaces. If this is achieved, it will be a major step forwards in the development of this fiber for a variety of high-performance applications.

Chapter 3 : Surface characterization of the PIII modified UHMWPE fabric

3.1 Introduction

There have been studies employing plasma treatments to modify the surfaces of UHMWPE fabric, but nothing is known about the specific surface properties of UHMWPE fabric after being modified by a nitrogen plasma based PIII treatment. UHMWPE fibers have a low surface energy and a hydrocarbon linear molecular structure without polar molecules groups on the surface. As a result, these fibers have a high chemical inertness, resulting in very weak interfacial adhesion between the fiber reinforcement and the matrix material, severely limiting their use in composite materials. As a result, it's especially critical to alter the surface properties of UHMWPE fibers[76].

Surface changes can be implemented in a variety of ways, including mechanical machining, chemical treatments, and physical treatments. Plasma-surface modification techniques including as plasma spray, oxygen plasma, and plasma immersion ion implantation have already been widely used in the semiconductor and biomedical industries and have proven to be cost-effective. The ability to selectively enhance surface attributes (to a depth of a few hundred nanometers) while bulk contributions remain unaffected is plasma modification's distinct advantage over other approaches [20–23]. Because it combines the advantages of traditional plasma and ion beam technologies, PIII is a versatile approach that can perform several processes, such as simultaneous and successive implantation, deposition, and etching, among the many plasma-based techniques.

Another significant benefit of plasma immersion ion & deposition (PIII&D) is the ability to modify the surface properties of a variety of biomaterials, such as metals, ceramics, and polymers, by introducing a variety of different elements and functional groups into materials with complicated geometries [24,25].

S. Puertas et al. have been reported that carboxyl group of polymers can be activated by carbodiimide chemistry[142]. N-hydroxysuccinimide (NHS) or sulfo-NHS is also used to increase the coupling efficiency of material[122]. Salinization and plasma functionalization have been used for pretreatment of surfaces for the generation of reactive sites for covalent coupling on polymer surface [232, 233].

UHMWPE, PIII, shows dynamic characteristics defined by gradual oxidation of the surface and a decreasing concentration of radicals when treated under the same conditions used in this investigation. The dynamic surface properties, resulting in a stable hydrophilic surface. PIII treated UHMWPE has been associated with better cell contacts because to its increased surface hydrophilicity, changed chemical structure, and radical content. Generally, earlier studies of PIII treated UHMWPE with nitrogen plasma showed increased hydrophilicity, wear resistance[234, 235], and cell contact qualities in general, but they didn't look into surface functionalization for UHMWPE fabrics and it's specific applications. It is required to provide a certain level of knowledge about the surface properties after receiving the nitrogen based PIII treatment before starting the experiments on the surfaces in terms of immobilization capabilities and cell responses. Understanding the composition of a medical device material and its potential for an undesirable biological effect when the device is implanted is based on materials characterization[236].

As a result, the primary goal of this chapter is to build a basic understanding of the topography, wettability, free radicals, and surface energy levels of nitrogen based PIII-treated UHMWPE fabric surfaces, as well as to identify any functional groups present on the surface. The characterization will be conducted by scanning electron microscopy (SEM), contact angle measurements, XPS, ESR study along with a variety of PIII treatment parameters. It's intended

that the knowledge gathered here will help us understand and explain any observations we make later. Because the focus of this study is on biological applications, variables emerging from the PIII treatment will be minimized and standardized to avoid inconsistencies in the biological experimental data.

Due to the high price and limited number of suppliers, finding a dependable and well characterized source of UHMWPE fabric proved to be a difficult endeavor.

3.2 Grades of UHMWPE fabric

Two different grades of UHMWPE fabric have been chosen here due to the following reasons: rationale for including two sources of UHMWPE fabric.

1. To validate lower price industrial grade material for establishing experimental conditions for cost saving reasons
2. To provide extra confidence in results by comparing findings from fabrics sourced from two different suppliers.
3. To gain information as to possible predictors of fabric performance

The first stage of the project included testing two types of UHMWPE fabric samples,

(i) UHMWPE fabric (DSM Dyneema SK78, Dimension-Polyant, Kempen, Germany)- Industrial grade, UHMWPE was in the form of 0.75mm thickness woven fabric.

(ii) UHMWPE fabric (Spectra 1000, Goodfellow Cambridge Ltd. Catalogue no: ET303510). Scientific grade, UHMWPE was in the form of 0.45mm thickness woven fabric. A yarn of ultra-high strength and composed of 118 filaments each of diameter 0.038mm.

(iii) Industrial grade-Price $25 per square m.

(iv) Scientific grade- Price $ 125 per square m.

The huge price difference between the different grades of UHMWPE fabric was assumed to be the result of the extensive quality control, material characterization and

documentation procedures required. (3.1 Initial experiments were conducted on both types of UHMWPE fabric.

Due to the cell culture facilities, the UHMWPE samples were cut into small rectangular sheets that were easy to handle and that allowed experiments to be conducted in the wells of tissue culture plates.

Table 3.1 Physical properties of two grades of UHMWPE fabric

UHMWPE fiber type	Color	Density	Filament diameter	Filament linear density
Dyneema SK-78	Opaque/white	0.97-0.98 g/cc	12-21 μm	1-3 dpf
SPECTRA fiber 1000	Opaque/white	0.97 g/cc	0.023 μm	1-7 dpf

3.3 Aim & hypothesis of the chapter

Overall, the aim & hypothesis of studies described in this chapter can be described as follows:

1. To gain a fundamental knowledge of the physical and chemical properties of two different grades of UHMWPE fabric surfaces after they have been treated with the nitrogen based PIII procedure.
2. Characterize the surface properties of two different grades of UHMWPE fabric.

It's also assumed that the knowledge gained in this chapter will help us better understand the properties of plasma-treated polymers in general, as well as develop theories about the underlying mechanism for covalent binding, resulting in the development of new applications for this new plasma treatment technology.

This chapter's hypothesis is that two distinct grades of UHMWPE fabric can have their surface qualities changed by plasma immersion ions (PIII). Surface quality can be enhanced by PIII treatment over untreated material.

3.4 Experimental methods

3.4.1 PIII treatment

PIII was created at the end of the 1980s [115] to solve the limitations of traditional ion implantation[237], such as the complexity of ion beam scanning, low beam current, non-uniform ion implantation profile, and the necessity for a mask to avoid excessive sputtering. The implanted target is placed directly in plasma and then pulse biased to a high negative potential in PIII. Without the requirement for target manipulation, a plasma sheath is generated around the target (Fig 3.1), and ions from the plasma are accelerated by the electric field in the sheath to bombard the entire surface of the target.

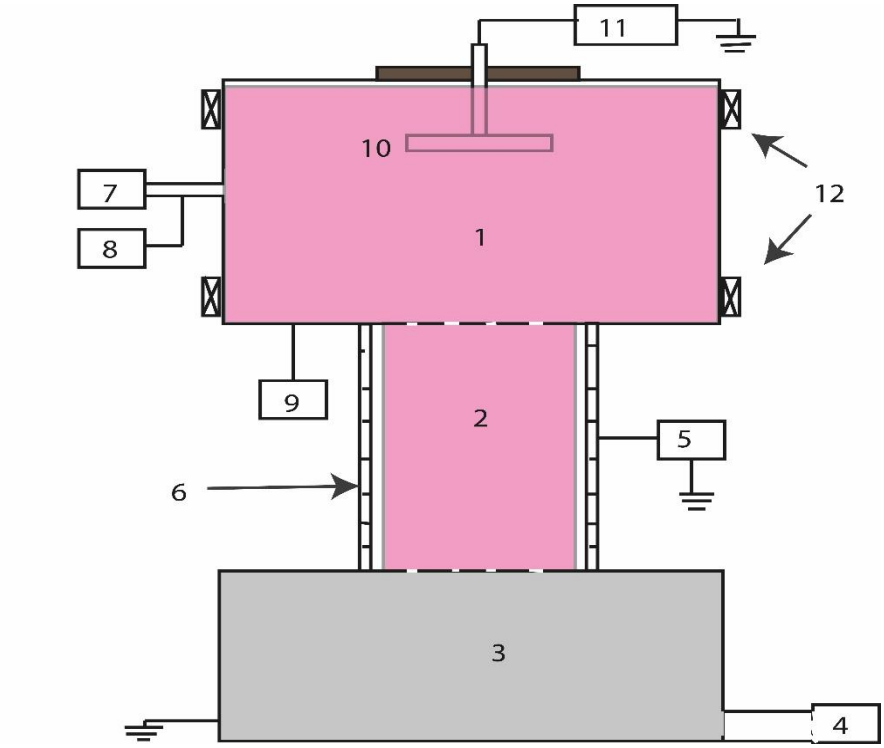

Figure 3. 1 Schematic of the treatment setup in the PIII plasma chamber. Plasma immersion ion implantation system is shown in a schematic diagram. (1). aluminium chamber; (2). Glass tube; (3). stainless steel; (4). vacuum pump; (5). RF generator; (6). inductively c coupled antenna; (7). Gas source; (8&9). Pressure sensors; (10). Sample holder; (11& 12). Magnetic coils.

Plasma immersion ion implantation was conducted in a specially manufactured plasma chamber, as shown in the schematic Fig (3.1). The ion implantation technology utilized in this work was designed at the University of Sydney's School of Physics.

An aluminum chamber 1, a glass tube 2, and a stainless-steel chamber 3 make up the system. A vacuum pump 4 is linked to the stainless-steel chamber. Plasma is created by utilizing an RF generator to apply radio frequency (RF) power (13.75 MHz, 100 W) to an inductively coupled antenna 6 wound around the glass tube 5. Impedance matching the RF generator to the plasma discharge provides stable plasma power with optimal power transfer into the plasma. A gas source 7 is linked to the aluminum chamber 1. 10^{-4} Torr is the starting pressure. Pressure sensors 8 and 9 at the gas inlet and chamber 1, respectively, monitor the pressure. In these tests, the operating chamber pressure was $2x10^{-3}$ Torr. Setting the optimum flow rate with a gas flow controller ensures a consistent pressure of the working gas in the chamber.

The treated sample is put on a sample holder 10 that is coupled to a high voltage pulse generator 11. A stainless-steel mesh was positioned at 5 cm from the sample surface and electrically attached to the sample holder to cover the sample. The introduction of a mesh decreases the charging of the polymer sample and eliminates arcing [7, 8]. To provide uniform PIII treatment, the mesh geometry and the distance between the mesh and the sample were tuned [8]. The plasma sheath forms around the mesh when it covers the sample, and the ions are propelled towards the mesh and subsequently pass through it to implant into the sample. To avoid sample warming, the pulse was 20 seconds long. The pulse rate was 50 hertz. Two magnetic coils 12 create a magnetic field inside the aluminum chamber 1 to increase plasma density.

The plasma source was a 13.56 MHz inductively coupled radiofrequency plasma. When matched, the plasma power was 100 Watts with a reverse power of 12 Watts. A Langmuir probe

from Hiden Analytical Ltd was used to detect plasma density during treatment. During implantation, the basal pressure was 106 Torr (104 Pa), and nitrogen gas was employed at a pressure of $2x10^3$ Torr ($4.4x10^2$ Pa). The application of high voltage (20 kV) bias pulses of 20 seconds length to the sample holder at a frequency of 50 Hz was used to accelerate ions from the plasma.

The samples were put on a stainless-steel holder with a diameter of 150 mm, a stainless-steel mesh covering it, and an electrical connection 45 mm above the sample surface shown in Fig 3.2. The numbers of high voltage pulses was multiplied by the fluence corresponding to one pulse to obtain the ion fluence. For the wide sample container with mesh, the fluence rate was determined to be 10^{13} ions/cm^2 per second of PIII treatment duration. The samples were exposed to implantation ion fluences of (4–16) 10^{14} ions/cm^2 for 400, and 800 seconds, respectively.

Parameters for PIII treatment:

- Radiofrequency: 13.56 MHz
- Plasma power: 100 watts
- Reverse power: 12 watts
- Base pressure: 10^{-6}
- Gas pressure of nitrogen: $2x\ 10^{-3}$ Torr ($4.4x\ 10^{-2}$ Pa)
- Voltage: 20kV
- Pulse bias: 20 us

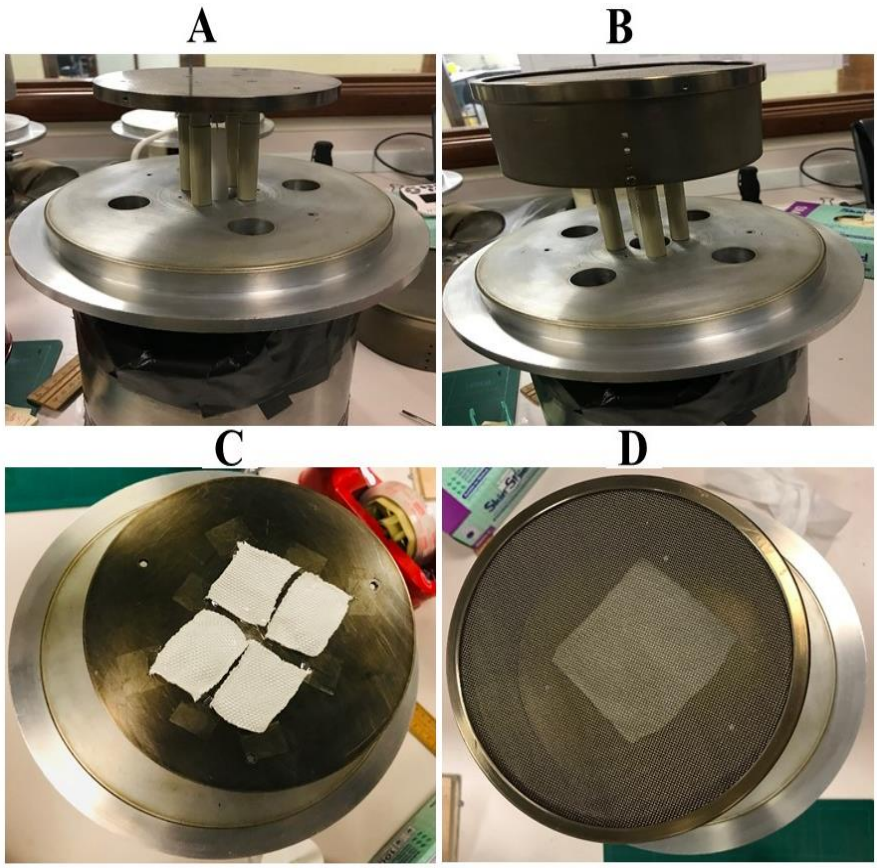

Figure 3. 2 (A) photo of the sample holder 150mm in diameter; (B) stainless steel metal mesh attached 45mm of the sample stage;(C) UHMWPE fabric on the sample stage: (D) UHMWPE sample secured with top mesh screen.

3.4.2 Contact angle & surface energy.

The surface energy of a material can be determined by wetting it with liquids which have well-known surface tensions. The measurement can be obtained by the sessile drop method, through the contact angle of a pure liquid droplet on the solid substrate. In this method, a syringe filled with liquid pointed vertically down onto the sample surface deposits the liquid droplet. Several different types of liquids have been used for this method and is referred d to as probe liquid. For each experiment, at least two liquids with known surface tension and its polar and dispersive components are required. This is a straightforward method. To determine the heterogeneity of

the sample, multiple droplets can be deposited in various locations on the sample. Fig 3.3 shows the Kruss DS10 contact angle measuring machine and experiment on UHMWPE fabric (Fig 3.3 A & B)

Surface energy of a polymer can be determined by measuring the contact angle of the sample with several test liquids and evaluated according to Owen-Wendt method.

The Owens-Wendt-Rabel-Kaelble Method: the authors[204] divide the data in this method. Surface tension is divided into two parts: dispersion and polar portions. The contact angles on the sample's surface are measured using two probing liquids (diiodo methane and formamide) with known dispersion and polar fractions. Test liquids are:

1. Liquid 1: Water
2. Liquid 2: Diiodomethane
3. Liquid 3: Glycerol
4. Liquid 4: Formamide

Liquid 2 and liquid 4 were used in this experiment. To estimate the changes of UHMWPE fabric surfaces after the PIII treatment and subsequent ageing in air. Kruss DS10 contact angle measuring equipment was used with two different fluids: The liquids were dropped on UHMWPE fabric surfaces. This process was repeated several times across the surface of the sample to get a proper contact angle.

The surface tension is then computed by combining the Owens and Wendt equation with Young's equation:

$$\gamma_{SL} = \gamma_S + \gamma_L - 2\left(\sqrt{\gamma_S^D \cdot \gamma_L^D} + \sqrt{\gamma_S^P \cdot \gamma_L^P}\right)$$

$$\gamma_S = \gamma_{SL} + \gamma_L \cdot \cos\theta$$

Where: θ is the contact angle of the liquid on the solid surface; γ, γD and γP are surface tension, disperse and polar fractions respectively; The subscripts S, L and SL denote the solid-air, liquid-air, and solid-liquid interfaces respectively.

Untreated UHMWPE fabric, for instance, have a very low polar portion of the surface energy compared to PIII treated UHMWPE fabric.

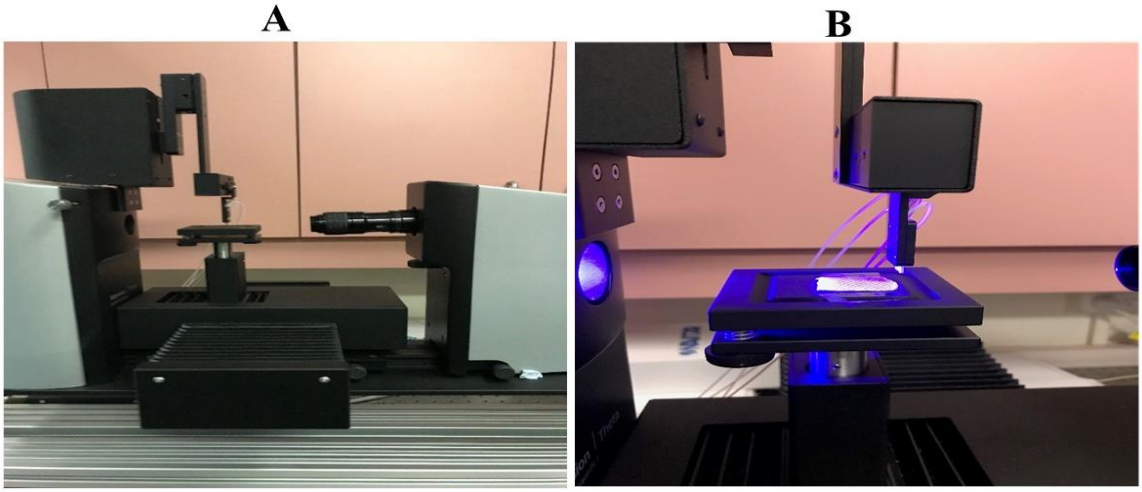

Figure 3. 3 (A) The Kruss DS10 contact angle measuring machine;(B) Experiment on UHMWPE fabric.

3.4.3 X- ray photoelectron spectroscopy (XPS) study

One of the most common methods for analyzing surfaces is X-ray photoelectron spectroscopy. XPS is a surface sensitive quantitative technique used to detect the elements that present within a material or on its surface. It can also identify their chemical state, overall electronic structure and density of the electronic states in the material[238].

Surface analysis is used to figure out the surface chemistry of a material and investigate the adequacy of a material. X-ray photoelectron spectroscopy (XPS) was performed to examine the surface chemistry of the PIII/PI[3] treated UHMWPE fabric with FlexMode SPECS

spectrophotometer. The spectrophotometer was equipped with monochromatic A1 K alpha radiation source, a hemispherical analyser, and an MCD9 electron detector. Sample charging was alleviated by an argon gun source[239]. A K X-ray beam was created using (Mode XP-50 High Performance Twin Anode with Focus 500 Ellipsoidal Crystal Monochromator and PHOIBOS 150 MCD-9 analyzer).

XPS spectra are produced by irradiating a solid surface with an X-ray beam when measuring the kinetic energy of electrons released from the top 1-10 nm of the material being studied[240]. The number of expelled electrons and their kinetic energy are measured. Counting expelled electrons over a variety of electron kinetic energies produces a photoelectron spectrum. Peaks in the spectrum are caused by atoms releasing electrons with a specific energy. Fig 3.4 demonstrates the photo emission process of XPS analysis.

3.4.3.1 Mechanism of XPS

During the process, an electron may be expelled when an atom or molecule receives an X-ray photon. The electron's kinetic energy (KE) is determined by the photon energy (hv) and the electron's binding energy (BE)[239].

It is possible to calculate which elements are near a material's surface, their chemical states, and the binding energy of the electron by calculating the kinetic energy of the released electrons. The binding energy is determined by a variety of factors, including the ones mentioned below:

- The portion that the electron is expelled from.
- The orbital that the electron is ejected from.
- The chemistry of the atmosphere

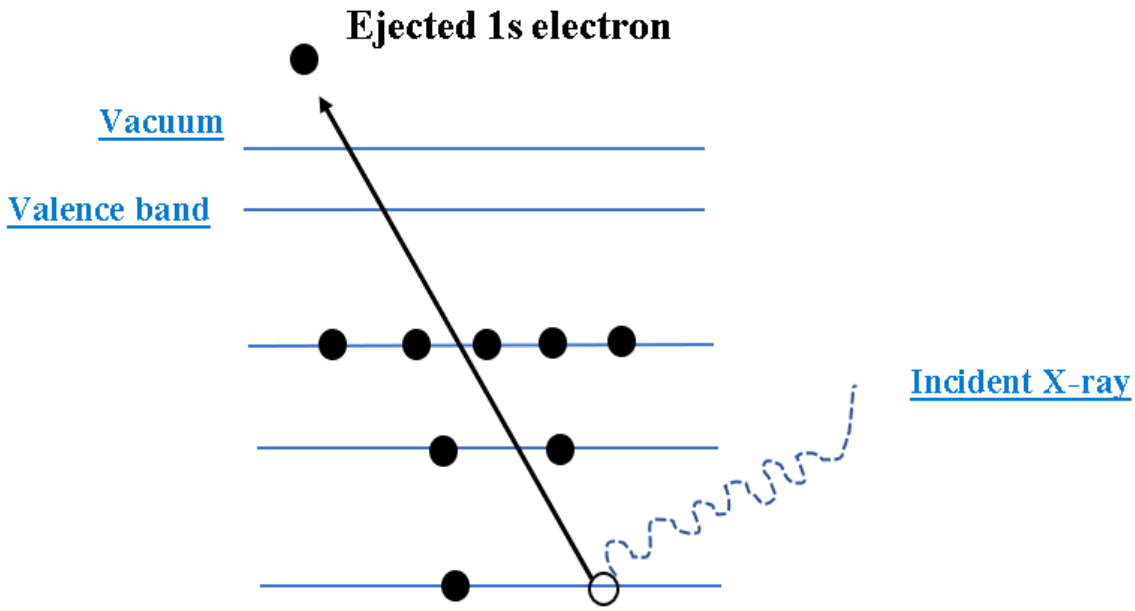

Figure 3. 4 Photoemission process for XPS surface analysis.

3.4.4 Electron spin resonance (ESR) study

The foundation of ESR spectroscopy is the microwave radiation that an unpaired electron absorbs when subjected to a high magnetic field. Magnetic resonance absorption is a term used to describe this excitation. The spectroscopic method of electron spin resonance (ESR), also known as electron paramagnetic resonance (EPR), is restricted to the investigation of elements with one or more unpaired electrons. The most significant paramagnetic systems, or those with one or more unpaired electrons, include free radicals, transition metal ions, and ions and molecules with an odd number of electrons.

Electron spin resonance (ESR) spectroscopy was conducted for studying unpaired electrons on materials surface. ESR spectra were acquired at room temperature using a spectrometer Spin Scan X (ADANI) operating in the X band with a microwave frequency of (9.2-9.55) GHz and a central magnetic field of 336 mT. The UHMWPE fabrics (before and after the PIII treatment)

were cut into strips of (5mmx 40mm x 0.9mm) and attached to an ESR tube for the measurement. They were placed in the equipment cavity and scanned 5 times with a microwave power of (0.946 mW) and a sweep width of 15 mT. The spectra were double integrated to obtain the peak areas which correlate to the number of unpaired electrons in the samples. Table 3.2 represents the parameters of ADANI spectrometer SPINSCAN. Simple balanced bridge ESR spectrometer block diagram is shown in Fig 3.5.

Table 3.2 Parameters of ADANI spectrometer spin scan

Operating frequency	9.2 — 9.55 GHz
Microwave cavity power	250 mW
Sensitivity	8 x 10^9 spin/0,1mT
Cavity	TE_{102}
Q unloaded	5000
Magnetic field modulation	Magnetic field modulation
Magnetic field	0,01 to 0,65 T
Magnetic field homogeneity	± 5 µT over sample volume in active region TE_{102}
Power	400 W, 115/230 VAC
Dimension /weight	47 x 38 x 26 cm / 45 kg

A X-band ESR spectrometer's fundamental parts are as follows:

(i) An electromagnet that can produce a uniform magnetic field that can be linearly changed on both sides of the magnetic field.
(ii) Source of microwave radiation at 9.5 GHz in frequency.
(iii) An appropriate sample cavity.
(iv) Arrangements to allow the radiation energy to enter the sample cavity.
(v) A system for detecting changes in microwave power.
(vi) An appropriate oscilloscope or recorder.

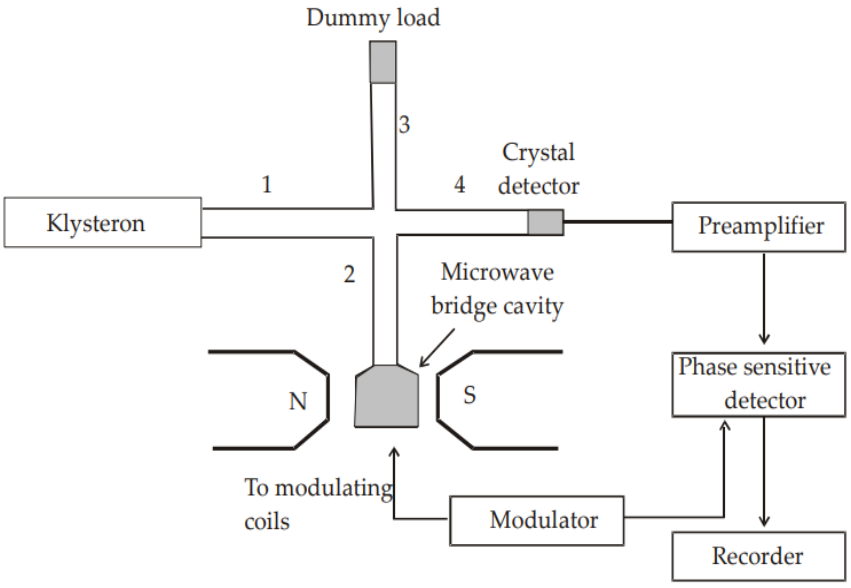

Figure 3. 5 Simple balanced bridge ESR spectrometer block diagram.

3.4.4.1 Mechanism of ESR

ESR spectroscopy is based upon the absorption of microwave radiation by an unpaired electron when it is exposed to a strong magnetic field. Atoms or molecules will split into different amounts of electronic energy and this excitation is known as magnetic resonance absorption[241]. A static/magnetic field and microwave are utilized in an ESR apparatus to investigate the behavior of unpaired electrons in the material under study. In theory, ESR detects paramagnetic centers (such as radicals) which may or may not be caused by radiation. An applied microwave energy is absorbed in resonance when a strong external magnetic field produces a difference between the energy levels of the electron spins, ms = +1/2 and ms = -1/2 presented in Fig 3.6 below. The absorption of microwave radiation by unpaired electrons in a magnetic field as well as the energy levels of the electrons are observed and measured using ESR[242].

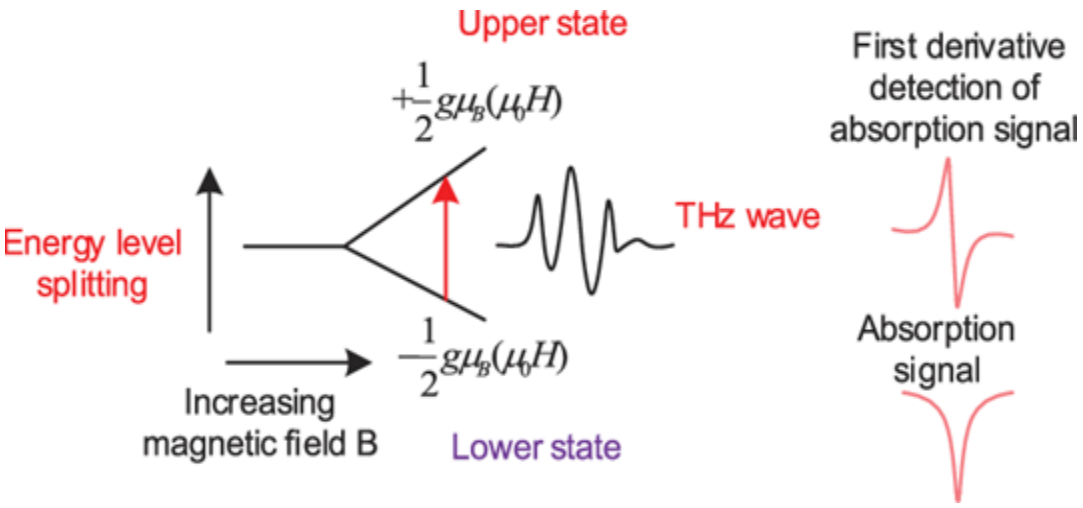

Figure 3. 6 A discrepancy between the energy levels of the electron spins, ms = +1/2 and ms = -1/2, is produced by a strong external magnetic field.

3.5 Data Presentation and Statistical Analysis

All figures and statistical analyses relevant to the results in this chapter were analyzed and evaluated using Microsoft Excel (version 2013), and ORIGINPRO 2020. For group comparisons, two tailed t-tests with a P value of 0.05 indicating significance were used.

3.6 Experimental results

3.6.1 Physical appearance of industrial grade UHMWPE fabric

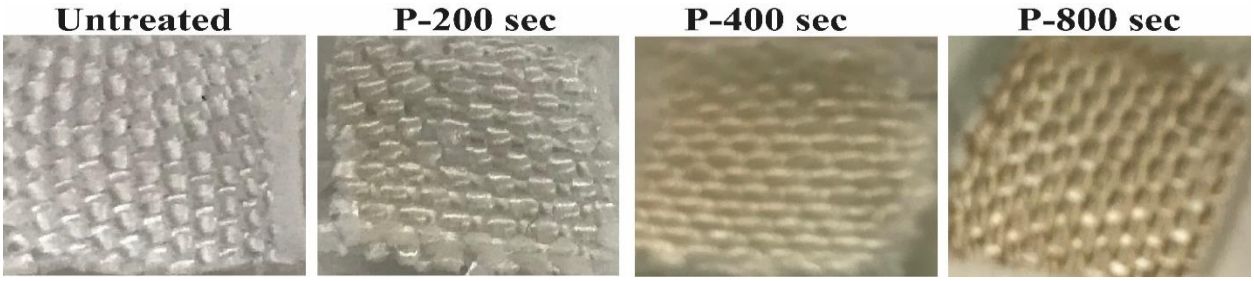

Figure 3. 7 Physical appearance of untreated and PIII treated industrial grade UHMWPE fabric.

The above figure shows the appearance of UHMWPE fabric before and after the plasma treatment. The surface of UHMWPE fabric is rough and glossy. The untreated UHMWPE fabric was white in color and after different treatment time, this color deepened and appears more intense. These results proved the dehydrogenation and creation of highly cross-linked sp^2 amorphous carbon structures on industrial grade UHMWPE fabric.

3.6.2 Contact angle and surface energy of industrial grade UHMWPE fabric

The contact angle of untreated as well as PIII treated industrial grade UHMWPE fabric with various PIII treatment periods is summarized in the following Fig 3.8. All surfaces became noticeably more hydrophilic after being treated with PIII treatment. The decrease in contact angle is proportionate to the decrease in temperature, according to a small trend. After treatment, the end contact angle ranged from 66.27° to 49.53° for the 800s treated sample at 1.8 sec. Fig 3.8 illustrated the change of liquid (formamide) contact angles on untreated and PIII treated UHMWPE with time. As shown in Fig 3.8, at each time point, formamide droplet contacted the PIII treated fabric with a lower angle (approximately 20^o) than the untreated fabric during the recording period.

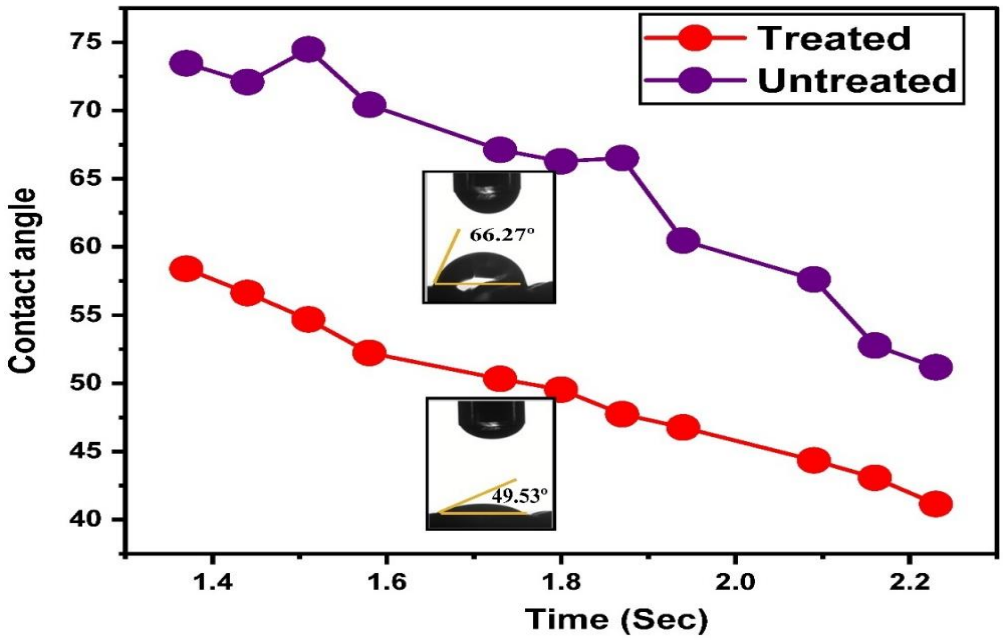

Figure 3. 8 Values of contact angles in relation to PIII treatment times. The measurements were taken as soon as the PIII therapy was completed. The untreated and PIII treated surface is represented by two data point.

Total surface energy is a measure of all the forces that entice molecules to come together. Even though it is a minor and undulating component, dispersive surface energy is included in the total. The component of surface energy that occurs from the dispersion of electron clouds in molecules on the material's surface is known as dispersive surface energy.

Molecules can contain structures that result in permanent dipoles, which means that, in addition to electrons being randomly dispersed throughout the molecule, there are portions that are always more positive or negative than others. Due to their structure, some molecules have permanently charged areas, either positively or negatively. They are more attracted to each other than the dispersive interactions. Polar surface energy is a component of surface energy that arises because of the attraction between molecules whose areas are permanently charged positively or negatively. Some molecules have areas that are permanently charged by their structure, either po sitively or negatively.

Surface energy and polar-dispersive components of untreated and PIII treated UHMWPE fabric is presented in Table 3.1. The surface energy of the UHMWPE increased from 47.33 mN/m to 58.87 mN/m after the PIII treatment in which the majority increases come from polar component which is shown in Fig 3.9 (A), (B) & Table 3.3.

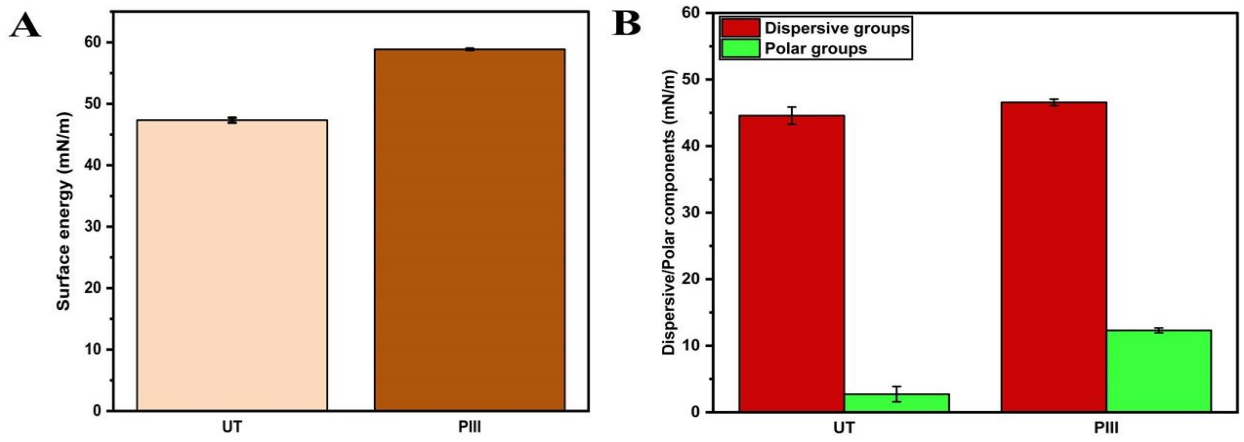

Figure 3. 9 (A) Surface energy of untreated and PIII treated industrial grade UHMWPE fabric; (B) Dispersive and polar groups of untreated and treated UHMWPE fabric. Error bars here indicate standard deviations of quadruplicates and an asterisk (*) indicates a significant difference ($P<0.05$) between the untreated and PIII treated groups. There were no differences detected in between the two treated groups.

Table 3.3 Surface energies and their dispersive and polar contributions evaluated according to Owen-Wendt method.

Material	**Surface energy (mN /m)**	**Dispersive (mN /m)**	**Polar (mN /m)**
Untreated	47.33	44.58	2.73
PIII treated.	58.87	46.57	12.30

3.6.3 Surface chemistry of industrial grade UHMWPE fabric

XPS with a sensitivity depth of 8-10 nm [243, 244] was used to measure the elemental composition of surfaces before and after PIII treatment. After the PIII treatment, nitrogen content

significantly increased due to the nitrogen implantation onto the surface of the material. Oxygen slightly increases due to the reaction of radicals with oxygen in the air after the treatment.

The chemical structure of both treated and untreated industrial grade UHMWPE fabric was also determined by means of XPS. A survey scan spectrum was obtained to identify the chemical species present from each sample, followed by a high-resolution scan spectrum of the peaks associated with each species. As shown in Fig 3.10, carbon, oxygen, and nitrogen are the main elements present on the surface of the untreated sample. A high-resolution spectrum of the C1s signal was collected to pinpoint the chemical bond at the surface.

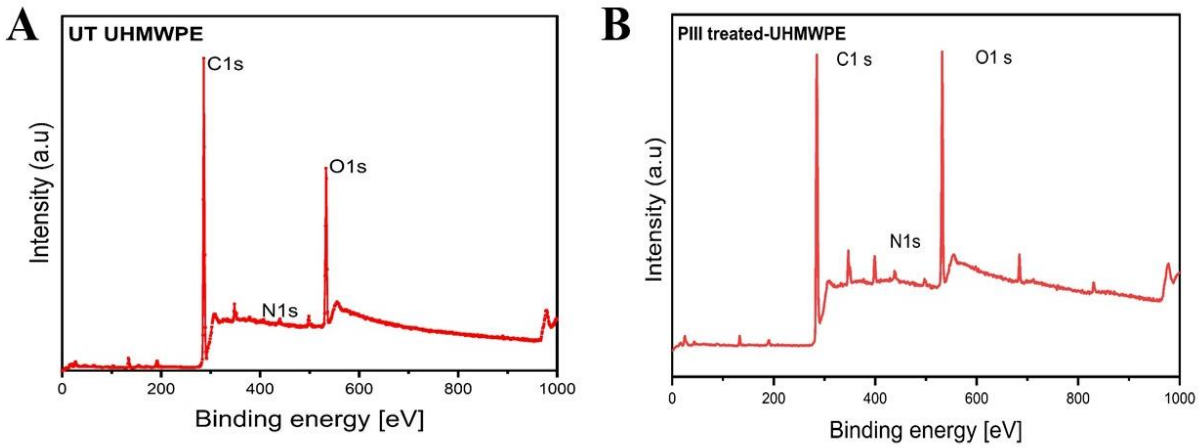

Figure 3. 10 (A) Whole spectra of Untreated UHMWPE fabric; (B) Whole XPS spectra of PIII treated UHMWPE.

Fig 3.10 illustrates the XPS carbon high resolution spectrum. It shows the XPS carbon high resolution spectra for C–C/C–H, C–O/C–N, and C O/N–C O components with relative fractions of 284.6, 286.5, and 287.5 eV, respectively. The peak centered at 284.0 eV indicates that C - C and C - H bonding are the predominant states of carbon. The asymmetric peaks in nitrogen spectra indicate the presence of new chemical components on the surface. Several new peaks have formed that overlap with the main C1s. The functional groups C – O, C = O, and O – C – O

36,37, as well as a C – N peak in nitrogen-treated samples, can be attributed to them. Plasma polymerized films are exposed to ambient oxygen, they oxidize, resulting in the presence of oxygen. Percentage of Carbon decreased as carbon is the backbone of the material, it covered by Plasma treatment. This demonstrates that after exposure to the plasma treatment and then to an oxygen-containing environment, oxygen functional groups are integrated into the surface.

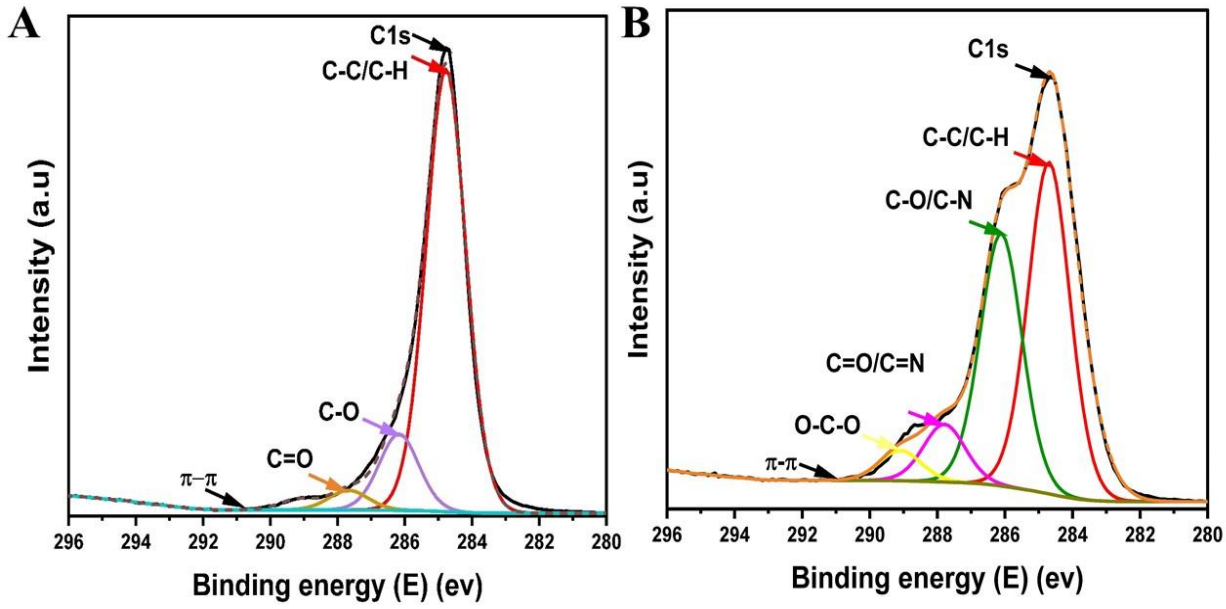

Figure 3. 11 (A) Peak fitted XPS C1s high resolution spectra obtained for UT UHMWPE; (B) Peak fitted XPS C1s high resolution spectra obtained for PIII treated UHMWPE.

Fig 3.11 shows peak fitted C1s high resolution spectra of Untreated (UT) and PIII treated industrial grade UHMWPE fabric. UT UHMWPE contains 82.95% of C-C/C-H, 12.38 % of C-O/C-N & 2.63 % C=O/N=C (Table 3.4). On the other hand, XPS spectra of PIII treated UHMWPE is composed of C-C/C-H, C-O/C-N & C=O/N=C bonds at a concentration of 57.60%, 23.80%, and 7.84%. Additional π-π satellite increased in PIII treated UHMWPE from 2.04 % to 6.51%. Presence of oxygen and nitrogen containing substance increased due to the

introduction of nitrogen from the injected gas that polymerized onto the surface of the material. Table 3.4 illustrated the comparison of deconvoluted peaks of C1s of untreated and PIII treated UHMWPE fabric.

Table 3.4 Atomic composition of industrial grade untreated and PIII treated industrial grade UHMWPE fabric from XPS analysis.

Functional groups	Atomic percentage (%)	
	UT	PIII
C–C/C–H	82.95%	57.60%
C–O/C–N	12.38%	23.80%
C= O/N=C	2.63%	7.84%
π-π satelite	2. 04%	6.51%
-COO-	Nil	4.24%

3.6.4 Radicals detection on UHMWPE fabric after the PIII treatment

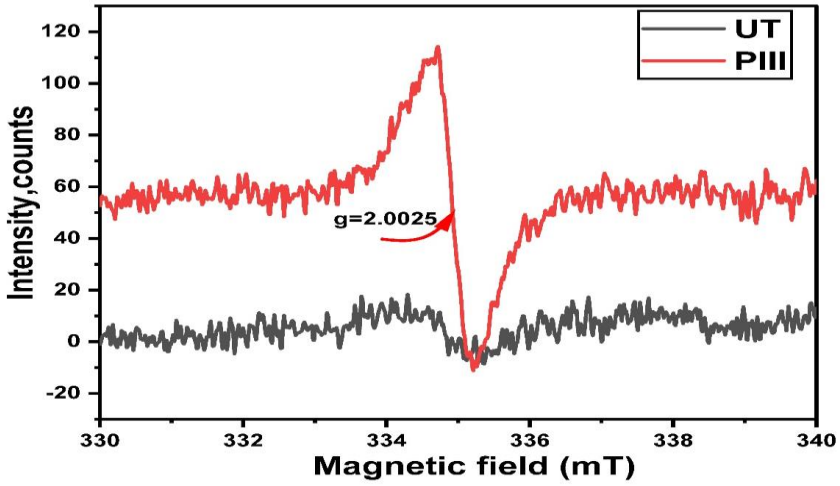

Figure 3. 12 ESR spectra of untreated and PIII treated industrial grade UHMWPE fabric.

PIII treatment induced radicals forming on the surface of UHMWPE from nitrogen bombardment as detected by ESR spectroscopy (Fig 3.12). A comprehensive knowledge of the relationship of free radicals with surface-contacting protein molecules is essential to provide the

precision required to build implant surfaces covered in patient suitable proteins. Fig 3.12 compares the derivative ESR signals measured on PIII treated UHMWPE and untreated UHMWPE with the differences in g-factor values and peak intensity. The untreated UHMWPE didn't show any free radicals while PIII treated UHMWPE has free radicals with g-factor of 2.0025. The shift of g-factor and the broader peak suggest that the PIII treatment produces a type of free radicals on UHMWPE surfaces with much higher number of radicals.

3.6.5 Physical appearance of scientific grade UHMWPE fabric

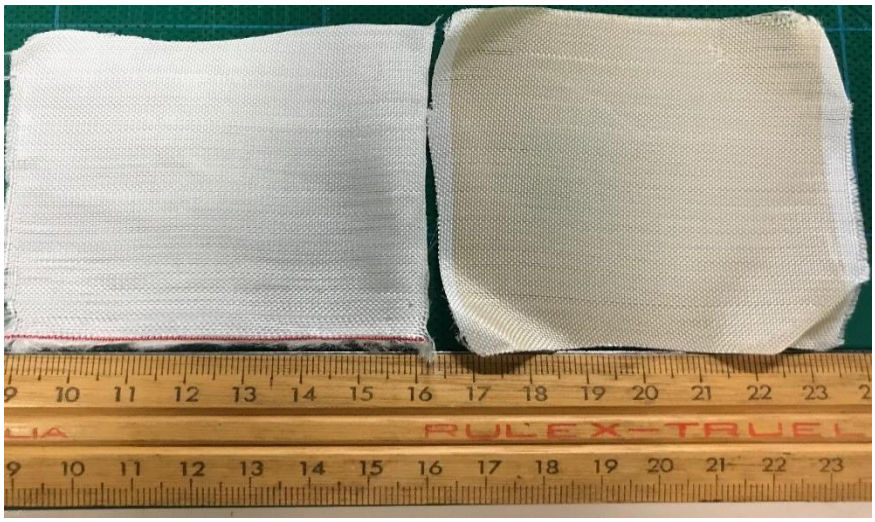

Figure 3. 13 Left side image showing untreated fabric and right-side image showing PIII treated scientific grade UHMWPE fabric.

We activated the UHMWWPE constructs using the PIII treatment and evaluated the changes in their physical and chemical properties. The color of the UHMWPE transformed from white to light brown after the PIII treatment treatment as shown in Fig 3.13. It shows the appearance of UHMWPE fabric before and after the plasma treatment. The surface of UHMWPE fabric is smooth and glossy. It could be observed that the PIII treatments developed a darkened appearance in the UHMWPE fabric which is identical to the previous results shown in Fig 3.7. The untreated UHMWPE fabric was white in color and after 400 seconds of PIII treatment this

color deepened and appears more intense. Due to the masking effect of the sticky tape used for this sample fixation, white edges on the top and bottom ends of the samples could be noticed after the 400 seconds plasma treatment.

The level of darkening increases by increasing the treatment time which is shown in Fig 3.14. This darkening is due to dehydrogenation and creation of highly cross-linked sp^2 amorphous carbon structures as it has been previously observed for polycarbonate and low density polyethylene [245, 246] . The color dispersion was consistent across the surface, showing that the ion bombardment occured evenly on the sample surface.

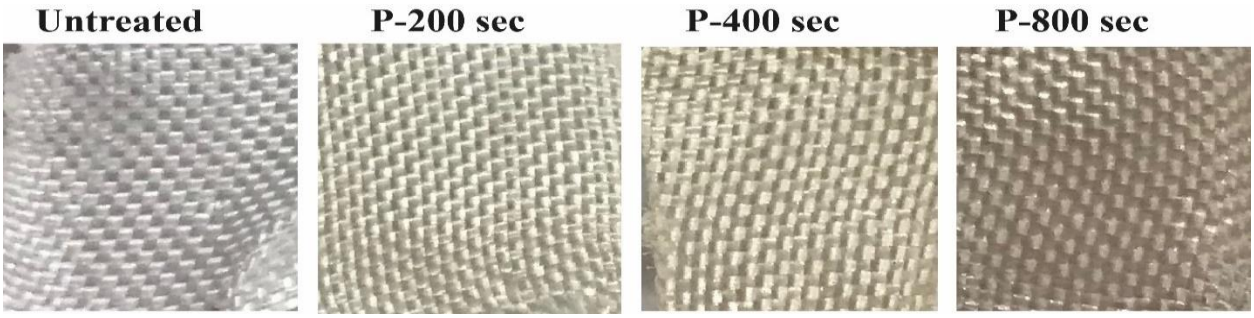

Figure 3. 14 Physical appearance of Untreated and plasma treated (different treatment times) scientific grade UHMWPE fabric.

3.6.6 Contact angle and surface energy of scientific grade UHMWPE fabric

Fig 3.15 shows shadow images of liquid droplets when placed on untreated & PIII treated scientific grade UHMWPE fabric. From the figure, it can be observed that the contact angle of untreated fabric is much higher than the treated fabric. The contact angle of the untreated UHMWPE fabric samples was 45.53° suggesting that the untreated UHMWPE fabric has a mildly hydrophobic surface. However, water droplet on PIII treated UHMWPE fabric was much more flattened out, water contact angle was around 23.06°, indicating surface wettability.

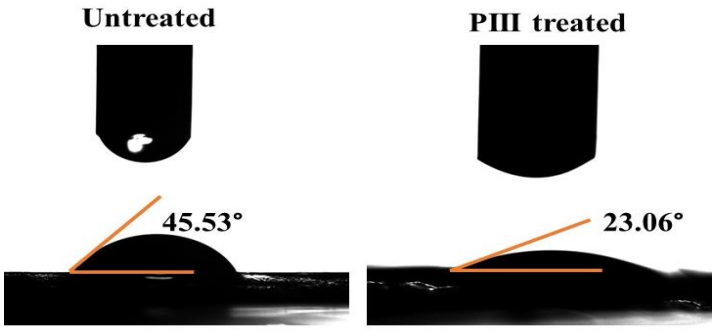

Figure 3. 15 Drop shape analysis shadow image showing water droplet on untreated and PIII treated scientific grade UHMWPE fabric. Contact angle of Untreated UHMWPE fabric is 45.53° and PIII treated is 23.06º.

The contact angle of untreated as well as PIII treated scientific grade UHMWPE fabric with various PIII treatment periods is summarized in the Fig 3.16. The contact angle of untreated UHMWPE is around 45.53° at 2.6 sec, according to these results. All surfaces became noticeably more hydrophilic after being treated with PIII. The decrease in liquid contact angle is proportionate to the decrease in temperature, according to a small trend. After treatment, the end water contact angle ranged from 45.53° to 23.06° for the 800s treated sample at 2.6 sec. Due to the introduction of active free radicals on top of the polymer surface, it became hydrophilic. Oxygen from the environment reacts with molecules from the surface of material and produces C-O and C=O and makes the surface more hydrophilic.

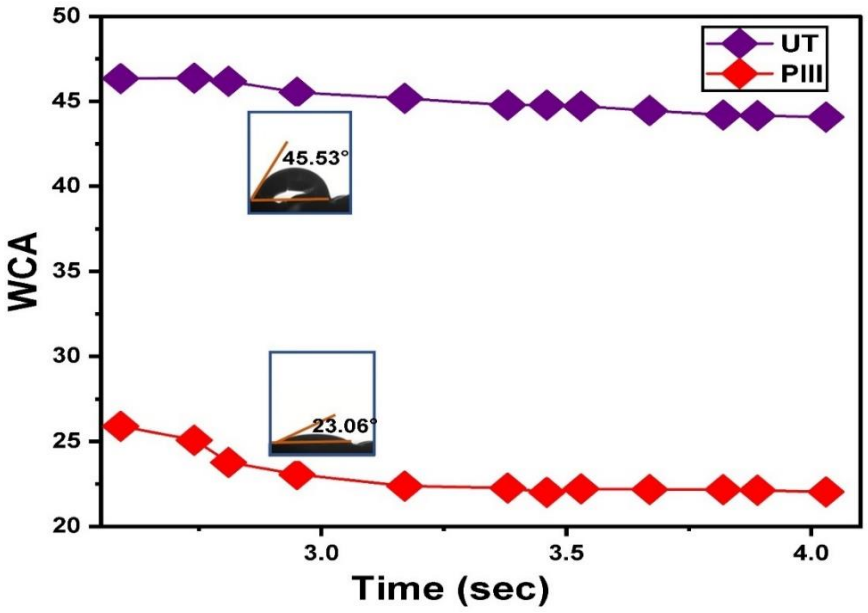

Figure 3. 16 Values of contact angles in relation to PIII treatment times. The measurements were taken as soon as the PIII therapy was completed. The untreated and PIII treated surface is represented by two data point.

Surface energy of untreated and PIII treated scientific grade UHMWPE fabric is presented in Fig 3.17 A. So, by measuring the angle created by the height of a drop of water on a surface, we can determine how the polar component of surface energy is changing with great precision. Because the water drop is so attracted to the surface and spreads or wets out, the smaller the angle will be the higher the surface energy. Water beads up and constricts into a small bubble on the surface due to low surface energy, resulting in a wide contact angle.

The wettability of a substrate with a low surface energy is poor. For satisfactory wettability, a high surface energy is necessary. The Surface energy of PIII treated scientific grade UHMWPE fabric is 58.24 mN/m. This is high compared to the surface energy of untreated UHMWPE fabric which is 47.33 mN/m. In Fig 3.17 B: a comparative study has been noticed on Untreated and PIII treated UHMWPE fabric. Main reason for increasing the surface energy of PIII treated

material is due to the presence of more polar groups than the untreated UHMWPE after the treatment which is presented in Fig 3.17 (B) & Table 3.5.

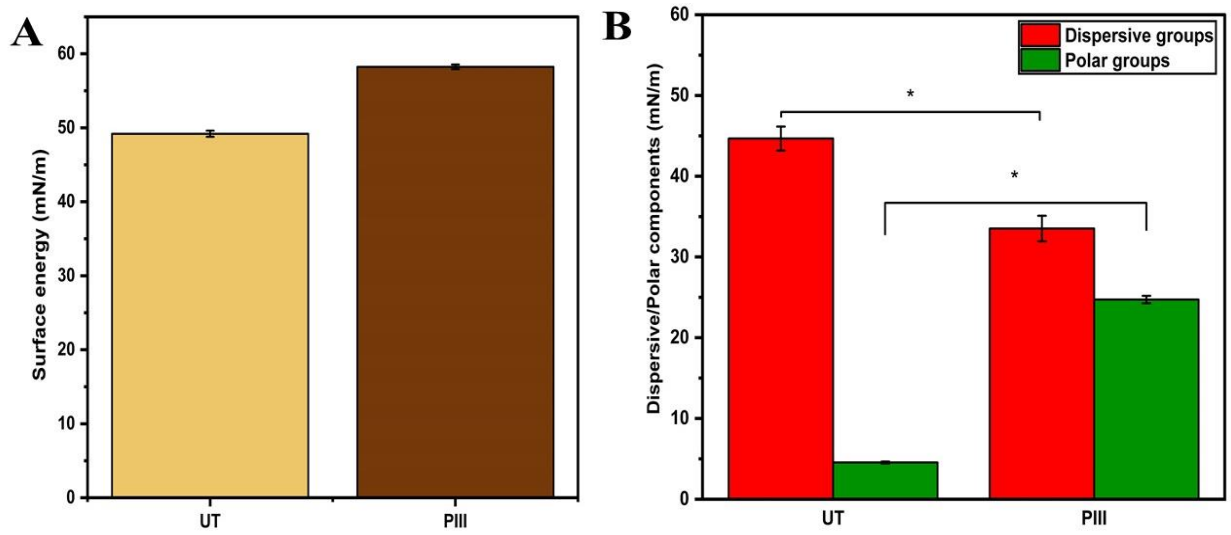

Figure 3. 17 (A) Surface energy of untreated and PIII treated scientific grade UHMWPE fabric; (B) Dispersive and polar groups of untreated and treated UHMWPE fabric. Error bars here indicate standard deviations of quadruplicates and an asterisk (*) indicates a significant difference ($P<0.05$) between the untreated and PIII treated groups.

There is no significant difference in dispersive groups between two materials. Table 3.4 illustrated the atomic composition of untreated and PIII treated UHMWPE. As plasma polymerized films are exposed to ambient oxygen, they oxidize, resulting in the presence of oxygen. The percentage of carbon decreased as carbon is the backbone of the material, is covered by Plasma treatment.

Table 3.5 Surface energies and their dispersive and polar contributions evaluated according to Owen-Wendt method.

Material	**Surface energy (mN /m)**	**Dispersive (mN /m)**	**Polar (mN /m)**
Untreated	49.2	44.66	4.54
PIII treated.	58.24	33.52	24.72

3.6.7 Surface chemistry of scientific grade UHMWPE fabric

Percentage of elements detected on each surface were shown in Table 3.6. UT UHMWPE contains Carbon, Nitrogen, and oxygen at a concentration of 79.09 %, 0.07%, and 20.84%. On the other hand, XPS spectra of PIII treated UHMWPE is composed of Carbon, Nitrogen, and oxygen at a concentration of 72.40%, 4.11%, and 23.49%. The fundamental element of UHMWPE is Carbon and hydrogen. After the PIII treatment, nitrogen content significantly increased due to the nitrogen implantation onto the surface of the material. Oxygen slightly increases due to the reaction of radicals with oxygen in the air after the treatment.

Table 3.6 Atomic composition of Untreated and PIII treated UHMWPE from XPS analysis

Name	Elements	Peak BE	Atomic percentage (%)
UT	C	286.27	79.09
	N	400.82	0.07
	O	533.18	20.84
PIII	C	285.01	72.40
	N	532.01	4.11
	O	399.02	23.49

We peak fitted the C 1s high resolution spectra to better understand the bonding of carbon to other elements, as shown in Fig 3.18 and the percentage of the peaks are shown in Table 3.7. After the PIII treatment, there is significant reduction of C-C/C-H bonds while C-O and C-N bonds significantly increase. There is also an appearance of COO group after the treatment. The amount of unsaturated carbon–carbon groups present decrease after the PIII treatment because these groups react further with active radicals to produce aromatic rings or branching crosslinked structures. The observed decrease in unsaturated carbon–carbon groups could potentially be attributed to oxidation as a result of reaction with atmospheric oxygen. The increase of surface nitrogen atomic concentration and nitrogen-containing functional groups upon PIII treatment is due to the implantation of nitrogen atoms into the surface. The nitrogen and oxygen-containing

functional groups greatly influence surface charge of the fabrics in a buffer solution and the subsequence immobilisation of functional biomolecules.

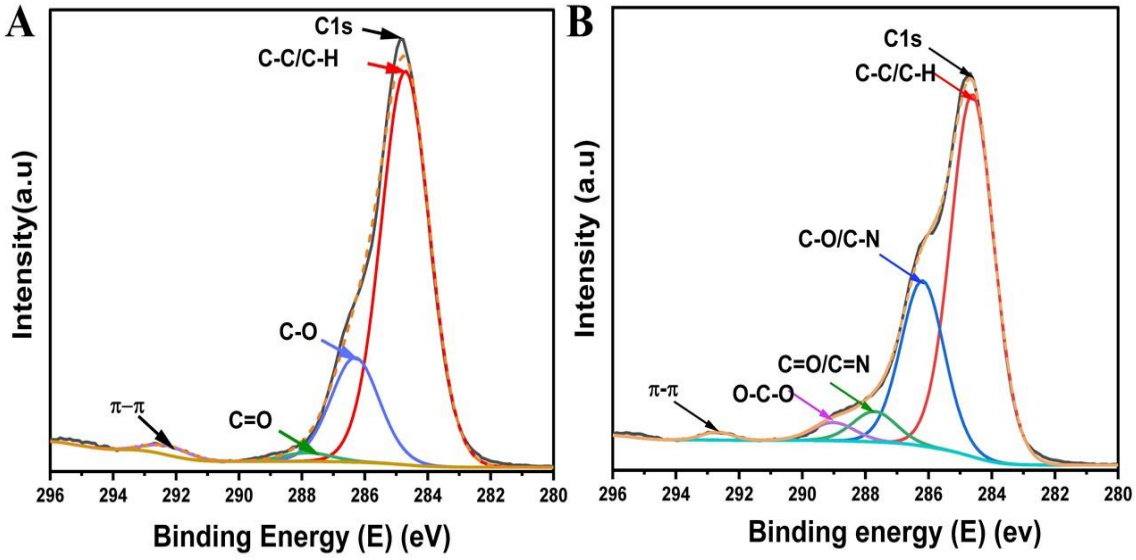

Figure 3. 18 (A) Peak fitted XPS C1s high resolution spectra obtained for UT UHMWPE;(B) Peak fitted XPS C1s high resolution spectra obtained for PIII treated UHMWPE.

Table 3.7 Comparison of deconvoluted peaks from C1s of untreated and PIII treated scientific grade UHMWPE fabrics .

Functional groups	Atomic percentage (%)	
	UT	PIII
C–C/C–H	80.67%	62.25%
C–O/C–N	13.94%	28.42%
C= O/N=C	3.60%	5.24%
π-π satelite	1. 79%	0.96%
-COO-	Nil	3.13%

3.6.8 Radicals detection on scientific grade UHMWPE fabric after the PIII treatment

PIII treatment induced radicals forming on the surface of UHMWPE from nitrogen bombardment as detected by ESR spectroscopy (Fig 3.19). A comprehensive knowledge of the relationship of free radicals with surface-contacting protein molecules is essential to provide the

precision required to build implant surfaces covered in patient suitable proteins. Fig : 3.19 compares the derivative ESR signals measured on PIII treated UHMWPE and untreated UHMWPE with the differences in g-factor values and peak intensity. The untreated UHMWPE has free radicals with a g-factor of 2.0005 while PIII treated UHMWPE has free radicals with g-factor of 2.0025. The shift of g-factor and the broader peak suggest that the PIII treatment produces a different type of free radicals on UHMWPE surfaces with much higher number of radicals. Those radicals measured on untreated UHMWPE could be due to the polymer synthesis in manufacturing process.

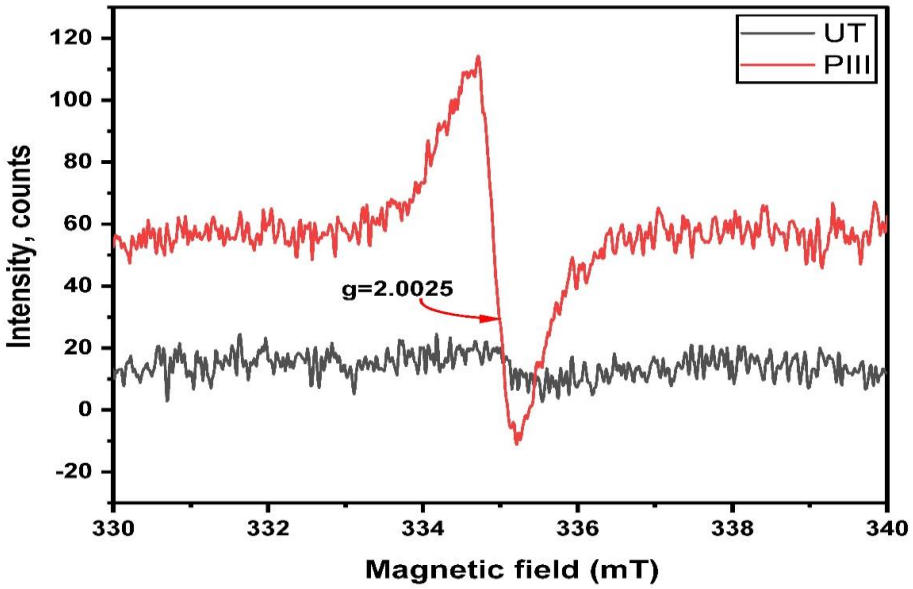

Figure 3. 19 ESR spectra of the untreated and treated UHMWPE. The ESR lines with g values of 2.0025 is marked for PIII treated UHMWPE.

3.6.9 Comparative study between industrial grade and scientific grade UHMWPE fabric

Though both grades of UHMWPE fabric are identical in chemical structure, but they possess several different characteristics. Industrial grade UHMWPE fabric is thick and shiny, on the other hand scientific grade UHMWPE is thin and matt in appearance. Due to the thick fabric

structure of industrial grade UHMWPE fabric, it has less plasma penetration throughout the fabric compared to the scientific grade UHMWPE fabric. Contact angle of scientific grade UHMWPE fabric changed from 66.27° to 49.53° and scientific grade UHMWPE changed from 45.53° to 23.06°. Contact angle of scientific grade UHMWPE changed at a higher rate than the industrial grade UHMWPE fabric.

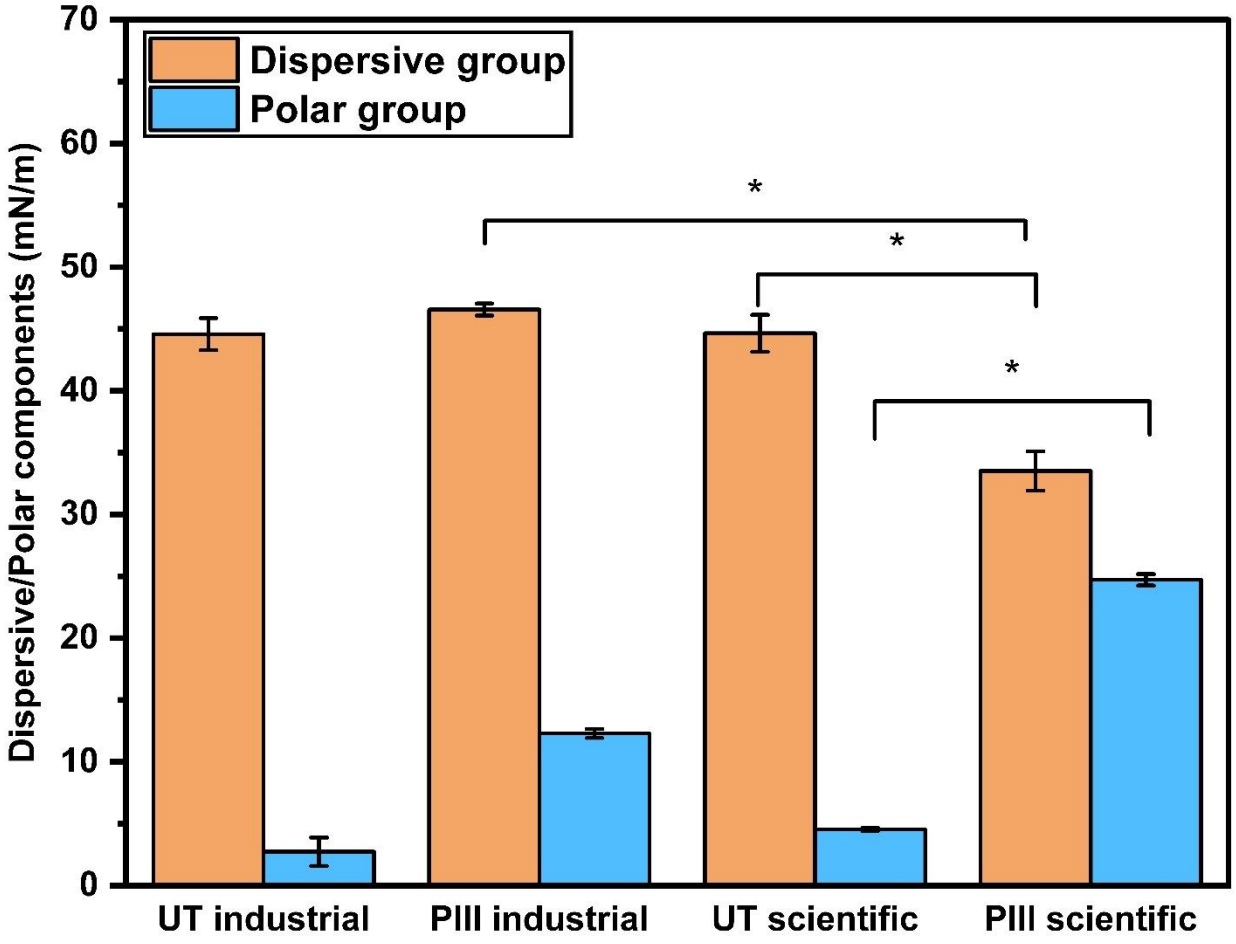

Figure 3. 20 Comparative study of dispersive and polar components of two grades of UHMWPE fabrics.

Fig 3.20 represents the comparative study of dispersive and polar components of two grades of UHMWPE fabrics. Surface energy is similar for untreated and PIII treated UHMWPE fabrics, but the dispersive and polar components ratio is different. More polar groups are noticed in

nitrogen based PIII treated scientific grade UHMWPE fabric than the scientific grade UHMWPE fabric.

Table 3.8 illustrated the comparative study on atomic percentages of industrial grade & scientific grade UHMWPE fabric after XPS analysis. C-C/C-H, C-O/C-N, C=O/N=C and -COO functional groups on both grades of UHMWPE fabric changed in a same percentage after the PIII treatment. The only difference observed for π-π bonds, it increased in industrial grade UHMWPE fabric but decreased for scientific grade UHMWPE fabric.

Table 3.8 Comparative study on atomic percentages of two different grades of UHMWPE.

Functional groups	**Atomic percentage (%)**			
	Industrial grade		**Scientific grade**	
	UT	**PIII**	**UT**	**PIII**
-C-C/C-H	82.95 %	57.60 %	80.67 %	62.25 %
C-O/C-H	12.38 %	23.80 %	13.94 %	28.42 %
C=O/N=C	2.63 %	7.84 %	3.60 %	5.24 %
π-π satellite	2.04 %	6.51 %	1.79 %	0.96 %
-COO-	Nil	4.24 %	Nil	3.13 %

3.7 Discussion and Conclusion

The goal of this thesis is to investigate the adhesion properties of nitrogen based PIII activated UHMWPE fabric surfaces. It was critical to create a consistent technique early in the investigation to assure a clean surface and generate repeatable results. A broad range of surface

factors influence the successful attachment of a protein molecule to polymer surfaces. The outcomes of the preliminary study also permitted the selection of a set of parameters that minimized the presence of potentially confounding variables throughout the subsequent operation.

Based on the initial evaluation of the surface uniformity of the various UHMWPE materials and the material costs, the UHMWPE materials assessed were the industrial grade UHMWPE fabric (Dyneema SK-78) in the form of 0.75mm thickness woven fabric and Scientific grade, UHMWPE fabric (Spectra-1000) was in the form of 0.45mm thickness woven fabric. These materials were selected decided because industrial grade UHMWPE fabric was cheap and easily available, while on the other hand, scientific grade UHMWPE fabric was a closer match for implantable grade UHMWPE materials.

Well-known validation, traceability, and control rules based on ISO 13485 are tightly enforced for biomaterial manufacturers. These materials frequently need to undergo extensive biological analysis and chemical characterization to support regulatory applications for associated goods. Because of these factors, implantable biomaterials continue to be far more expensive than materials of a lower quality. It was predicted that both scientific and industrial grade UHMWPE fabrics would be adequate to achieve the goals of this study. This was supported by the similar findings in the material characterization process. Even though the results of this study were based on UHMWPE of an industrial and scientific grade from different sources, results are anticipated to transfer to UHMWPE of an implantable quality for the intended uses.

As previously stated, the effective attachment of a protein molecule to polymer surfaces is determined by a few surface and protein features. Characterization studies of PIII treated fabric

surfaces were carried out to better understand the mechanisms of the process. Contact angle studies provide information on the surface energy and wettability of, while XPS allows the detection of structural changes on the UHMWPE fabric surface after the nitrogen based PIII treatment. It is hoped that the investigation of these properties will provide a reference for later results and may also better understand the covalent connection process. Also, the effect of the plasma treatment of the polymer is not permanent, because the surface it is often partially restored to its untreated state after storage. Even while a plasma treatment can be used to raise a polymer's surface energy, as it ages, the active surface will also experience post-plasma oxidation processes[85].

Typically, the initial surface characterization results matched the reported values in the literature quite closely. Untreated UHMWPE had contact angles and surface energy values that were comparable to those seen in other sources[123, 153]. Untreated UHMWPE fabric had liquid contact angles and surface energy values that were comparable to those seen in other sources[52, 58]. While there haven't been any studies of the nitrogen based on PIII treatment being applied to UHMWPE fabric surfaces, other energetic bombardment surface treatments have frequently revealed a considerable increase in wettability, surface energy, and oxygen content, all of which are related to the intensity of the treatment used. Plasma can modify the function of the polymer to insert or activate it. The surface of polymer is expected to undergo chemical and morphological changes, because high-energy ions in plasma can react with the outer atomic layer of the substrate down to several nanometers. The impacts caused by particle assault are chain scission and presentation of components to form modern chemical bunches, radical arrangement, cross linking and oxidation when exposed to air[247].

Initially, ion bombardment at some stage in PIII treatment effects in preferential sputtering of hydrogen and therefore dehydrogenation. Enhancement of the wear resistance and surface hardening can be done with this technique. Plasma adjustment is one of the normal strategies to improve or lessen the wetting properties of polymers. Generally biocompatible materials have a hydrophilic nature however, as received, from the supplier, UHMWPE is hydrophobic with a water contact point of around 69°. The treatment makes the fabric surface become more hydrophilic as demonstrated from the contact angle of formamide (Fig 3.8,3.16). In previous study, the PIII treatment on LDPE reduced the water contact angles from 90° to 60°[248]. The hydrophilicity of UHMWPE can be improved by presentation of polar groups such carboxyl, carbonyl, and hydroxy groups from oxidation.

The PIII treatment has been known to create a reservoir of radicals on the sub-surface of the polymer which emerge to the surface and react with oxygen when samples are exposed to the air [249].The formation of oxygen and nitrogen containing groups as detected by XPS (Fig 3.11 & 3.18) contributes to the increased hydrophilicity of the PIII treated surface, although we cannot directly measure the water contact angle on the fabrics. The PIII treatment & surface characterization results were similar for industrial & scientific grade UHMWPE fabric, but this could be different in biological testing.

Section 3.5.9 has been discussed on physical and chemical difference between two grades of UHMWPE before and after the PIII treatment. Some similar results observed for free radical measurements, surface energy calculations etc. However, a few results showed variations observed between industrial and scientific grade UHMWPE fabric such as presence of more polar groups, higher rate of contact angles changes, less pi-pi bonds in scientific grade UHMWPE fabric than industrial grade UHMWPE fabric. This may have been due to the

presence of impurities introduced in the manufacturing process as indicated by the stronger discoloration of industrial material with the PIII treatment.

The work done in this chapter enabled the creation of a uniform operating procedure for all upcoming tests using the same UHMWPE fabric. Studies on surface characterization have shown an unanticipated hydrophobic recovery effect, which is thought to be caused by the production of low molecular weight fragments at high ion bombardment levels occurred on both grades of UHMWPE fabric.

In summary, we may state that the experimental component of this chapter's findings supported the hypothesis.

Chapter 4 : Design and evaluation of a prosthetic ligament/tendon graft

4.1 Introduction

Ligaments and tendons play a significant role in musculoskeletal biomechanics. Ligament attaches bone to bone and tendon at taches bone to muscle[250]. Ligaments are strong mechanical connective fibers that can extend across a joint and be attached to bones at either end. They bind two bones together, prevent dislocation, and limit joint movement. They are distinct in terms of their location, size, shape, and orientation. Tendons and ligaments are elastic fiber structures made up of densely packed collagen fibers that are arranged in a pyramid pattern[251]. Rod-like collagen molecules align in a quarter-stagger array parallel to the tendon's longitudinal axis to produce a fibril, the smallest structural unit in the tendon. Water, collagen, proteoglycans, glycoproteins, cells, and ground substance are the main components of tendons and ligaments.

Tendons and ligaments are soft tissue components that are typically damaged by direct injury or prolonged stress. Tendon or ligament perforation often occur as a result of sudden, extreme loading, which can arise as a result of athletic injuries or motor vehicle accidents[161].

Tendon and ligament injuries are a huge category of musculoskeletal injuries that cause pain and functional impairment in millions of people and account for a significant amount of health-care spending. Soft tissue injuries account for thirty to fifty percent of all injuries in athletes, and this number is expected to continue to climb. One of the most common procedures performed by orthopedic surgeons is the reconstruction of Ligaments/Tendons (L/T) of the knee following their rupture[252]. The number of patients receiving Ligament/Tendon (L/T) reconstruction is rapidly increasing, and while it is a generally safe technique, it is not uncommon for these patients to require further knee surgery, particularly in young and female patients[162].

Many procedures have been used to restore the (L/T) 's activity and function, including allograft, autograft, and synthetic graft surgery. Autograft reconstruction is a typical procedure in which a piece of the patient's own tissue, usually from the patellar tendon or hamstrings, is taken and used as a ligament replacement due to the benefits of using human tissues such as the existence of stretch receptors, vascularity, and the lack of graft rejection problems [253]. Quadrupled hamstring grafts, bone patellar tendon bone (BPTB), the double looped semitendinosus/gracilis tendon (DLSGT) have been used widely around the world as an autograft for L/T reconstruction.

Quadriceps tendon and iliotibial band have been used as autograft as well[40]. Autografts have several disadvantages. These grafts have issues include crepitation, flexion contracture, and post-operative knee discomfort. A gradual switch from using BPTB grafts to using DLSGT grafts has occurred in recent years due to problems with donor site morbidity, specifically arthrofibrosis, patello-femoral pain when kneeling, quadriceps weakness, and loss of sensitivity associated with these grafts[183]. Generally, donor site morbidity with hamstring grafts is often lower than with patellar tendon transplants, but saphenous nerve injury and hamstring weakening have been documented. The need for a further harvesting technique results in lengthier operation and recuperation times, which is another drawback of autograft reconstructions.

Allografts can used in the same way that autografts are. Patellar tendon, quadriceps tendon, Achilles' tendon, tibialis anterior tendon, tibialis posterior tendon, hamstring tendon, and fascia lata are among the allografts used. Because of its mechanical qualities, the Achilles tendon is a viable candidate[254]. A graft diameter that is easily matched to the patients, a more cylindrical shape than a patellar graft. On the other hand, patellar tendon has a bigger cross-sectional area that offers for superior strength, and a graft diameter that is easily matched to the patients. Allografts have several advantages compared to other grafts. The use of allografts avoids donor

site complications such as: patellar fracture, muscle weakness and knee pain etc. Negative outcomes for allografts include expense, delayed graft incorporation compared to autografts, tendon allografts that are weaker than autografts, higher risk of contamination, and limited availability.

Autografts can cause donor site morbidity, while allografts can cause patients to develop blood and bone disorders. Physical activity restrictions are currently the most significant limitation for L/T repairs using synthetic grafts. Even though early rehabilitation of autograft can reduce these issues, but biological graft is fragile. The increased activity that occurs during the early post-operative period can cause further issues. Excessive tension on the graft could harm the graft tissue, leading to graft fracture.

Synthetic ligament grafts could be a useful choice for L/T restoration due to the disadvantages of allografts and autografts. To address the drawbacks of biological grafts, artificial ligaments have been suggested as a substitute. The synthetic ligament graft is a device that connects the ends of two bones using artificial ligaments. A layered or tubular woven ligament with an extra-articular region, at least one bending region, and at least one end region makes up the device. Each area should be weaved to provide support and flexibility in response to certain stresses. Ligament grafts would ideally have the following properties:

- Strength and stiffness comparable to a natural L/T
- Minimal inflammation upon implantation into the body
- Degradable over time to facilitate tissue ingrowth
- Excellent resistance to abrasion against bones and joints

Various biomaterials have been developed over the past few years as artificial ligaments such as poly -l-lactic acid (PLLA), poly carbonates, poly arylates, polycaprolactone, PDS, poly(diaxonane), PLGA, poly(lactic-co-glycolic acid), PLLA, poly(L-lactic acid)[205, 255–258]. However, the selection of biomaterials for such regeneration is a major challenge due to the lack of biocompatibility of mechanically suitable materials that are capable of appropriately handling in vivo mechanical loadings [1]. In the last few decades, bioabsorbable and non-bioabsorbable biopolymers have been applied for use in orthopaedic applications due to their high mechanical strength and biocompatibility compared to metals and ceramics [65]. Ultra-high molecular weight polyethylene (UHMWPE) is among the non-bioabsorbable polymers which are commonly used for joint replacement and other applications where sustained function in required. The market demand for medical-grade UHMWPE has increased tremendously from 60.9 kilotons (2015) to 204.8 kilotons (2024) according to a survey conducted by Grand view research [67]. The comprehensive use of UHMWPE in the medical field is due to its low wear volume, ultimate tensile strength and low coefficient of friction [79].

In this research two different types of UHMWPE fabric have been chosen based on their sources. One is industrial grade UHMWPE fabric which is cheap and easily available, and another is scientific grade UHMWPE fabric potentially free from impurities and costly.

4.2 Design criteria for ligament/tendon graft

To accommodate varying patient knee sizes, the synthetic graft can be manufactured in a variety of lengths and diameters. A prosthetic ACL has some advantages over biological grafts, one of which is that it allows for better overall design and production control without being constrained

by the need to modify the acquired tissue. The human load bearing capability and body weight were considered during the creation of the graft, and these factors will determine the desired strength of the synthetic ligament graft. In contrast side, a graft may lose 50% of its volume during the remodelling period, thus it's critical to maintain the graft's strength during insertion. When designing the UHMWPE ligament graft, three essential elements were considered such as graft diameter, cross sectional area and strength of graft [259–261].

Table 4.1 Relationship of graft diameter and cross-sectional area with strength of the graft[261]**.**

Change in graft diameter (mm)	% Increase in cross-sectional area	% Increase in strength of graft
6 to7	36	38
7 to 8	31	20
6 to 8	78	66
7to 9	65	34
6 to9	125	85

The graft's diameter has been reported to be important for graft strength as shown in Table 4.1. There would be more space for tissue ingrowth if the transplant had a large surface area. Prior to graft design, the length of the graft was considered. Scientists have discovered that the bone tunnel's overall length might range from 85 to 105mm[260].

Tunnel sections should be designed in a way that it can play an important role in cellular adhesion, proliferation, and differentiation. The proposed hollow cylindrical shape of the UHMWPE ligament graft would support osteogenesis and tissue integration. The design needs to include high porosity for tissue ingrowth and simple access to vascularization across the entire system should be features of the UHMWPE prosthetic design [262]. A synthetic ligament/tendon

graft should have strength and stiffness to match the properties of human L/T without any side effects. This UHMWPE graft is designed to in such a way so that it can mimic the properties of natural L/T.

(i) It has a cylindrical shape of 100mm length and 10mm diameter to mimic the structure of human L/T.
(ii) It is highly porous and can provide large surface area for cells to grow and proliferate.
(iii) It has high strength and stiffness.

4.3 Aim & hypothesis of the chapter

The following summarises the goal and focus of studies described in this chapter:

1. Development of a synthetic ligament graft prototype by combining of Ultra high molecular weight polyethylene (UHMWPE) fabric in a woven fabric structure
2. Conduct testing for tensile mechanical properties under immediate physiological loading to validate the mechanical performance of the synthetic ligament graft. Conduct Cyclic loading evaluation of ligament/tendon graft prototype which mimics the initial phase of ligament healing.
3. Assuring that acceptable standards and literature guidelines were used in this test work.
4. Compare the mechanical properties for industrial grade versus scientific grade UHMWPE.
5. Determine the impact of plasma treatment on tensile mechanical properties of the synthetic UHMWPE ligament graft by measuring these properties before and after plasma treatment.
6. Compare the porosity of industrial grade UHMWPE graft versus scientific grade UHMWPE graft.

According to the theory, industrial-grade UHMWPE is more robust than scientific-grade UHMWPE fabric and both grades of UHMWPE graft can support human weight. Both substances would be sufficiently porous to support blood supply and osteogenesis.

4.4 Experimental method for designing, manufacturing, and testing a prototype synthetic ligament/tendon prosthesis.

4.4.1 Material selection

UHMWPE was selected as the material for the prototype synthetic prosthesis. UHMWPE is a subgroup of the thermoplastic polyethylene (PE) family that is obtained from a monomer of ethylene by a polymerization reaction. UHMWPE is also known as a high modulus PE or high-performance PE because of its toughness and good impact strength. It also has extraordinary properties such as nontoxicity, high resistance to corrosive chemicals and wear resistance that makes it reliable for orthopaedic applications and is widely used in other orthopaedic applications requiring long term implant performance. Two grades of UHMWPE fabric would be used here to conduct mechanical testing as they could represent alternative weave design, cost, and purity for assessment.

4.4.2 Fabrication of UHMWPE prosthetic prototype

In order to evaluate the mechanical properties of a UHMWPE fabric prototype including performance with and without the PIII treatment, a rectangle of UHMWPE fabric was sewed with a Lumina N190 sewing machine into a tubular shape of similar dimensions to human anterior cruciate ligament (ACL) for mechanical testing. Approximately 125 mm x 20mm of UHMWPE fabric was used for sewing. Nylon thread was used as a sewing thread due to its excellent biocompatability strength and abrasion resistance properties.

After sewing, the excess portion of the fabric was trimmed by using heated scissors blade to make a tubular shape. One end of the graft was stitched closed with nylon thread. It was then

pushed by a knitting needle (diameter 4.0 mm) to reverse inner and outer surfaces to produce a hollow tubular shape. with a length of 100 mm and a width of 10 mm. This shape and dimensions was selected to reproduce the dimensions of current ACL autografts. The fabrication process is illustrated in Fig 4.1.

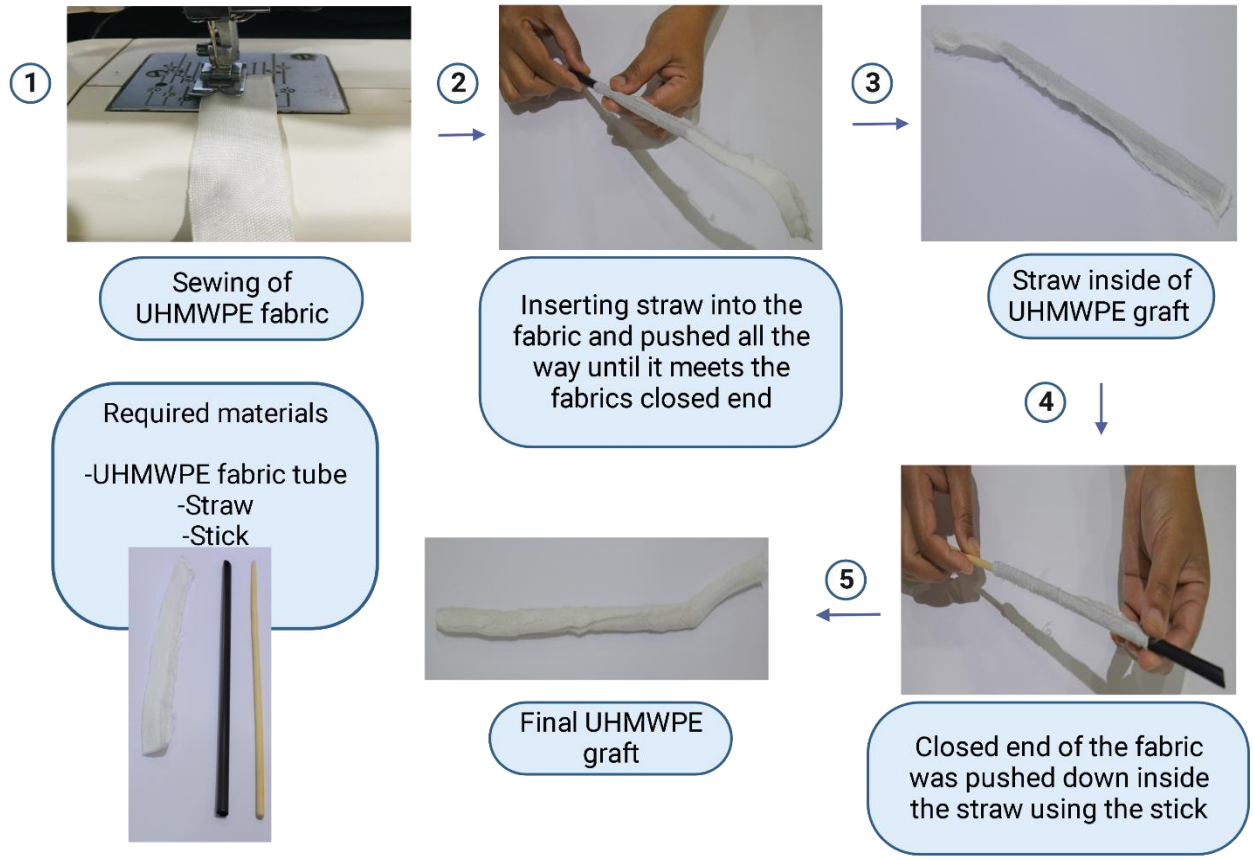

Figure 4. 1 Fabrication of UHMWPE ligament graft prototype from UHMWPE fabric.

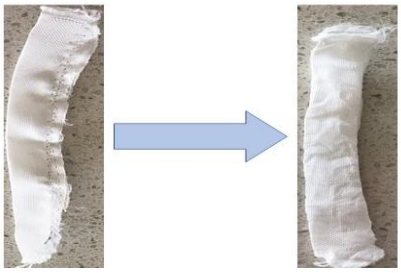

Figure 4. 2 Left side image showing stitched UHMWPE fabric and right-side image showing the inside out transformation to the final fabric graft.

4.4.3 Tensile testing of the graft

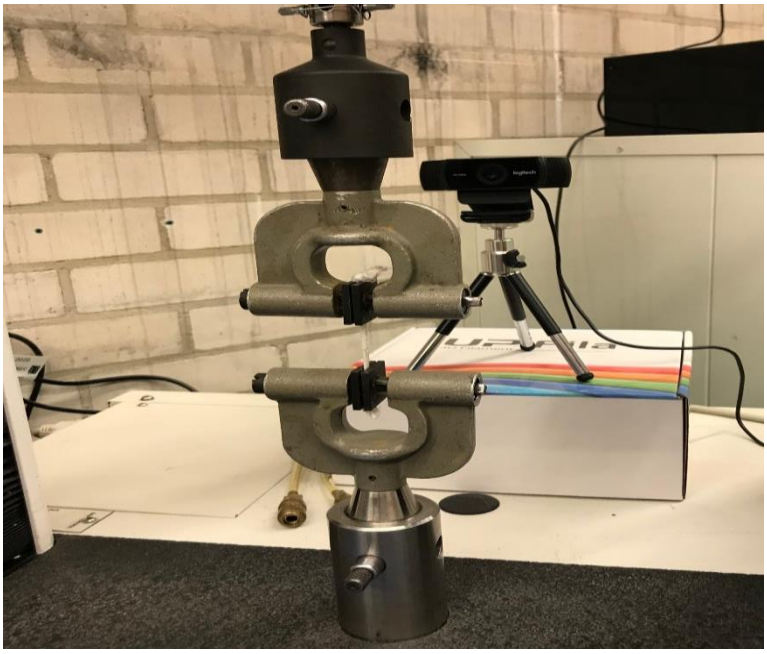

Figure 4. 3 Mechanical testing of graft using Instron machine.

A tensile test was performed using an Instron 3366 testing machine to compare the mechanical properties of the untreated and PIII treated UHMWPE ligament grafts (tubular structure). Mechanical properties of the grafts were calculated from the stress-strain relationship. The graft was gripped by clamps at each end where a knot was made to prevent it from slipping through the clamps. The load was continuously increased, and the UHMWPE ligament graft extended gradually until failure. The gauge length was set at 10 cm. The maximum tensile load, maximum strain, and stiffness were measured from the stress-strain relationship.

4.4.4 Cyclic loading of the graft

The goal of the cyclic loading was to see how simulated physiological loads affected the untreated UHMWPE grafts mechanical performance. Each graft was first cyclically loaded in a load control mode using a sinusoidal wave ranging from 50 to 1000 N for varying amounts of cycles at 1 Hz. The forces in the ligament/tendon specially anterior cruciate ligament (ACL)

during walking and running were simulated using this technique [263]. We selected to examine each specimen for 1000 and 100,000 cycles at two distinct loading strengths in our research ranging from 50 and 700 N, 50 and 800 N and 50 and 1000 N. This number of cycles is higher than what Beynnon and Amis (1998)[264] and Beynnon, Johnson, and Fleming (2002)[265] prescribed, and it was chosen to optimize prosthesis loading. The difference between strains at the first and last cycle was used to compute the displacement after loading.

4.4.5 Porosity of the graft

When enzymatic degradation takes place, the device's surface area and porosity play a key role in regulating the pace of degradation. The functionality of the implant and the overall cellular response can be modified by the implant's porosity[266, 267]. The porosity of UHMWPE graft was evaluated based upon the protocol reported in the literature of Chun[268]. Based on the concept of liquid displacement the porosity of the UHMWPE ligament graft was assessed. The porosity of the PET-ALs was calculated using the following equation.

$$\varphi = \frac{\frac{[(PT - PS) - (PR - PP)]}{\rho H2O}}{VP - (PR - PP)/\rho H2O} X\ 100\%$$

Here, Porosity of the graft is denoted by φ

PT= Weight of the pycnometer's weight after being fully filled with pure water and the tested UHMWPE graft.

PS= Weight of the dried pycnometer and the UHMWPE graft

PP= Weight of the dried pycnometer

VP= Volume of pycnometer

ρH_2O= Density of water at room temperature

4.5 Data presentation and statistical analysis

All figures and statistical analyses relevant to the results in this chapter were analyzed and evaluated using Microsoft Excel (version 2013), and ORIGINPRO 2020. For group comparisons, two tailed t-tests with a P value of 0.05 indicating significance were used.

4.6 Experimental Results

4.6.1 Mechanical testing of industrial grade UHMWPE graft

Load-strain curves were constructed for deformation rate to investigate the impact of strain rates on the mechanical properties of the prosthesis. The mechanical behaviour of this prostheses reflected the ligament behaviour which is shown in Fig 4.4 and Table 4.2.

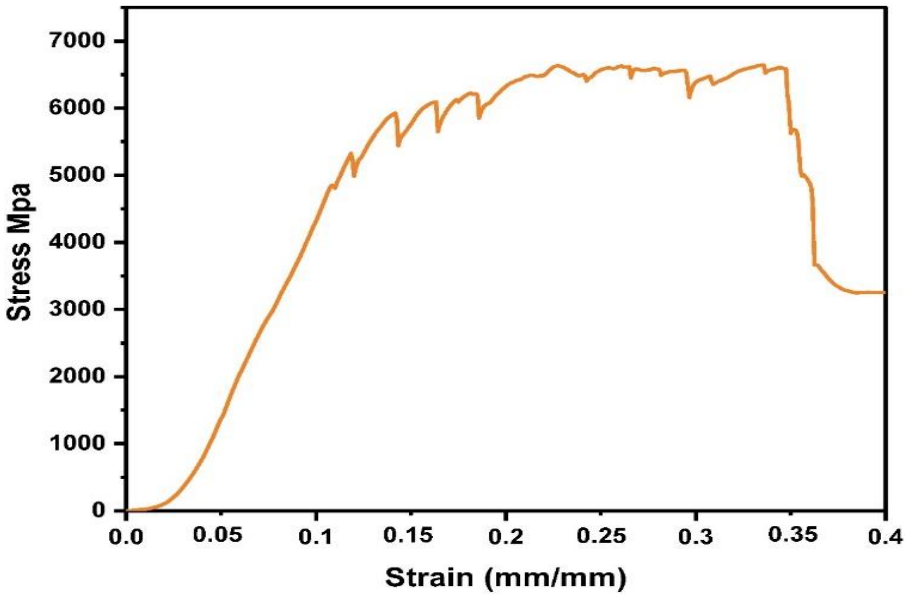

Figure 4. 4 Stress-strain curve for UHMWPE graft.

The load–strain curve of industrial grade UHMWPE prosthesis is shown in Fig 4.5. This curve can be also broken down into various categories. The first region is nonlinear and has a high

starting stiffness. Then there's a linear zone with a higher rigidity. The fibers are stretched in this phase, which is followed by a plastic region in which the distortion is irreversible. The curve eventually achieves the maximum load that the structure can bear. The prosthesis will fail if it is overloaded. The young's modulus of UHMWPE graft is 10844.97 Mpa.

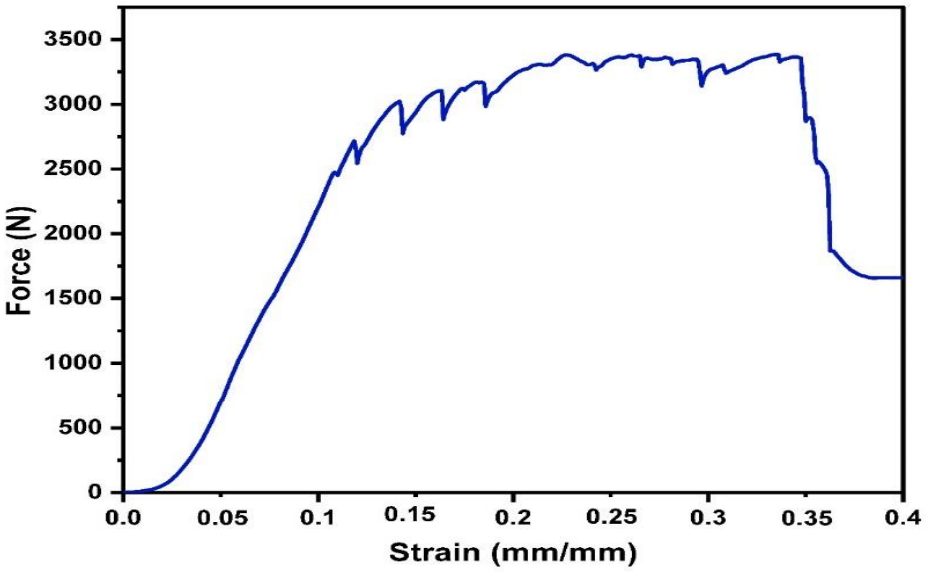

Figure 4. 5 Load versus strain curve for industrial grade UHMWPE graft.

Table 4.2 Tensile properties of industrial grade UHMWPE prostheses.

Ligament/graft	Tensile load (N)	Yield strain (%)	Stiffness (N/mm)	Youngs modulus (MPa)	Yield strength
UHMWPE graft	3739.21±216.9	3.02±0.6%	5547±316.5	10844.97±608.37	1119.8±87.2
Human Ligament/tendon	1725–2160		306	110	

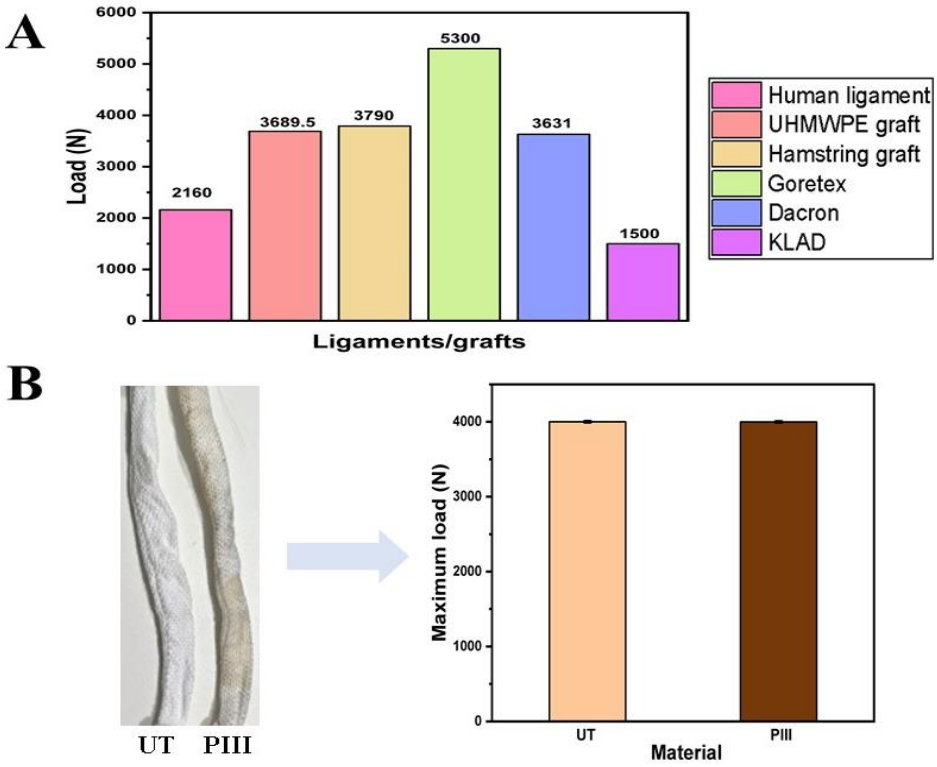

Figure 4. 6 (A) Load comparison of several types of grafts from mechanical testing [1] (B) Load comparison of Untreated and PIII treated UHMWPE grafts.

Fig 4.6 (A) compares industrial grade UHMWPE graft with other grafts obtained from literature including human Anterior cruciate ligament (ACL) graft. UHMWPE can withstand 3689.5 N till it breaks. From analysis of essential criteria of other synthetic grafts, UHMWPE could be considered an option for ligament/tendon reconstruction.

Fig 4.6 (B) shows the mechanical performance comparison of UHMWPE ligament graft before and after the plasma treatment, in which the value remains unchanged after the plasma treatment. Low variability indicated by the error bar indicates the consistency of measurements between repeats. Comparable results proved that PIII treatment did not change the bulk properties of the material, whilst it changes the material's surface properties.

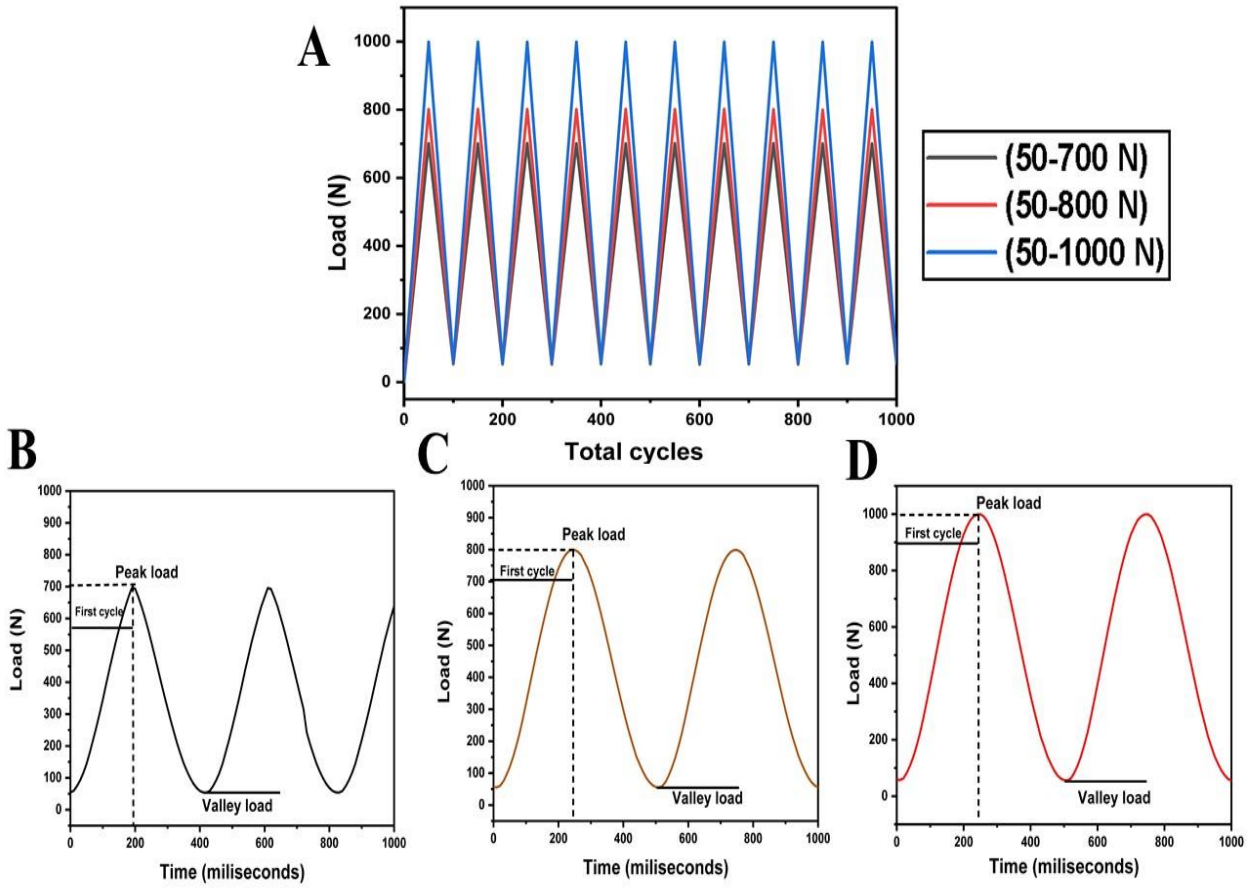

Figure 4. 7 (A) Cyclic loading of UHMWPE at 1000 cycles within different load ranging from (50-1000 N); (B), (C) & (D) Peak and valley load of the UHMWPE grafts at each cycle during cyclic loading.

4.6.2 Cyclic loading of industrial grade UHMWPE graft

The mean deformation and peak load measured on untreated UHMWPE graft after cyclic loading are reported in Table 4.3. The maximum load is defined as the peak load level in the load–time curve, and it can be used to estimate the prosthesis' failure load during cyclic loading is shown in Fig 4.7 & 4.8. At 1000 cycles, the UHMWPE graft presented a residual deformation of 0.53 mm for 700 N, 1.05 mm for 800 N, and 1.49mm for 1000 N load. On the other hand, at 100000 cycles, a residual formation of 1.32mm found for 700 N and 1.69 mm for 800 N. Each prosthesis was first cyclically loaded in a load control mode using a sinusoidal wave between

different load ranges (50 - 1000 N) for various amounts of cycles at 1 Hz is shown in Fig 4.7 (B, C, D) & Fig 4.8(B, C). The forces in the ligament/tendon specially in (Anterior cruciate ligament) during walking and running were estimated using this mode[263].

Table 4.3 Cyclic loading data of untreated industrial grade UHMWPE graft.

No of cycles	Peak load (N)	Deformation (%)
1000	701.69	0.53
	802.25	1.05
	999.6259	1.49
100000	699.71	1.32
	799.41	1.67

Cyclic loading of ACL grafts has yet to be defined as a standard procedure. To analyze the first cyclic loading response, Beynon and Amis [264] proposed loading the knee to 1000 load cycles at 150 N of displacement. Jarvinen et al. [263] loaded grafts for 1500 loading cycles at 0.5 Hz between 50 and 200 N. In this work, the UHMWPE grafts were loaded between 50 - 800 N for 1,000 cycles and 50-1000N for 100,000 cycles to imitate stresses exerted to the ACL during walking and intensive physical therapy[269].This number of nodes are higher than that suggested by Beynnon and Amis(1998) and Beynnon, Johnson, and Fleming(2002), Jedda and Ben(2011) and it was chosen to maximize prosthesis loading[263].

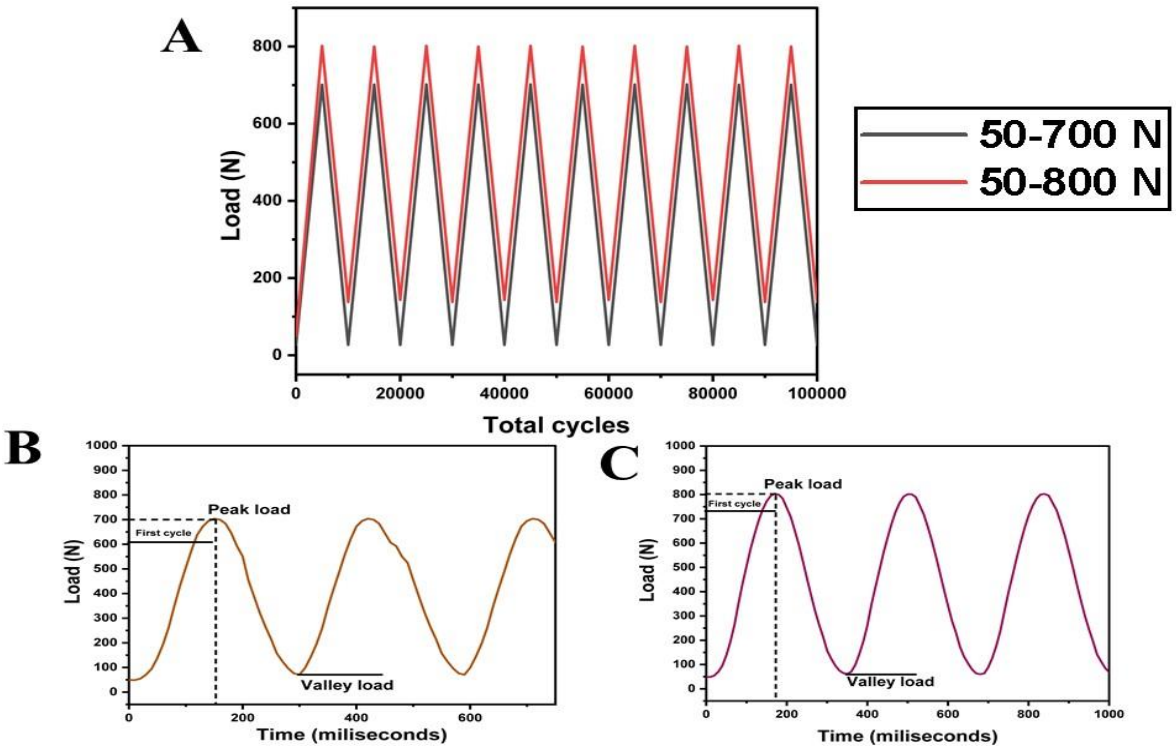

Figure 4. 8 (A) Cyclic loading of UHMWPE at 100000 cycles within different load ranging from (50-800 N); (B) & (C) Peak and valley load of the UHMWPE grafts at each cycle during cyclic loading.

4.6.3 Mechanical strength of scientific grade UHMWPE graft

Stress-strain curves were constructed for deformation rate to investigate the impact of strain rates on the mechanical properties of the prosthesis. The mechanical behaviour of this prostheses reflected the ligament behaviour which is shown in Fig 4.9 and Table 4.4.

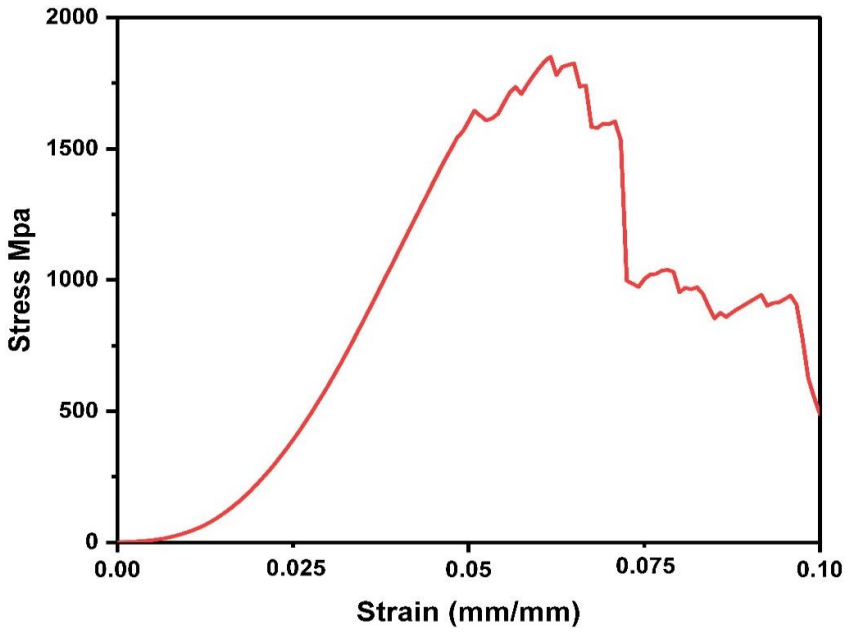

Figure 4. 9 Stress-strain curve for scientific grade UHMWPE graft.

The load–strain curve of UHMWPE prosthesis is shown in Fig 4.10. This curve can be broken down into various categories. The first region is nonlinear and has a low starting stiffness. Then there's a linear zone with a higher rigidity. The fibers are stretched in this phase, which is followed by a plastic region in which the distortion is irreversible. The curve eventually achieves the maximum load that the structure can bear. The prosthesis will fail if it is overloaded.

Table 4.4 Summarizes the mechanical features of the scientific grade UHMWPE prosthesis.

	Tensile load (N)	Yield strain (%)	Stiffness (N/mm)	Youngs modulus (MPa)	Yield strength (Mpa)
UHMWPE graft	2238.9±245	5.1%±0.04	47355.5±200	46424±167	1625.9±50
Human Ligament/tendon	1725–2160		306	110	

The average tensile load bearing capacity of the scientific grade UHMWPE prostheses is higher than that of the natural ACL (2195; 1725–2160) N. We found that the strain values are lower (< 6%) than that of the natural ACL, and the stiffness is higher than that of the natural ACL (242–306 N/mm).

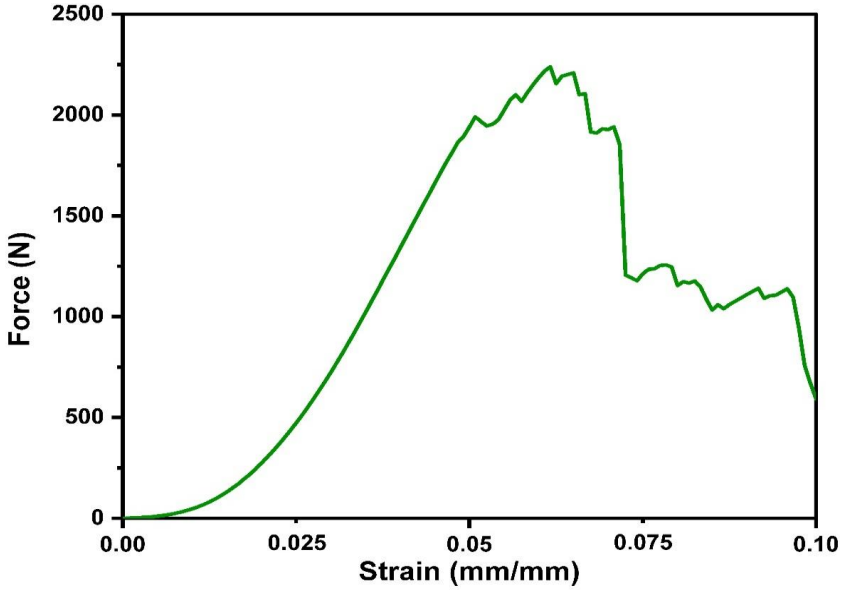

Figure 4. 10 Load-strain curve of scientific grade UHMWPE graft.

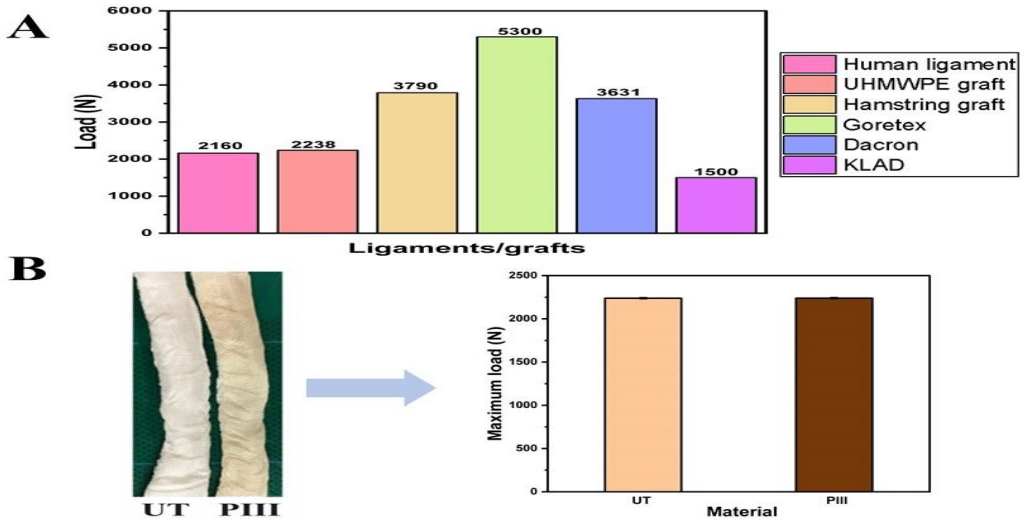

Figure 4. 11 Load comparison of several types of grafts from mechanical testing.

When repairing hard tissues such as ligaments, tendons, cartilage, and bone, the mechanical qualities of the graft/scaffold are typically crucial. In this section mechanical strength of UHMWPE graft was calculated and compared with PIII treated scientific grade UHMWPE graft. Fig 4.11(A) compares UHMWPE graft with other grafts obtained from literature including human Anterior cruciate ligament (ACL) graft. UHMWPE can withstand 2238 N till its break. From analysis of essential criteria of other synthetic grafts, UHMWPE could be considered the best option for ligament/tendon reconstruction.

Fig 4.11 (B) shows the mechanical performance comparison of scientific grade UHMWPE ligament graft before and after the plasma treatment, in which the value remains unchanged after the plasma treatment. Minor error bar indicates the consistency of measurements among repeats. Comparable results proved that PIII treatment did not change the bulk properties of the material, whilst it changes the material's surface properties.

4.6.4 Cyclic loading

The mean deformation and peak load measured on untreated scientific grade UHMWPE graft after cyclic loading is reported in Table 4.5. The maximum load is defined as the peak load level in the load–time curve, and it can be used to estimate the prosthesis' failure load during cyclic loading is shown in Fig 4.12 & 4.13. At 1000 cycles, the UHMWPE graft presented a residual deformation of 1.62 mm for 700 N, 1.77 mm for 800 N, and 1.88mm for 1000 N load. On the other hand, at 100000 cycles, a residual formation of 2.08mm found for 700 N and 2.37mm for 800 N. Each prosthesis was first cyclically loaded in a load control mode using a sinusoidal wave between different load ranges (50 - 1000 N) for various amounts of cycles at 1 Hz is shown in

Fig 4.12 (B, C, D) & Fig 4.13(B, C). The forces in the ligament/tendon specially in (Anterior cruciate ligament) during walking and running were estimated using this mode[263].

Table 4.5 Cyclic loading data of untreated UHMWPE graft.

No of cycles	Peak load (N)	Deformation (%)
1000	701.69	1.62
	802.25	1.77
	1002.28	1.88
100000	749.71	2.08
	802.12	2.37

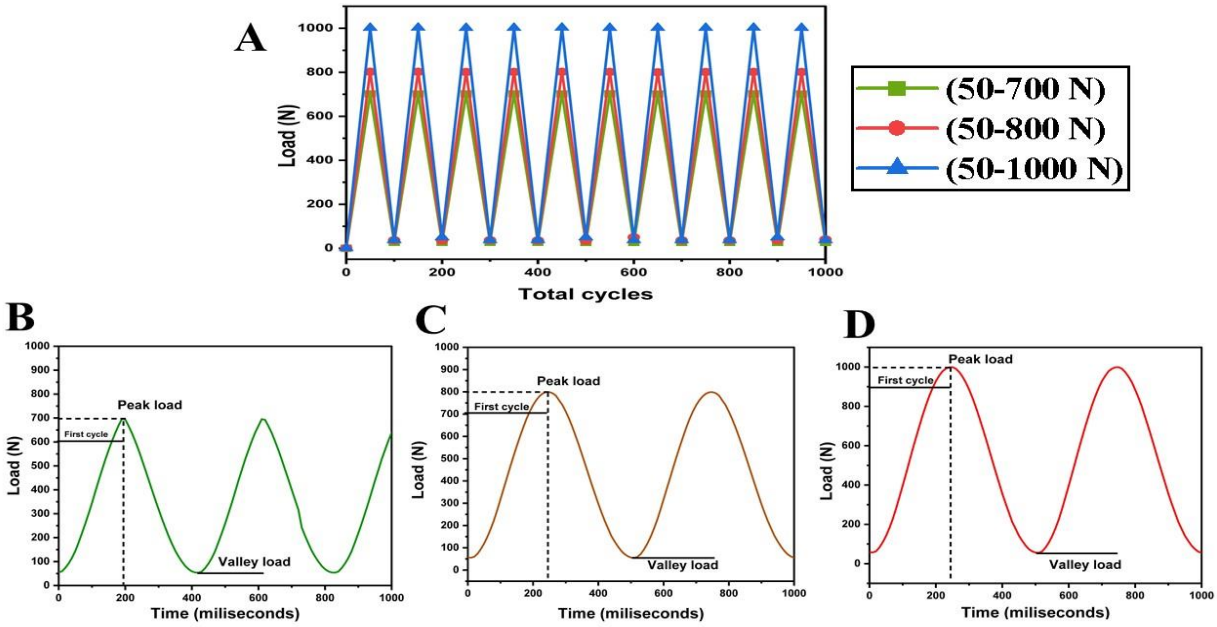

Figure 4. 12 (A) Cyclic loading of UHMWPE at 1000 cycles within different load ranging from (50-1000 N); (B), (C) & (D) Peak and valley load of the UHMWPE grafts at each cycle during cyclic loading.

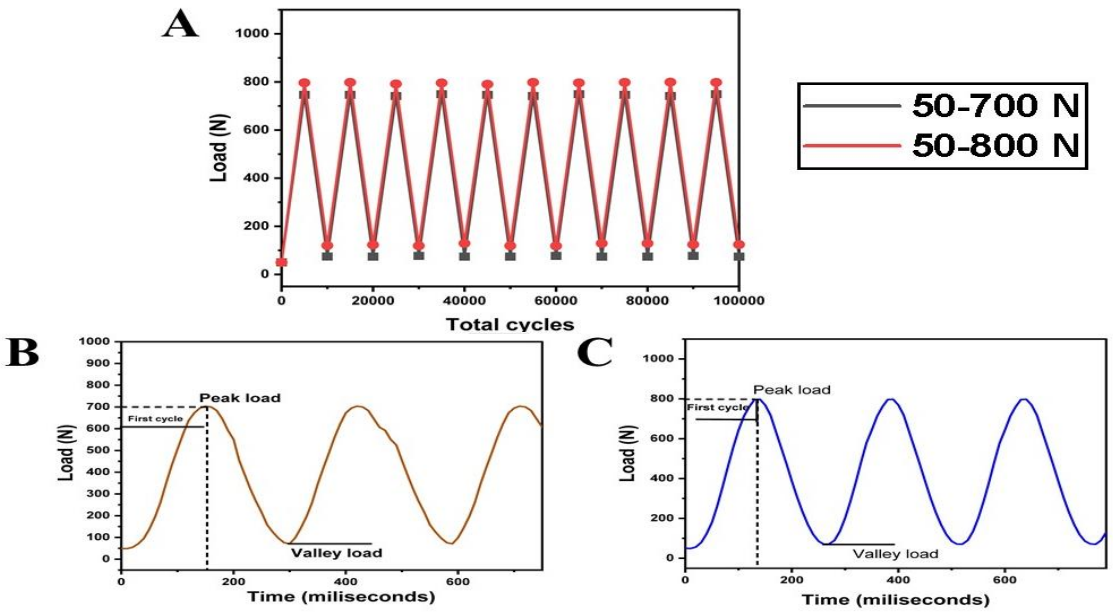

Figure 4. 13 (A) Cyclic loading of UHMWPE at 100000 cycles within different load ranging from (50-800 N); (B) & (C) Peak and valley load of the UHMWPE grafts at each cycle during cyclic loading.

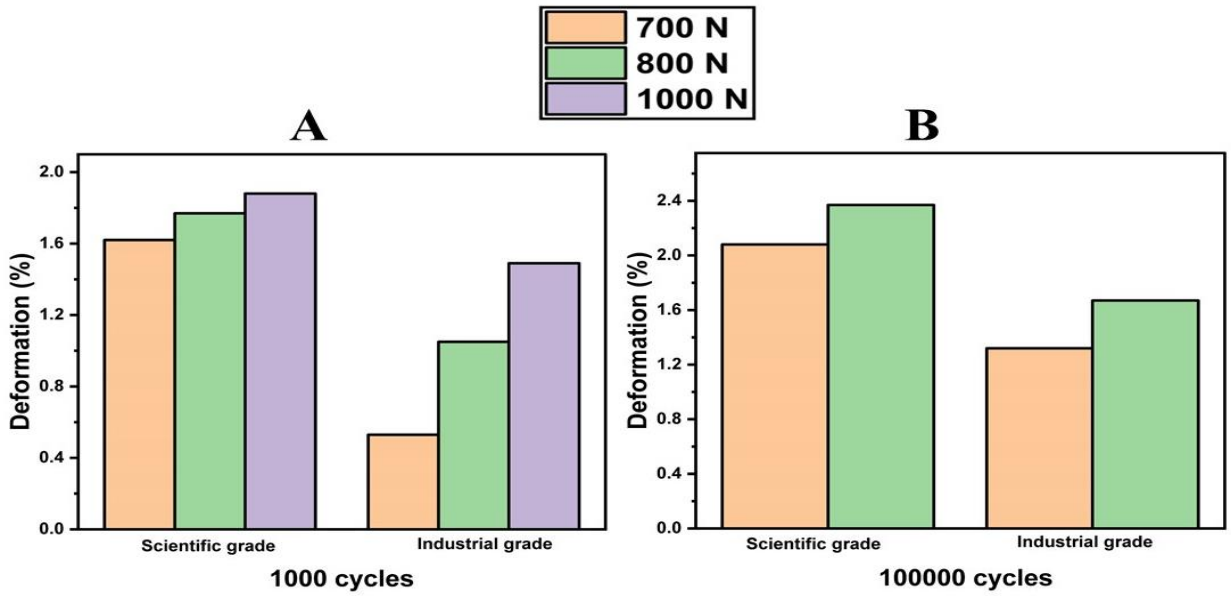

Figure 4. 14 Variation in residual deformation during cyclic loading; (A) Comparison of residual deformation for scientific and industrial grade UHMWPE graft at 1000 cycles; (B) Comparison of residual deformation for scientific and industrial grade UHMWPE graft at 1000 cycles; (B) Comparison of residual deformation for scientific and industrial grade UHMWPE graft at 100000 cycles.

Fig 4.14 depicts residual deformations for industrial and scientific grade UHMWPE prostheses at various cycle counts. Residual deformation is higher for scientific grade UHMWPE. It is obvious that residual deformation rises as the number of cycles rises, yet it tends to settle at high cycle counts and never rises above 3%.

4.7 Porosity of the graft

Porosity of two different types of UHMWPE fabric has been calculated and plotted in Fig 4.15. It's been observed that there is no significant difference in porosity between these two types of UHMWPE graft. Porosity of industrial grade UHMWPE graft is 62.05 and scientific grade UHMWPE is 61.07.

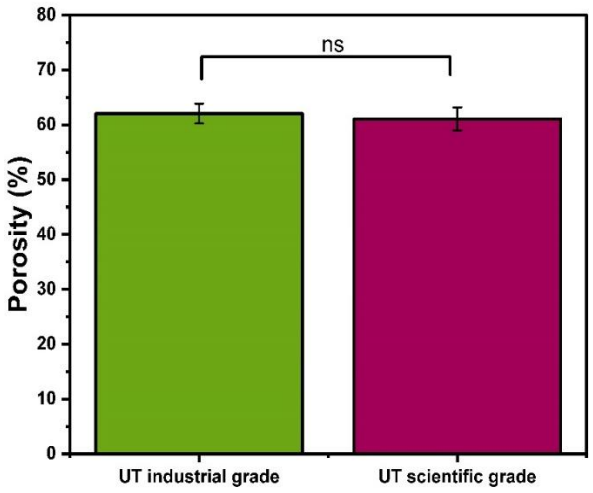

Figure 4. 15 Variation in porosity of two different types of untreated UHMWPE graft.

4.8 Comparative study between two grades of UHMWPE graft

Industrial grade UHMWPE fabric is cheap but may contain more impurities compared to the scientific grade UHMWPE fabric. Here, we studied their load bearing capacities to use them as a medical implant. Industrial grade UHMWPE fabric graft can withstand 3689.5 N which is higher than the scientific grade UHMWPE graft (2238.9 N). From the cyclic loading data, it is obvious

that both grafts can bear 700-1000 N within 1000 cycles and 700-800 N within 100000 cycles. Residual deformation rate is higher for scientific grade UHMWPE graft but very minimal compared to the load bearing capacity which is shown in Fig 4.14. Porosity of both types of UHMWPE graft is similar. The above differences is due to the structure of industrial grade UHMWPE fabric. The fabric thickness and filament diameter are higher in industrial grade UHMWPE fabric than the scientific grade UHMWPE fabric which is mentioned in Table 3.1.

4.9 Discussion and Conclusion

The mechanical qualities of two types of UHMWPE grafts are sufficient for use as the ligament-replacing portion of a prosthetic ligament/tendon device. The design criteria of UHMWPE graft provided by Ge et al.[1]. In comparison to earlier prosthetic devices and currently available L/T replacement choices, a prosthetic with the mechanical behavior and performance provided by the suggested design would have advantages. Currently available alternatives have drawbacks, such as donor site morbidity and the requirement for the harvest operation in the case of autografts and disease transmission risk, slower incorporation, and increased procurement costs in the case of allografts. These drawbacks would be eliminated with a functional prosthetic alternative[270]. The ultimate strength of the suggested design was found to be greater than 2100 N, surpassing that of natural ligament/tendon, which were found to be susceptible to rupture as a failure mode[263].

In younger donors, the linear stiffness of the ACL has been measured between 182 N/mm and 242 N/mm, and as low as 124 N/mm in elderly donors. Autografts and allografts are stiffer than the natural ligament. For example, hamstring graft stiffness can reach 1000 N/mm, yet there have

been no reports of this severely reducing functionality. Here we found that both of our UHMWPE grafts are stiffer than the hamstring graft.

The mechanical behavior of the graft construct throughout healing is not covered by single-cycle load-to-failure testing of ACL grafts, which offers information regarding the mechanical properties at the time of implantation[264]. The early healing phase is characterized by submaximal cyclic stress. Therefore, the purpose of this study is to give a more accurate analysis of the impact of cyclic loading on the parameters of the graft. A suitable ligament/tendon replacement should have high fatigue characteristics in addition to biocompatibility, sufficient mechanical properties (high initial tensile strength, sufficient strain, and high stiffness), and sufficient mechanical properties due to different degrees of forces are repeatedly applied to the artificial ligament graft. This study looked at how cyclic stress affected the artificial ligaments' mechanical behavior to provide an indication of their durability after implantation.

Other issues like fatigue and bending creep were not adequately described in this thesis. These tests are not standardized and might or might not be relevant to in vivo ligament performance, even though they are significant conceptually. The cyclic loading test was carried out in force control mode as opposed to displacement control mode, even though displacement limits would also apply to the native ligament or a ligament replacement to some extent.

To analyze the initial cyclic loading response, Beynon, and Amis (1998) advised loading the knee to 1000 load cycles at 150 N of displacement. Jarvinen et al. chosen to apply 1500 loading cycles ranging from 50 to 200 N at 0.5 Hz to the grafts. Weiler, Richter, Schmidmaier, Kandziora, and Sudkamp (2001) gradually increased force until tendon collapse while applying forces ranging from 50 to 300 N. In a force-relaxation test, Numazaki, Tohyama, Nakano, Kikushi, and Yasuda (2002) stretched the graft by 2 mm every cycle for 5000 cycles. 100 cycles

were repeated with increasing loads up to 850 N by Jarvinen, Kannus, and Jarvinen (2001) and Kousa (2003a, 2003b).

In this study, the prosthetic ligaments were loaded between 50 and 700 N until 60,000 cycles to replicate the stresses placed on the ACL while walking and engaging in vigorous physical therapy, which served as a representation of the equivalent activity for eight weeks. Therefore, it appears that the mechanical performance of the proposed graft declines as the number of cycles increases. It is obvious that residual deformation rises as the number of cycles rises, yet it tends to settle at high cycle counts and never rises above 3%. As a result of the textile structure reaching a fully jammed condition, where further fiber slippage is impossible, after many cycles, residual deformation is stabilized.

Industrial grade UHMWPE graft was superior in mechanical strength rather than scientific grade UHMWPE ligament graft. It may have been due to slight differences in molecular or filament structure of UHMWPE fabrics. The primary differentiation between them is in the filament pattern and braids. Spectra has thicker individual filaments but less filaments to make a weave pattern in fabric. On the other hand, Dyneema has thinner filaments & more of them are added to make an individual weave. Although having excellent mechanical properties of industrial grade and scientific grade UHMWPE graft is it safe to be used for prosthesis is dependent on cell culture studies.

The porosity of two types of UHMWPE graft has been calculated and studied. It's been observed that there is no significant difference between these two types of ligament grafts. Porous membranes are also used in research labs to sustain various multi-compartment microenvironments that mimic intricate physiological functions. The majority of studies on how cells react to porous membranes have indicated a multiphase response in which pore size

increases and frequently pore-pore spacing results in better interactions between cells and their substrate[271, 272].

Further studies needed to understand the surface properties of both UHMWPE fabric. Material properties (weave pattern, thread dimension, molecular weight plays an important role in mechanical strength of material. A greater level of control in manufacturing and characterization of impurities of scientific grade UHMWPE could make it preferred material for implants for regulatory reasons. By changing the fiber composition, diameter, braiding and twisting angles, as well as yarn density, the architecture of the UHMWPE fabric can be altered in terms of pore diameter, porosity, and surface area.

Summary of this chapter

1. Two synthetic UHMWPE ligament graft prototypes were developed by combining Ultra high molecular weight polyethylene (UHMWPE) fabric in a woven structure. Industrial grade and scientific grade UHMWPE ligament graft's tensile behaviour is similar to the native ligament/tendon.
2. Tensile mechanical properties validated the mechanical performance of the synthetic ligament graft prototype. Cyclic loading evaluation of ligament/tendon graft prototype mimics the initial phase of ligament healing. The cyclic loading results indicated both graft materials were able to withstand physiological loads without exceeding the acceptable strain percentage. All experiments were conducted based on standards and literature guidelines.

3. Comparative study between two grades of UHMWPE graft indicated that both were able to carry human loads but the industrial grade graft capacity was higher than that for the industrial grade UHMWPE graft.
4. The mechanical properties of UHMWPE grafts before and after plasma treatment were identical which indicates that plasma treatment does not change the bulk properties of the materials.

The porosity of industrial grade and scientific grade UHMWPE graft was similar and was predicted to be supportive for cell growth and expansion.

In conclusion, the claim made in the introductory part is validated by our data analysis and the results of our experiment.

Chapter 5 : Protein Immobilization on UHMWPE fabric

5.1 Introduction

Over the last few decades, numerous attempts have been made to produce surface immobilized enzymes with the goal of making them easier to utilize in continuous flow processes. When an enzyme or other sort of catalyst is dissolved in the reaction media, it can be difficult to monitor and to recycle. Immobilizing an enzyme can be a simple way to permit the sustained activity of an enzyme, which can considerably improve biocatalytic process economics while also preventing the enzyme activity from being carried over to subsequent steps. The effectiveness of every assay utilizing protein microarrays hinges on selecting the right surface for protein immobilization. An ideal surface should be able to maintain protein functionality with excellent signal-to-noise ratios while also having a high protein-binding capacity and providing an extended shelf life (Smith et al., 2005; Tao et al., 2007).

Immobilization of peptides or growth factors on well-known biodegradable polymers has shown significant promise in terms of increasing bioactivity and establishing a more supportive environment for cells to attach, expand, and generate matrix [273]. Immobilized peptides or growth factors can improve stem cell homing capacity and have important consequences for in vivo immune responses. Growth factors delivered by scaffolds can modulate local cellular responses as well as induce neo-vascularization and encourage mesenchymal stem cells from neighboring tissues[274, 275]. Protein immobilization on an orthopedic surface enables more precise control of the implant's biological interactions with the body. Since the beginning of protein functionalization for orthopedics, several techniques have been examined. Some of the most commonly used immobilization methods include entrapment, encapsulation, connection to a solid support, and self-immobilization [221].

The tendon/ligament-bone interface is a continuous slow transition of three different types of tissues within the body: tendon/ligament, fibrocartilage, and bone. Such transition zones also include the associated cells fibroblasts, fibro chondrocytes, and osteoblasts[276]. Collagen is the major component of tendons and ligaments, and the appearance of collagen types I and III, as well as decorin in minor levels, is typical of these tissues[277]. The fibrocartilage portion, which connects the tendon/ligament and bone tissues, is the most important part of this interaction. The Musculoskeletal (MSK) tissue recovery process after an injury can be broken down into five different phases: hematoma formation, inflammation, progenitor cell recruitment, matrix deposition, and matrix remodeling[278].

Plasma treatments are one of the recent techniques widely explored in the field of biomedical device development. Various functional reactive species on the surface of the plasma treated material changes the surface properties of the material[52, 279, 280]. Several patents covering the use of plasma activated polymer substrates to bind functional biological molecules have been successfully submitted by Prof. Marcela's group in the last few years[247, 281]. The innovation describes a simple method for generating a polymer substrate functionalized with a biological molecule that only requires two stages.

During plasma immersion ion implantation, the first stage entails exposing a surface of a polymer substrate to plasma treatment with a suitable plasma generating gas. The second stage is to simply incubate a desired biological molecule on the surface that has been treated in the first stage. Numerous peer-reviewed studies have supported the invention, which covers a variety of substrate materials such as PEEK, polystyrene, nylon, PET, and PTFE, as well as a variety of biomolecules such as horseradish peroxidase (HRP), catalase, and soybean peroxidase (SBP), as well as the extracellular protein monomer tropoelastin[247]. However, the number of clinical

procedures based on the patent claims is still limited, particularly in the field of biomedical and orthopedic polymers. The goal of this research is to extend the use of the patented method to UHMWPE polymers, with an emphasis on biomedical applications.

Altering the fundamental substrate polymer may result in new and unexpected consequences due to the random and unpredictable nature of plasma treated polymer surfaces. As a result, it's critical to perform a thorough investigation to see if the patented technology can be applied to binding biomolecules to UHMWPE. The binding of different proteins to modified UHMWPE surfaces will be investigated in this chapter through immunostaining.

Immunostaining is used here to examine differences in protein expression, localization, and distribution in UHMWPE structures. We can visualize the protein attachment on the surface. How much the surface is covered with proteins can be detected easily through immunostaining. Immunostaining is used here for (i) clarity (ii) high specificity (iii) high sensitivity (iv) ease of operation (v) sample positioning etc.

Since UHMWPE polymers are now used mostly in the musculoskeletal engineering, some bone-muscle related ECM proteins, such as collagen, and fibronectin, will be examined here. Furthermore, to assess the functionality of the immobilized biomolecules directly, release kinetics of Fluorescein Isothiocyanate Conjugated-Bovine Serum Albumin (FITC–BSA) from UHMWPE was observed. Furthermore, the predicted covalent bond between the activated polymer and the biomolecules will be investigated because it could have a direct impact on the technology's durability and variety of potential uses. The purpose of the study is also to differentiate the binding events between two different samples (industrial & scientific grade) of pure UHMWPE fabric and PIII treated UHMWPE fabric. Additionally, determining whether the immobilization impacts the proteins' functions is crucial for the technology's future usefulness.

5.2 Aims & hypothesis of the chapter

Overall, the aims of this chapter can be summarized as the following:

1. Evaluation and comparison of protein absorption or immobilization on treated and untreated industrial grade & scientific grade UHMWPE fabric surfaces

2. Evaluation and comparison of PIII mediated covalent bonding of industrial & scientific grade UHMWPE with immobilized proteins BSA, collagen and fibronectin.

3. Determine the release kinetics of Fluorescein Isothiocyanate Conjugated-Bovine Serum Albumin (FITC–BSA) from UHMWPE fabric.

It is expected to immobilize protein molecules on the PIII treated UHMWPE fabric due to the presence of free radicals but not on the untreated UHMWPE fabric. For release kinetics assay, Scientific grade UHMWPE can show better results than the industrial grade UHMWPE fabric based on previous results mentioned in the thesis.

5.3 Experimental methods

5.3.1 Materials

Collagen type 1 from calf skin (catalogue no: Sigma C9791), Fibronectin (Gibco Cat# 33016-015), were among the proteins identified in this thesis. Monoclonal anti-Collagen type I antibody produced in mice (Sigma 2456). and Collagen type 1 antibody produced in mouse (catalogue no: C2456). bovine serum albumin, sodium dodecyl sulphate (SDS), phosphate buffered saline (PBS), dimethyl sulfoxide, Goat Anti-mouse-IgG antibody, and Alexa flour 488 were also used

in this thesis. Bovine plasma was purchased from Merck. Fluorescein labeled Bovine Serum Albumin conjugate (FITC-BSA) was purchased from Life technologies Australia. The secondary antibody employed in all these tests was a conjugated anti-mouse IgG antibody generated in goats (Sigma A4416).

5.3.2 PIII treatment procedure

The PIII treatment technique followed the protocol developed in the early stages of this investigation, and the surface characterization chapter provides all the details. The industrial & scientific grade UHMWPE fabric samples were sterilized under UV treatment and cut into 6 cm x 8 cm strips for protein binding experiments, then plasma treated on both sides and trimmed down to 0.8 cm x 0.8 cm rectangles that just fit into the bottom of the wells of a 24 well plate.

5.3.3 SDS washing protocol

The organic chemical sodium dodecyl sulfate (SDS) has the formula $CH_3(CH_2)_{11}OSO_3Na$. It is an anionic surfactant that's often employed in the Sodium dodecyl sulfate Polyacrylamide gel electrophoresis (SDSPAGE) procedure to prepare proteins for electrophoresis. SDS operates by disrupting non-covalent interactions in proteins, causing them to denature and change their original shape. SDS coats proteins with a significant negative charge, allowing them to be separated on an SDSPAGE gel only by size. SDS is employed in this thesis to remove non-covalently bound proteins that are just physically adsorbed onto a polymer surface since it eliminates all non-covalent linkages.

To build productivity, the SDS washing stage was carried out under harsh conditions, with the incubation temperature raised to 95°C for 10 minutes. All non-covalently bound proteins should

be removed during this rigorous washing process, and any proteins identified on the surface afterward are assumed to have made at least one covalent connection to the surface.

5.3.4 Protein immobilization on UHMWPE fabric

One of the goals of this thesis was to immobilize biomolecules covalently onto a UHMWPE woven fabric surface without the use of complex chemical procedures or linkers. To coat each ECM protein or enzyme onto the fabric surface, a sample was simply soaked in a sufficient concentration of protein for long enough to guarantee that the maximum quantity of proteins attached to the surface. The concentration of the collagen and fibronectin proteins used was 8ug/ml.

5.3.5 Immobilization of Alexa fluor 488

The Alexa Fluor 488 dye is a vivid, green, fluorescent dye with excitation perfectly matched to the 488 nm laser line. High molar ratios of Alexa Fluor 488 dye molecules can be used to bind to proteins without considerable self-quenching, resulting in brighter conjugates and more accurate detection. For cellular labelling and detection, Alexa Fluor 488 dye has been attached to a wide range of antibodies, peptides, proteins, tracers, and amplification substrates.

The nature of protein attachment on untreated and PIII treated UHMWPE was investigated in this experiment. The nature of protein attachment on untreated and PIII treated UHMWPE was investigated by IgG binding assay. The UHMWPE samples were cut into 6 cm x 8 cm strips for the protein binding assay, plasma treated on both sides, and then trimmed down to 0.8 cm x 0.8 cm rectangles that just fit into the bottom of the wells on a 24 well plate.

In the IgG binding assay,it is assumed that Alexa fluor 488 conjugated fluorescent proteins will bind to the untreated and treated surfaces and washing will remove non covalent proteins from the surfaces. Samples were incubated in Alexa fluor 488 labeled goat anti mouse IgG (H+L) protein in PBS buffer for 1 hour with a concentration of 8 μg/mL. After incubation, the samples were carefully washed with 3 X 1 ml PBS to eliminate any remaining unattached protein.

Samples of Each of the above UHMWPE fabrics are placed in 50ml falcon tubes filled with 5% sodium dodecyl sulfate in MiliQ water and rotated for the same number of hours as above to remove any non-covalently bound IgG from the surface of the fabric to provide an indication or what proportion of the fluorescently labelled protein covalently bound. Physisorbed molecules were removed by washing whereas covalently bound protein was retained.An Olympus Bx51 microscope was used for fluorescence imaging to observe the immobilized protein on the UHMWPE surfaces.

5.3.6 Collagen covalent attachment assay

The Collagen type I was used to examine the protein attachment capabilities of the UHMWPE surfaces. Collagen is the primary and most important extracellular matrix component of the human body[182]. It is vital for functions as diverse as cell separation, cell relocation and mechanical properties of tissues. It is mainly observed in the form of elongated fibrils in connective tissues such as tendon, ligament, skin, cartilage, bone etc.[282]. Mechanical strength of ligament and tendon comes from the collagen. Increased interior crystallinity and a broad range of fibril sizes / are observed in Collagen type-I structures [283]. Each collagen has a unique triple helix structure that serves as their identifying characteristic. Three polypeptide chains with a glycine residue in every third position constitute its structure. The amino acid

sequence of collagen is unique, and the mandatory glycine is essential for the formation of the triple helix. The three-dimensional structure of collagen is formed by the three polypeptide chains[284]. In vitro and in vivo, collagen type-I has been employed in ligament/tendon tissue engineering[285].

In various tissues, including tendons, collagen type III, fibrillar collagen made up of a homotrimer of chain type 1(III) amino acids, is a copolymer of collagen I. It is also known to be abundant at tissue healing and repair sites[286]. Collagen type III can be expressed in very small amount during L/T differentiation[287]. Some published articles have used collagen type III as an L/T marker for gene expression assay[288, 289].

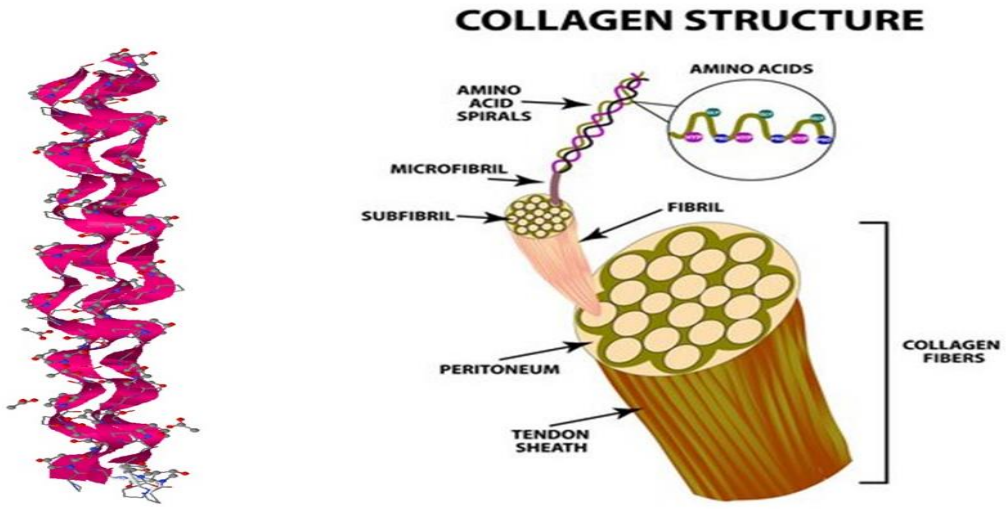

Figure 5. 1 Structure of collagen Type-I.

For the collagen binding assay, 0.8 cmx 0.8 cm strips of untreated and PIII treated UHMWPE fabric were incubated with collagen (15 μg/mL in PBS) for 1 hour and then washed with 1 ml PBS twice. Collagen molecules were then labeled with primary antibody (anti collagen type 1 antibody) for 1 hour at room temperature and then washed with 1ml PBS for three times. Then the primary antibody was labeled with a secondary antibody (anti-mouse IgG antibody produced

in goat and conjugated with Alexa fluor 488) for 1 hour at room temperature followed by 1ml PBS washing step for 3 times to remove any unbound antibodies. An Olympus Bx51 microscope was used for fluorescence imaging to observe the immobilized protein on the UHMWPE fabric surfaces.

5.3.7 Fibronectin

The adherence of numerous cell types is significantly influenced by fibronectin. In tissues and the extracellular matrix of cultivated cells, fibronectin can either be found as an insoluble protein or soluble in plasma, other body fluids. Numerous additional macromolecules that interact with fibronectin including collagen[290]. Collagen and fibronectin are important components of extracellular matrix in vertebrates. The development and properties of various tissues are influenced by their connection and redistribution[291].

Fibronectin (Fn) is a large, glycosylated protein that forms fibrils in the ECM and is made up of many copies of three domain classes: Fn-I, Fn-II, and Fn-III. It is involved in a variety of physiological processes, including embryogenesis, wound healing, hemostasis, and thrombosis etc. [290].

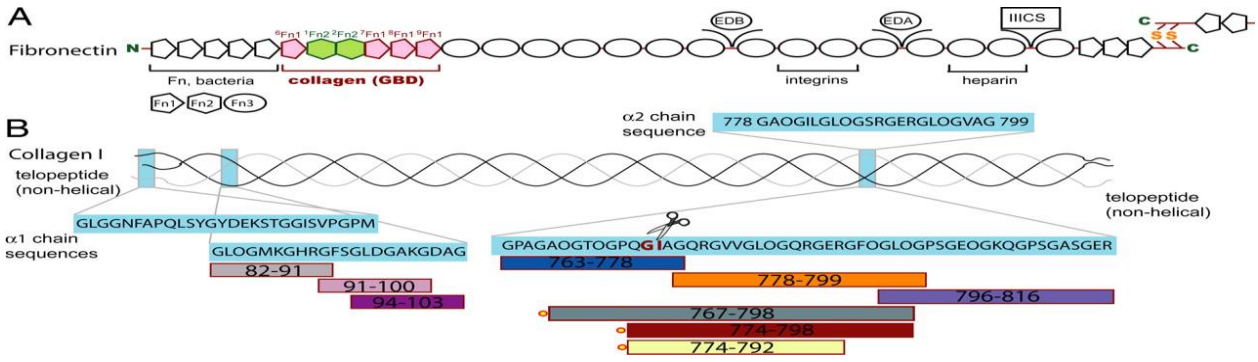

Figure 5. 2 Fibronectin fragments and collagen-derived peptides are shown schematically. (A) Domain structure of human fibronectin, showing the dimerization site and the alternatively spliced EDB, EDA, and IIICS sections. The gelatin-binding domain (GBD) is colored and

numbered according to the type of domain (pink, type I; green, type II). (B) Type I collagen is made up of two chains: one (black) and one (grey). Peptides from various regions are color-coded, and fluorescent tags are represented by red circles.

5.3.8 Release kinetics of FITC-BSA

The aim of this study is to observe the release kinetics of protein (BSA) coated UHMWPE fabric alone and in the presence of collagen /fibronectin. As we know that release kinetics of proteins (growth factors such as basic fibroblastic growth factor, endothelial growth factor, insulin like growth factor etc.) plays an important role in ligament/tendon regeneration during the three phases of L/T healing process. The release kinetics of FITC-BSA observed with both industrial and scientific grade untreated and PIII treated UHMWPE fabric. BSA used as a model protein in this experiment due to its availability, similarity to albumin in body fluid. This experiment was conducted to examine the prolonged release kinetics, protein-protein interactions, and how they have interacted with the PIII treated material. 10ug of FITC-BSA conjugate was observed here as a model protein (as growth factors) based on experiments conducted by Natalie[226]. It was delivered into the UHMWPE fabric as described below.

The UHMWPE fabrics (UT+ PIII treated) samples were cut into small pieces with a 1.9 cm^2 area. Samples were divided into 3 groups: (i) samples were incubated in FITC–BSA solution (BSA only); (ii) samples were incubated in FITC–BSA combined with collagen solution (Col BSA); and (iii) samples were incubated in FITC-BSA combined with fibronectin (Fibronectin BSA). FITC-BSA, collagen and fibronectin solutions were prepared with a concentration of 10ug/mlin (solution) respectively. Each sample was placed in a well of a 24-well tissue culture plate with (volume) incubation solution and incubated for 24 hours. They were washed in serum-free media at 37^oC for an hour and dried in ambient conditions. They were then placed in a well of a 24-well tissue culture plate containing 0.5 ml of serum-free medium. The whole volume of

media was taken from each well and thoroughly replaced at 1 hour, 5 hours, 1, 4, 7, 11, 15, 18, and 21 days. The fluorescence absorption of the taken media was measured using a plate spectrophotometer (Multiskan EX microscope spectrophotometer, Thermo Scientific).

5.4 Data Presentation and Statistical Analysis

Origin and Microsoft Excel were used to construct and assess all figures and statistical analyses relevant to the conclusions in this chapter. Two-tailed t-tests were performed to compare groups, with a P value of 0.05 indicating significance. Unless otherwise noted, each experiment employed at least three triplicates and a minimum of three biological replicates to assure statistical validity of the results.

5.5 Experimental Results

5.5.1 Protein (Alexa fluor 488) covalent bio-functionalization of PIII-treated industrial grade UHMWPE fabrics

We compared the strength of protein binding on the fabrics before and after the PIII treatment by observing the signal of Alexa fluor 488 fluorescently labeled IgG. Fig 5.3 shows images taken on untreated and PIII treated fabrics after each step. Higher levels of autofluroscence noticed from the untreated control industrial grade UHMWPE fabric compared to that for scientific grade UHMWPE fabric. Possible reasons could be the presence of contaminants not removed during the manufacturing process.

After the immobilisation with IgG bound Alexa fluor 488, strong fluorescence can be seen on both UT and PIII-treated surfaces with brighter signal on the PIII-treated surface. The SDS wash

removed IgG entirely with deappearance of fluorescencs from the untreated fabric while fluorescence still visible on the PIII treated fabric, as evidenced by the dark colour on the UT versus the bright green observed on the PIII treated surafce. This suggests that the robust protein attachment observed on the PIII treated surfaces is due to covalent bonding rather than physical adsorption. This finding is consistent with protein attachment from previous studies of PIII treatment on other flat polymer surfaces such as polyurethane[85] in which the covalent bonds were assigned to the reaction between the protein molecules with radicals embedded on the polymer surfaces[85].

Thus it can be concluded that that the robust protein attachment found on the PIII ion-implanted surfaces is the result of a covalent connection rather than physisorption. The technology to covalently immobilise proteins onto a hydrophilic surface is a significant advance that potentially allows protein structure and bioactivity to be preserved (Fig 5.3D &E).

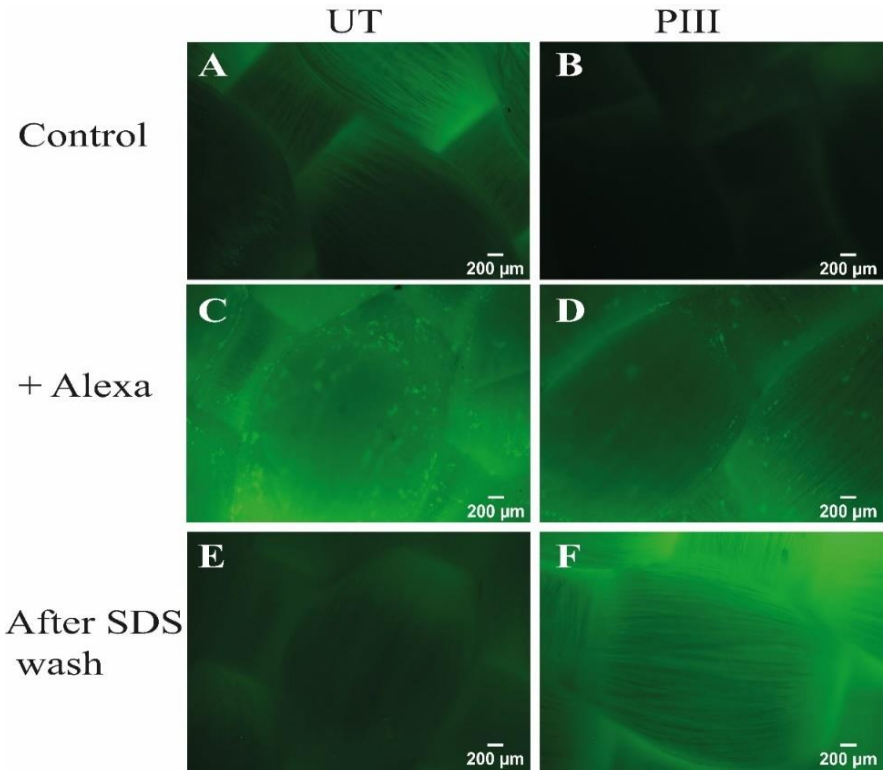

Figure 5. 3 Fluorescence images of the fabrics; (A) and (B) Bare Untreated (UT) and PIII treated UHMWPE. (C) and (D) UT and PIII treated UHMWPE immobilized with Alexa. (E) and (F) UT and PIII treated UHMWPE immobilized with Alexa after SDS wash.

5.5.2 Protein (Collagen Type-I) covalent bio-functionalization of PIII-treated fabrics

Similar observations were found when collagen was immobilized on the UT and PIII treated industrial grade fabrics (Fig 5.4). The significant increase of fluorescence signal on both surfaces after the secondary antibody (anti-mouse IgG antibody produced in goat and conjugated with Alexa fluor 488) indicates that collagen molecules attached on both surfaces and hence enabled the attachment of the first antibody where the secondary antibody bound.

The SDS wash substantially reduced the collagen molecules on the untreated UHMWPE surface, which is consistent with the decrease in fluorescence intensity. In contrast, the strong signal that was still present after PIII treatment of the surface confirmed that collagen had adhered there

covalently. This demonstrates that the protein molecules that were physically adsorbed onto the UT surface are rinsed off due to weak bonding mechanism were responsible for the UT signal.

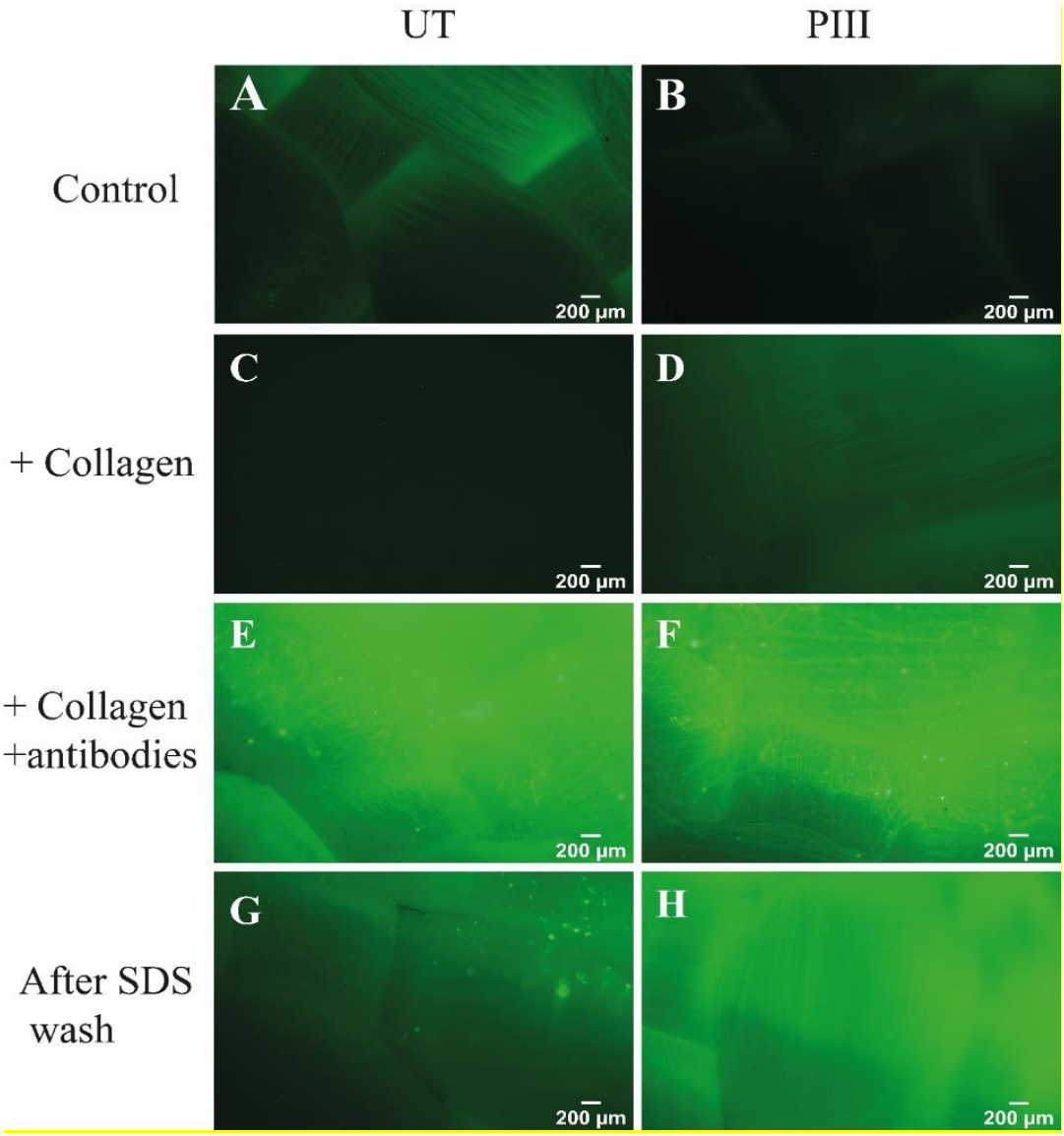

Figure 5. 4 Collagen type I immobilization on treated and untreated UHMWPE. (A) and (B) bare Untreated and PIII treated UHMWPE; (C) and (D) UT and PIII treated UHMWPE incubated in collagen solution only; (E) and (F) UT and PIII treated UHMWPE incubated in collagen--antibody solution; (G) and (H) Incubated UT and PIII treated UHMWPE in collagen-antibody solution; after SDS wash.

5.5.3 Release kinetics of FITC-BSA on untreated & PIII-treated industrial grade UHMWPE fabrics

In this study, the kinetics of the release of fluorescently labeled BSA into the surrounding media were determined (in contrast to the previous study which assessed retention of labeled protein on the UHMWPE).

Fig 5.5 illustrated the release kinetics of FITC-BSA on untreated and two different types of plasma treated UHMWPE fabric. It's clearly observed that absorbance isn't consistent for untreated industrial grade UHMWPE fabric. First few hours 5,18 & 20 hours absorbance of untreated industrial grade UHMWPE is considerably higher. Absorbance is decreased over the next few days and then increased and again decreased till day 30.

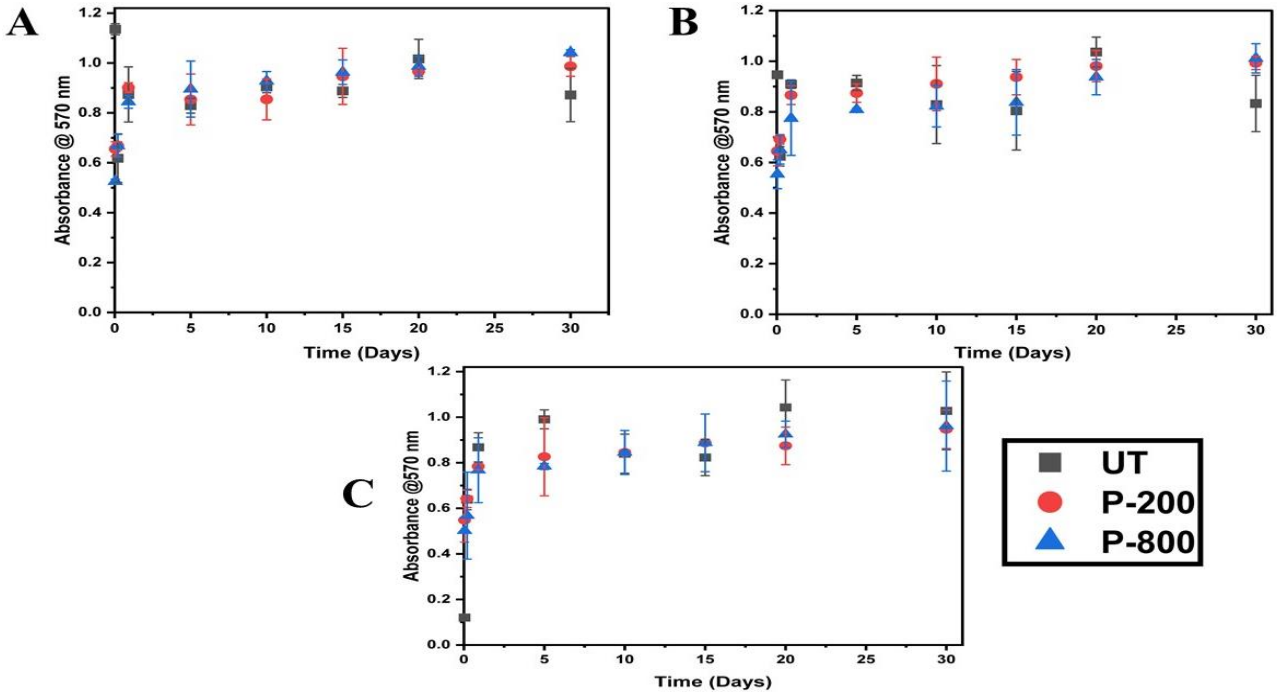

Figure 5. 5 Release kinetics of fluorescein isothiocyanate conjugated BSA from 3 different types of UHMWPE fabric(A) FITC-BSA without any protein released from untreated & PIII treated industrial grade UHMWPE fabric (B) FITC-BSA-Collagen released from untreated & PIII treated industrial grade UHMWPE fabric (C) FITC-BSA-Fibronectin released from untreated & PIII treated industrial grade UHMWPE fabric.

FITC-BSA molecules were immobilized on untreated and PIII treated surfaces (200s and 800s treatment) with or without additional presence of collagen type I or Fibronectin protein. The FITC-BSA sustained release from these samples is shown in Fig 5.5 (A),(B) & (C). Untreated UHMWPE has burst release with BSA alone. Fibronectin has some effect on BSA release. A burst release pattern for FITC-BSA was noted during the first 1 hour in untreated UHMWPE fabric with or without additonal protein. In contrast, the PIII treated 200s and PIII treated 800s samples did not display an initial burst release of BSA; instead, they showed a consistent steady release of BSA within the first 21 hours of the experiment. Concurrent collagen and fibronectin coating didn't influence the release pattern for industrial grade UHMWPE fabric.

5.5.4 Protein (Alexa fluor 488) covalent bio-functionalization of PIII-treated fabrics

The evidence for covalent immobilization of Alexa fluor 488 has also been assessed on scientific grade UHMWPE fabric. Samples were incubated with IgG conjugated with Alexa fluor 488 and in PBS overnight at room temperature to achieve the attachment. After the immobilization, samples were either rinsed with water or washed stringently in SDS.

Fig 5.6 shows images taken on untreated and PIII treated fabrics after each step. After the immobilisation with Alexa fluor 488, strong fluorescence can be seen on both surfaces with brighter signal on the PIII-treated surface. The SDS wash removed IgG entirely from the untreated fabric while it still remained on the PIII treated sample, evidenced by the dark colour on the UT versus the bright green observed on the PIII treated surafce. This suggests that the robust protein attachment observed on the PIII treated surfaces is due to a covalent bonding rather than physical adsorption.

This finding is consistent with protein attachment from previous studies of PIII treatment on other flat polymer surfaces such as industrial grade UHMWPE & polyurethane[85] in which the covalent bonds were assigned to the reaction between the protein molecules with radicals embedded on the polymer surfaces[85]. This reveals that the robust protein attachment found on the ion-implanted surfaces is the result of a covalent connection rather than physisorption. The technology to covalently immobilise onto a hydrophilic surface is a significant advancement that potentially allows protein structure to be preserved for in vitro experiments (Fig5.6 D &E).

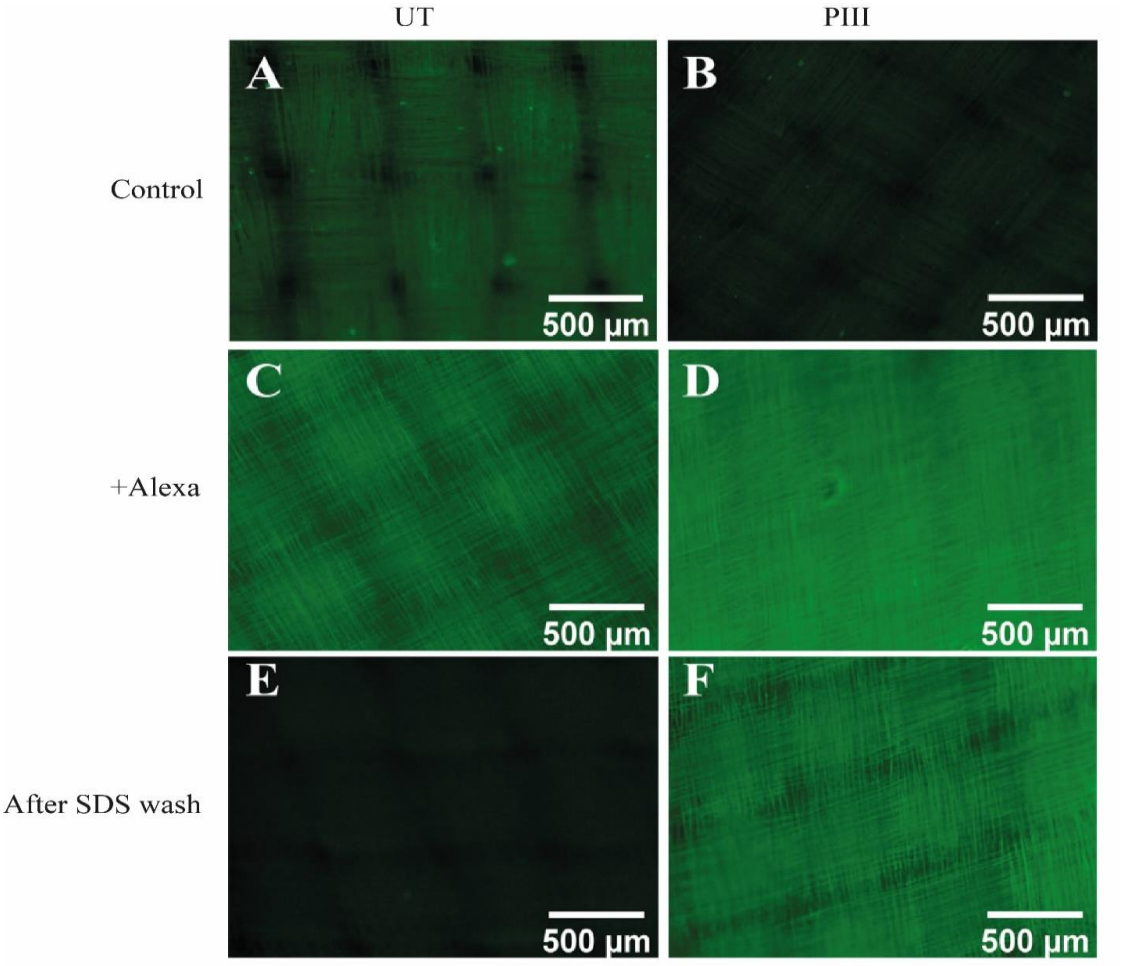

Figure 5. 6 Fluorescence images of the fabrics; (A) and (B) Bare Untreated (UT) and PIII treated UHMWPE. (C) and (D) UT and PIII treated UHMWPE immobilized proteins labelled with Alexa fluor 488. (E) and (F) UT and PIII treated UHMWPE immobilized with Alexa fluor 488 after SDS wash.

5.5.5 Protein (Collagen Type-I) covalent bio-functionalization of PIII-treated fabrics

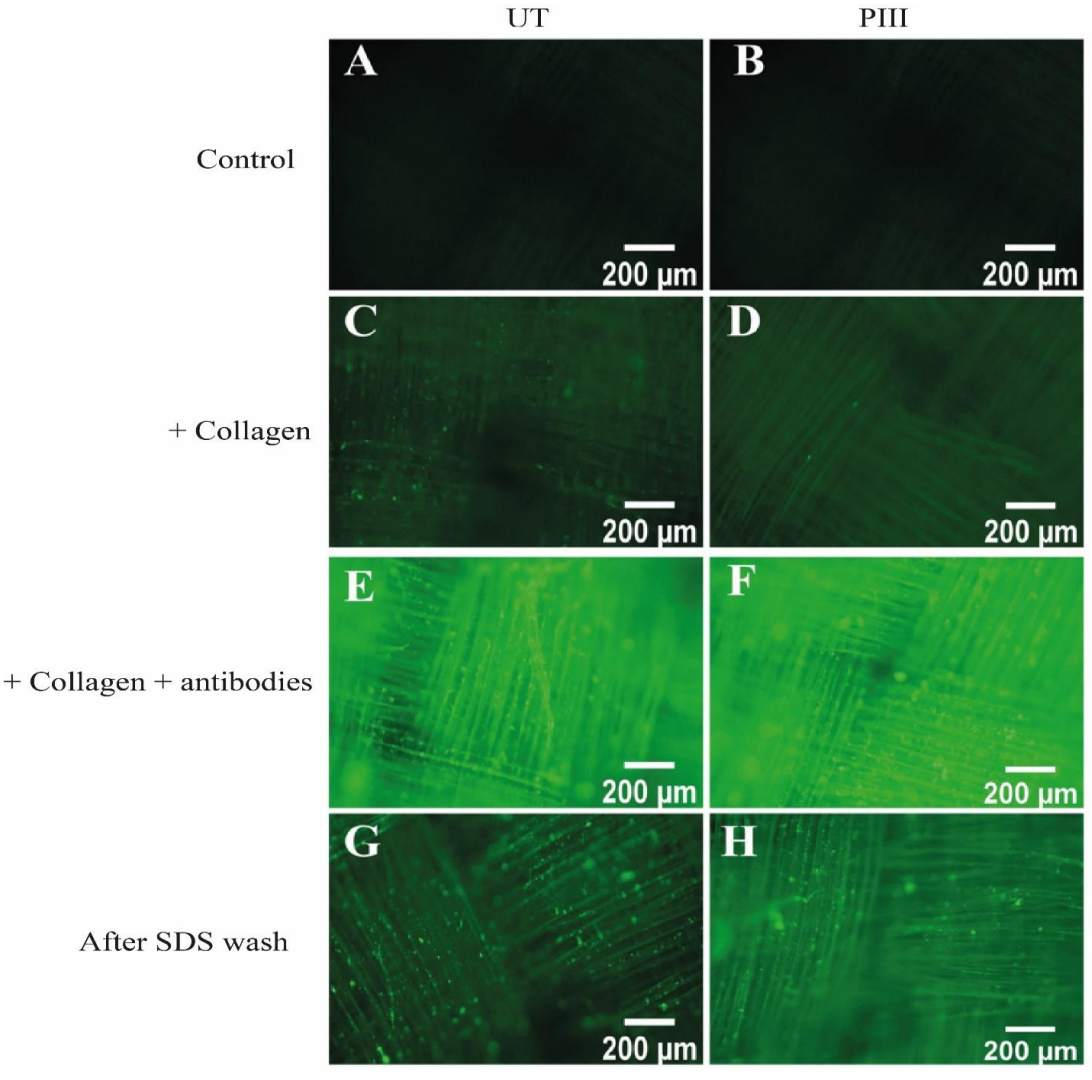

Figure 5. 7 Collagen type I immobilization on treated and untreated UHMWPE. (A) and (B) bare Untreated and PIII treated UHMWPE; (C) and (D) UT and PIII treated UHMWPE incubated in collagen solution only; (E) and (F) UT and PIII treated UHMWPE incubated in collagen-antibody solution; (G) and (H) Incubated UT and PIII treated UHMWPE in collagen-antibody solution; after SDS wash.

Similar observations were found when collagen was immobilized on the UT and PIII treated fabrics (Fig 5.7). The significant increase of fluorescence signal on both surfaces after the secondary antibody (anti-mouse IgG antibody produced in goat and conjugated with Alexa fluor 488) indicates that collagen molecules attached on both surfaces and hence enabled the

attachment of the first antibody where the secondary antibody bound. The SDS wash largely removed the collagen molecules on the UT, correlating to the fluorescence intensity reduction, which is in contrast to the bright signal on the PIII treated surface, confirming the covalent attachment of collagen on the PIII treated fabrics as opposed to the physical adsorption on the UT surface.

5.5.6 Release kinetics of FITC-BSA on untreated & PIII-treated scientific grade UHMWPE fabrics

FITC-BSA molecules were immobilized on untreated and PIII treated surfaces (200s and 800s treatment) with or without protein is showed in Fig 5.8 (A ,B & C). Untreated scientific grade UHMWPE fabric showed fast release pattern during first few hours but later decreased compared to the collagen and fibronectin coated UHMWPE fabric. Collagen and fibronectin induced initial release pattern for untreated UHMWPE surface. PIII treated -200 s & 800s with BSA alone showed very slow release pattern compared to the untreated UHMWPE fabric.

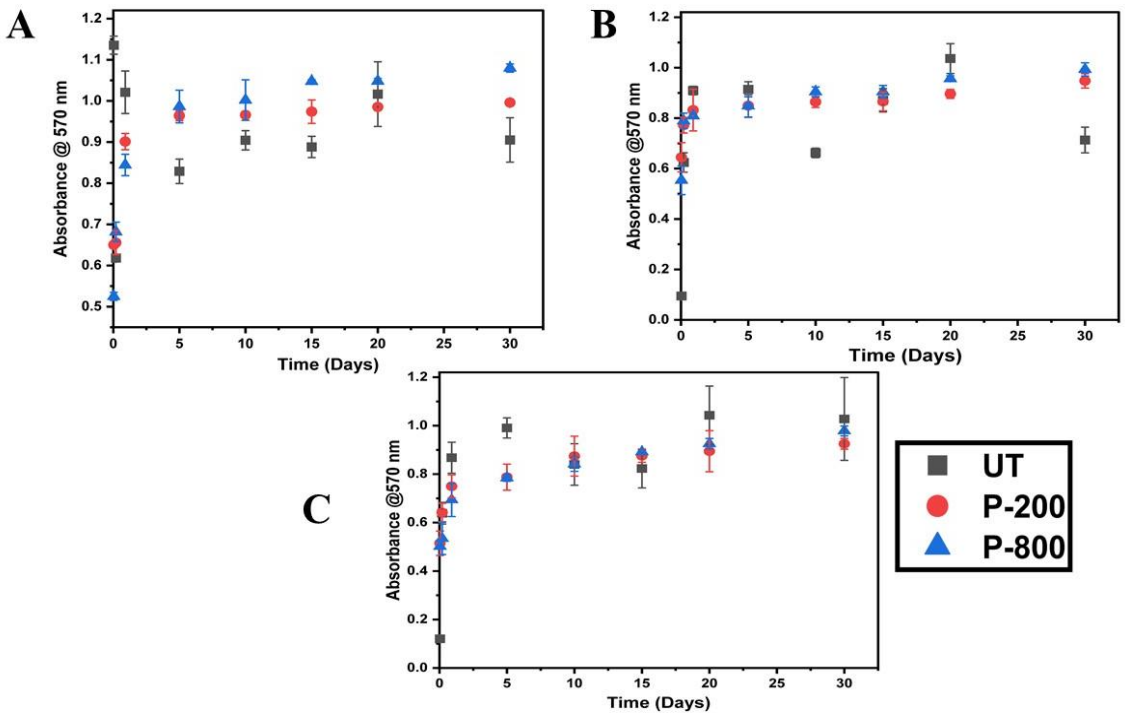

Figure 5. 8 Release kinetics of fluorescein isothiocyanate conjugated BSA from 3 different types of UHMWPE fabric(A) FITC-BSA without any protein released from untreated & PIII treated UHMWPE fabric (B) FITC-BSA-Collagen released from untreated & PIII treated UHMWPE fabric (C) FITC-BSA-Fibronectin released from untreated & PIII treated UHMWPE fabric.

Collagen and fibronectin have effect on release kinetics on untreated UHMWPE fabric but not on PIII treated surface. An initial burst release was noted during the first 1 hour in untreated UHMWPE with or without protein for FITC-BSA. In contrast, the PIII 200s and PIII 800s samples did not display an initial burst release of BSA; instead, they showed a consistent steady release of BSA within the first 21 hours of the experiment. After day 5, release kinetics from all PIII treated surfaces were constant, steady, and insignificant.

This slow release pattern is recommended over a burst release because growth factors are primarily needed in the second and third stages of ligament healing (hemostasis and inflammation, cellular proliferation and matrix deposition, and long-term remodeling) rather than

during the first inflammatory reaction[220]. Similar to observations with industrial grade fabric, the presence of collagen and fibronectin coatings also did not influence the release pattern.

5.6 Discussion and Conclusion

The objective of this chapter was to examine the protein binding properties of the UHMWPE surfaces with and without PIII treatment. Protein immobilization was observed for two different types of UHMWPE fabric with PIII providing more stable binding. Generally, there are two main aspects to this discussion. The properties of the layer of bound proteins were first looked at in terms of the fluorescence signal of the bound protein itself or its binding to fluorescently labeled secondary antibodies. Second, and perhaps more crucially, it was determined whether the immobilization of proteins served the goal of regulating protein release from the UHMWPE material surface as required for full biofunctionalization. This was simply demonstrated in this chapter by immobilizing proteins on the surfaces and monitoring their release kinetics. The goal of biofunctionalization is further examined using living cells as a model and assessing their biological reactions using various techniques in the next chapters.

According to the fluorescence results in this case, both PIII treated UHMWPE fabric surfaces were able to bind a substantially higher quantity of proteins, such as Alexa fluor 488 and collagen, to the surface. In this chapter, it was demonstrated that UHMWPE fabric may covalently bind biomolecules following the nitrogen based PIII treatment. Our group has already shown in several prior investigations that PIII treatment of various polymers, such as PC, PS, and PUR, results in the capacity to covalently bind biomolecules[85, 144, 249].

The SDS washing experiment was crucial in enabling the drawing of this conclusion. After SDS washing, surfaces treated with PIII treatment were able to retain a substantial amount of protein,

but untreated surfaces had their protein detection reduce to background levels comparable to the negative controls. Proteins are known to bind to hydrophobic polymer surfaces quickly, and the PIII treatment typically changes the surface so that it is much more hydrophilic. When there is a larger difference in hydrophilicity levels, there is a higher degree of confidence in this judgement.

Whereas the SDS washing technique has already been demonstrated in the literature, there are still certain drawbacks to the technique that need to be mentioned. SDS, a potent anionic detergent, breaks the tertiary structure of the protein by breaking all non-covalent bonds. The way the epitope is exposed to the antibodies because of this significant alteration in protein structure affects the degree of detection during ELISA testing. Antibodies frequently recognize conformational epitopes, or the tertiary structure of the protein, and as soon as this ability is compromised by SDS washing, the antigen can no longer be distinguished.

Fluorescence microscope was used to identify the presence of bound proteins on the surface of the material before and after the PIII treatment. ESR is the preferred method for detecting the presence of free radicals responsible for covalent bonding with protein molecules and strengthen the protein attachment on the treated surface. The resistance of protein removal on the nitrogen based PIII treated UHMWPE fabric when using stringent wash with SDS is consistent with previous findings on the PIII treated LDPE and other polymers[246]. It has been shown that the conformation of the immobilized proteins on the PIII treated polymers was largely unchanged and hence, they likely remained functional as will be addressed in a later chapter.

Prolonged release kinetics, protein-protein interactions, and how they have interacted with the PIII treated material was evaluated in BSA release kinetics study. BSA has been chosen as a model protein due to its availability and similarity with albumin protein in the body fluid. It

needs further study. It's a complicated dynamic so pretty much difficult to explain but we can say that it has prolonged release kinetics of collagen and fibronectin. If we can add more protein can bind more and might have significant effect on release kinetics. The concurrent binding of several proteins on a material surface can result in interference if they compete for the same binding sites.

The release kinetics of BSA from untreated and PIII treated UHMWPE fabric alone and with collagen/fibronectin confirms that PIII treatment can influence slow-release pattern which is beneficial for L/T healing process. The half-life of growth factors is short, making it impossible for exogenous growth factors to play a role in regeneration without the help of a carrier that controls its release. It's been reported that sustained delivery of growth factors such as bone morphogenic protein (BMPs) to bone defect sites is beneficial for long-term bone/ligament regeneration compared to single high-dose bursts of BMPs[292].

Summary of this chapter

The following points serve as a summary of the main results of this chapter

- It has been demonstrated that the ECM protein collagen can be covalently immobilized on the PIII-treated surface.
- A small concentration of proteins can be detected on untreated surfaces due to the physical adsorption of biomolecules. However, as the results have revealed, a higher concentration of covalently bound proteins can be detected on the PIII treated samples. It is likely that this will vary depending on the physical characteristics of the proteins themselves.

- Release kinetics of BSA protein suggest that slow-release patterns can be achieved through PIII treatment. Sustained exposure of connective tissues cells to growth factors is likely superior to burst release kinetics where the growth factor is quickly cleared by body fluids[293].
- Both industrial grade and scientific grade fabrics have shown similar results for protein immobilization and release dynamics, but industrial grade UHMWPE fabric had a higher fluorescent indicating higher levels of impurity.

Hypothesis was supported by the data provided and explained in the above sections.

Chapter 6 : The Biocompatibility & Bioactivity of PIII modified UHMWPE fabric

6.1 Introduction

Polymeric materials have been widely investigated and analyzed for biomedical applications due to their low density, flexibility, simplicity of manufacture, and cost-effectiveness characteristics. But frequently, their surface characteristics fall short of the requirements of different biomedical applications[294]. Biomaterials that come into direct interaction with the human body must have a challenging blend of bulk mechanical properties and surface properties to function effectively in the physiological environment.

As a result, to achieve the necessary surface properties while maintaining the bulk properties of the polymers utilized, an extra surface modification step is frequently required. Plasma treatment is one of the most common procedures for achieving such an outcome. Plasma is used for surface treatment of polymers for a variety of scientific and technological objectives. Although most polymers have excellent chemical inertness and weight-to-strength ratios, they frequently have poor bioactive characteristics[120].

Plasma treatments can be utilized to easily change surface chemistry of biomaterials by bonding functional species onto their surfaces. Plasma only affects the surface of polymers; it doesn't change the bulk properties of the material. Plasma methods are also more ecologically friendly than traditional wet chemistry procedures, as well as being quick and cost-effective to deploy in a production process. Plasma treatments could aid in the improvement of polymer materials' bioactivity by either improving protein adsorption or directly boosting cell growth support. Protein adsorption is influenced by the chemical and physical properties of the biomaterial, as detailed in previous chapters. Plasma treatments allow for the creation of certain surface qualities, whether very hydrophilic or very hydrophobic surfaces are preferred[295].

The protein adsorption properties of PIII treated UHMWPE fabric have already been discussed in earlier chapters, thus in this chapter we will concentrate on how cells react to the PIII treated UHMWPE surfaces directly, without the need for an intermediary functional protein coating. Although the widespread use of UHMWPE fabric in the biomedical industry[71], one of the main disadvantages is that it is inert in the body, which limits its ability to actively encourage cell proliferation and adhesion. As seen in the earlier sections, functionalizing UHMWPE fabric surfaces with bioactive compounds has been a proactive strategy to get around these restrictions. The commercialization of such goods, however, may face considerable challenges as a result of the added difficulties that connecting bioactive biomolecules to UHMWPE may bring about in securing the necessary regulatory permission [296]. If UHMWPE fabric could be modified with a straightforward PIII treatment to significantly increase bioactivity, many orthopedic industries may find the approach to be quite beneficial.

In this chapter, we will compare the performance of the untreated and nitrogen based PIII-treated two different grades UHMWPE surfaces in terms of cellular responses to determine whether such a strategy is practical or not. The bioactivity of UHMWPE sheet has been found to be improved by a variety of plasma procedures in multiple investigations [153, 297], but the effects of the much more intense PIII treatment have not yet been completely explored on UHMWPE fabrics.

Several in vitro experiments were conducted to examine the cellular responses on various untreated and PIII treated UHMWPE fabrics. These experiments are necessary to show that the new surface can enable cell adhesion and proliferation successfully, without producing any negative harmful effects. These evaluations will be made using tissue culture assays with a

variety of cells from our laboratory. Additionally, any improvements in bioactivity will be measured and analyzed in relation to UHMWPE that has not been plasma treated as a control.

Alkaline Phosphatase (ALP) assay and mineralization of fibroblastic cells were carried out to see the differentiation of cells [288]. Firstly, these cells can differentiate in several different pathways, and we were looking for specific different forms of cell expressions[298].

Secondly, the ligament, unmineralised fibrocartilage, mineralised fibrocartilage, and bone are the four transitional zones that make up the natural Ligament/Tendon (L/T) insertion, for a functionally graded material system. Restoring the natural histological structure at the tendon-ligament insertion zone and function is still challenging. To ensure joint function during restoration, the optimal ligament graft should be able to replicate the natural L/T'S anchoring structure as closely as feasible[175]. The repair of ligament injuries significantly influences the process by which tendinous fibroblasts differentiate at the tendon-bone junction, and the differentiation of cells could induce the anchoring system through mineralisation[276].

6.2 Aim & hypothesis of the chapter

The goal of this study was to examine the in vitro biocompatibility of two different grades UHMWPE fabric surfaces for ligament/tendon (L/T) cells and see how the PIII treatment of UHMWPE surfaces impacted biocompatibility. The cell interactions with the bare PIII modified UHMWPE surfaces in the absence of any protein functionalization are studied in this section using two easily obtainable and well-known cells, Human primary fibroblast cells (FB) and human primary adipose-derived stem cells (ADSC). Fibroblast is the primary cell of ligament and tendons [299–301]. It has been reported that ADSCs were more effective in

promoting fibroblast migration and procollagen synthesis for Anterior cruciate ligament (ACL) reconstruction[302].

Based on our previous scientific experimental data, it is expected to have get good cell biocompatibility for PIII treated UHMWPE fabric. Cells could be easily attached on the surface of treated UHMWPE fabric due to the increased hydrophilicity created by plasma treatments.

6.3 Experimental methods

Based on the findings of previous surface characterization studies on Chapter 4, it was determined that the surface properties of the 800 second PIII treated UHMWPE samples have significantly higher covalent properties, so these samples, as well as an untreated UHMWPE control, were included in most of the following studies. The PIII treatment settings were set in accordance with the procedure outlined in the earlier chapters of this thesis. In contrast to the protein investigations in the previous chapter, all cell samples were solely PIII treated on the side that interacts directly with the cells. The UHMWPE fabric was cleaned and cut into 0.8 cm x 8 cm strips for most cell experiments, then plasma treated and further cut into 0.8 cm 1.2 cm rectangles that just fit into the wells of a 24 well plate. To determine the orientation of the sample and ensure that the treated side is always facing upwards, a small cut was made in the upper right corner of each sample. Additionally, overall gene expression investigations were carried out on much larger round discs with a diameter of 3/4 inch. The bigger discs provided more surface area for growth and fit precisely inside the wells of a 12 well plate. The larger samples were required to support a greater number of cells, resulting in a greater amount of RNA to aid in the RNA extraction process.

6.4 The primary Fibroblast cells

Tendons and ligaments are both comprised of connective tissue. Fibroblasts are the primary cell type of ligamentous/tendinous tissue [303]. Biocompatibility of untreated and PIII treated UHMWPE with FB cells are crucial for ligament/tendon regeneration. The cells were kept in a Dulbecco's Modified Eagle Medium (DMEM) (Gibco Laboratories catalogue #11995) with 25 mM D-glucose, 4 mM L-glutamine, 1 mM sodium pyruvate, and phenol red but no HEPES, and supplemented with 10% heat-inactivated fetal calf serum (FBS) (Gibco Laboratories catalogue # 16000-044). In biomaterials research, the primary fibroblast has been frequently employed to investigate the impact of substrates on tenogenic development.

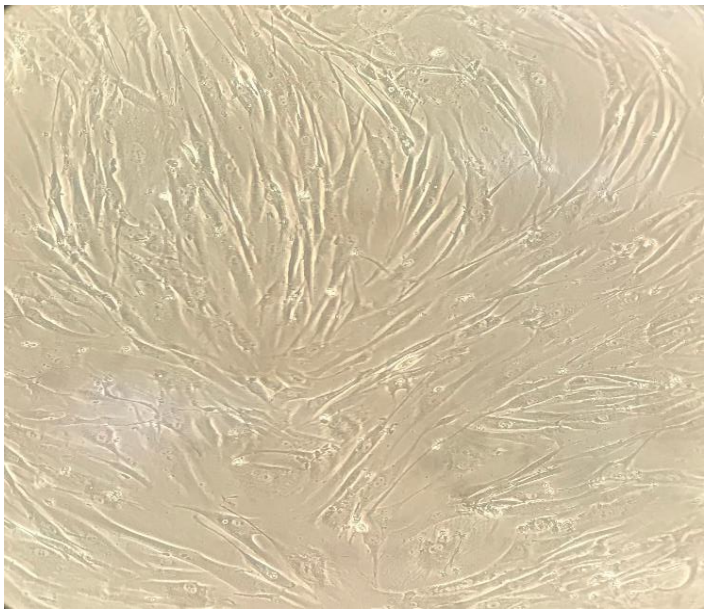

Figure 6. 1 Fibroblast cells.

6.5 Adipose derived stem cells

ADSCs (adipose-derived stem cells) are a kind of adult mesenchymal stem cell that may self-renew and proliferate. Currently, tendon graft integration employing ADSCs has been demonstrated[304]. For this reason, we chose ADSC to observe its interaction with the surface

of UHMWPE. These cells were cultured in a special minimal essential medium (MEM) with 4mM L-glutamine and Phenol Red but no nucleosides (Gibco Laboratories catalogue #12561). The MEM was only supplemented with 10% fetal bovine serum (Gibco Laboratories catalogue #16000-044) for regular cell expansion. Antibiotics of 30 mg/mL penicillin and 100 mg/mL streptomycin (Gibco Laboratories catalogue #15070-063) were also required in very long-term trials to prevent bacterial contamination.

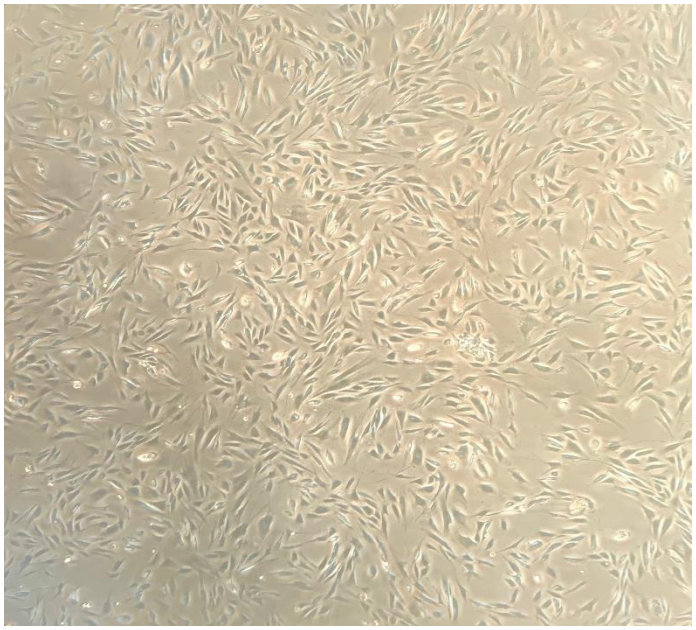

Figure 6. 2 ADSC cells.

6.6 Cell culture procedures

T-175 cell culture flasks were used to increase the number of FB cells, while T-75 cell culture flasks were utilized to increase the number of ADSC cells. The investigations were carried out utilizing 12 or 24 well plates with UHMWPE samples trimmed to fit in the wells. Every three days, as well as the day before any trials, fresh medium was provided. A fresh passage was made with 10% of the cells from the confluent flask when they achieved a confluence level close to 100%. After removing all medium, the cells were digested and lifted with 5 mL TrypLETM

Express Enzyme (Gibco catalogue #12605) for 5-6 minutes before being re-suspended in 5 mL complete medium for T-75 flasks. Cells were digested and lifted with 17mL TrypLETM Express Enzyme for 5-6 minutes before being resuspended in 17mL complete medium for T-175 flasks. After that, enough cells would be moved to a new T-75 flask with 15 mL fresh media. After that, enough cells would be moved to a new T-75 and T-175 flask with 15 mL and 30mL fresh media.

6.6.1 Freezing and reviving of cells

Liquid nitrogen was used to cryo-preserve cells that needed to be kept for a long time. The cells were trypsinized and centrifuged under 0.5 G for 10 minutes prior to freezing. The cell pellet was then re-suspended in a small volume of standard complete medium, adjusted to contain 1-2 million cells per mL, and to this volume an equal volume of FBS containing 10 percent DMSO. This cell suspension was then transferred into a cryo-vial, and then inserted in an isopropanol-filled freezing container and kept in the -80°C freezer. The freezing container's isopropanol functions as an insulator, causing the temperature of the cells to decrease gradually at a rate of 1 C per minute. The cells were then taken out of the freezing container the following day and kept in liquid nitrogen for a very long time. The cryo-vials were taken out of the liquid nitrogen tank and put into a 37°C water bath to thaw the cells. The cells were promptly suspended in warm normal complete medium when all the ice in the cryo-vial had completely melted. Two methods have been followed to revive the cells after melting. One-way cells were then gently combined and centrifuged once more under 0.5g for 10 minutes. After discarding the DMSO-containing supernatant, the cell pellet was re-suspended and plated into a brand-new T-75 flask. Second way- after melting the cells were carefully transferred into a T-75 flasks and incubated to settle down into the flaks. The following day cell media was removed and replaced with a fresh complete media.

6.6.2 Cell attachment assays

Cell attachment assays were modified from Humphries protocol [305] to measure cell density on the fabrics. Cell attachment assays were used to determine the degree of attachment between a cell and the treated surface, as well as other cellular activities like spreading. Single-side PIII-treated samples were cut into 0.8 cm × 1.2 cm rectangles and put at the bottom of a 24-well plate. Six samples were used to reduce experimental variation and improve statistical analysis. All assays were additionally subjected to a minimum of three biological replicates to ensure that the results obtained were consistent. To minimize bacterial contamination, all UHMWPE samples were sterilized in the biosafety cabinet under UV radiation for 20 minutes on each side.

The cells were harvested at 80–90 percent confluence while continuing growth. Trypsin digestion was employed to lift the cells into the solution.The solution waas then incubated for 5-6 minutes and then resuspended in fresh media. The solution was then centrifuged at 1.8rpm for 5 minutes. To avoid serum proteins disguising the action of the treated or functionalized surfaces, they were re-suspended in serum-free media. A haemocytometer was used to count the cells at this point, and the cell density was adjusted to an appropriate level for seeding. The optimal cell density seeded ranged from 20,000 to 50,000 cells per cm^2 depending on the cell type and well plate size employed.

The cells were seeded into the well plates with the UHMWPE samples in a random order and then placed in the cell incubator for the length of the test.During the experiment care was taken to ensure that UHMWPE didn't float on top of the media. The test samples were washed twice with 1 mL warm PBS at the end of the attachment time to eliminate any non-adherent or loosely attached cells. At this stage, pipette tips having their end tips cut off or an automatic repeating

pipette that exerts the same amount of force during each dispensing phase were used to pipette the PBS onto the samples with a mild but steady force.

Fibroblast (FB) cells were harvested when actively growing at 80–90 p ercent confluence. They were seeded at a density of 2.5 X 10^4 cells per well in serum free medium and were allowed to attach for 1 and 3 hours in an incubator. After the attachment, the unbound cells were removed by washing with PBS. Cells attached to the fabrics were fixed and stained for 20 minutes in 0.1% crystal violet solution. A volume of 300 µL acetic acid (10%) was used to solubilize cells and release the stain. The amount of stain released per sample was then quantified with a Thermo Scientific Multiskan EX microplate spectrophotometer at 570 nm. Error bars are standard deviations of triplicates.

6.6.3 Cell proliferation assay (MTT)

Traditionally, viable cells were counted following trypan blue staining to measure cell proliferation. But the technique lacked sensitivity, was prone to handling mistakes, and was challenging to modify for high throughput tests.

The cytotoxicity of the samples was determined using an MTT assay. This method is extensively used to assess a drug's cytotoxic potential in established cell lines or primary or secondary cultures[306]. Thiazolyl Blue Tetrazolium Blue (MTT) assay was used to analyze cell growth and metabolic activity on the modified UHMWPE surfaces. In living cells, MTT is converted into formazan crystals. MTT is a yellowish solution that is reduced by the mitochondrial reductase enzyme to produce a purple water-insoluble MTT formazan product, which can then be solubilized with DMSO and detected colorimetrically at 570 nm. The conversion rate is

propotional to the overall metabolic activity of the viable cells within the well. Dark color of the solution represents the greater number of cells (more viable cells) with high absorbance pattern.

UHMWPE samples were plasma treated, cut into 0.8 X 0.8 cm squares, and placed in 24 well plates in order to quantify cell proliferation on the modified UHMWPE. In order to ensure that the results obtained in each case were comparable, a minimum of three biological replicates were performed. To further limit the danger of bacterial contamination, all UHMWPE samples were sterilised in the biosafety cabinet for 20 minutes on each side under UV light. The ADSC and low passage primary fibroblast cells were consistently grown in T-75 flasks and reached a confluent level of roughly 90% before being employed in the tests.On day 0, the cells were seeded onto the samples in a randomized order at a density of 20,000 cells per well in 100 µL of DMEM culture medium supplemented with 10% FBS and 1% P/S and incubated at 37 °C in humidified atmosphere with 5% CO_2.

Cells were cultured for 3, 5 and 7 days, with medium changed every other day. To measure the metabolic activity of the cells, the samples were gently washed and incubated in 2.5 mM MTT for 2 hours. The MTT solution was prepared using PBS, a 0.22 um syringe filter, and 2.5 mM Methylthiazolyldiphenyl-Tetrazolium Bromide (Sigma M2128). It was also protected from light. After the two hours of incubation, dark purple needle-shaped formazan crystals that were proportional to the number of cells present could be seen on the samples and well plates. By aspiration, the leftover yellow MTT solutions were eliminated. No PBS washing step was carried out in this stage due to the fragility of the cell layer. To solubilize the formazan, 300 µL of DMSO was added to each well after the samples had been transferred to a new 24 well plate. To allow the formazan crystals to completely dissolve, the well plates were then covered in foil and set on a well plate shaker for 10 minutes. The optical density of the released stain corresponds to

the amount of metabolic activity and was measured by a Thermo Scientific Multiskan EX microplate spectrophotometer set at 570 nm.

6.6.4 SEM sample preparation

Because cells could not be easily seen by optical microscopy due to the opaque nature of UHMWPE surfaces, SEM was employed to investigate cellular adhesion, morphology, and proliferation.The JEOL Neoscope JCM 6000 microscope was used to obtain field emission scanning electron microscopy (SEM) pictures. Cell-containing samples went through a series of fixation and dehydration processes to prepare them for SEM observation. The specimens were initially fixed for an hour at room temperature in the primary fixative, which contained 2.5 percent glutaraldehyde in 0.1M phosphate buffer at pH 7.2–7.4. A secondary fixation using 1 percent Osmium tetroxide (OsO_4) in 0.1M phosphate buffer was carried out with incubation at room temperature for an additional hour after the primary fixative was removed by rinsing three times in the solution. The samples were then dehydrated sequentially in graded ethanol from 30 percent to 100 percent, followed by three Milli-Q water rinses. The samples were then dried by adding hexamethyldisilazane (HMDS) for 3 minutes, removed, and stored overnight in a desiccator. The properly dried samples were placed into conducting sample holders, 15 nm gold was sputtered on top, and then the samples were examined under the microscopes. Samples without any biological components were simply mounted into the sample holders after sputter-coated with 15 nm gold.

6.6.5 The Induced Differentiation of Fibroblasts

The fibroblast cells were cultured on the modified two different types of UHMWPE under tenogenic conditions. The experimental design is quite identical to the proliferation assay;

however, it is carried out over a considerably longer period. The UHMWPE samples were single-sided PIII treated, cut into rectangles measuring 0.8 by 0.8 cm^2, placed on 24-well plates, and sterilized with UV light for 20 minutes per side. The fibroblast cells were cultivated in T-75 flasks using standard expansion medium until they were 90% confluent. Cells were digested and lifted by trypsin on the day of cell seeding (Day 0), cleaned by centrifuging, and adjusted with normal media to a concentration of 80,000 cells per mL. In the typical expansion media, the cells were seeded onto the samples at a density of 20,000 cells per cm^2. After the medium had been aspirated out on day three, tenogenic media was employed to encourage differentiation. The tenogenic medium contained connective tissue growth factor (CTGF) (100 ng/mL) and ascorbic acid (50 μg/mL) with standard cell culture medium. Depending on the experiment, the cells were taken from the culture at days 7, 14, 21, and the degree of differentiation was assessed using the techniques described in the following sections. To ensure that the results obtained were consistent across all cases, a minimum of three biological replicates were carried out for each of the experiments.

6.6.6 ALP assay

An essential technique for measuring osteogenesis is the alkaline phosphatase (ALP) assay. According to earlier research, human periodontal ligament cells (hPDLCs) have osteoblastic characteristics such as high alkaline phosphatase (ALP) activity, the ability to produce matrix proteins that resemble bone, and the potential to form mineralized nodules[307].

6.6.7 Mineralization assays for untreated & treated UHMWPE

The degree of calcification in the extracellular matrix was assessed by Alizarin red S staining. To investigate the stage of mineralization that could be seen by staining the calcium deposits with

Alizarin Red S, Fibroblast cells were cultured on the modified UHMWPE under long-term tenogenic conditions. The cells were fixed in 10% formalin and PBS for 10 minutes. The preserved cells were stained with Alizarin red S solution for 5 minutes after being washed twice with double-distilled water. The cells were stained and then rinsed with double-distilled water. After being fixed and stained, the plates were allowed to air dry at room temperature. To quantify the degree of mineralization is achieved by dissolving the cell-bound Alizarin red S in 10% acetic acid and measured at 415 nm. For imaging the samples were meticulously placed on a microscope slide the following day, left to cure for three days, and imaged under Olympus Bx51 fluroscence microscope.

6.6.8 RNA extraction and gene expression

Gene expression tests were carried out utilizing untreated and treated UHMWPE on 24 well plate to obtain a suitable quantity of RNA. The samples were UV sterilized for 20 minutes on both sides before cell seeding. Due to the primer availability in our lab, only primary human fibroblasts were employed in the gene expression experiment. A density of 100,000 cells per 12 well plate, or about 25,000 cells per cm^2, was used to seed the cells. Throughout all tests, regular expansion media was employed to emphasize any variations in gene expression brought on only by the various surface qualities. Every three days, the medium was changed, and on days 7 and 10, the total RNA content was extracted. Each experiment employed a minimum of three duplicates to establish its statistical validity. For all subsequent experiments, a minimum of three biological replicates were also carried out to ensure that the results were consistent across all cases.

The TRI Reagent® (Sigma T9424) was used to separate the total RNA from the primary human fibroblasts according to the manufacturer's instructions. The media was quickly removed, and the cells were given a quick rinse in cold PBS. Immediately after the addition of 0.7 mL of Tri Reagent, the cells were homogenized by pipetting and washing the sample surfaces. Phase separation was achieved by transferring the cell lysates into a fresh Eppendorf tube free of RNAse, adding 0.14 mL of chloroform, aggressively mixing by shaking and incubated at room temperature for 2-3 minutes. Samples were centrifuged at 10,000xg for 30 minutes at 4°C, the samples were divided into three phases: an upper, translucent aqueous phase; a lower, red, phenol-chloroform phase; and an organic interphase. The RNA-containing aqueous phase was carefully taken out and collected in a brand-new tube. After that, RNA from the aqueous phase was precipitated using 0.4 mL of isopropyl alcohol and incubated for 10-15 minutes. After centrifuging, the RNA forms a pellet that resembles a gel, and the supernatant was discarded. The RNA pellet was once more washed in 75% ethanol, dried by air, and then dissolved once more in 20 µL of DEPC-treated water by incubation at 55°C for 15 minutes.

The Tetro cDNA Synthesis Kit (Bioline Cat. # BIO-65054) was used to create first strand cDNA from the purified total RNA in accordance with the manufacturer's instructions. In a summary, the kit's included buffer was poured to an RNAse-free reaction tube along with random primers, a 10 mM dNTP mix, an RNAse inhibitor, and the tetro reverse transcriptase. Reverse transcription was allowed to occur in the mixture by incubating it at 45°C for 30 minutes. The reaction was then stopped by raising the temperature to 85°C for 5 minutes. For the RT-PCR process, the final reaction products were further diluted with DEPC-treated water.

RT-PCR was carried out using the SensiFAST SYBR® No-ROX Kit (Bioline Cat. # BIO-86005) in the Quant Studio™ 7 Flex Real-Time PCR System (Thermo Fischer scientific). To cover the

gene region, enough forwards and reverse primers were added to the SensiFAST Probe No-ROX Mix along with the cDNA templates. After that, the mixture was placed into the Quant Studio™ 7 Flex Real-Time PCR device and conducted through a pre-set PCR cycle. The DNA strands were split at 95 degrees, and the annealing and extension temperatures were set at 60 degrees. At the conclusion of each cycle, the probe's temperature was measured. To ensure the accuracy of the results collected, melting curve analysis was also carried out to evaluate the dissociation properties of the DNA products. By comparing to the house-keeping gene GAPDH, the relative gene expression levels for many genes relevant to ligament/tendon were standardized. The relative gene expression, expressed as $2^{-\Delta Ct}$, and the Ct values were measured using a threshold of 3000 relative fluorescence units. The following table shows lists of the primer sequences for the chosen genes.

6.7 Data presentation and Statistical analysis

Origin and Microsoft Excel were used to construct and assess all figures and statistical analyses relevant to the conclusions in this chapter. Two-tailed t-tests were performed to compare groups, with a P value of 0.05 indicating significance. Unless otherwise noted, each experiment employed at least three triplicates and a minimum of three biological replicates to assure statistical validity of the results.

6.8 Experimental Results

6.8.1 Cell attachment & proliferation study of industrial grade UHMWPE

It ‘s been observed in Fig 6.3 that PIII-treated industrial grade UHMWPE fabric had a higher number of Fibroblast (FB) cells adhere within the 1& 3 hour time frame. The PIII-treated

industrial grade UHMWPE fabric samples had higher absorbance, compared to the untreated industrial grade UHMWPE samples. This demonstrated that after PIII treatment, FB cells could bind to the treated surface more frequently rather than untreated UHMWPE, indicating that it may be more biocompatible.Furthermore, no significant differences were detected between the untreated UHMWPE from 1 hr to 3 hr period.

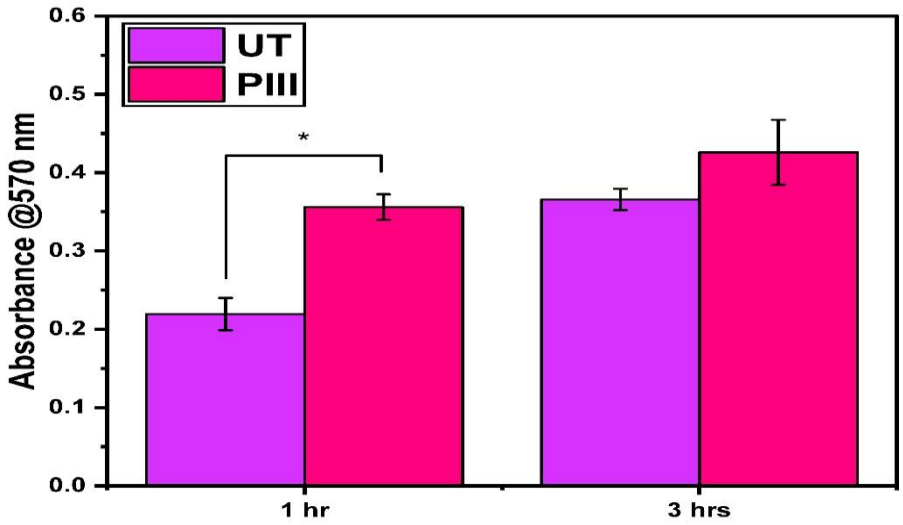

Figure 6. 3 Fibroblast cell attachment on untreated (UT) & PIII treated industrial grade UHMWPE under serum free conditions. Error bars here indicate standard deviations of quadruplicates and an asterisk (*) indicates a significant difference ($P<0.05$) between the untreated and PIII treated groups. There were no differences detected in between the two treated groups.

The Fibroblast cells that are adhered to the various UHMWPE surfaces can be seen clearly in the SEM images of Fig:6. 4 (A&B). It is clearly observed that untreated industrial grade UHMWPE fabric has less cells after 1 hour's period. Whereas PIII treated surfaces, contains a greater number of cells on the fabric surface.

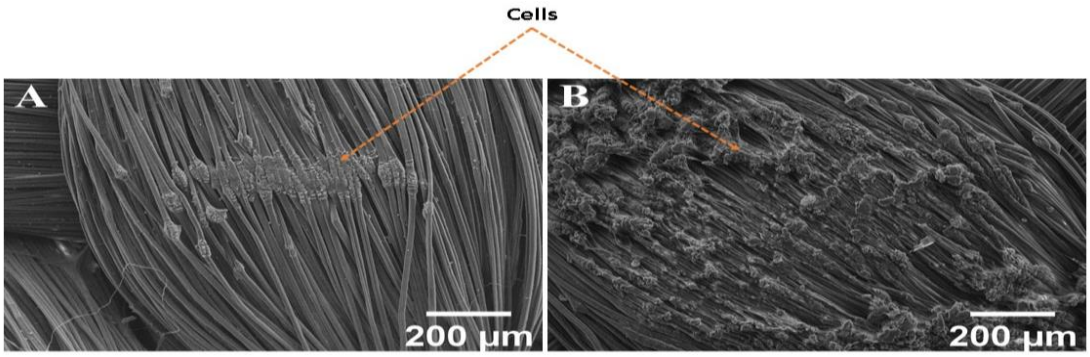

Figure 6. 4 Scanning Electron Microscopy imaging of the cell attachment of the Fibroblast cells for 1 hour on industrial grade UHMWPE under lower magnification. The groups presented here are: (A) Pure industrial grade UHMWPE at lower magnification (100X); (B) PIII treated industrial grade UHMWPE at lower magnification (100X). All cells were seeded on the samples at a density of 50,000 cells per cm^2 in serum free medium and allowed to attach in a cell culture incubator for 3 hours.

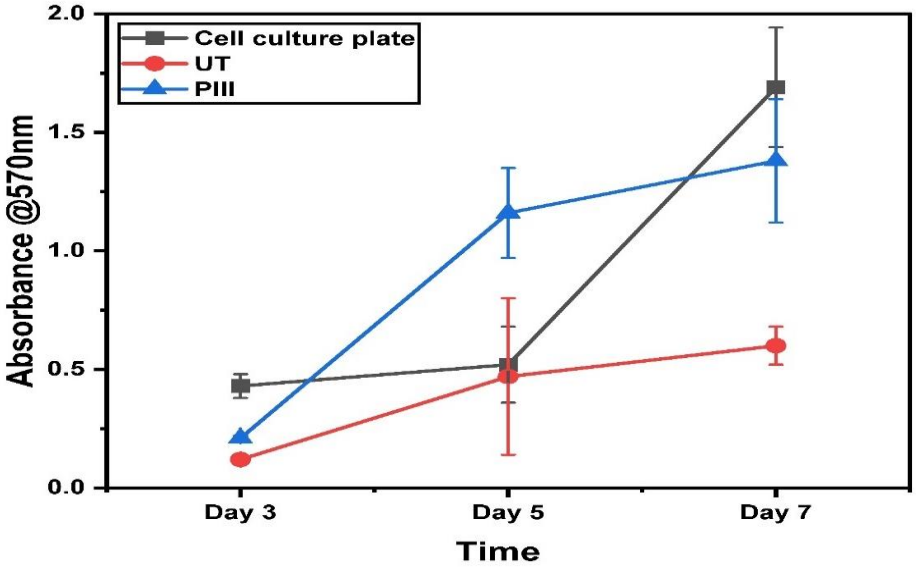

Figure 6. 5 Growth curve of FB cells cultured on pure and PIII modified industrial grade UHMWPE over 2-7 days. A density of 20,000 cells per cm2 was seeded onto the samples in regular expansion medium on day 0. To measure the metabolic activity of the cells, the samples were incubated in 2.5 mM MTT for 2 hours, gently washed then transferred into a new plate with 300 µL DMSO to solubilize the formazan crystals. The optical density of the released stain corresponds to the amount of metabolic activity and was measured by a Thermo Scientific Multiskan EX microplate spectrophotometer at 570 nm. Error bars here indicate standard deviations of quadruplicates and an asterisk (*) indicates a significant difference ($P<0.05$) between the untreated and PIII treated groups. There were no significant differences detected in between the two treated groups.

Fig 6.5 presented the cell proliferation assay of untreated and PIII treated industrial grade UHMWPE fabric. It's been observed that cell proliferation is consistent for untreated industrial grade UHMWPE fabric. Cell proliferated over the week. Cell proliferated rapidly from days 3 to days 5 for PIII treated industrial grade UHMWPE fabric but in day 7 it didn't follow the same trendline. Cell proliferation trendline is similar for both untreated and treated fabric but the rate is higher in PIII treated industrial grade UHMWPE fabric than untreated industrial grade UHMWPE fabric.

6.8.2 Cell adhesion & morphology study on scientific grade UHMWPE

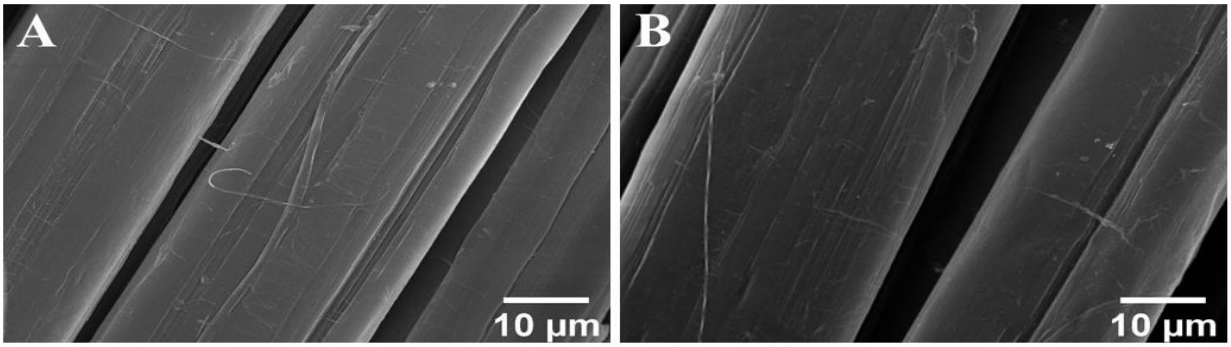

Figure 6. 6 SEM images of (A) Untreated and (B) PIII treated UHMWPE.

SEM image of untreated and PIII treated scientific grade UHMWPE is shown in Fig 6.6.UHMWPE is a gel spun multifilament fiber. Fibers are alligned and clear. PIII treated UHMWPE is relatively darker in appearance than the untreated UHMWPE fabric.

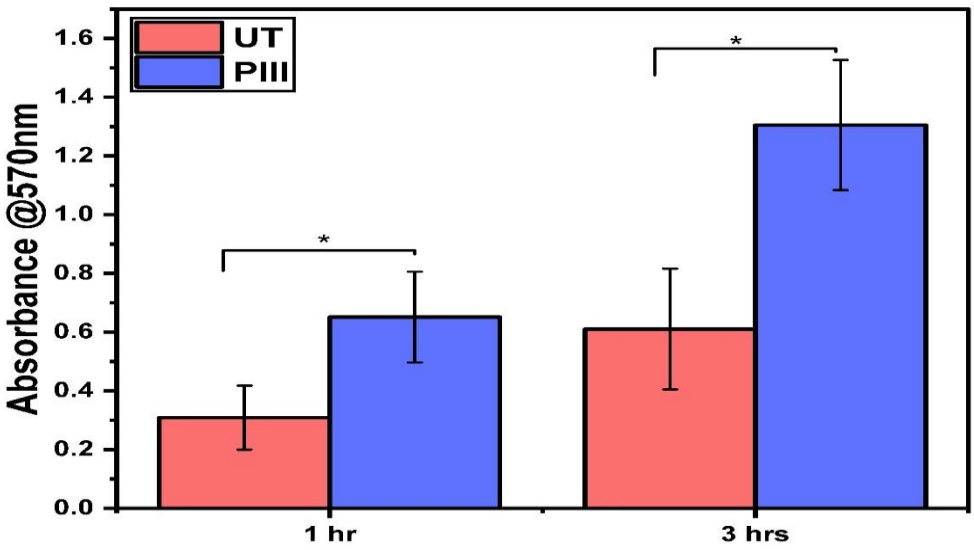

Figure 6. 7 Fibroblast cell attachment on untreated (UT) & PIII treated UHMWPE under serum free conditions.

Fig 6.7 It was clear that PIII-treated scientific grade UHMWPE fabric had a markedly larger number of Fibroblast (FB) cells adhere within the 1& 3 hour time frame. The PIII-treated scientific grade UHMWPE samples had higher absorbance, compared to the untreated scientific grade UHMWPE samples. This showed that more than twice as many FB cells could bind to the treated surface after PIII treatment, suggesting that it might be more biocompatible. Furthermore, no significant differences were detected between the untreated csientific grade UHMWPE from 1 hr to 3 hr period. Whereas, PIII treated UHMWPE it markedly increased.

The Fibroblast cells that are adhered to the various UHMWPE surfaces can be seen clearly in the SEM images of Fig 6.8. It is apparent that the bottom row 8 (C) &(D), which belongs to the PIII treated surfaces, contains a greater number of cells.

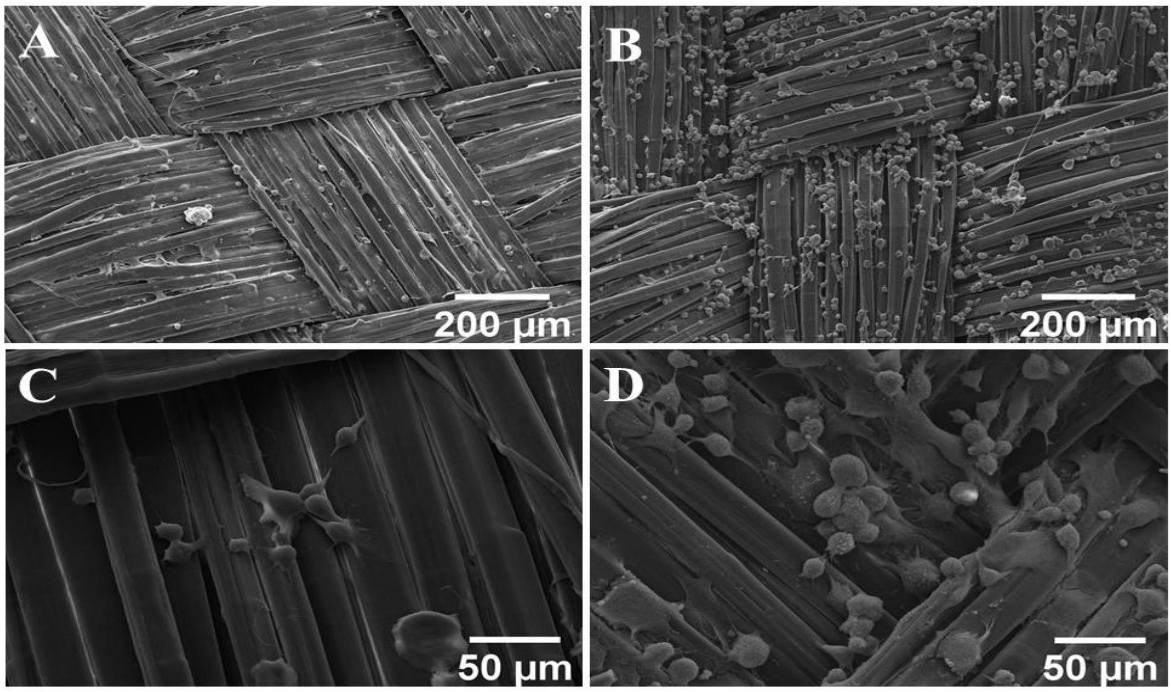

Figure 6. 8 Scanning Electron Microscopy imaging of the cell attachment of the Fibroblast cells for 1 hour on UHMWPE under higher and lower magnification. The groups presented here are: (A) Pure UHMWPE at lower magnification (100X); (B) PIII treated UHMWPE at lower magnification (100X), (C) Pure UHMWPE at 400X magnification, (D) PIII treated UHMWPE at 400X magnification. All cells were seeded on the samples at a density of 50,000 cells per cm^2 in serum free medium and allowed to attach in a cell culture incubator for 1 hour.

The Fibroblast cells that are connected to the various UHMWPE surfaces have seen under higher magnification in the SEM images from Fig 6.9. The cells on the PIII treated surfaces seemed to be larger in diameter and tended to be more dispersed, even at the same magnification levels. Although cells on the PIII treated surfaces exhibited isotropic protrusions and had formed fingers suggesting a later spreading stage, but cells on the untreated pure scientific grade UHMWPE surfaces still seemed to be spherical in shape at an early initial spreading stage.

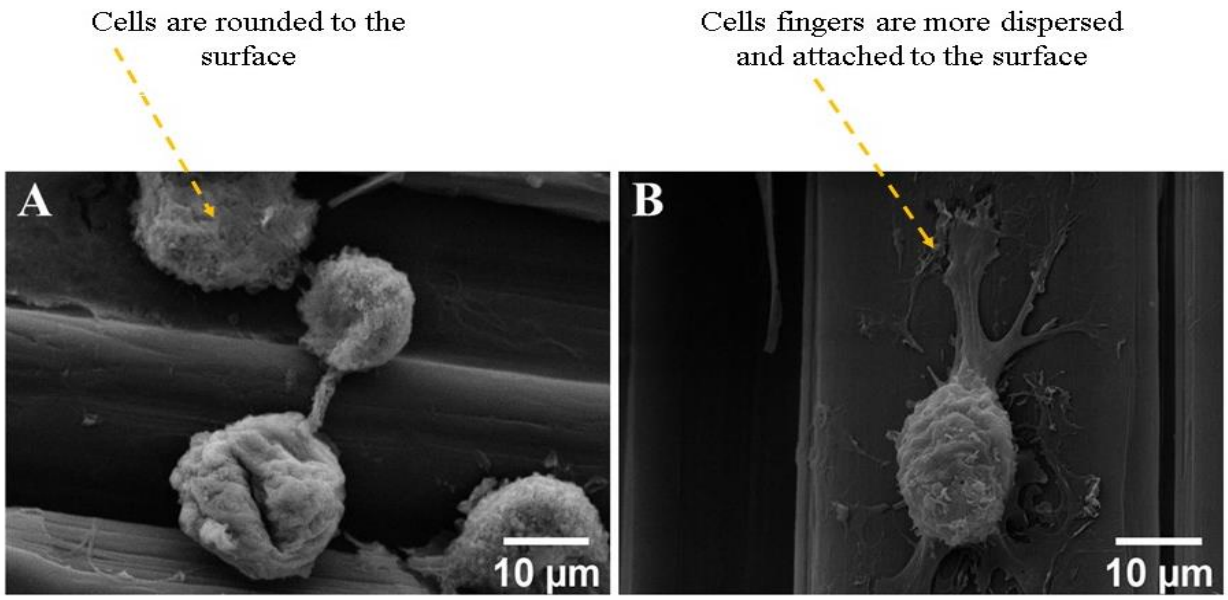

Figure 6. 9 Scanning Electron Microscopy imaging of the cell attachment of the Fibroblast cells for 1 hour on UHMWPE under high magnification. The groups presented here are: (A) Pure UHMWPE, (B) PIII treated UHMWPE.

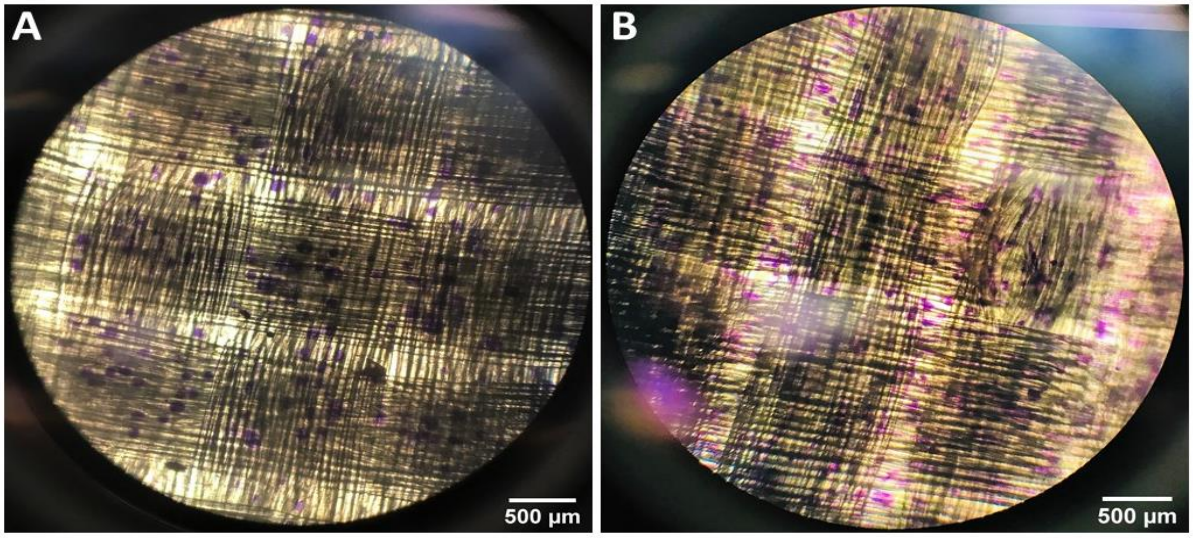

Figure 6. 10 Inverted microscopic images of the FB cell attachment for 1 hour. (A) Pure UHMWPE under low power, (B) PIII treated UHMWPE under low magnification.

All cells were seeded on the samples at a density of 25,000 cells per cm^2 in serum free medium and allowed to attach in a cell culture incubator for 1 hour. The samples were fixed by 3% PFA, stained by crystal violet and inverted to achieve a better contrast against the opaque UHMWPE

background. On both the untreated and PIII treated surfaces of Fig 6.10, the primary Fibroblasts have been observed. The PIII treated surfaces generally had more cells visible on them. Additionally, a clear distinction in terms of cell shape has been seen in this situation. Although a greater proportion of the cells on the untreated surface looked to be still spherical, the cells that had spread out appeared to extend further and took on the appearance of needles. On the other hand, although having a greater overall number of spreading cells on the PIII-treated surface, the surface area that the cells covered appeared to be smaller. It's likely that on treated surfaces, cells can connect relatively quickly whereas they may need to extend further on untreated surfaces to find sufficient anchor points.

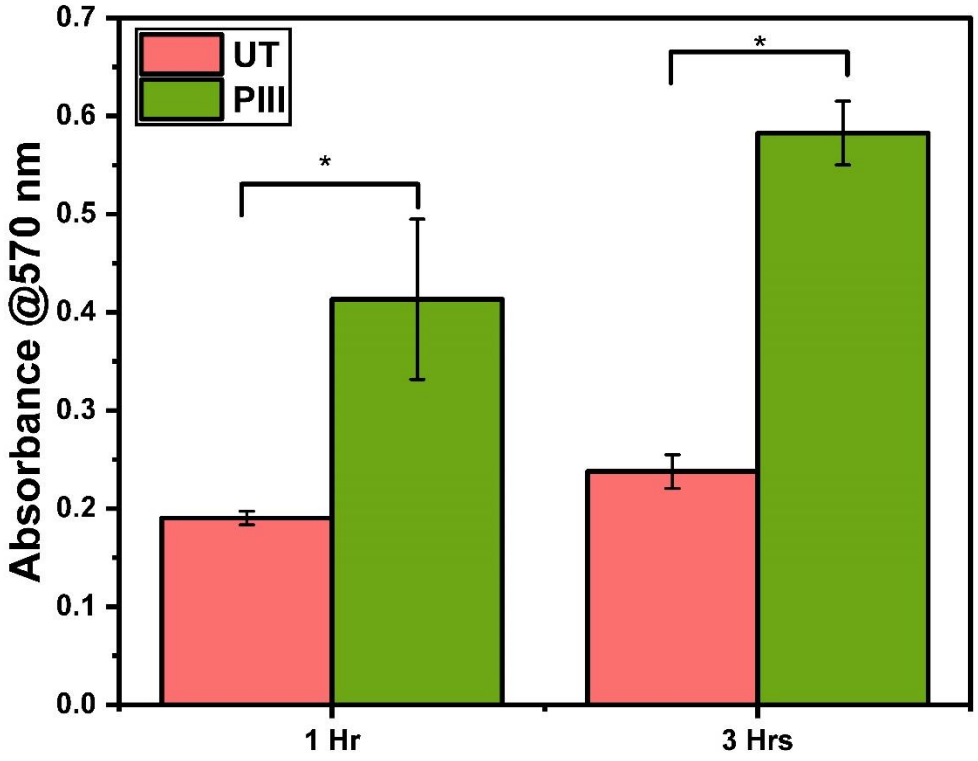

Figure 6. 11 ADSC cell attachment on untreated (UT) & PIII treated UHMWPE under serum free conditions.

It's been observed in Fig 6.11 that during 1 & 3hour period a significantly higher number of Adipose derived stem (ADSC) cells adhered to UHMWPE fabric. The PIII-treated scientific grade UHMWPE samples had higher absorbance, compared to the untreated scientific grade UHMWPE samples. This shown that after PIII treatment, ADSC cells could bind to the treated surface like FB cells. Furthermore, no significant differences were detected between the untreated scientific grade UHMWPE from 1 hr to 3 hr period. On the other hand, it is markedly increased on PIII treated UHMWPE fabric.

6.8.3 Cell Proliferation on scientific grade UHMWPE

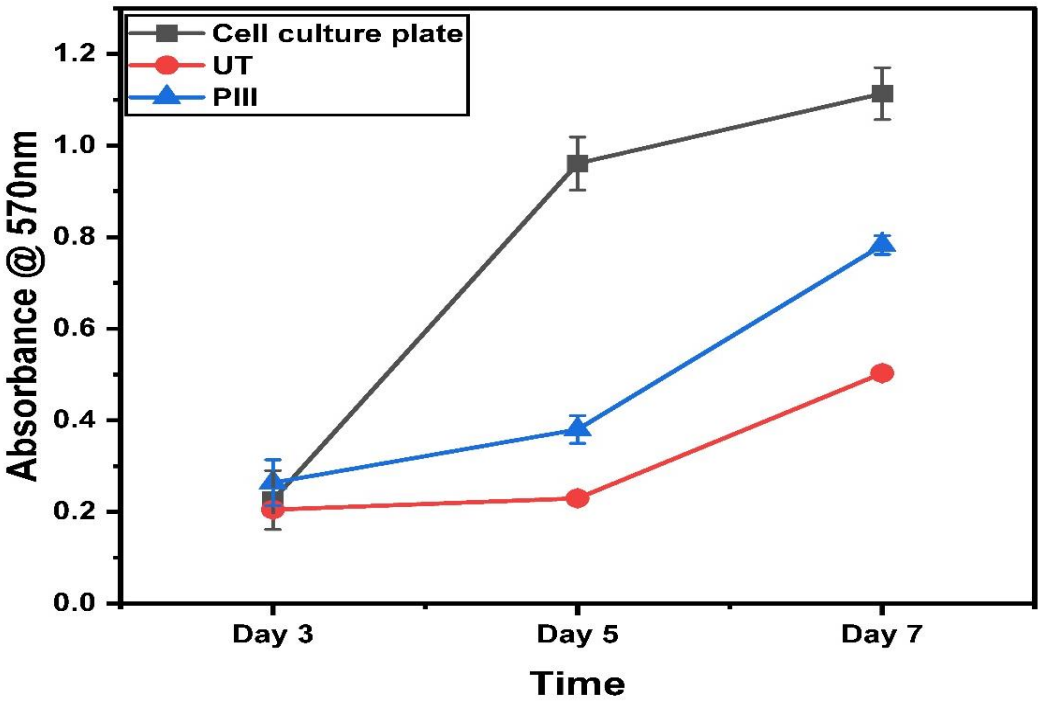

Figure 6. 12 Growth curve of FB cells cultured on pure and PIII modified industrial grade UHMWPE over 2-7 days. A density of 20,000 cells per cm2 was seeded onto the samples in regular expansion medium on day 0. To measure the metabolic activity of the cells, the samples were incubated in 2.5 mM MTT for 2 hours, gently washed then transferred into a new plate with 300 µL DMSO to solubilize the formazan crystals. The optical density of the released stain corresponds to the amount of metabolic activity and was measured by a Thermo Scientific Multiskan EX microplate spectrophotometer at 570 nm. Error bars here indicate standard deviations of quadruplicates between the untreated and PIII treated groups. There were no differences detected in between the two treated groups.

The proliferation of FB cells on untreated and PIII-treated UHMWPE over the course of a week is shown in Fig 6.12. As evidenced by the rising trend in metabolic activity, the FB cell was able to successfully multiply on all surfaces examined here. Additionally, it is evident that starting on day 3, the cells growing on the two PIII-treated surfaces showed a significantly increased metabolic activity. Cells on the PIII-treated surfaces by the end of the week at day 7 display roughly twice the metabolic activity compared to the untreated UHMWPE surfaces. These results indicate that PIII-treated surfaces are superior to pure untreated UHMWPE in encouraging the growth of FB cells and in exhibiting no harmful effects. Rapid increase of FB cells on cell culture plate observed from day 3 to day 7.

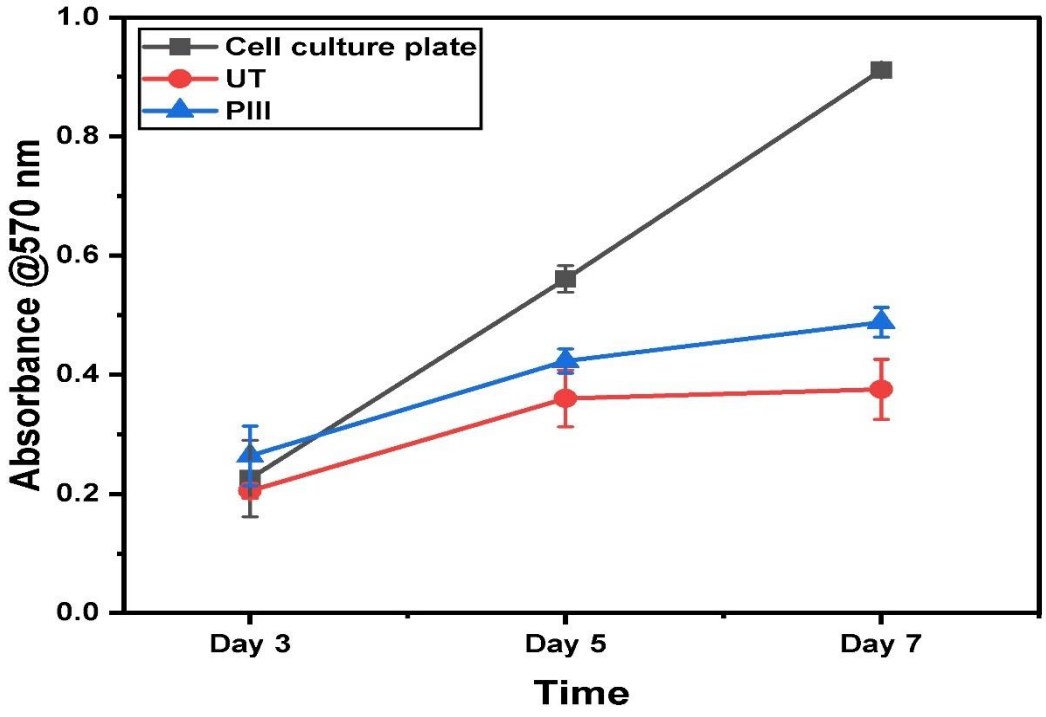

Figure 6. 13 Growth curve of ADSC cells cultured on pure and PIII modified UHMWPE over 2-7 days. A density of 20,000 cells per cm2 was seeded onto the samples in regular expansion medium on day 0. To measure the metabolic activity of the cells, the samples were incubated in 2.5 mM MTT for 2 hours, gently washed then transferred into a new plate with 300 µL DMSO to solubilize the formazan crystals. The optical density of the released stain corresponds to the amount of metabolic activity and was measured by a Thermo Scientific Multiskan EX microplate spectrophotometer at 570 nm.

The growth curve of ADSC cells on untreated UHMWPE and PIII-treated UHMWPE over the course of one week is shown in Fig 6.13. The clear rising trend in metabolic activity indicates that the ADSC cell was able to successfully multiply on all surfaces examined here. Additionally, it is evident that starting on day 3, the cells growing on the two PIII-treated surfaces showed a significantly increased metabolic activity. Cells on the PIII-treated surfaces display roughly twice the metabolic activity compared to the untreated UHMWPE surfaces on days 5, and 7. These findings strongly indicate that PIII-treated surfaces are superior to pure, untreated UHMWPE in enabling the proliferation of the ADSC cell and in exhibiting no harmful consequences. Cell proliferated constantly from day 3 to 7 in cell culture plate.

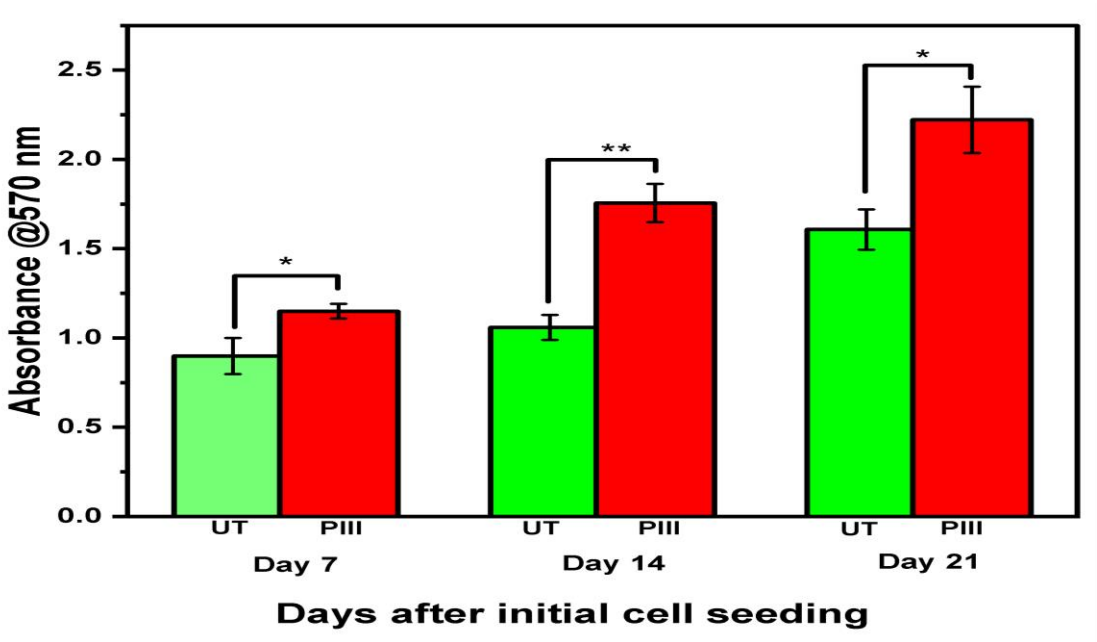

Figure 6. 14 ALP (Alkaline Phosphatase Activity) activity from the FB cell lysate cultured on pure and PIII treated UHMWPE samples in tenogenic medium. 20,000 cells per cm2 were cultured on UHMWPE under tenogenic medium. ALP activity was measured and recorded at 405 nm. The Error bars here indicate standard deviations of quadruplicates and an asterisk (*) indicates a significant difference ($P<0.05$) compared to the untreated groups while a hash symbol (#) indicates a significant difference ($P<0.05$) between the two PIII modified groups.

The ALP activity levels of fibroblast cells grown on scientific grade UHMWPE under tenogenic conditions are shown in Fig 6.14. The healing of grafted tendon-to-bone tunnels is largely dependent on the development of new bone around ligament/ tendon grafts. ALP's composition could be a direct indicator of osteoblasts' activity or functionality. The greater concentration of ALP shows that cells have a larger capability for mineralisation. After staining and quantitative analysis the content of ALP was less in untreated UHMWPE and higher in PIII treated UHMWPE. The PIII treated UHMWPE displayed considerably higher levels of FB mineralisation than the untreated UHMWPE fabric, according to the ALP quantitative data. This was also showed in the Alizarin red stain-ing quantitative analysis. After 21 days of induction, an osteogenic differentiation assay indicated that the majority of the cells had mineralization calcium deposits, as seen by Alizarin red staining (Fig 6.15).

Figure 6. 15 Alizarin Red S. positive staining examples of the calcium mineral deposits.

Using quantitative PCR, the mRNA expression levels of T/L-and bone-associated markers were examined to measure the differentiation of FB cells implanted on scientific grade UHMWPE (Fig 6.16). It is noted that connective tissue growth factor (CTGF), collagen, fibronectin were used in culture to induce T/L differentiation.

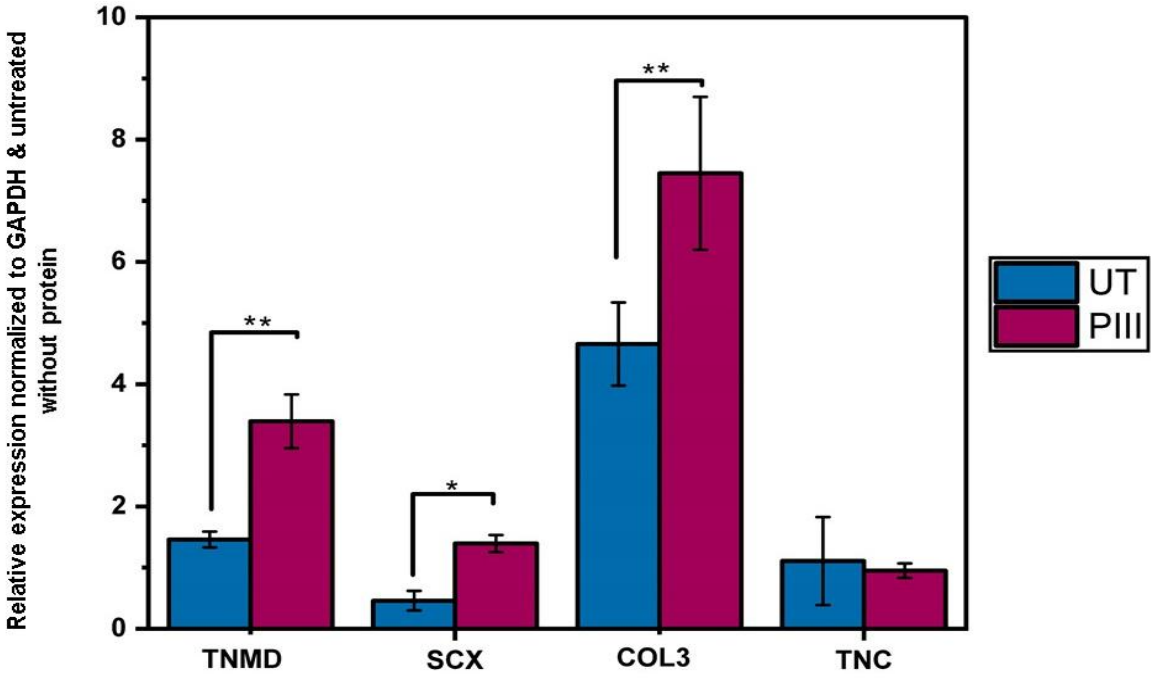

Figure 6. 16 Gene expression profile of human primary fibroblasts cultured on pure (UT) and PIII modified (PIII) UHMWPE with no protein coatings. This experiment is similar to the one produced in chapter 4 but at earlier time points. A density of 50,000 cells per cm^2 was seeded onto the samples in regular expansion medium and RNA was collected using Trizol on day 3 and 10. The RNA was reverse transcribed into cDNA and quantified by the method described earlier. The relative gene expression levels were obtained by normalizing to the house-keeping gene GAPDH and the pure UHMWPE control. The Error bars here indicate standard deviations of triplicates. A hash symbol (#) indicates a significant difference ($P<0.05$) between the unmodified pure UHMWPE and PIII modified UHMWPE surfaces.

The gene expression profile of primary fibroblasts cultivated on untreated and PIII-treated UHMWPE without protein coatings is shown in Fig: 16. The PIII-treated surfaces showed a definite increasing trend in a number of tenogenic genes. Particularly type III Collagen (COL 3) expression levels were markedly elevated compared to tenomodulin(TNMD) and Scleraxis (SCX). Adversely, when compared to the untreated control group, the expression levels of Tenascin-c (TNC) were dramatically down regulated after the PIII treatment.

6.9 Discussion and Conclusion

The purpose of this study was to examine the in vitro biocompatibility of two different types of UHMWPE surfaces for ligament/tendon cells and to assess how PIII treatment of UHMWPE fabric surfaces affected biocompatibility. In this chapter, we explore the cell interactions with the bare PIII modified UHMWPE fabric surfaces in the absence of any protein functionalization using two easily accessible and well defined fibroblast and ADSC cell cultures. The evaluation of biological safety and biocompatibility is a crucial phase in the early development stages of new biomaterials[308]. Future in vivo animal investigations can be built upon the cell culture analyses carried out here to see if the novel substance exhibits any substantial cytotoxicity. Overall, the results showed much higher growth and differentiation capabilities of all cell types on PIII modified UHMWPE fabric surfaces, supporting the hypothesis that the PIII may be employed to enhance and overcome the inert qualities of both industrial and scientific grade UHMWPE. The discussion is split into two main sections to go into more detail on the results that were noticed. In terms of typical cellular attachment and proliferation, the first section discusses cellular responses. The second section analyses the gene expression outcomes, ALP activity, and mineralisation potential to determine the changed surface's tenogenic & osteogenic potential.

We know that the inertness & lack of biocompatibility of UHMWPE is due to the absence of hydhophilic groups present on its surface[71]. Therefore, it was in our intention to ascertain whether the PIII treatment may enhance cell attachment characteristics as a result of the alteration in the hydrophilic features. Early on in the chapter, attention was placed on identifying any distinctions between the two forms of UHMWPE fabric that were available: industrial grade, and scientific grade. This brief cell attachment assay was performed to offer additional

information on whether any changes in the biological performance could be discovered. Surface characterisation investigations have shown that the differences in terms of physical attributes can be minimal. The findings showed that there were no noticeable variations in cell attachment between the two types of UHMWPE fabric, which was expected given the similarity of the surface features. Industrial grade UHMWPE fabric was able to show positive cellular responses, but it was quite difficult to maintain the sterile environment for cell culture.

The effects of PIII treatment on sientific grade UHMWPE and its interactions with fibroblasts and ADSC were the subject of our next investigation. Due to several problems associated with industrial grade UHMWPE in cell culture, we didn't further study with it. It was quite difficult to maintain the aseptic environment for industrial grade UHMWPE fabric. The number of cells connected during the 1-hour attachment assay increased by two times for all varieties of UHMWPE. The results of a SEM study also showed that the PIII-treated surface had a greater number of cells adhered to it as well as better cell spreading.

The stark variations in cell shape that can be seen in the SEM photos suggest that the cells were reacting to the surfaces differently. Similar results were seen when the same experiment was run on the Fibroblast cells, with a marginally faster total coverage. The characteristic of the Fibroblast cell itself may be the cause of the quicker attachment. On the other hand,adipose derived stem cells attached to the surfaces more slowly than the fibroblast cells did, but after three hours, the same pattern was seen again, with the PIII-treated samples attracting around twice as many cells.Industrial grade UHMWPE fabric showed less cell attachment than scientific grade due to the structural properties. Yarn of fabrics are tightly binded to one another and there were no porous structure in industrial grade UHMWPE fabric whereas it is quite prominent for scientic grade UHMWPE fabric.

The outcomes from this study are consistent with reports in the literature for various plasma treatments of UHMWPE. Studies have demonstrated that the biocompatibility of UHMWPE fabric was enhanced by plasma treatments that added new functional groups to the surfaces[67, 246]. However, our findings show that a comparable improvement might also be attained with the PIII treatment with high intensity nitrogen ion bombardment. Wetability of polymer surfaces can change as a result of oxidised groups produced by plasma treatments[6]. The improvement shown here most likely results from the rise in functional groups C – O, C = O, and O – C – O, as well as a C – N groups discovered in chapter 2 by XPS study. Additionally, it is commonly acknowledged that the wettability of a surface has a significant impact on cell adhesion[305]. According to the investigations on surface characterisation, the PIII treatment was able to lower the contact angle from 47° to roughly 28°.

It's also significant to note that a few difficulties were experienced when carrying out the cell attachment assays. Numerous times, not only between samples but also within the same portion of sample, the cell adhesion on untreated UHMWPE fabric for all cell types examined was very inconsistent. In many cases, cell attachment led to a haphazard, uneven coverage of cells that revealed few to no cells adhered which lead to a large variation of results. It was hypothesized that this might be because there are still some additives in the product that were added during processing. On the other hand, none of the PIII-treated samples showed this behaviour, likely as a result of the severe surface alteration eliminating any local differences. Furthermore, the assay depends on PBS washing procedures to eliminate any non-adherent cells, the cell attachment assay itself was incredibly vulnerable to handling errors.

Previous research had already shown that pure UHMWPE sheet/block is not cytotoxic or mutagenic[309]. However, the effect of PIII treated UHMWPE fabric on long term cell

proliferation remained unknown and was investigated in this study. It's been noted that FB & ADSC cells proliferated easily and constantly in both fabrics. The cell culture plate could be more receptive surface for adhesion and growth or could be indicative of cells being pushed down the differentiation path for the UHMWPE which is typically associated with reduce proliferation. Both industrial grade & scientific grade PIII treated UHMWPE samples were superior to the pure untreated industrial grade & scientific grade UHMWPE fabric samples in terms of cell growth. In cell cultures, significant increases in metabolic activity have been seen as early as 3 days following the initial cell seeding. Approximately twice as much metabolic activity was present in cells cultivated on PIII-treated surfaces by the end of a one-week period, indicating that the cells were multiplying twice as quickly on the changed surfaces. We can draw the conclusion that PIII-treated UHMWPE fabric did not exhibit any harmful effects. In contrast to the untreated UHMWPE fabric, there was also a noticeable robust promotion of cell growth. Similar findings from other studies have been published in the literature for sheet or block[42, 79]. The modified surface features of PIII treated UHMWPE fabric offered a much better foundation for the cells to connect, which further boosts the proliferation and total metabolic activity.

A thorough examination of the surface proteins adsorbed as well as the cellular receptors that are controlled on the cells to adhere to the various UHMWPE fabric surfaces would be beneficial. Although there have been a few reports on the biocompatibility testing of plasma-treated UHMWPE in the literature, the vast majority of these research reports concentrated on gingival&periodental ligament cells that are unable to develop into the full spectrum of ligament and tendon cells and thus cannot accurately represent the physiological behaviour of earlier primary cells[307]. When an orthopedic implant is inserted into the body, the adsorbed ECM

proteins are primarily responsible for determining the host response. The repair of the bone tunnel surrounding the transplanted ligament/tendon (L/T) depends on the production of new bone [310]. As a result, in the second section of this chapter, we concentrated on using primary fibroblast cells in longer-term studies and analyzing its differentiation parameters, which still could differentiate into cells that have a mature tenocyte-like phenotype.

The developmental sequence can be divided into three major phases using primary L/T cell cultures as a model: proliferation, ECM maturation, and mineralisation. Each of the three phases displays an unique phenotype for gene expression. The results of the RT-PCR helped establish whether the modified UHMWPE fabric surface can exhibit tenogenic qualities by giving a snapshot of how the cells are reacting to the surfaces in terms of gene expression. After 10 days of culture, the data showed that several genes, TNMD,SCX and COL3A, had significantly increased expression. In addition, TNC expression levels showed a trend towards downregulation. It is assumed that the culture is most likely in the matrix development and maturation stage based on the expression pattern. Additionally, it is important to note that a large rise in numerous genes was seen for PIII treated UHMWPE in comparison to the untreated UHMWPE, and similar findings were obtained during cell attachment and proliferation assays. It indicates that the variance in the gene expression profile was caused by the differences in surface properties between the two material surfaces. It is well known that differences in the surface properties can be seen in the development of fibroblasts in vitro. This affects not just how responsive the cells are to the substrate but also how differently they differentiate. There is no doubt that changes in the functional groups on the surfaces could have led to such a result.

The primary fibroblast gene expression data offered some evidence that the PIII-treated surface might be able to facilitate differentiation, but longer-term tissue culture studies were still

required for definitive proof. It has been suggested that bone formation and calcification are mediated by high levels of ALP activity, which is a characteristic biochemical characteristics of osteogenic differentiation of cells [311].

Overall, the findings from this chapter demonstrated that PIII treatment alone significantly increases UHMWPE's bioactivity for bone cells without the need for additional biofunctionalization.

Summary of this chapter

1. The two types of UHMWPE that were examined for cell attachment were found to be to give similar results, indicating that, for exploratory studies, less expensive forms of UHMWPE fabric should produce biological responses that are comparable to implantable grade UHMWPE, which is frequently used in clinical settings. However, the evidence of the presence of impurities in the industrial grade material would be of concern.
2. In comparison to untreated UHMWPE, the percentage of cell attachment was roughly twice as high on surfaces modified with PIII.
3. SEM and optical microscopy analyses proved that the cells initially adhered in greater numbers to the PIII treated surfaces and tended to be more dispersed.
4. According to proliferation experiments, the PIII enhanced UHMWPE fabric surfaces had much higher metabolic activity than the untreated pure UHMWPE control for FB & ADSC cells, which was around twice as high.
5. The PIII treated UHMWPE surfaces were able to enable tenogenic differentiation, with the PIII treatment demonstrating a higher effect, according to the gene expression investigation.

6. All the substances studied were able to support differentiation, according to ALP activity assays, although the PIII-treated samples had a notably greater impact.
7. All the studied materials were able to support mineralisation, according to Alizarin Red S staining.

Our hypothesis predicted outcomes resemble the outcomes of our experimental work and data analysis.

Chapter 7 : The adhesion, proliferation, and differentiation of primary human fibroblasts and ADSC grown on PIII treated and Protein Functionalized UHMWPE

7.1 Introduction

The surface of UHMWPE continues to be passively inert despite its substantial success as a biomaterial for orthopedic implants[71]. There are obstacles to overcome to apply UHMWPE in more orthopedic applications, such as for implantation locations that are affected by poor bone quality. Shojaee and Parham reported that the most crucial and difficult part of the implanted ligament/tendon graft is tenogenic differentiation[312]. Modern biomaterials development for tissue engineering applications has recently concentrated on creating biomimetic materials that can trigger specific cellular responses through bio-molecular recognition, to guide the synthesis of new tissues[312].

The use of rational growth factors that can regulate the cellular activities of the parent cells and their capacity to differentiate into specific cell types is crucial, in addition to providing appropriate scaffolds that act as a mechanical support for cell growth[313]. The discovery of the attachment of ligament stimulatory factors to implants surfaces was described was an exciting area by Molloy et al.[220] in 2003. Implant surface topographic design has already been extensively researched and implemented. Additional physical alterations, such as raising the implant's surface energy, may further enhance tenogenic differentiation. The use of ligament/tendon L/T growth stimulating substances, however, may result in the greatest advancements and improvements in implant design as our knowledge of the roles of ECM proteins and growth factors involved in the control of fibroblast growth [276].

Among various areas or research, Bax reported utilizing PIII to covalently link tropoelastin to polystyrene in 2009, significantly enhancing the fibroblast cells' ability to proliferate[314]. The study also showed how a metal mask could be used to regulate how much of the polymer surface was exposed to the plasma treatment, allowing surface patterning to control biological responses.

Applying the plasma treatment as a switch to regulate whether cells may adhere to the surface. We have acquired enough foundation knowledge to use PIII as a surface treatment on UHMWPE surfaces through the experiments in the prior chapters.

We have demonstrated that covalent immobilization of proteins onto PIII-treated surfaces is possible through a straightforward one-step procedure and that covalent attachment does significantly improve the immobilized protein's long-term retention. However, large increases in differentiation and mineralization occurred when L/T cells were cultivated directly on the bare treated surfaces, leading to considerable bioactivity improvements. Depending on these encouraging findings, we plan to incorporate the knowledge gained and described in the earlier chapters of this thesis in the project's next stage to immobilize proteins and evaluate how well the functionalized layer performs in terms of cellular responses. Full-length proteins were chosen for this study's immobilization procedure and examined for their capacity to promote L/T cell development. To facilitate fibroblast attachment and to encourage fibroblast differentiation, surface coatings made of ECM proteins that serve as sites of attachment for fibroblasts have been investigated.

The primary structural protein in L/T, collagen type I, has already been described as an effective scaffold material for directed L/T regeneration [315]. In a rat model study, collagen-coated titanium pins were also found to result in enhanced L/T remodeling. Similarly, fibronectin is an essential protein for the processes of wound healing and embryonic development and plays a significant role in cell adhesion, proliferation, migration, and differentiation[220]. Numerous studies have shown that covering a surface in cell adhesive proteins like fibronectin and collagen enhances preliminary cell attachment, cell spreading, and overall cell activity[220, 316].

Connective tissue growth factor (CTGF) was chosen to be immobilized and assessed in this investigation in addition to the previously described two ECM proteins. CTGF is related to wound healing and connective tissue regeneration and found in many tissues[317]. CTGF, also referred to as CCN2, is a 38 kDa extracellular matrix protein that is cysteine-rich (with 22 cysteines in the N-terminal and 16 cysteines in the C-terminal area) and belongs to CCN family of proteins. Connective tissue growth factor is a polypeptide growth factor that induces chemotaxis and promotes DNA synthesis. Cheng et al.[318] have reported the influence of CTGF in tendon healing in 2008. It's been observed that by Olvera [319] CTGF induced higher levels of expression of L/T genes.

7.2 Aim & hypothesis of the chapter

The purpose of this study is to assess the performance of the immobilized protein in tests conducted in in vitro cell culture. The following points could be used to summarize this chapter's goal:

1. To determine whether the biomolecules fibronectin, collagen type I, and CTGF retain biological function after becoming attached on the surface of UHMWPE.
2. To determine whether the PIII treatment leads to better bioactivity results than passive binding without PIII.

It is assumed that the PIII treatment will be able to enhance and safeguard the function of the protein coatings because of the lowered hydrophobicity and through the covalent immobilization of the procedure, which is based on the literature describing the success of similar applications. We can better understand if the immobilized protein coating can enhance UHMWPE bioactivity by using the results from this chapter, which could lead to the creation of new applications.

7.3 Experimental methods

7.3.1 Surface Preparation and Functionalization

Based on the previously established results, scientific grade UHMWPE fabric is used because it was difficult to maintain the aseptic environment of the cell culture technique for industrial grade UHMWPE fabric. Industrial grade UHMWPE fabric was quite thick, so ethanol wash/UV sterilization didn't work several times. Protein functionalization was simply carried out by incubating proteins overnight in a buffer solution containing collagen and fibronectin at concentrations in three different solutions that had previously been shown (chapter 5) to saturate surface binding after overnight soaking and to produce CTGF in vitro activity. Prior to being sterilized under UV for 20 minutes per side, surfaces were first cleaned, dried, and plasma treated in accordance with the specified protocols. After that, surfaces were exposed to the sterile protein solutions for an overnight incubation period at 37°C in a humidified cell culture incubator. The protein concentrations employed were fibronectin at 10 μg/mL, collagen type I at 30 μ/mL, and CTGF at 100 ng/mL. The surfaces were cleaned three times with PBS the following day to eliminate any non-bound proteins, and cells were promptly seeded on the surfaces.

Based on research in the literature that claimed a stimulating effect may be seen when a dose level of 100 ng/mL was utilized in the medium, this concentration for the CTGF protein was chosen.

7.3.2 Cell Attachment and Proliferation Studies

Studies on cell adhesion and proliferation for protein-coated UHMWPE were carried out according to the same technique as described in chapter 5. To reduce the overall size of the trials, the experiment was carried out in triplicate rather than quadruplicate using primary human fibroblasts (FB) & Adipose derived stem cells (ADSC). Collagen and fibronectin and CTGF were evaluated among the proteins because they have a substantial impact on cell attachment and proliferation. It has been demonstrated that connective tissue growth factor (CTGF) stimulates endogenous tendon stem cells, hence promoting tendon regeneration[320].

7.3.3 Gene expression studies of ligament and tendon cell specific genes

The procedure outlined in chapter 6 was followed while carrying out gene expression tests on the protein-coated UHMWPE. Using primary human fibroblasts (FB), the experiment was once more carried out in triplicate. The UHMWPE surfaces with collagen, fibronectin, and CTGF coatings as well as a control group without any protein coatings were investigated. Additionally, two early time points—day 3 and 10—were selected to track the early alterations since it was anticipated that the protein coatings would be extremely effective at producing impacts. A larger range of genes, such as COL3 A1, Tenomodulin (TNMD), Scleraxis (SCX), and Tenascin-C (TNC) were also evaluated which are characteristic genes for ligament/tendon differentiation. To find any fold change differences, all findings were compared to the uncoated and untreated pure UHMWPE surface after being normalized to the Glyceraldehyde 3-phosphate dehydrogenase GAPDH housekeeping gene.

7.3.4 Cell differentiation towards the osteoblast lineage

Repetition of the chapter 5 methodology was used to investigate differentiation towards the osteoblast lineage for the protein-coated UHMWPE studies by evaluating induction of alkaline phosphatase (ALP) activity. Because of the shortage of ADSC cells and the short study duration, the experiment was performed in triplicate using only fibroblast (FB) cells. To identify any early alterations brought on by the various protein coatings. Time points 7,14, and 21 days were selected for the ALP activity experiment. The identical methods described in chapter 5 were used for all cell culturing conditions and for image analysis.

7.4 Data presentation and statistical analysis

Origin and Microsoft Excel were used to construct and assess all figures and statistical analyses relevant to the conclusions in this chapter. Two-tailed t-tests were performed to compare groups, with a P value of 0.05 indicating significance. Unless otherwise noted, each experiment employed at least in triplicates and a minimum of three biological replicates to assure statistical validity of the results.

7.5 Experimental results

7.5.1 Cellular responses on biomolecule immobilized UHMWPE

The attachment of primary human osteoblasts to the functionalized UHMWPE fabric surfaces after one and three hours may be seen in Figures 7.1 (A-F). Fig 7.1 B shows that the bare PIII-treated surfaces have a greater total number of attached and spreading cells. After applying collagen to every surface, it was possible to see improvements in the number of cells and spreading intensity (Fig C &D). The PIII-treated surface promoted cell adhesion and spreading

far better than the untreated UHMWPE fabric surface (Fig B). According to results obtained from Fig (E &F) fibronectin coating has a positive impact on cell attachment in untreated & treated UHMWPE fabric surfaces.

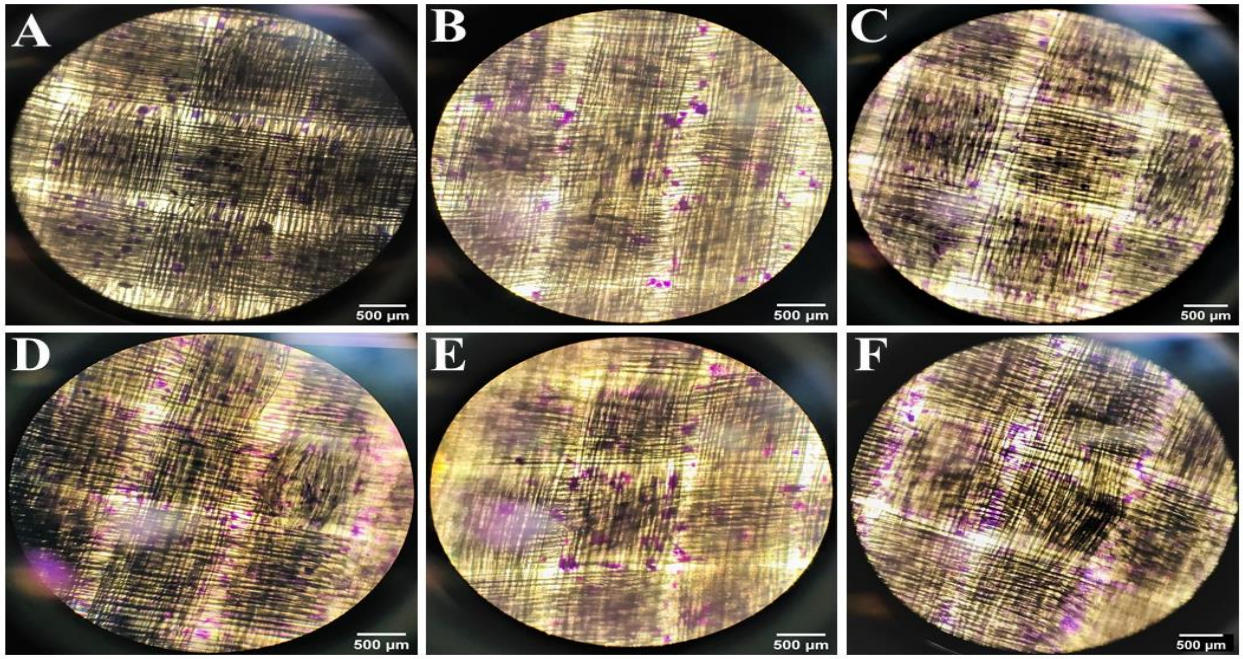

Figure 7. 1 Microscope image of primary human fibroblast cells attaching onto untreated or PIII-treated UHMWPE samples (A) Pure UHMWPE 1 hour, (B) PIII treated UHMWPE 1 hour, (C) Pure UHMWPE +Collagen 1 hour, (D) PIII treated UHMWPE+ Collagen 1 hour, (E) Pure UHMWPE + Fibronectin 1 hour, (F) PIII treated UHMWPE +Fibronectin 1 hour. All cells were seeded on the samples at a density of 25,000 cells per cm^2 in serum free medium and allowed to attach in a cell culture incubator for 1 hour. The samples were fixed by 3% paraformaldehyde, stained by crystal violet, and inverted before imaging to achieve a better contrast against the opaque UHMWPE background.

7.5.2 Fibroblast adhesion and morphology

Tendons and ligaments are both comprised of muscular connective tissue in which fibroblasts are the primary cell type [303]. Biocompatibility of untreated and PIII treated UHMWPE with FB cells are crucial for our ligament/tendon regeneration study. The adhesion of primary fibroblasts to functionalized UHMWPE surfaces after 1 hour and 3 hours is shown in Fig 7.2. Fibroblast

adherence to the fabrics at 1 and 3 hours after seeding was quantified and shown in Figures 7.2(A) and (B). Fig 7.2 (A) shows that during the first hour, the direct cell attachment to the PIII treated surfaces without protein pre-coating was twice the cell number on the untreated UHMWPE.

There was significant improvement in cell attachment when the untreated fabrics were incubated with collagen or fibronectin prior cell seeding but this improvement was only observed on the PIII treated fabrics after 3 hours with fibronectin (Fig 7.2 B). On both surfaces, fibroblast showed much more improvement with immobilized fibronectin compared to that with collagen.

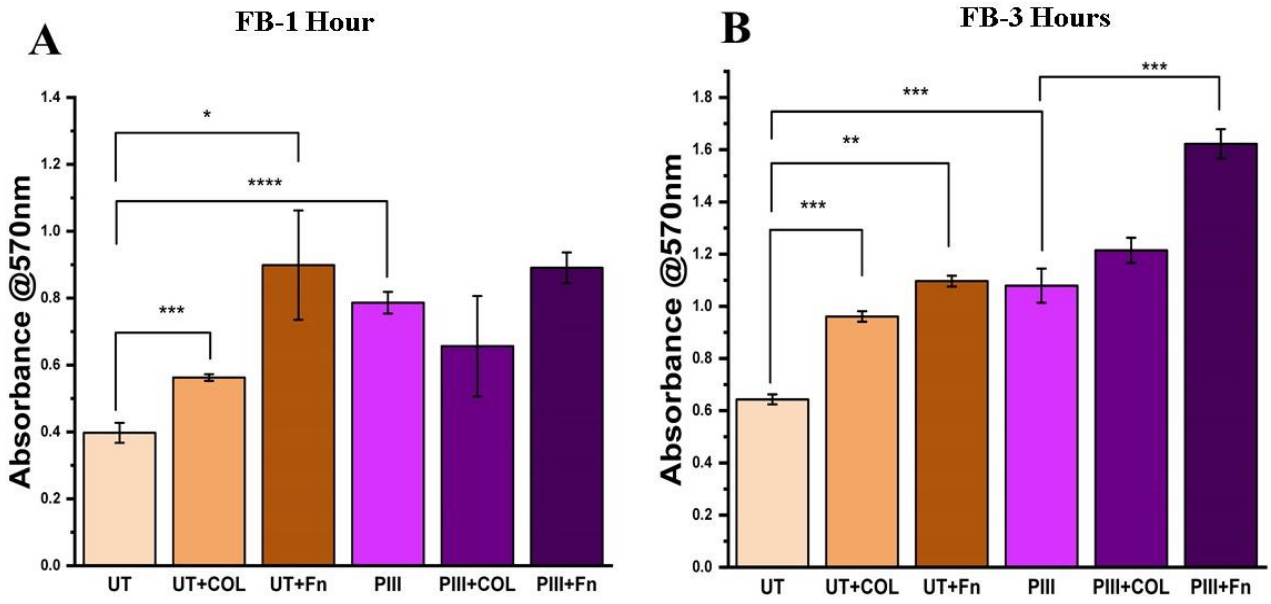

Figure 7. 2 Absorbance of crystal violet released from fibroblast cells attaching onto untreated or PIII treated UHMWPE samples measured after 1 hour (A) and 3 hours (B). Error bars here indicate standard deviations of triplicates before and after the PIII treatment. Symbol meaning (*) =$P \leq 0.05$, (**) = $P \leq 0.01$, (***) = $P \leq 0.001$, (****) = $P \leq 0.0001$.

SEM was utilized to examine and measure the adherence of fibroblast cells to the material surface. A notable change in cell morphology was observed. On untreated surface, a great number of cells are in round shape while those on the PIII-treated surface showed a higher overall number of spreading cells. It's likely that the higher wettability of the treated surfaces enables the cells to adhere quickly.

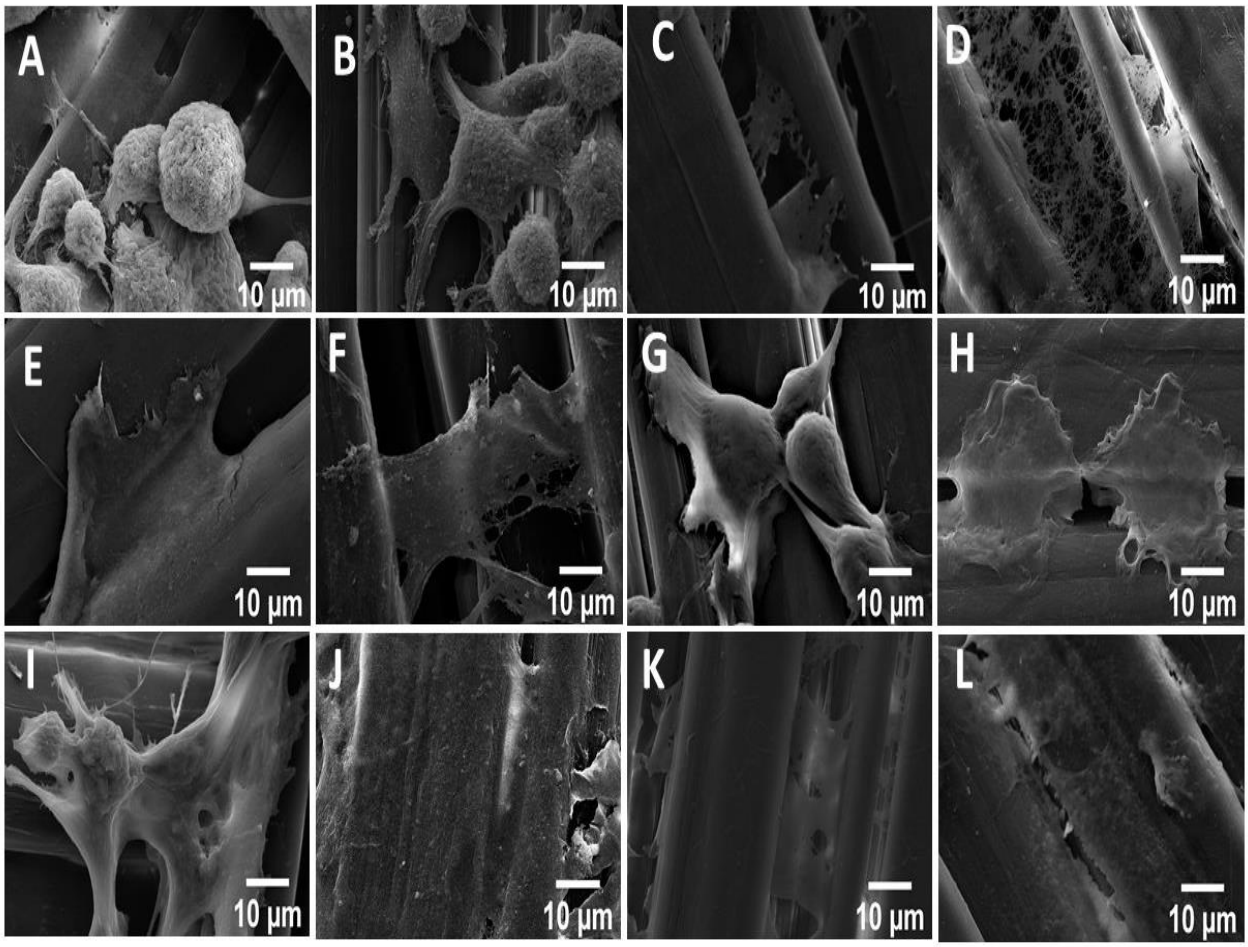

Figure 7. 3 Scanning Electron Microscopy (SEM) imaging of the fibroblast cells on UHMWPE under low magnification. (A-F) represents cell attachment after 1 hour. (G-L) represents cell attachment after 3 hours. The groups presented here are: (A & G) Untreated UHMWPE, (B & H) PIII treated UHMWPE, (C &I) Untreated UHMWPE+ Collagen, (D &J) PIII treated UHMWPE+ collagen, (E &K) UT(Untreated) UHMWPE+ Fibronectin, (F& L) PIII treated UHMWPE+ Fibronectin.

Fig 7.3 depicts the shapes and distribution of adherent cells on UHMWPE after 1 hour and 3 hours with magnification of 1700 X. Fibroblast cells were in round shapes when attaching to the untreated fabrics (Fig 7.3A) and only less than half of the cells have spread after 3 hours (Fig7. 3G) while those on the PIII treated surfaces spread more at one hour (Fig 7.3B) and completely spread after 3 hours (Fig 7.3H). The spreading is an indication that cells can develop focal adhesion to the surface. Surfaces coated with collagen (Fig 7.3 C, D, I and J) show an improvement in both cell number and degree of spreading. Both PIII treated and untreated surfaces had obtained nearly 100 percent surface coverage by the three-hour mark. Figures 7.3E, F, K and L show that the Untreated and PIII treated surface promoted cell adhesion and dissemination substantially similar at both time points when all surfaces were coated with fibronectin.

7.5.3 FB proliferation

The growth curves of fibroblast cells cultivated on various functionalized surfaces is shown in Fi g 7.4. The data is shown as a mean of the cell survival absorbance for each condition. The FB cells did not proliferate effectively on the untreated with no protein but still proliferated on the PIII treated surface after 7 days. The addition of proteins (collagen or fibronectin) significantly improved cell growth on both surfaces but with higher rates on the PIII treated surfaces compared to the untreated surfaces immobilized with the same protein.

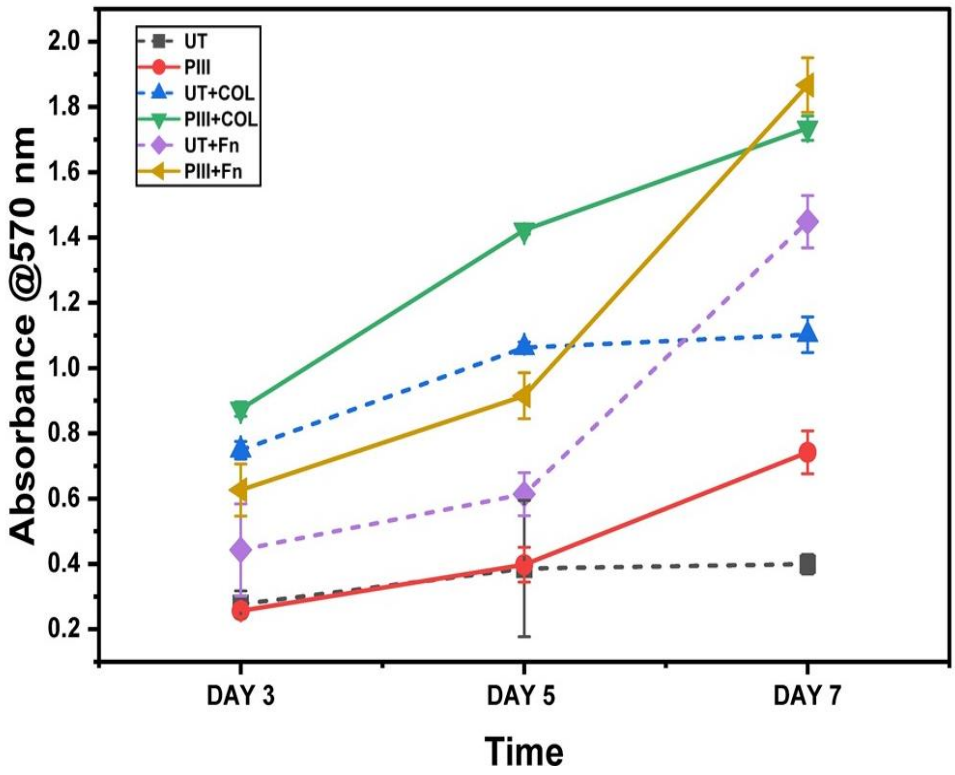

Figure 7. 4 Growth curve of human primary fibroblasts cultured on untreated (UT) and PIII treated (PIII) UHMWPE coated with collagen (+COL), fibronectin (+FN) over 3-7 days.

Fig 7.5 shows Cell on the UHMWPE fabric displayed flat and broad morphology after 7 days of incubation, bridging between adjacent fibers. Additionally, small cell colonies developed on PIII treated and protein coated UHMWPE fabric surfaces which is prominent for collagen and fibronectin coated PIII treated UHMWPE fabric surfaces. On the PIII-treated sample, cell colonies expanded and covered more of the layer of UHMWPE fibers. Compared to those at untreated UHMWPE fabric surfaces, these cells developed an even larger colony as they expanded in the direction of the fiber. Additionally, these cells displayed additional attachment sites that were anchored to nearby fibers (Fig 7.5B, C, E).

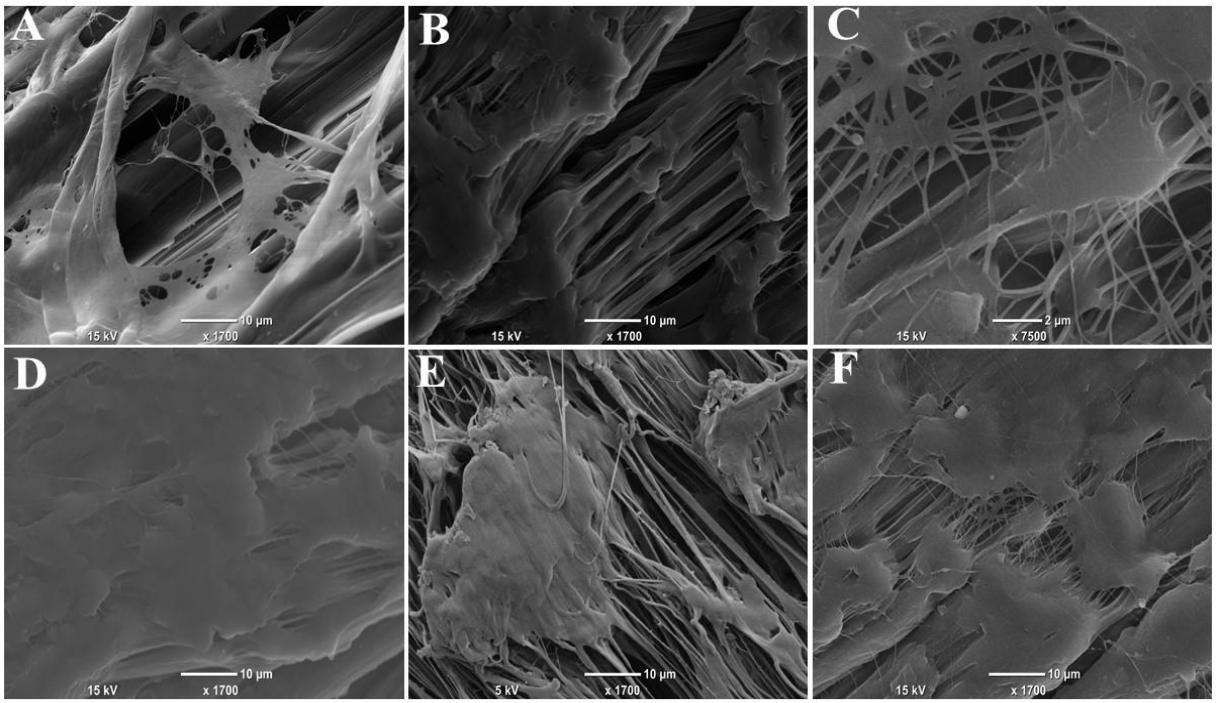

Figure 7. 5 Fibroblast cell attachment on UHMWPE fabric (A) Untreated UHMWPE fabric (B) PIII treated UHMWPE fabric (C) Untreated UHMWPE +Collagen (D) PIII treated UHMWPE +Collagen (E) Untreated UHMWPE + Fibronectin (F) PIII treated UHMWPE +Fibronectin on day 7 at higher magnification.

In the meantime, cells on collagen and fibronectin-coated UHMWPE fabric similarly proliferated in the direction of the fibers and developed into a bigger colony that covered the entire surface before attaching to the fibers (Fig 7.5 D &F). In comparison to cells on the UHMWPE fabric, cells on PIII treated COL+UHMWPE and Fn+ UHMWPE also seemed to be stretched out and have a wider shape.

7.5.4 ADSC adhesion and morphology

ADSC cells has been used in tendon graft integration due to their ability to self-renew and proliferate [304]. For this reason, we chose ADSC to observe its interaction with the surface of UHMWPE. The amount of ADSC cells adhered to the functionalized surfaces at 1 hour after

seeding is quantified in Fig 7.6. Similar improvement was observed with ADSC cells on the untreated fabrics when the surfaces were incubated with either collagen or fibronectin before cell seeding. On the PIII treated fabrics, the number of ADSC cells attached to the surface without any protein was much higher than the number on the untreated fabrics and the addition of the protein improved this number further but not as obviously as observed on the untreated fabrics. ADSC cells preferred fibronectin coated surfaces to collagen coated surfaces at 3 hours' time point.

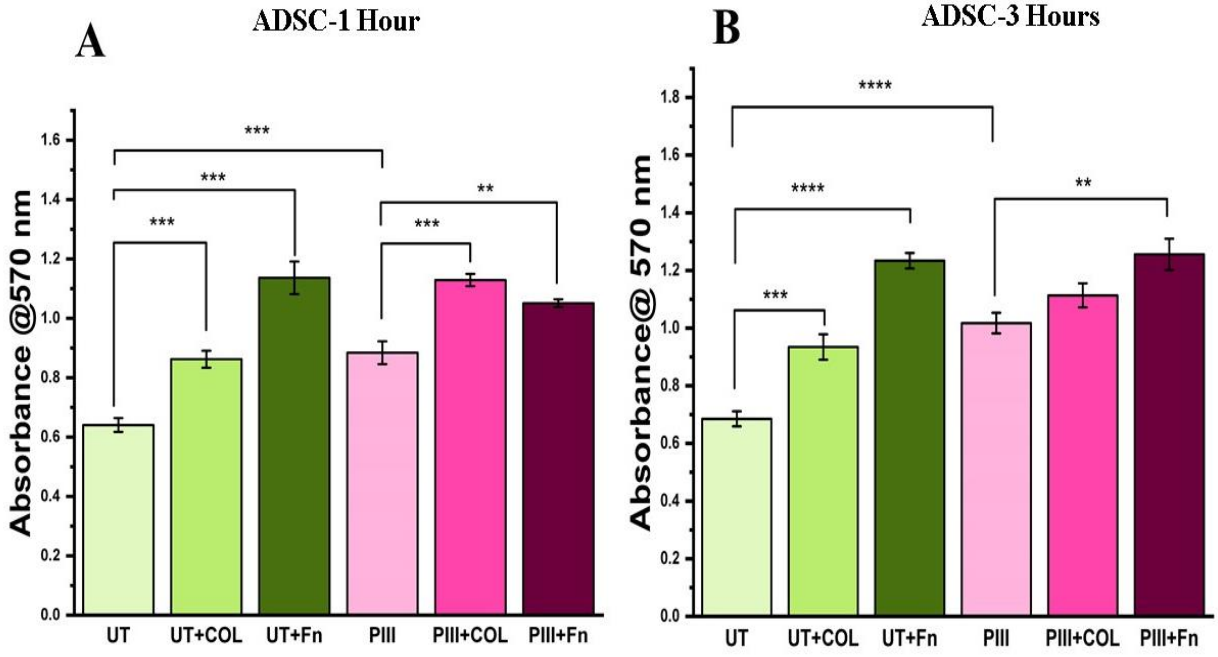

Figure 7. 6 Absorbance of crystal violet released from ADSC cells attaching onto untreated or PIII treated UHMWPE samples measured after 1 hour (A) and 3 hours (B). Error bars here indicate standard deviations of triplicates before and after the PIII treatment. Symbol meaning (*) =$P \leq 0.05$, (**) = $P \leq 0.01$, (***) = $P \leq 0.001$, (****) = $P \leq 0.0001$.

Cell spreading and attachment of ADSC cells are shown in Fig 7.7 from (A-L). The presence of pseudopodia and cell spreading on the fibrous region was observed. Cells are quite rounded at 1 hour in untreated UHMWPE than PIII treated UHMWPE. PIII treatment may increase the

effective contact area and interaction force between the material surface and the ADSC cells due to the increased hydrophilicity, and covalent bonding. Most cells on the surface had developed pseudopodia and seemed to be active for PIII treated and with protein coated UHMWPE samples. Greater cell spreading was observed for PIII treated & with protein coated UHMWPE samples.

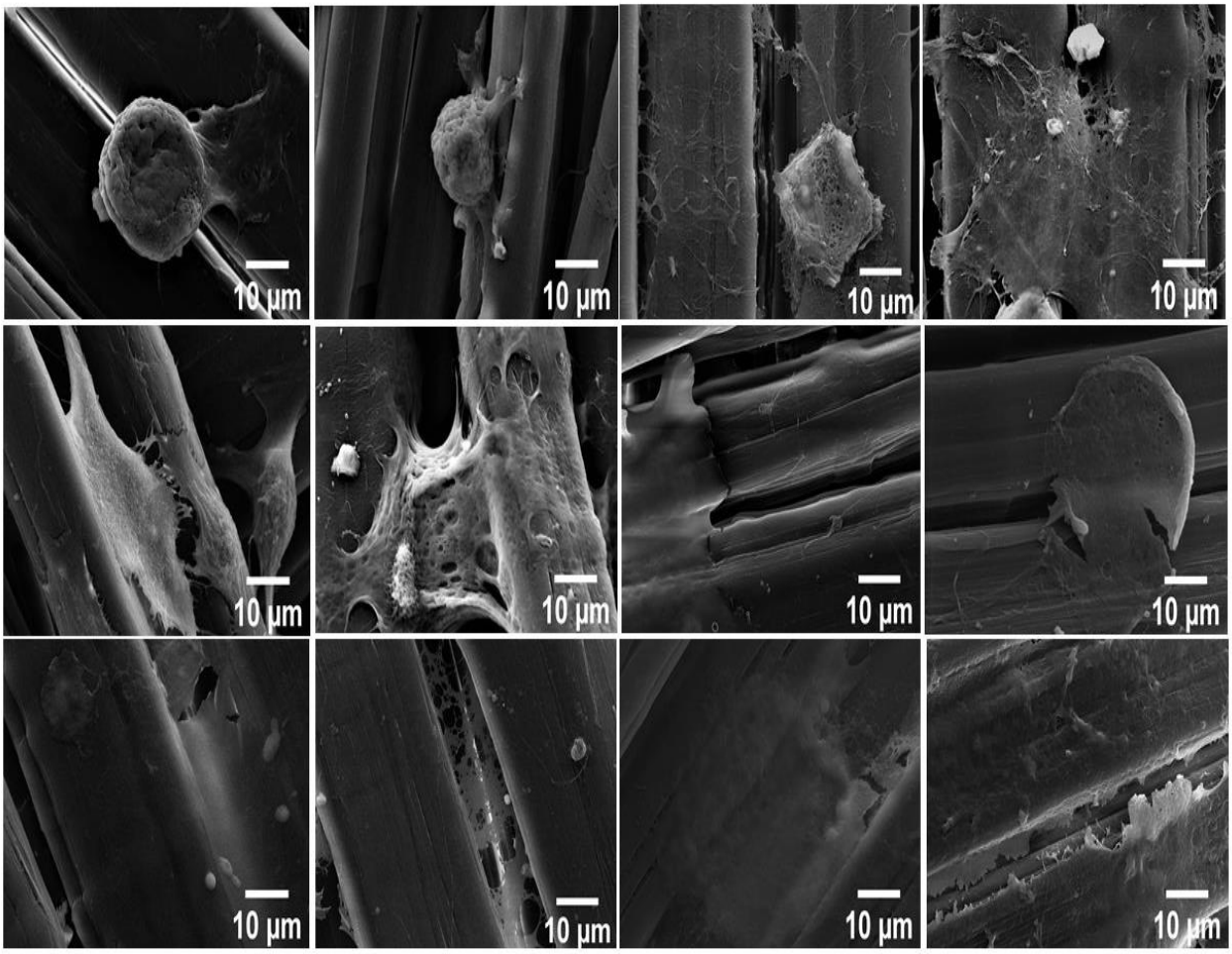

Figure 7. 7 Scanning Electron Microscopy (SEM) images of ADSC cells on UHMWPE under low magnification. (A-F) represents cell attachment after 1 hour. (G-L) represents cell attachment after 3 hours. The groups presented here are: (A & G) Untreated UHMWPE, (B & H) PIII treated UHMWPE, (C &I) Untreated UHMWPE+ Collagen, (D &J) PIII treated UHMWPE+ collagen, (E &K) Untreated UHMWPE+ Fibronectin, (F& L) PIII treated UHMWPE+ Fibronectin.

7.5.5 ADSC proliferation

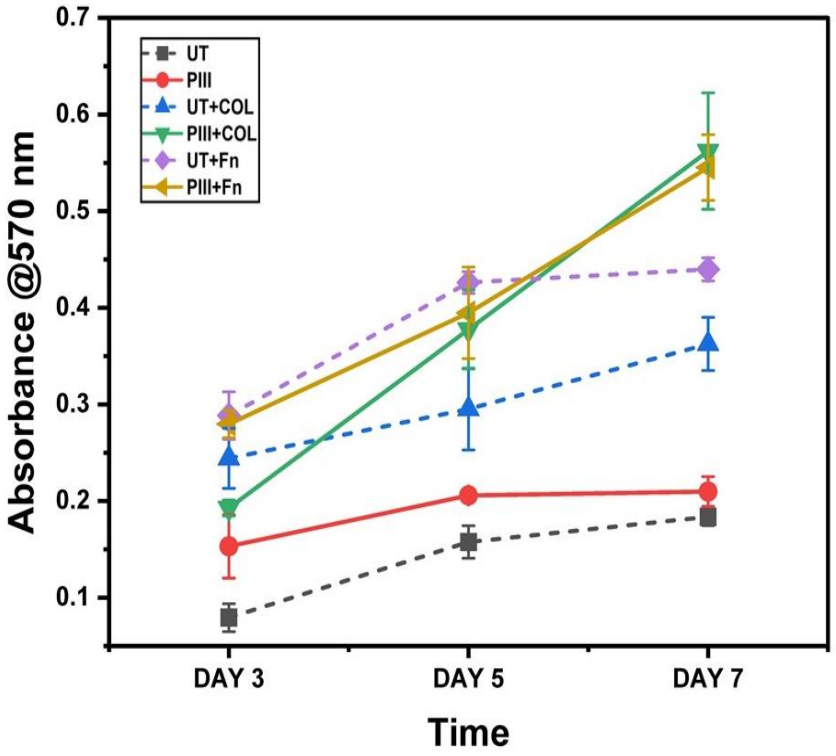

Figure 7. 8 Growth curve of ADSC cells cultured on untreated (UT) and PIII treated (PIII) UHMWPE coated with collagen (+COL), fibronectin (+FN) or untreated (UT) over 3-7 days. Error bars are standard deviations of triplicates.

Fig 7.8 depicts the growth curves of ADSC cells, with statistical analysis used to assess the growth period's ultimate results. Like findings with fibroblasts, the PIII-treated surfaces had the maximum metabolic activity till day 5 but later decreased. Collagen coating significantly improved cell adhesion on the untreated and treated surfaces. However, the metabolic activities observed for untreated and PIII treated UHMWPE with and without fibronectin are significantly different. Metabolic activity of fibronectin coated untreated UHMWPE increased till day 5 and then decreased.

7.5.6 Gene expression study

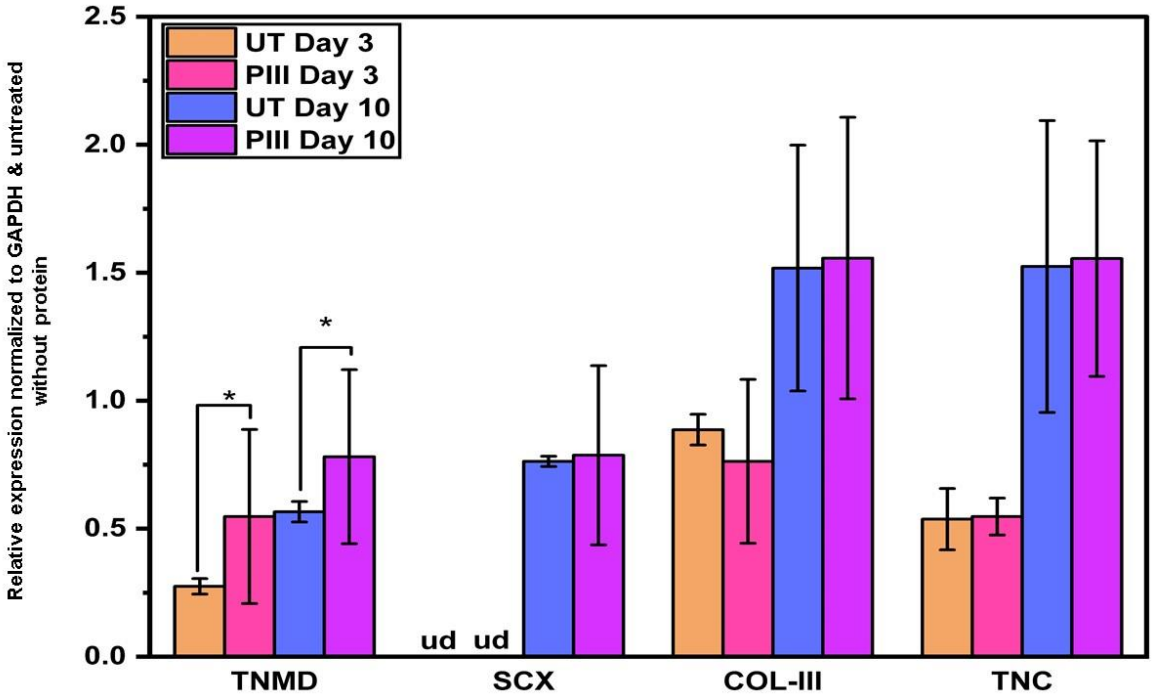

Figure 7. 9 Gene expression profile of human primary fibroblasts cultured on pure (UT) and PIII modified (PIII) UHMWPE with no protein coatings. Error bars here indicate standard deviations of triplicates before and after the PIII treatment. Symbol meaning (*) =P ≤0.05, (**) = P ≤ 0.01, (***) = P ≤ 0.001, (****) = P ≤ 0.0001.

Fig 7.9 shows gene expression profiles of primary fibroblasts cultured in untreated and PIII-treated UHMWPE fabric without protein coating. Although a general pattern appeared to indicate that many of the tenogenic genes were expressed at higher levels on the PIII treated surface, few significant differences were found because of the limited number of samples and high degree of heterogeneity. After day 3 & 10 when the PIII treated, group was compared to the untreated group, TNMD expression was higher. These differences were statistically significant for only TNMD. After day 3, SCX expression was undetected for both untreated and PIII treated UHMWPE fabric surfaces. But, after 10 days expression level was increased for untreated & PIII

treated UHMWPE fabric surfaces. On the other hand, a higher expression of the Collagen-III & TNC gene were found on both untreated & PIII treated UHMWPE fabric surfaces after 10 days.

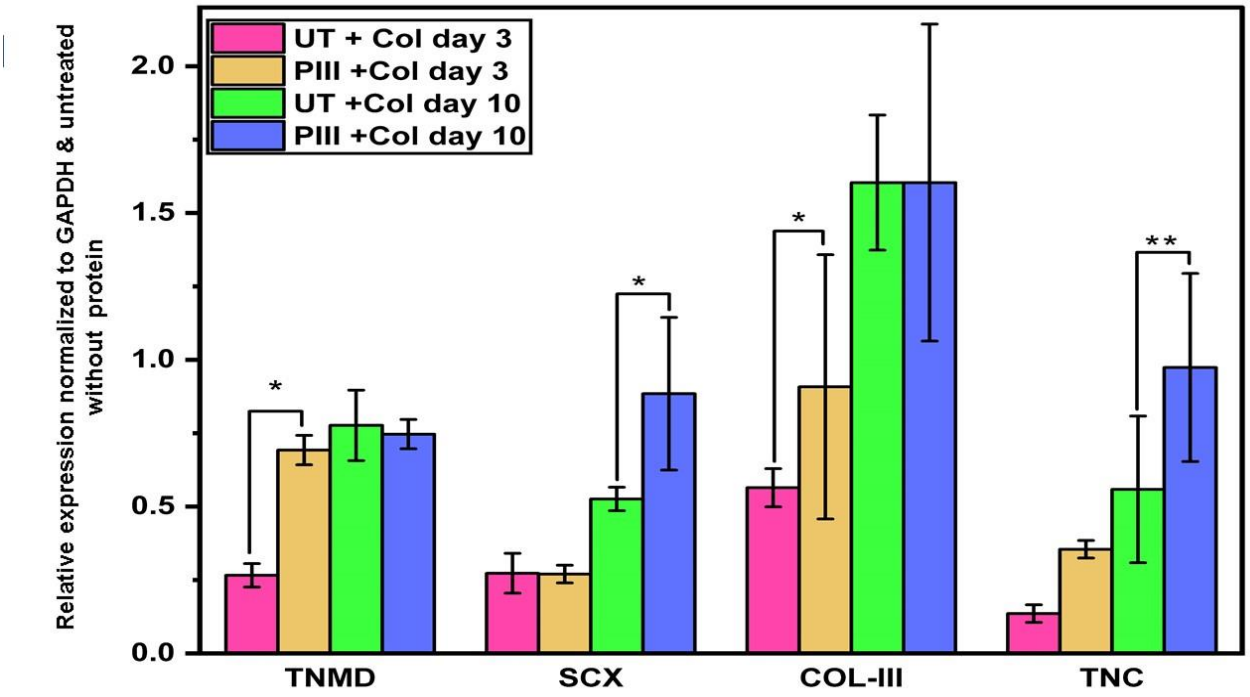

Figure 7. 10 Gene expression profile of human primary fibroblasts cultured on pure (UT) and PIII modified UHMWPE with collagen type -I protein coatings. Error bars here indicate standard deviations of triplicates before and after the PIII treatment. Symbol meaning (*) =$P \leq 0.05$, (**) = $P \leq 0.01$, (***) = $P \leq 0.001$, (****) = $P \leq 0.0001$.

The gene expression profile of primary fibroblasts cultivated on collagen coating PIII treated UHMWPE fabric and untreated fabric is shown in Fig 7.10. The TNC, COL-III, TNMD expression levels rose markedly after day 3. While the TNMD gene expression was increased for both surfaces but less for PIII treated UHMWPE fabric surfaces compared to the untreated surface. In addition, after day 10, a large increase in the expression of SCX, COL-III & TNC were seen on the PIII treated UHMWPE fabric surface compared to the untreated surface, but this trend was similar on the COL-III gene expression levels.

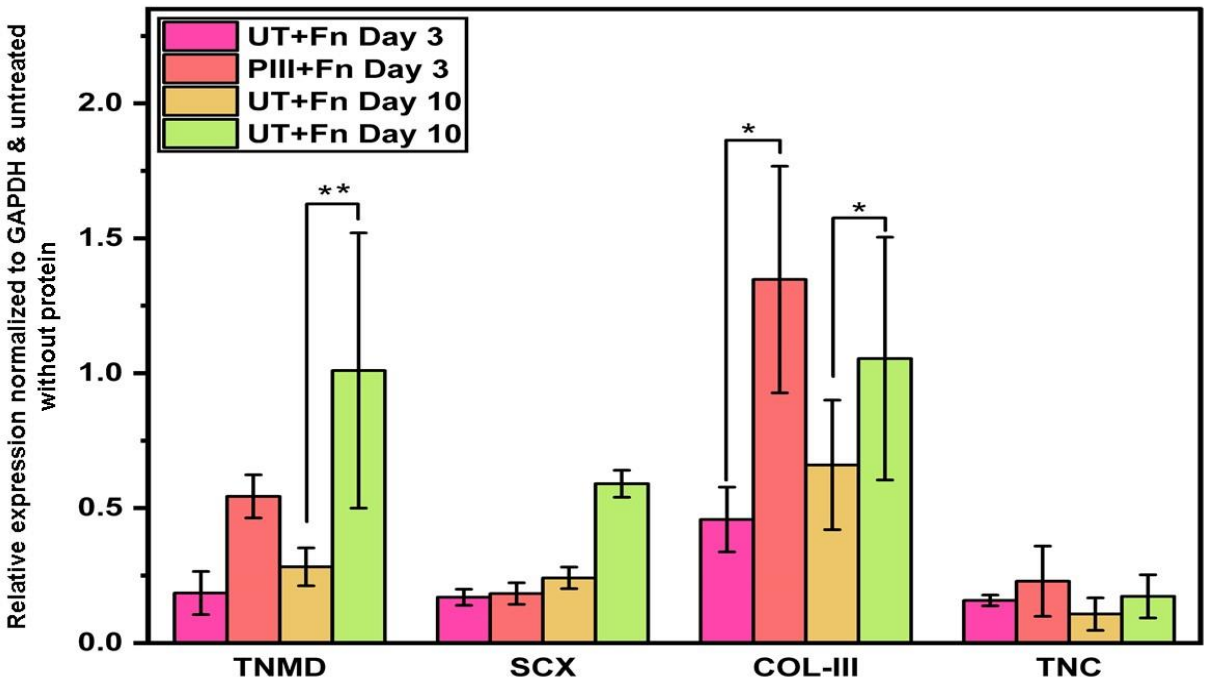

Figure 7. 11 Gene expression profile of human primary fibroblasts cultured on pure (UT) and PIII modified (PIII) UHMWPE with Fibronectin protein coatings. Error bars here indicate standard deviations of triplicates before and after the PIII treatment. Symbol meaning (*) =P ≤ 0.05, (**) = P ≤ 0.01, (***) = P ≤ 0.001, (****) = P ≤ 0.0001.

The gene expression profile of primary fibroblasts cultivated on untreated and PIII-treated UHMWPE fabric with a fibronectin coating is depicted in Fig7.11. Even though few statistically significant changes could be seen, the untreated surface exhibited a tendency for increased TNMD expression levels after days 3, and 10 respectively. SCX expression levels increased after 10 days. COL-III and TNC expression level increased after 3 days but this was reversed after 10 days.

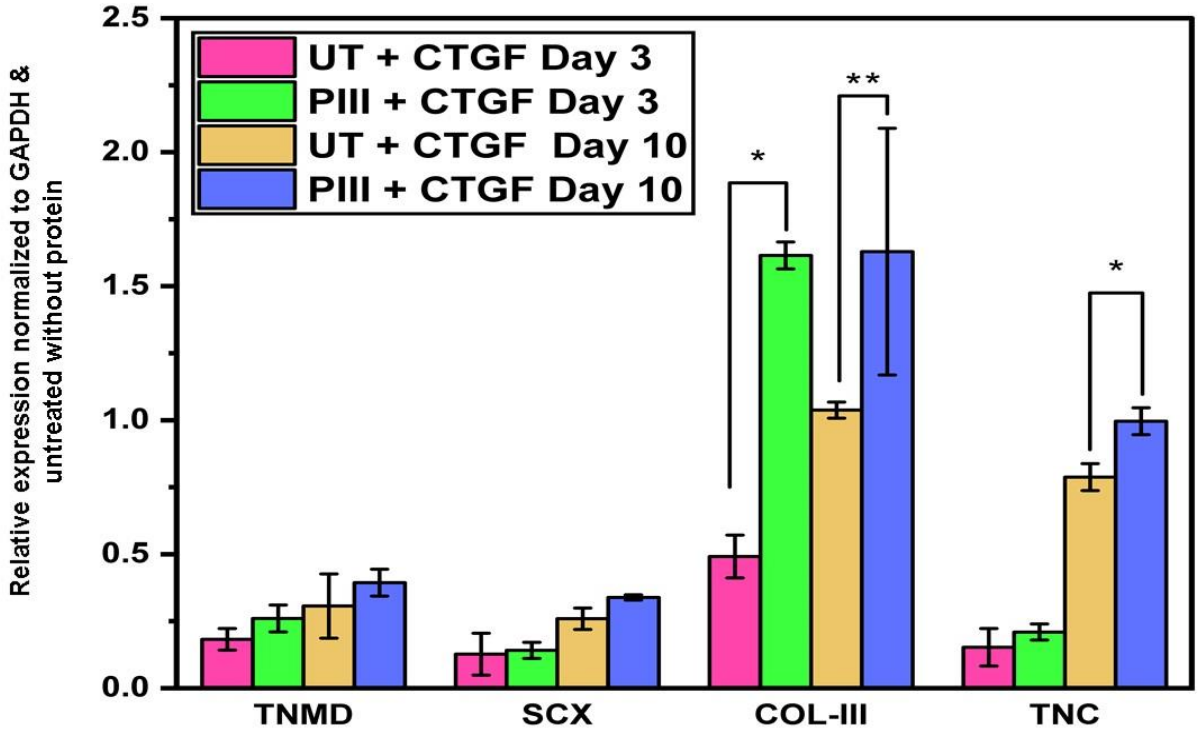

Figure 7. 12 Gene expression profile of human primary fibroblasts cultured on pure (UT) and PIII modified (PIII) UHMWPE with CTGF protein coatings. Error bars here indicate standard deviations of triplicates before and after the PIII treatment. Symbol meaning (*) =$P \leq 0.05$, (**) = $P \leq 0.01$, (***) = $P \leq 0.001$, (****) = $P \leq 0.0001$.

Fig 7.12 displays the gene expression profile of primary fibroblasts cultivated on untreated and PIII-treated UHMWPE fabric with CTGF coating. Apart from an up-regulation of Col-III and TNC on the untreated & PIII treated surface after days 3 &10, not many statistically significant alterations could be seen. After days 3 and 10, a rise in expression was seen in the untreated and PIII-treated group for several genes, including those encoding SCX and TNMD but changes were minor.

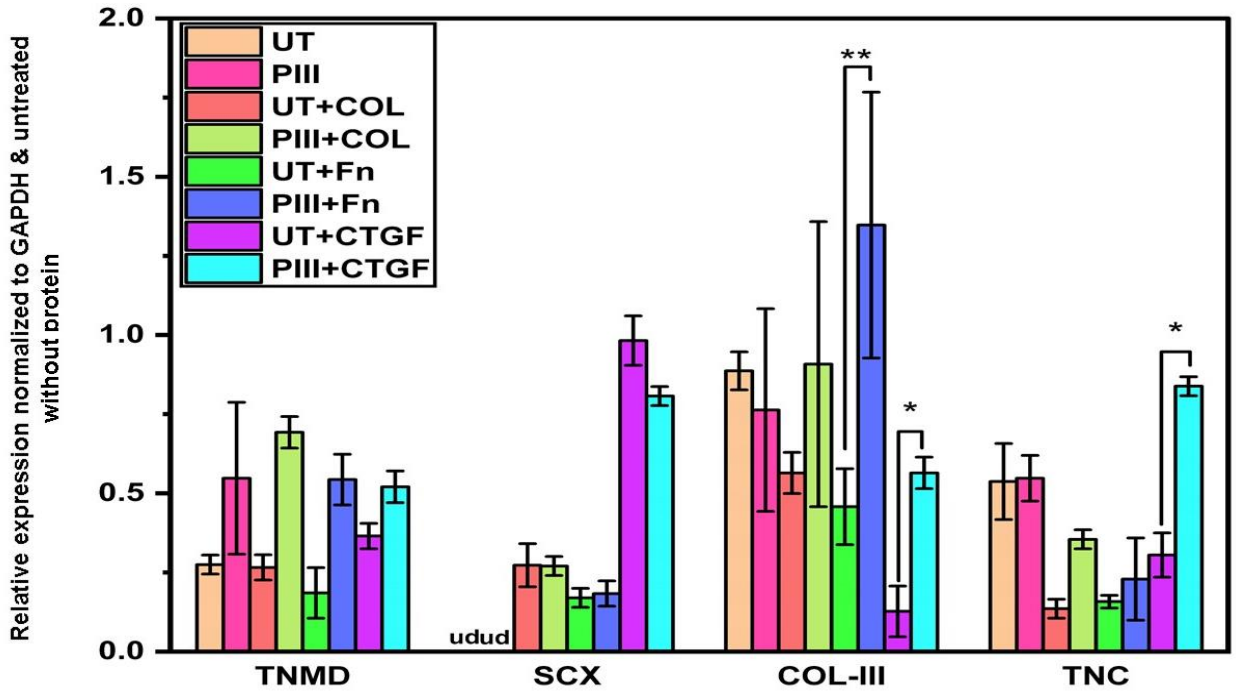

Figure 7. 13 Comparison of gene expression profile of human primary fibroblasts cultured on pure (UT) and PIII modified (PIII) UHMWPE with protein (COL-I, Fn, CTGF) coatings after 3 days. Error bars here indicate standard deviations of triplicates before and after the PIII treatment. Symbol meaning (*) =$P \leq 0.05$, (**) = $P \leq 0.01$, (***) = $P \leq 0.001$, (****) = $P \leq 0.0001$.

Fig 7.13 shows the relative comparison of gene expression profile of primary fibroblasts cultured on pure and PIII modified UHMWPE fabric with protein (COL-I, Fn, CTGF) coatings after 3 days. It's been observed that higher levels of COL-III & TNC genes expressed on untreated UHMWPE fabric after 3 days period. PIII treated UHMWPE fabric showed higher expression levels for TNMD, TNC & COL-III genes. Fibronectin coating improved gene expression on PIII treated UHMWPE fabric for TNMD & COL-III. On the other hand, CTGF coating improved gene expression levels for almost all genes such as TNMD, SCX & COL-III after 3 days for PIII treated UHMWPE fabric surfaces. SCX gene expression wasn't detected for untreated and PIII treated UHMWPE without protein coating. Collagen and fibronectin didn't show any progressive outcome in general, but CTGF showed promising results for untreated and PIII treated surfaces.

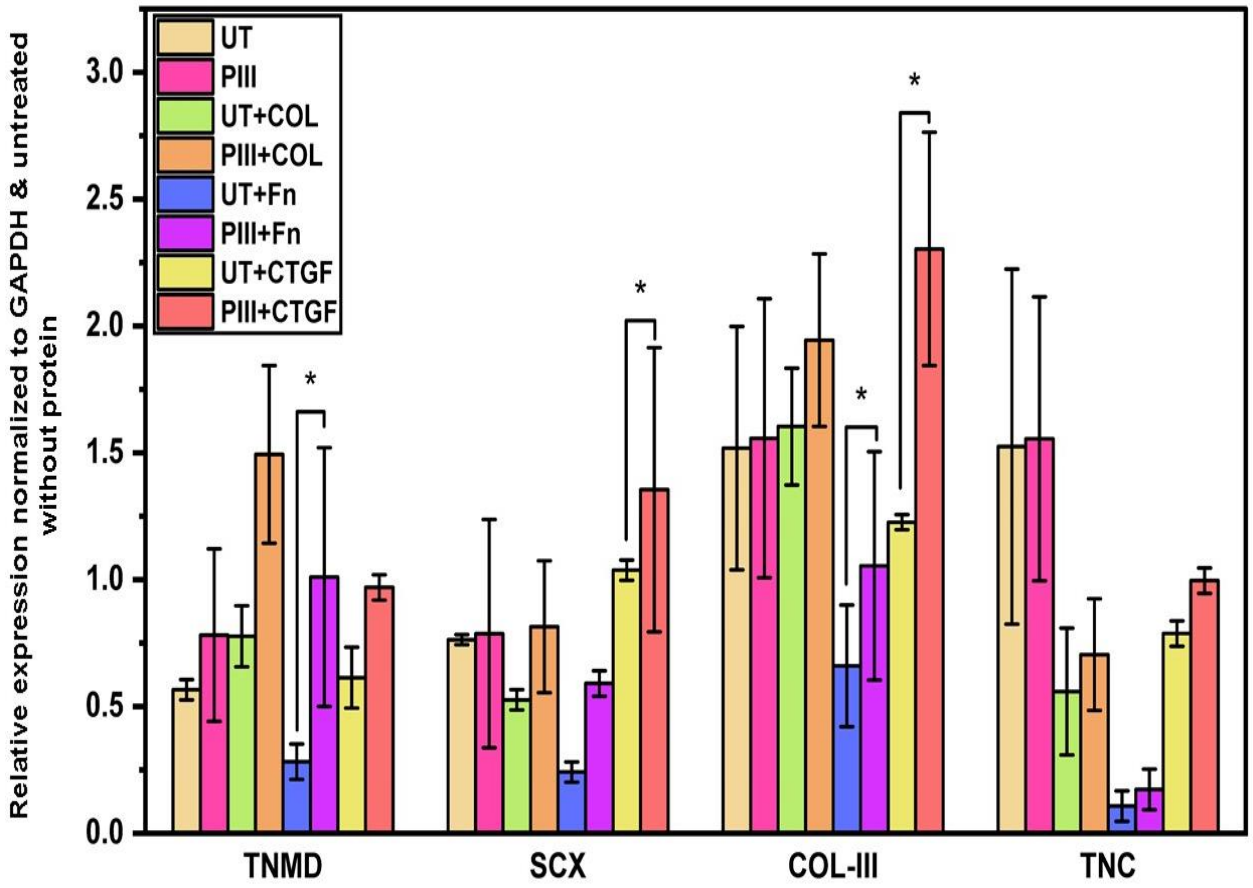

Figure 7. 14 Comparison of gene expression profile of human primary fibroblasts cultured on pure (UT) and PIII modified (PIII) UHMWPE with protein (COL-I, Fn, CTGF) coatings after 10 days. Error bars here indicate standard deviations of triplicates before and after the PIII treatment. Symbol meaning (*) =$P \leq 0.05$, (**) = $P \leq 0.01$, (***) = $P \leq 0.001$, (****) = $P \leq 0.0001$.

Fig 7.13 shows the relative comparison of gene expression profile of primary fibroblasts cultured on pure and PIII modified UHMWPE fabric with protein (COL-I, Fn, CTGF) coatings after 10 days. It's been observed that higher levels of COL-III & TNC genes were expressed on untreated UHMWPE fabric after the 10 days period. PIII treated UHMWPE fabric showed higher expression levels for TNC & COL-III genes. Collagen coating improved gene expression on PIII treated UHMWPE fabric for TNMD & COL-III. Fibronectin (Fn) coating didn't show any

improvement for untreated and PIII treated UHMWPE fabric. On the other hand, CTGF coating improved gene expression levels for almost all genes such as TNMD, SCX & COL-III after 10 days for PIII treated UHMWPE fabric surfaces. TNC genes expression was also noticeable for PIII treated UHMWPE fabric surfaces.

7.5.7 ALP activity

Fig 7.15 depicts the primary fibroblasts' ALP activity levels after 7,14, and 21 days of culture on collagen-and fibronectin-functionalized UHMWPE fabric surfaces. Generally, it is evident that the expression levels rose for most surfaces as the time points proceeded.

Therefore, the expression levels at day 14 remained modest, whereas those at day 21 increased. On days 7 and 21, the PIII-treated surface on the uncoated surfaces appeared to stimulate more ALP activity. It appears that both surfaces might be seen to have an increasing tendency in the collagen coating except day 7. Specifically, the ALP activity levels were reduced on days 14 on the untreated surface respectively. Comparatively, the action of collagen and CTGF appeared to be supportive of the ALP activity, markedly raising activity levels in Day 7,14, and 21 days.

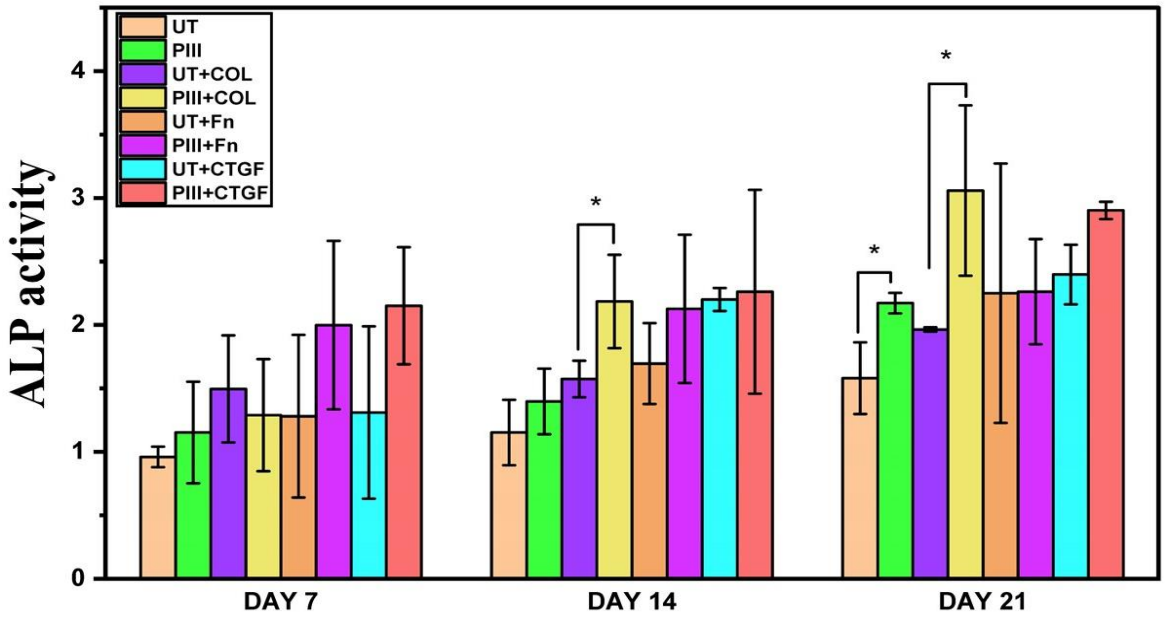

Figure 7. 15 ALP activity from the Fibroblast cell lysate cultured on pure (UT) and modified (PIII) UHMWPE fabric samples functionalized with Collagen-I, Fibronectin and CTGF. Error bars here indicate standard deviations of triplicates before and after the PIII treatment. Symbol meaning (*) =$P \leq 0.05$, (**) = $P \leq 0.01$, (***) = $P \leq 0.001$, (****) = $P \leq 0.0001$.

The mineral deposits made by the fibroblast cells on various functionalized UHMWPE fabric surfaces after they were cultured in tenogenic media are shown in Fig 7.16. The collagen & fibronectin showed a great effect on mineralization level on PIII treated surface. On the other hand, CTGF coating surface showed a higher level of mineralization for treated and untreated UHMWPE surfaces.

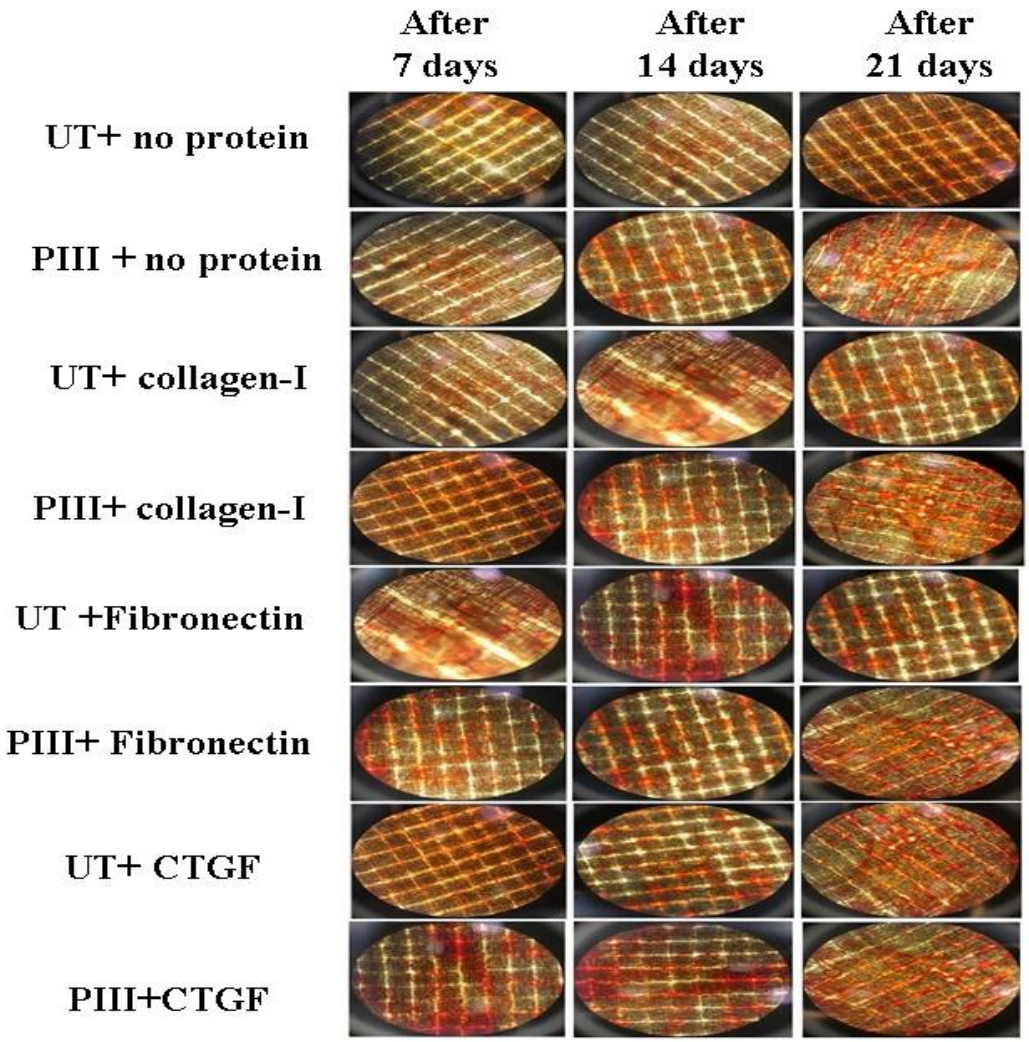

Figure 7. 16 Mineralization by the Fibroblast cell cultured on pure and modified UHMWPE samples coated with different proteins. 20,000 cells per cm2 were cultured on 0.8 × 0.8 cm sized UHMWPE fabric under tenogenic medium for the set period which ranged from 14 to 21 days.

7.6 Discussion and Conclusion

The objective of this study was to examine the in vitro biocompatibility and cell differentiation effects of UHMWPE fabric surfaces that have or have not been treated with PIII and further determining the impact of bio-functionalizing the surfaces by coating with various types of biomolecules. Consequently, we have developed surfaces that are loaded with the ECM proteins

fibronectin and collagen type -I. Furthermore, Connective tissue growth factor (CTGF) has been assessed for its ability to improve the functionality for tenogenic differentiation. ADSC cells have been used in tendon graft integration due to their ability to self-renew and proliferate. ADSC and FB cells were used to test the surfaces for short-term evaluations, and to measure differentiation and mineralization.

The graph in Fig 7.2: shows adhesion of FB cells on UHMWPE fabric was improved by PIII treatment, and by coating with either COL or Fn. The combination of Fn with PIII further improves adhesion at 3 hours but no further advantage for combining PIII and COL. PIII treatment has modest effect on FB cell proliferation. Fn improves cell proliferation in untreated UHMWPE fabric. On the other hand, the combination of PIII treatment with Col & Fn coating enhances the proliferation effect of UHMWPE fabric. PIII treatment enhances ADSC cell adhesion on UHMWPE fabric. Col & Fn coating increases adhesion alone and with PIII treatment as shown in Fig7.5. ADSC cell proliferation is not affected much by PIII treatment but was increased by combination treatment of PIII and Col & Fn coatings.

The evaluations of cell culture performed here provides information for upcoming whole animal experiments and are the initial step in figuring out whether the attached biomolecules could significantly increase bioactivity. The experiments selected here significantly increase our understanding of how the immobilized proteins may affect cells in contact and offer insight into potential results if the method was later applied in an in vivo investigation.

It was expected that the PIII might be used to augment and overcome UHMWPE's inert qualities, and the results showed that all cell types grew considerably better on PIII modified UHMWPE surfaces. SEM analysis demonstrated that not only was there a greater number of cells adhering to the PIII-treated surface, but also that cell spreading was better. The substantial changes in cell

shape visible in SEM pictures suggest that the cells were responding to the surfaces differently for both cells which already discussed in section 7.3,7.5 7.7. The results provided here are consistent with other UHMWPE plasma treatments reported in the literature. Plasma treatments that introduced additional functional groups to the surfaces improved the biocompatibility of UHMWPE, according to studies[98, 321].

The findings presented here show that a similar improvement can be achieved with the PIII treatment's high-intensity nitrogen ion bombardment. Plasma treatments are known to produce oxidized groups on polymer surfaces, which changes their wettability. The increase in oxidized groups such as (O-C-O) observed by XPS in section 3.10 &3.17 is most likely to be responsible for the improvement shown here. Additionally, it is commonly acknowledged that the wettability of a surface has a significant impact on cell adhesion[322].

The PIII treatment was able to reduce the contact angle from 45 degrees to around 23 degrees, according to surface characterization studies. It's also likely that the increased amount of carboxyl groups generated by plasma treatment improved cell adhesion, as seen in Tamada's work[323]. It was obvious from the attachment and proliferation investigations that the PIII therapy resulted in significant improvement in both cell adhesion and proliferation. Moreover, when an extra collagen coating was added, as shown in the cell attachment assays, improvements were detected for FB &ADSC cells after 1 & 3 hours. Although the effect was not as robust as on the PIII-treated surface effects. When employed alone on untreated UHMWPE, the collagen layer showed slightly higher levels of cell adhesion and proliferation than uncoated surfaces. Our findings are consistent with the literature, which suggests that collagen substrates can help cells growth[290]. When UHMWPE was coated with fibronectin, another ECM protein investigated

in this work, had some surprising effects. It enhanced cell attachment and this effect was superior to for collagen for both fibroblasts and ADSC's.

It was predicted that the PIII may be employed to enhance and safeguard the functionalities of protein coatings, due to the reduction of hydrophobicity level and the covalent immobilization procedure. Based on the findings, it appears that in some cases, the PIII treatment resulted in an improvement compared to untreated UHMWPE. The following discussion has been separated into two points based on the results. (i) Untreated UHMWPE uses hydrophobic and electrostatic communications to non-covalently bind proteins to the surface. This improvement is because of the expanded hydrophilicity coming about because of polar gatherings framed at the protein-surface point of interaction. The expanded hydrophilicity permits adsorbed protein particles to hold local like conformities. Unfortunately, non-covalent, adsorption has a variety of drawbacks, including low effective protein concentrations, protein denaturing, and unfolding. It doesn't perform well in physiological environment. (ii) A protein-binding surface that does not denature the protein could successfully hide the original implant surface, preventing it from being recognized as foreign. Hydrophilic surfaces, rarely hold adsorbed protein molecules. The findings demonstrated that when protein coatings get fixed on treated UHMWPE fabric surfaces, they can improve bioactivity to a level that is higher than the original PIII treated surface. This might be because the covalent linkage had a positive effect on the biomolecules' functions, increasing their potency[249].

It has been shown that the conformation of the immobilized proteins on the PIII treated polymers was largely unchanged and hence, they remained functional as demonstrated with enzyme activity[144, 324] . On contrary, the physiosorbed proteins on untreated polymers may require the exposure of hydrophobic domains to form hydrophobic interactions with the surface and

therefore, unfold their tertiary structure. The native conformation of proteins and the stability of the attached protein layer are important for the subsequent cell adhesion and proliferation as observed in the experiment with FB and ADSC cells. Although there was no significant difference between cell adhesion numbers on collagen and fibronectin conjugated UT and PIII treated fabrics after 1- or 3-hours incubation (Fig 7.2 & 7.6), the growth and proliferation of both cell types are consistently higher on both protein coated PIII treated fabrics compared to the protein coated untreated fabrics (Fig 7.4 & 7.8) after long incubation time (3-7 days). We hypothesize these results are largely related to the density and conformation of the attached protein layer where cells were seeded on, especially in the later stage of the cell culture in which the reversible physiosorbed protein layer changes more than the covalent attached protein layer.

Primary human fibroblasts cultured on UHMWPE fabric samples coated with fibronectin, Collagen-I, and CTGF protein were used for gene expression investigations. The raw fold change quantified was compared to the uncoated pure UHMWPE data set after first being standardized against GAPDH. Comparing the effects of the same plasma treatments versus different protein coatings, as well as the effects of the same plasma treatments versus the same protein coatings, allowed for the statistical evaluation of the results. A selective effect of PIII treatment on gene expression observed for UHMWPE fabric. PIII treatment induced the tendon ligament gene expression for TNMD, SCX & COL-III. Collagen coating increased COL-III expression levels on untreated surfaces. On the other hand, collagen coating has significant impact on TNMD & COL-III gene expressions on PIII treated surfaces. Results from the fibronectin coating suggested reduced levels of gene expression for all L/T genes. CTGF showed higher gene expression results for TNMD, COL-III, SCX & TNC compared to collagen and fibronectin coating.

The conclusions from this set of studies were often contradictory. Overall, PIII treated surface without protein showed significant impact in all tenogenic gene expressions. However, in contrast to the fibronectin coating, which was applied to untreated surfaces, the collagen coating generally increased the overall levels of gene expression. Fn did not exhibit a significant impact, to enhance tenogenic gene expression on the untreated & treated surfaces.

The time points considered were early in the fibroblast differentiation process, and modifications happening during later differentiation stages may not have yet occurred. This experiment employed only triplicates, which limited the statistical validity. Also, it's possible that the protein coatings by themselves were unable to induce complete differentiation because the gene expression tests were conducted in conventional expansion media. According to the findings, the L/T genes TNMD, COL-III, SCX were expressed more frequently on all surfaces, including those without a protein coating.

The ALP activity and mineralization activities measured throughout prolonged duration periods seem to exhibit a potential biological healing of tendon-to-bone interface using above protein & growth factors. PIII treated UHMWPE fabric showed promising results for mineralization. PIII treated coated UHMWPE fabric may encourage FB cell growth and boost the adsorption of osteogenic proteins onto the graft's surface. Collagen coated UHMWPE fabric enhanced mineralization compared to fibronectin & CTGF coated UHMWPE fabric.

Summary of this chapter

1. PIII treatment improved the FB cell adhesion. An additional layer of collagen could significantly improve cell attachment on untreated UHMWPE fabric surfaces but not for PIII treated UHMWPE fabric surfaces. Yet only the PIII-treated UHMWPE fabric surfaces shown the fibronectin effect in terms of increased cell adhesion.
2. PIII treatment has significant impact on cell proliferation for FB cells. Fn improves cell adhesion for untreated UHMWPE fabric. PIII treatment enhances the cell proliferative effect for Fn and collagen coating. Collagen has significant effect on FB cell proliferation for untreated and PIII treated UHMWPE fabric surfaces. Collagen improved cell adhesion for untreated UHMWPE fabric at a higher rate than the PIII treated UHMWPE fabric surfaces.
3. PIII treatment amplified the ADSC cell adhesion on UHMWPE fabric surfaces. Collagen and Fn both have effect on ADSC cell adhesion on untreated & PIII treated UHMWPE surfaces. PIII treatment doesn't improve the ADSC proliferation but increase the effect in combination of Fn and collagen coating.
4. ALP activity and mineralization data suggested that a collagen and fibronectin coating have a more supportive role which influenced cell differentiation in the osteoblast lineage which is beneficial for tendon-bone regeneration. Additionally, CTGF showed promising results in inducing differentiation for fibroblast cells.
5. Although the gene expression results were mixed, the data suggested that FB cells can differentiate towards ligament and tendon cells. Treatment promoted increased expression of ligament and tendon specific genes.

6. On both surfaces, collagen & fibronectin appeared to increase cell adhesion, proliferation, differentiation, and mineralization.

In this chapter, above mentioned proteins (fibronectin, collagen type I, and CTGF) coated Untreated & PIII treated UHMWPE fabric supported cell adhesion, proliferation of primary human fibroblasts and ADSC cells. PIII treated UHMWPE fabric showed promising results for mineralization of FB cells. CTGF exhibited good results for cell differentiation of FB cells as well.

Chapter 8 : Conclusion

8.1 Summary and Criticism of the Hypothesis

Biofunctionalization of UHMWPE fabric for ligament/tendon reconstruction is considered a promising research area. Many effective ideas have been created and implemented by numerous researchers, but none of them yet fully meet the requirements. This thesis evaluated the characterization of nitrogen based PIII treated UHMWPE fabric, mechanical strength of UHMWPE fabric graft, immobilization of proteins on UHMWPE fabric, bioactivity & biocompatibility of UHMWPE fabric for ligament/tendon regeneration.

The evidence provided in this thesis showed that the nitrogen based PIII treatment might be used to improve the bioactivity of UHMWPE fabric by treating its surface. The long-term impacts of the surface qualities after PIII treatment were confirmed by surface characterization investigations. This nitrogen based PIII treated UHMWPE fabric (Scientific grade) was able to introduce functional groups to the materials surface through oxidation and dehydrogenation due to energetic ion bombardment technique. The treatment makes the surface more hydrophilic, reduced the contact angles and increased the surface energy.

The PIII treatment created a reservoir of free radicals on the sub surface of UHMWPE polymer and created oxygen and nitrogen containing groups. Between two grades of fabrics scientific grade UHMWPE fabric has been chosen for further study due to several reasons already discussed in chapter 3 & 5. Surface characterization and protein immobilization results are similar for both UHMWPE fabrics. Mechanical strength is superior for industrial grade UHMWPE fabric but due to the presence of impurities in the industrial grade UHMWPE fabric and a dense fiber structure, it was difficult to maintain an aseptic environment for cell culture study of industrial grade UHMWPE fabric.

Excellent mechanical strength of UHMWPE graft was observed in chapter 4. Mechanical properties such as tensile strength and stiffness of UHMWPE graft is superior to natural T/Cyclic loading data confirmed that UHMWPE graft can replicate the normal accommodation of stresses placed on the ligament/tendon while walking/engaging in vigorous physical therapy.

The covalent bonding of the given biomolecules was validated by protein immobilization tests, which also showed that immobilization increased long-term stability. Studies on cell culture on the bare PIII-treated surfaces showed significantly increased bioactivity in terms of attachment, proliferation, tenocyte differentiation, and mineralization when compared to the untreated surface. Studies in cell culture on surfaces functionalized with proteins suggested that the PIII treatment could influence the gene expression and thus cell functioning. These results provide evidence that covalent binding or fibronectin, collagen type 1 and CTGF maintains significant levels of bioactivity of these proteins.

The initial goal of this thesis was to investigate whether nitrogen based PIII treatment might be used to increase the bioactivity and biocompatibility of inert UHMWPE fabric surfaces and compare characteristics between two grades of UHMWPE fabric. Based on the numerous observations presented throughout this thesis, it has been determined that the PIII treatment can increase the bioactivity of UHMWPE fabric surface. These results allow for the application of three basic methods to enhance UHMWPE bioactivity using PIII treatment. Firstly, without the use of any biomolecules, PIII treatment on UHMWPE fabric surfaces produced significantly increased indicators of bioactivity.

Secondly, the synthetic UHMWPE ligament/tendon graft is capable to take sufficient tensile & cyclic loading for daily human physical activities. Mechanical measurement confirmed the

strength of the untreated fabric was unchanged after the PIII treatment, proving that the treatment only changed the surface properties but not the bulk properties of the material.

Thirdly, the covalent immobilization of biomolecules using PIII treatment on UHMWPE fabric serves to extend the biological usefulness of the attached biomolecules. The type and concentration of protein utilized can influence how the immobilized protein layer controls desired biological consequences to attached primary human cells of the ADSC and fibroblast lineages.

Finally, we have shown that the nitrogen based PIII technology may be used to increase the bioactivity of UHMWPE fabric quickly and effectively. This information supports further efforts to design UHMWPE materials for next-generation Ligament/Tendon implants. The nitrogen based PIII-treated UHMWPE fabric surface was demonstrated to be able to promote tenogenic differentiation and to support the deposition on the fabric of mineralized tissues indicating bone production which required for fixation to bone of tendon grafts. It is supportive for greater tenogenic differentiation without compromising the material's exceptional bulk mechanical capabilities.

8.2 Limitations and future recommendations

Although the nitrogen based PIII treatment produced a satisfactory result, there are still some regions where the surface treatment might not be ideal. Additionally, all studies performed for this thesis were done in vitro in a well-controlled environment. Estimating the efficiency of the surface treatment in practical biomedical applications, particularly in long-term implantable devices, may be challenging. The work described here provides a picture of how effectively PIII

treated UHMWPE functions in vitro, even though there are still certain restrictions and difficulties that need more research. There are several limitations such as limited opportunity to optimize culture conditions for both covalent bonding of proteins to the fabric and to optimize cell culture conditions to detect biological responses to plasma treatment and protein loading for bio functionalizing coatings. It would be necessary to assess the use of rational combinations of proteins for coatings.

Surface characterization through Fourier-transform infrared spectroscopy (FTIR) and wear testing weren't possible for UHMWPE fabric. UHMWPE fabric graft wasn't specifically designed or optimized for use as a ligament and tendon and further work must be done to make it functional such as impregnation of the hollow UHMWPE graft so that it can give support and prevent it from flattening during implantation or ACL surgery.

An exhaustive analysis of the surface properties of the nitrogen based PIII treated UHMWPE fabric was not completed because the aim of this work was primarily focused on the biological results. To further clarify our understanding of the nitrogen based PIII treated UHMWPE fabric surfaces, the author recommends that the following further research be done.

(1) The biological consequences were the main emphasis of this investigation, hence a thorough examination of the surface properties of the PIII-treated UHMWPE fabric was not fully carried out.

(2) Thorough examination on the sources of the material for defined manufacturing specifications would provide valuable criteria for evaluating the properties of the material to optimize the fabric's correct fiber dimensions, weave structure, pore size, mechanical strength & reducing impurities etc.

(3) By cleaning the surfaces with solvents and looking at any detachable functional groups, it would be feasible to do additional examination of the surface characteristics that cover the detection of potential mobile fragments arising from the PIII treatment.

(4) Thorough research may be required to further assess the biological performance due to the intricacy of the biological phenomena taking place.

(5) As a result of the information gathered there, it may be possible to immobilize many proteins on a surface at once in the future. The most significant increases in bioactivity may be achieved by using a range of proteins to cover the initial implant surface and so produce a more biomimetic interface.

(6) By focusing on Proper design of UHMWPE ligament graft. The graft must be designed such a way that growth factors have strong influence on blood supply and connective tissue ingrowth, it would be beneficial to inject it at the midpoint of tissue-engineered ligaments as well as for optimized fixation in bone tunnels. Anti-wear mechanism should be improved to reduce inflammation due to the presence of fragments observed from UHMWPE polymers.

(7) The data described here should give a clear picture of how effectively the PIII treated UHMWPE operates in vitro, even though there are still a few issues and challenges that need more research. The objective of the following phase of research on this subject should be to assess PIII surface modification technologies in an in vivo model to pave the way for therapeutic use.

(8) The macrophage cytokine release assay would be an interesting assay to conduct in future to the in vivo studies of Ligament/Tendon for immune response.

(9) In vivo assessment of Ligament/tendon repair of PIII treated UHMWPE fabric material implants would be conducted in future research studies.

All in all, the novelty of this thesis includes the validation of methods to biofunctionalized UHMWPE fabric with nitrogen based PIII treatment for the design of ligament and tendon implants. Biofunctionalization of UHMWPE has been studied before in the form of sheet, rod, cubes, or fibers there is an absence of literature on fabrics.

Previous study also focused on ligament/tendon differentiation conducted on UHMWPE composite grafts or scaffolds but not on simple UHMWPE fabrics. The information presented could be useful in understanding and preventing the activity loss that occurs when some enzymes are immobilized on surfaces. The information offered here will be crucial for subsequent in vivo implant investigations and clinical trials, and it is expected to spur new UHMWPE fabric uses in the biomedical sector. Utilizing this nitrogen based PIII treatment to biofunctionalized UHMWPE for the research of L/T implants has the potential to be revolutionary.

Appendices

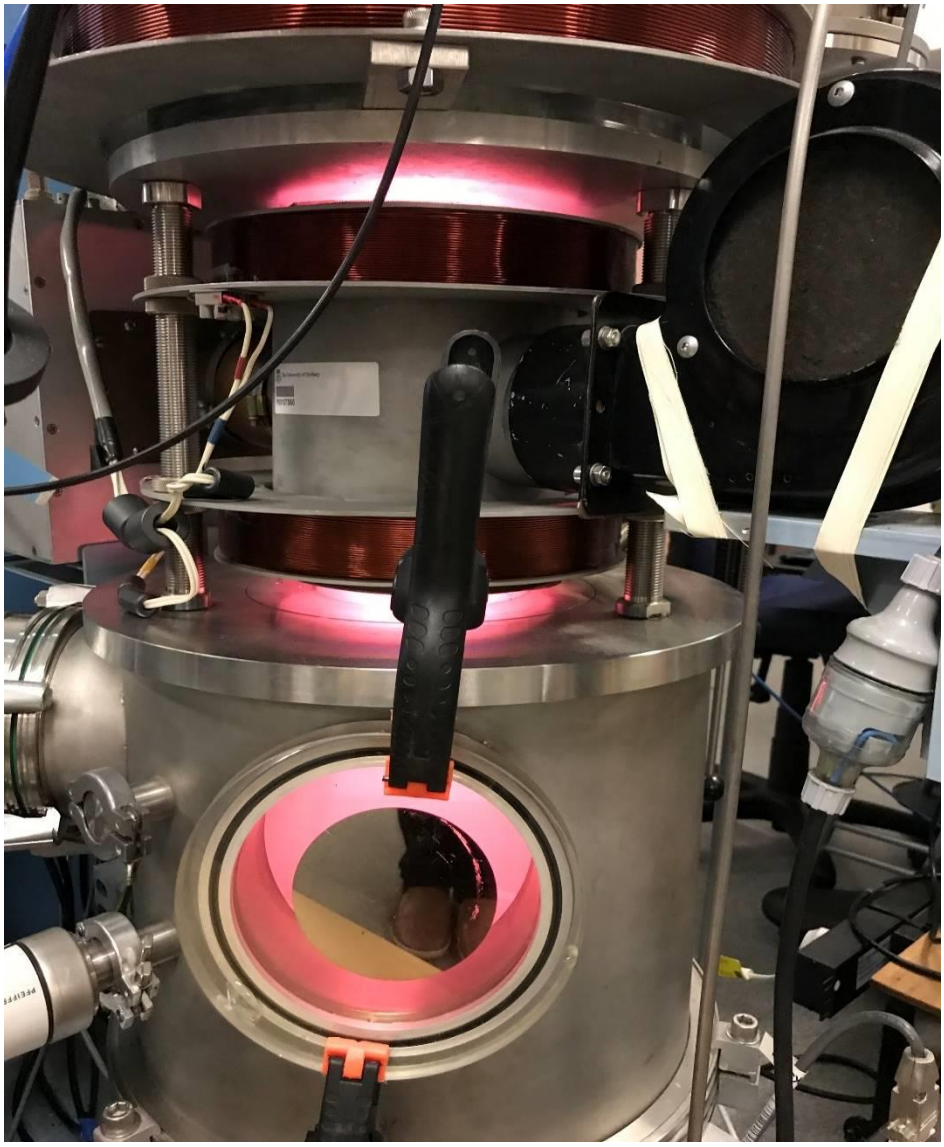

Figure A1 Photo of the PIII plasma chamber set up used for the surface treatment.

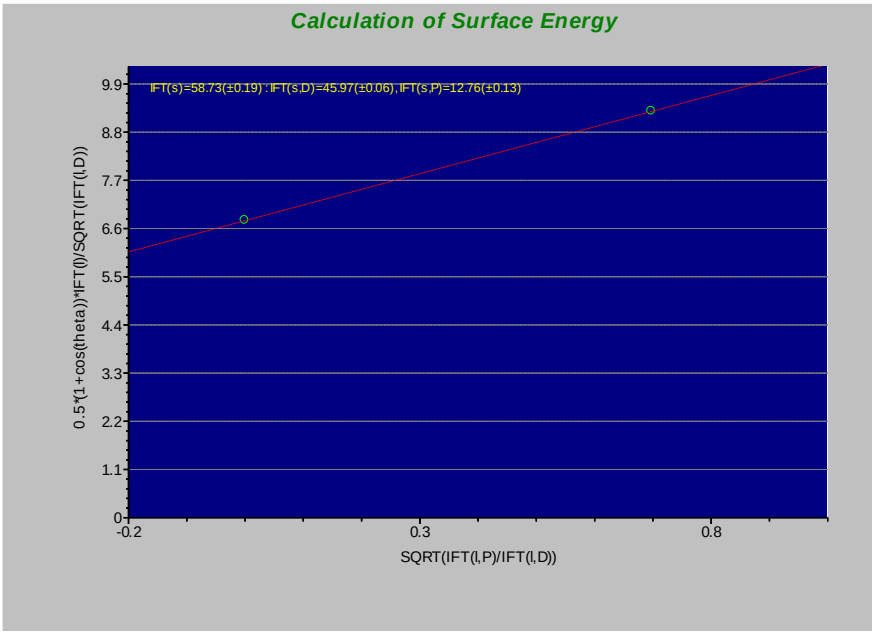

Figure A2 Surface energy of PIII treated UHMWPE based on Owen Wendt Rabel and Kaelble (OWRK) method.

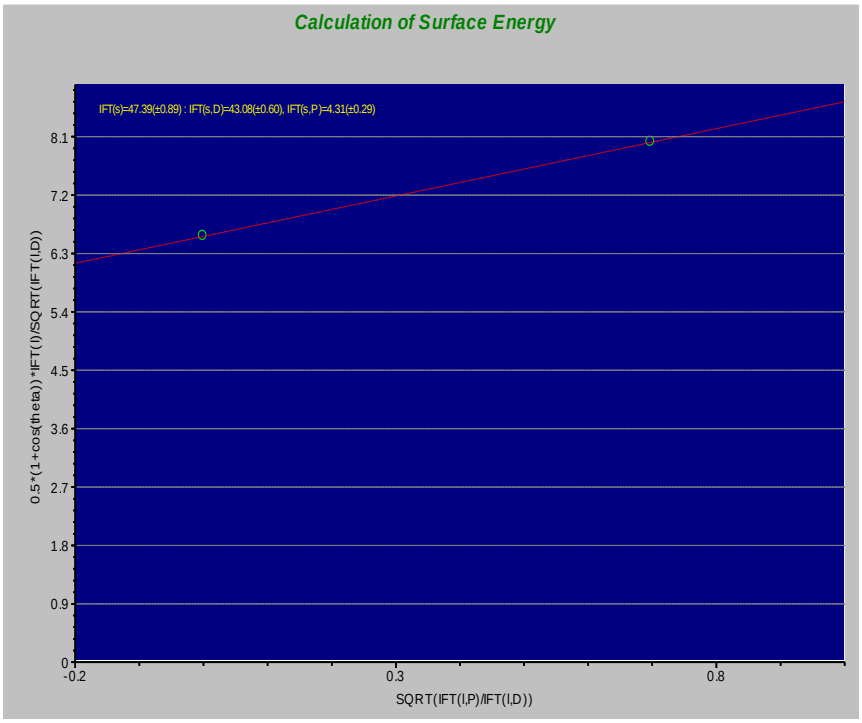

Figure A3 Surface energy of Untreated UHMWPE based on Owen Wendt Rabel and Kaelble (OWRK) method.

Figure A4 Hydrophilicity experiment of untreated & PIII treated UHMWPE fabric.

Contact angle test:

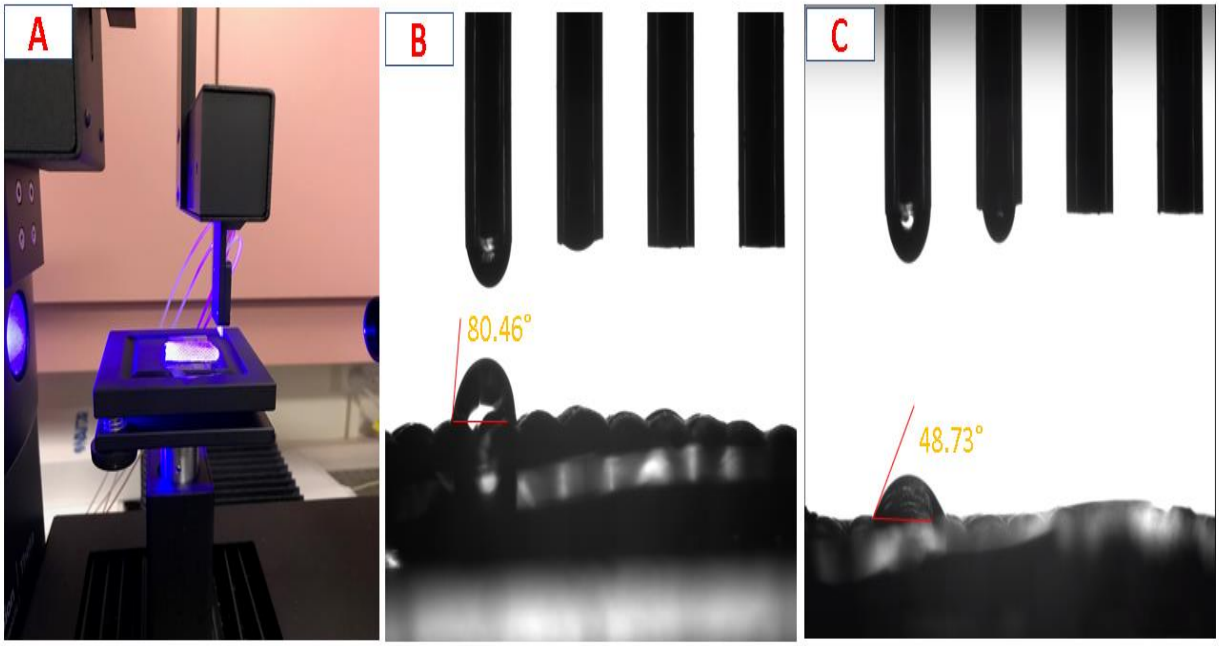

Figure A5 (A) Contact angle testing in optical tensiometer (B) Contact angles of water on untreated UHMWPE fabric (C) contact angle of water on PIII treated UHMWPE fabric.

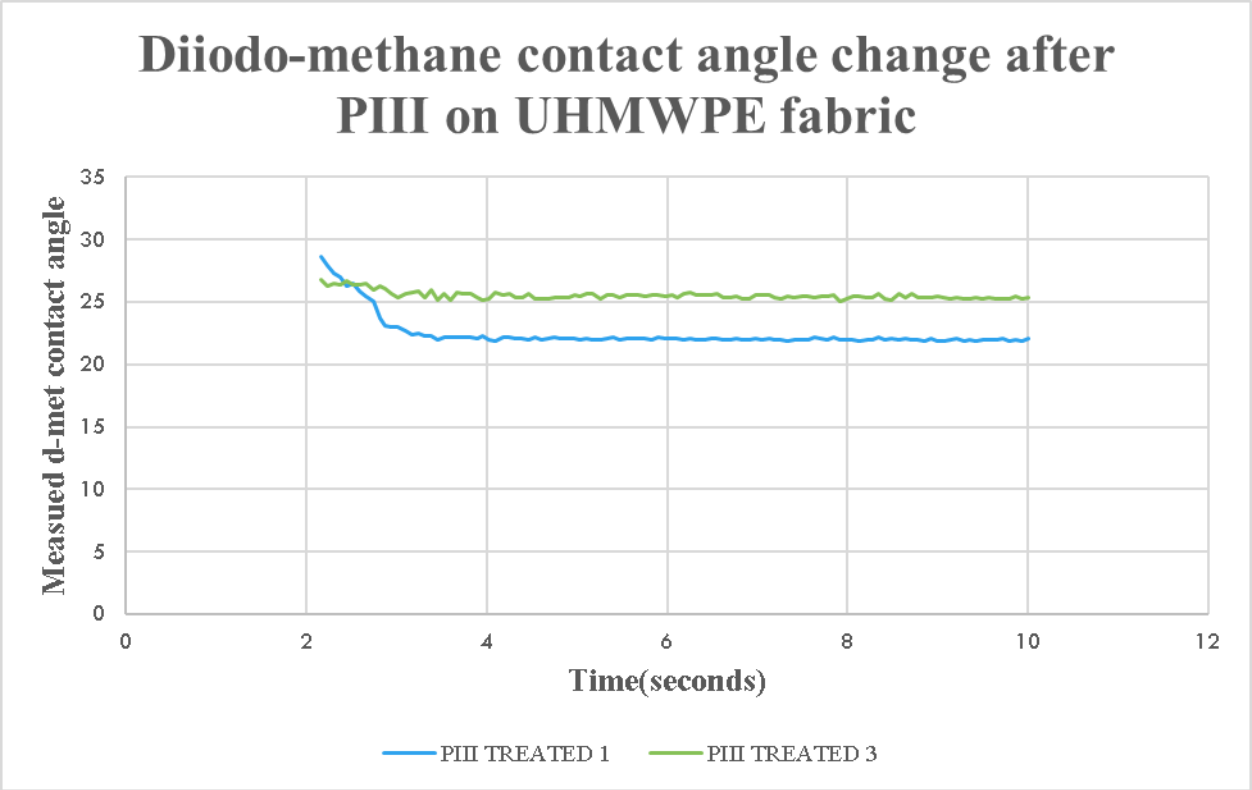

Figure A6 Diiodo-methane contact angle change after PIII treatment on UHMWPE fabric.

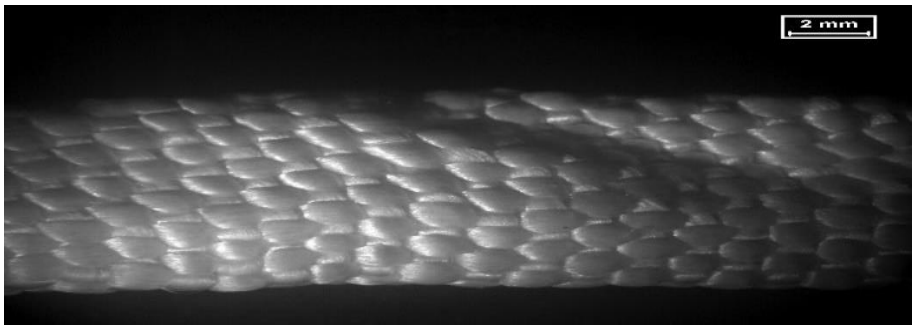

Figure A 7Fibers of graft before mechanical testing.

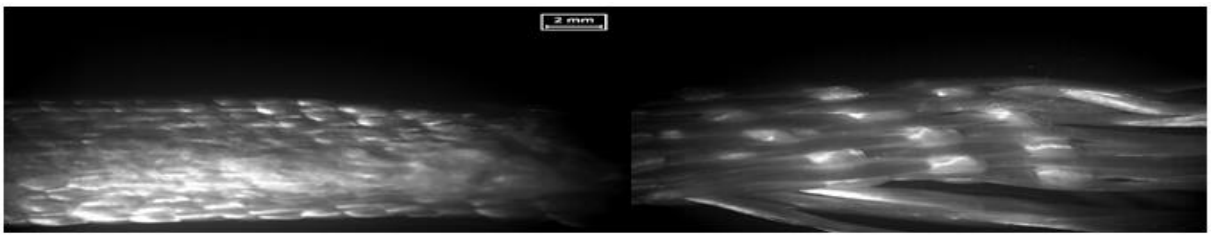

Figure A8 Stretching of fibers after mechanical testing.

TableA1 Contact angle measurement on untreated & PIII treated UHMWPE fabric

PIII					
Time [s]	CA left [°]	CA right [°]	CA mean [°]	Volume [µl]	Baseline [mm]
1.37	61.07	55.72	58.39	2.67	2.48
1.44	59.02	54.22	56.62	2.65	2.5
1.51	57.31	52.05	54.68	2.55	2.52
1.58	55.74	48.73	52.23	2.54	2.51
UT					
25/10/2019 1:46 PM					
Time [s]	CA left [°]	CA right [°]	CA mean [°]	Volume [µl]	Baseline [mm]
1.37	66.47	80.46	73.46	1.76	2.24
1.44	64.81	79.35	72.08	1.51	2.25
1.51	67.17	81.8	74.48	2.49	2.24
1.58	64.26	76.58	70.42	2.44	2.24

Dyneema®
With you when it matters

Ultra High Molecular Weight Polyethylene Fiber from DSM Dyneema

UHMWPE fiber combines excellent mechanical properties with low density, resulting in high performance-on-weight basis.

The UHMWPE fiber from DSM Dyneema is a gel-spun, multi-filament fiber produced from ultra high molecular weight polyethylene, with main characteristics: high strength, low weight, low elongation at break, and resistance to most chemicals. To stimulate developments, this sheet provides an overview of properties measured on UHMWPE fibers from DSM Dyneema.

Fiber range

UHMWPE fibers from DSM Dyneema are produced in three strength ranges and several linear densities with a characteristic very low filament diameter. The tensile properties are correlated with the fiber linear density. Detailed information per fiber type is available on request, as Product Data Sheets, Product Specification Sheets, Material Safety Data Sheets and Fact Sheets.

The disclosed data has been generated from test results of UHMWPE fibers from DSM Dyneema and can not be considered valid for other fibers from other UHMWPE suppliers.

UHMWPE Fiber Type	Tensile Strength			Tensile Modulus			Elongation to break %
	N/tex	g/den	GPa	N/tex	g/den	GPa	
SK99	4.3	48	4.1	159	1801	155	3 - 4
DM20*	3.2	36	3.1	96	1088	94	
SK75* SK78*	3.4 - 4.0	38 - 45	3.3 - 3.9	112 - 137	1267 - 1552	109 - 132	
SK60 SK62 SK65	2.3 - 3.4	28 - 38	2.4 - 3.3	67 - 102	759 - 1158	65 - 100	
SK38	1.7	19	1.6	35	396	34	6.5

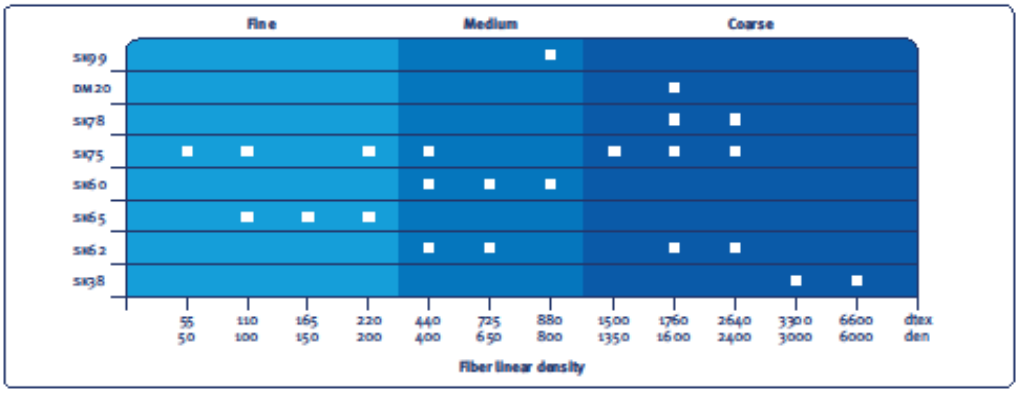

*: grades also available as 'XBO grades; XBO is an overlay finish to enhance bending fatigue performance

Please contact:
Gruschwitz Textilwerke AG
+49 (0) 7561 9098-0 · info@gruschwitz.com · www.gruschwitz.com

DSM

Spectra® Fiber 1000
high-strength, light-weight polyethylene fiber

PRODUCT DESCRIPTION: Spectra fiber 1000, the second in a series of Spectra fibers, was developed to meet customers' needs for increased performance. It is available in a multitude of deniers for use in a wide range of applications.

This extended-chain polyethylene fiber has one of the highest strength-to-weight ratios of any man-made fiber. Spectra fiber 1000 has a tenacity 15 to 20 percent higher than that of Spectra fiber 900. Spectra fiber is, pound for pound, 15 times stronger than steel, more durable than polyester and has a specific strength that is up to 40 percent greater than that of aramid fiber. Specific performance is dependent upon denier and filament count.

Applications:
- Police and military ballistic vests and helmets
- Composite armor for vehicles and aircraft
- Marine lines and commercial fishing nets
- Industrial cordage and slings
- Sailcloth, fishing line and other sporting equipment
- Cut-protection products

Product Benefits:
- Light enough to float (0.97 g/cc specific gravity)
- High resistance to chemicals, water and ultraviolet light
- Excellent vibration damping
- Highly resistant to flex fatigue
- Low coefficient of friction
- Good resistance to abrasion
- Low dielectric constant makes it virtually transparent to radar

PHYSICAL PROPERTIES												
(Nominal)	Spectra® Fiber 1000											
Weight/Unit Length (Denier) (Decitex)	75 83	100 111	130 144	180 200	215 239	275 306	375 417	435 483	650 722	1300 1444	1600 1778	2600 2888
Ultimate Tensile Strength (g/den) (Gpa)	43 3.68	39 3.34	38 3.25	38 3.25	38 3.25	36 3.08	35 3.00	35 2.95	36 3.08	35 3.00	36 3.02	34 2.91
Breaking Strength (lbs.)	7	9	11	16	18	22	29	33	52	100	123	195
Modulus (g/den) (Gpa)	1550 133	1450 124	1320 113	1350 116	1320 113	1320 113	1200 103	1180 101	1175 101	1150 98	1170 99	1135 97
Elongation (%)	2.9	3.0	2.8	2.9	2.9	3.1	3.1	3.2	3.5	3.3	3.5	3.5
Density (g/cc) (lbs/in³)	0.97 0.035	0.97 0.035	0.97 0.035	0.97 0.035	0.97 0.035	0.97 0.035	0.97 0.035	0.97 0.035	0.97 0.035	0.97 0.035	0.97 0.035	0.97 0.035
Filament/tow	40	40	40	50	60	60	60	120	120	240	240	480
Filament (dpf)	1.9	2.5	3.3	3.6	3.6	4.6	6.3	3.6	5.4	5.4	6.67	5.4

For more information:
Honeywell Advanced Fibers and Composites
15801 Woods Edge Road
Colonial Heights, VA 23834
Toll Free: 1-800-695-5969
Europe: +32 16 39 12 19
Asia: +86 21 2894 2000
www.honeywell.com/spectra

Honeywell

References

[1] Ge, Z.; Yang, F.; Goh, J. C. H.; Ramakrishna, S.; Lee, E. H. Review Biomaterials and Scaffolds for Ligament Tissue Engineering. **2006**. https://doi.org/10.1002/jbm.a.

[2] Chang, B. P.; Akil, H. M.; Nasir, R. M. Mechanical and Tribological Properties of Zeolite-Reinforced UHMWPE Composite for Implant Application. *Procedia Eng.*, **2013**, *68*, 88–94. https://doi.org/10.1016/j.proeng.2013.12.152.

[3] Gobbi, S. J. Requirements for Selection/Development of a Biomaterial. *Biomed. J. Sci. Tech. Res.*, **2019**, *14* (3). https://doi.org/10.26717/bjstr.2019.14.002554.

[4] Geetha, M.; Singh, A. K.; Asokamani, R.; Gogia, A. K. Ti Based Biomaterials, the Ultimate Choice for Orthopaedic Implants - A Review. *Prog. Mater. Sci.*, **2009**, *54* (3), 397–425. https://doi.org/10.1016/j.pmatsci.2008.06.004.

[5] Kurtz, S. M. *4 The Origins of UHMWPE in Total Hip Arthroplasty*, Third Edit.; Elsevier Inc., 1982. https://doi.org/10.1016/B978-0-323-35401-1/00004-1.

[6] Oosterom, R.; Ahmed, T. J.; Poulis, J. A.; Bersee, H. E. N. Adhesion Performance of UHMWPE after Different Surface Modification Techniques. *Med. Eng. Phys.*, **2006**, *28* (4), 323–330. https://doi.org/10.1016/j.medengphy.2005.07.009.

[7] Diabb Zavala, J. M.; Leija Gutiérrez, H. M.; Segura-Cárdenas, E.; Mamidi, N.; Morales-Avalos, R.; Villela-Castrejón, J.; Elías-Zúñiga, A. Manufacture and Mechanical Properties of Knee Implants Using SWCNTs/UHMWPE Composites. *J. Mech. Behav. Biomed. Mater.*, **2021**, *120* (January). https://doi.org/10.1016/j.jmbbm.2021.104554.

[8] Liu, Q.; Li, W.; Cao, L.; Wang, J.; Qu, Y.; Wang, X.; Qiu, R.; Di, X.; Wang, Z.; Liang, B. Response of MG63 Osteoblast Cells to Surface Modification of Ti-6Al-4V Implant Alloy by Laser Interference Lithography. *J. Bionic Eng.*, **2017**, *14* (3), 448–458. https://doi.org/10.1016/S1672-6529(16)60410-9.

[9] Zhu, X.; Chen, J.; Scheideler, L.; Reichl, R.; Geis-Gerstorfer, J. Effects of Topography and Composition of Titanium Surface Oxides on Osteoblast Responses. *Biomaterials*, **2004**, *25* (18), 4087–4103. https://doi.org/10.1016/j.biomaterials.2003.11.011.

[10] Gilman, A. B.; Piskarev, M. S.; Kuznetsov, A. A.; Ozerin, A. N. Modification of Ultrahigh-Molecular-Weight Polyethylene by Low-Temperature Plasma (Review). *High Energy Chem.*, **2017**, *51* (2), 136–144. https://doi.org/10.1134/S0018143917020059.

[11] Wahed, S. B.; Dunstan, C. R.; Boughton, P. A.; Ruys, A. J.; Faisal, S. N.; Wahed, T. B.; Salahuddin, B.; Cheng, X.; Zhou, Y.; Wang, C. H.; et al. Functional Ultra-High Molecular Weight Polyethylene Composites for Ligament Reconstructions and Their Targeted Applications in the Restoration of the Anterior Cruciate Ligament. *Polymers (Basel).*, **2022**, *14* (11). https://doi.org/10.3390/polym14112189.

[12] Ge, S.; Wang, Q.; Zhang, D.; Zhu, H.; Xiong, D.; Huang, C.; Huang, X. Friction and Wear Behavior of Nitrogen Ion Implanted UHMWPE against ZrO2 Ceramic. *Wear*, **2003**, *255* (7–12), 1069–1075. https://doi.org/10.1016/S0043-1648(03)00269-2.

[13] Rodrigues, M. M.; Fontoura, C. P.; Dotta Maddalozzo, A. E.; Leidens, L. M.; Quevedo, H. G.; Souza, K. dos S.; da Silva Crespo, J.; Michels, A. F.; Figueroa, C. A.; Aguzzoli, C. Ti, Zr and Ta Coated UHMWPE Aiming Surface Improvement for Biomedical Purposes. *Compos. Part B Eng.*, **2020**, *189* (December 2019), 107909. https://doi.org/10.1016/j.compositesb.2020.107909.

[14] Haque, E.; Wahed, S. B. A Systematic Review for Anterior Cruciate Ligament Reconstruction. *J. Anesth. Surg.*, **2016**, *3* (3), 1–9. https://doi.org/10.15436/2377-1364.16.031.

[15] Duraccio, D.; Strongone, V.; Malucelli, G.; Auriemma, F.; De Rosa, C.; Mussano, F. D.; Genova, T.; Faga, M. G. The Role of Alumina-Zirconia Loading on the Mechanical and Biological Properties of UHMWPE for Biomedical Applications. *Compos. Part B Eng.*, **2019**, *164* (July 2018), 800–808. https://doi.org/10.1016/j.compositesb.2019.01.097.

[16] Liu, Z.; Du, Y.; Ma, H.; Li, J.; Zhang, X.; Zhu, E.; Shi, C.; Zhu, Z.; Zhao, S. Mechanism of Boron Carbide Particles Improving the Wear Resistance of UHMWPE: Structure-Property Relationship. *Polymer (Guildf).*, **2022**, *245* (January), 124733. https://doi.org/10.1016/j.polymer.2022.124733.

[17] Reynolds, S. E.; Malkani, A. L.; Ramakrishnan, R.; Yakkanti, M. R. Wear Analysis of First-Generation Highly Cross-Linked Polyethylene in Primary Total Hip Arthroplasty. An Average 9-Year Follow-Up. *J. Arthroplasty*, **2012**, *27* (6), 1064–1068. https://doi.org/10.1016/j.arth.2012.01.006.

[18] Forster, A. L.; Forster, A. M.; Chin, J. W.; Peng, J. S.; Lin, C. C.; Petit, S.; Kang, K. L.; Paulter, N.; Riley, M. A.; Rice, K. D.; et al. Long-Term Stability of UHMWPE Fibers. *Polym. Degrad. Stab.*, **2015**, *114*, 45–51. https://doi.org/10.1016/j.polymdegradstab.2015.01.028.

[19] Silverstein, M. S.; Breuer, O. Relationship between Surface Properties and Adhesion for Etched Ultra-High-Molecular-Weight Polyethylene Fibers. *Compos. Sci. Technol.*, **1993**, *48* (1–4), 151–157. https://doi.org/10.1016/0266-3538(93)90131-Y.

[20] Stewart, C.; Akhavan, B.; Wise, S. G.; Bilek, M. M. M. A Review of Biomimetic Surface Functionalization for Bone-Integrating Orthopedic Implants: Mechanisms, Current Approaches, and Future Directions. *Prog. Mater. Sci.*, **2019**, *106* (July), 100588. https://doi.org/10.1016/j.pmatsci.2019.100588.

[21] Zeta-potential, T. R. B.; Strength, P. S.; Reinforced, F.; Composites, E. The Relationship Between Zeta-Potential and Pull-Out Shear Strength. 347–351.

[22] Costa, L.; Luda, M. P.; Trossarelli, L.; Brach Del Prever, E. M.; Crova, M.; Gallinaro, P. Oxidation in Orthopaedic UHMWPE Sterilized by Gamma-Radiation and Ethylene Oxide. *Biomaterials*, **1998**, *19* (7–9), 659–668. https://doi.org/10.1016/S0142-9612(97)00160-9.

[23] Wang, J.; Liang, G.; Zhao, W.; Lü, S.; Zhang, Z. Studies on Surface Modification of

UHMWPE Fibers via UV Initiated Grafting. *Appl. Surf. Sci.*, **2006**, *253* (2), 668–673. https://doi.org/10.1016/j.apsusc.2005.12.165.

[24] Serro, A. P.; Degiampietro, K.; Colaço, R.; Saramago, B. Adsorption of Albumin and Sodium Hyaluronate on UHMWPE: A QCM-D and AFM Study. *Colloids Surfaces B Biointerfaces*, **2010**, *78* (1), 1–7. https://doi.org/10.1016/j.colsurfb.2010.01.022.

[25] Kostov, K. G.; Ueda, M.; Tan, I. H.; Leite, N. F.; Beloto, A. F.; Gomes, G. F. Structural Effect of Nitrogen Plasma-Based Ion Implantation on Ultra-High Molecular Weight Polyethylene. *Surf. Coatings Technol.*, **2004**, *186* (1-2 SPEC. ISS.), 287–290. https://doi.org/10.1016/j.surfcoat.2004.03.033.

[26] Kar, R.; Barve, S. A.; Singh, S. B.; Barve, D. N.; Chand, N.; Patil, D. S. Diagnostics of Microwave ECR Generated Plasma: Effect of Contaminated Reference Electrode. *Vacuum*, **2010**, *85* (2), 151–155. https://doi.org/10.1016/j.vacuum.2010.05.003.

[27] Struszczyk, mh; Puszkarz, ak; Wilbik-Hałgas, B.; Cichecka, M.; Litwa, P.; Urbaniak-Domagała, W.; Krucinska, I. The Surface Modification of Ballistic Textiles Using Plasma-Assisted Chemical Vapor Deposition (PACVD). *Text. Res. J.*, **2014**, *84* (19), 2085–2093. https://doi.org/10.1177/0040517514528559.

[28] Tomita, N.; Kitakura, T.; Onmori, N.; Ikada, Y.; Aoyama, E. Prevention of Fatigue Cracks in Ultrahigh Molecular Weight Polyethylene Joint Components by the Addition of Vitamin E. *J. Biomed. Mater. Res.*, **1999**, *48* (4), 474–478. https://doi.org/10.1002/(SICI)1097-4636(1999)48:4<474::AID-JBM11>3.0.CO;2-T.

[29] Ahmadi, M.; Masoomi, M.; Safi, S. Mechanical Property Characterization of Carbon Nanofiber/Epoxy Nanocomposites Reinforced by GMA-Grafted UHMWPE Fibers. *Compos. Part B Eng.*, **2015**, *83*, 43–49. https://doi.org/10.1016/j.compositesb.2015.08.006.

[30] Chagas, N. P. da S.; Aguiar, V. de O.; Garcia Filho, F. da C.; Figueiredo, A. B. H. da S.; Monteiro, S. N.; Huaman, N. R. C.; Marques, M. de F. V. Ballistic Performance of Boron Carbide Nanoparticles Reinforced Ultra-High Molecular Weight Polyethylene (UHMWPE). *J. Mater. Res. Technol.*, **2022**, *17*, 1799–1811. https://doi.org/10.1016/j.jmrt.2022.01.104.

[31] Stürzel, M.; Kempe, F.; Thomann, Y.; Mark, S.; Enders, M.; Mülhaupt, R. Novel Graphene UHMWPE Nanocomposites Prepared by Polymerization Filling Using Single-Site Catalysts Supported on Functionalized Graphene Nanosheet Dispersions. *Macromolecules*, **2012**, *45* (17), 6878–6887. https://doi.org/10.1021/ma301376q.

[32] Hamedi, G. H.; Ranjbar Pirbasti, Z. The Effects of UHMWPE/Nanoclay on Rheological Properties of Modified Asphalt Binder. *Pet. Sci. Technol.*, **2020**, *38* (4), 309–315. https://doi.org/10.1080/10916466.2019.1703740.

[33] Hussain, O.; Ahmad, B.; Saleem, S. Tribological Performance of Biomedical Grade UHMWPE/Nano-Al2O3/Vitamin-C Hybrid Composite for Cartilage Replacements. *Mater. Lett.*, **2021**, *291*, 129515. https://doi.org/10.1016/j.matlet.2021.129515.

[34] Xiong, D.; Yang, Y.; Deng, Y. Bio-Tribological Properties of UHMWPE against Surface

Modified Titanium Alloy. *Surf. Coatings Technol.*, **2013**, *228* (SUPPL.1), S442–S445. https://doi.org/10.1016/j.surfcoat.2012.05.033.

[35] Kumar, N. N.; Yap, S. L.; Samsudin, F. N. D. bt; Khan, M. Z.; Srinivasa, R. S. P. Effect of Argon Plasma Treatment on Tribological Properties of UHMWPE/MWCNT Nanocomposites. *Polymers (Basel).*, **2016**, *8* (8), 1–15. https://doi.org/10.3390/polym8080295.

[36] Bracco, P.; Brunella, V.; Luda, M. P.; Zanetti, M.; Costa, L. Radiation-Induced Crosslinking of UHMWPE in the Presence of Co-Agents: Chemical and Mechanical Characterisation. *Polymer (Guildf).*, **2005**, *46* (24), 10648–10657. https://doi.org/10.1016/j.polymer.2005.08.095.

[37] Shen, J.; Costa, L.; Xu, Y.; Cong, Y.; Cheng, Y.; Liu, X.; Fu, J. Stabilization of Highly Crosslinked Ultra High Molecular Weight Polyethylene with Natural Polyphenols. *Polym. Degrad. Stab.*, **2014**, *105* (1), 197–205. https://doi.org/10.1016/j.polymdegradstab.2014.04.018.

[38] More, S. E.; Dave, J. R.; Makar, P. K.; Bhoraskar, S. V.; Premkumar, S.; Tomar, G. B.; Mathe, V. L. Surface Modification of UHMWPE Using ECR Plasma for Osteoblast and Osteoclast Differentiation. *Appl. Surf. Sci.*, **2019**, No. October, 144665. https://doi.org/10.1016/j.apsusc.2019.144665.

[39] Liu, H.; Xie, D.; Qian, L.; Deng, X.; Leng, Y. X.; Huang, N. The Mechanical Properties of the Ultrahigh Molecular Weight Polyethylene (UHMWPE) Modified by Oxygen Plasma. *Surf. Coatings Technol.*, **2011**, *205* (8–9), 2697–2701. https://doi.org/10.1016/j.surfcoat.2010.08.120.

[40] Bach, J. S.; Detrez, F.; Cherkaoui, M.; Cantournet, S.; Ku, D. N.; Corté, L. Hydrogel Fibers for ACL Prosthesis: Design and Mechanical Evaluation of PVA and PVA/UHMWPE Fiber Constructs. *J. Biomech.*, **2013**, *46* (8), 1463–1470. https://doi.org/10.1016/j.jbiomech.2013.02.020.

[41] Ianuzzi, A.; Mkandawire, C. *Applications of UHMWPE in Total Ankle Replacements*, Third Edit.; Elsevier Inc., 2009. https://doi.org/10.1016/B978-0-12-374721-1.00011-0.

[42] Ai, C.; Sheng, D.; Chen, J.; Cai, J.; Wang, S.; Jiang, J.; Chen, S. Surface Modification of Vascular Endothelial Growth Factor-Loaded Silk Fibroin to Improve Biological Performance of Ultra-High-Molecular-Weight Polyethylene via Promoting Angiogenesis. *Int. J. Nanomedicine*, **2017**, *12*, 7737–7750. https://doi.org/10.2147/IJN.S148845.

[43] Deng, Y.; Xiong, D.; Wang, K. Biotribological Properties of UHMWPE Grafted with AA under Lubrication as Artificial Joint. *J. Mater. Sci. Mater. Med.*, **2013**, *24* (9), 2085–2091. https://doi.org/10.1007/s10856-013-4970-x.

[44] Sun, R.; Feng, Y.; Zhang, Z.; Yan, L.; He, Z.; Zhang, Z.; Yan, L. Research Progress on Surface Modification and Application Status of UHMWPE Fiber Research Progress on Surface Modification and Application Status of UHMWPE Fiber. **2022**. https://doi.org/10.1088/1742-6596/2263/1/012016.

[45] Sa, R.; Wei, Z.; Yan, Y.; Wang, L.; Wang, W.; Zhang, L.; Ning, N.; Tian, M. Catechol

and Epoxy Functionalized Ultrahigh Molecular Weight Polyethylene (UHMWPE) Fibers with Improved Surface Activity and Interfacial Adhesion. *Compos. Sci. Technol.*, **2015**, *113*, 54–62. https://doi.org/10.1016/j.compscitech.2015.03.017.

[46] Hu, J.; Feng, X.; Liu, Z.; Zhao, Y.; Chen, L. Surface Amine-Functionalization of UHMWPE Fiber by Bio-Inspired Polydopamine and Grafted Hexamethylene Diamine. *Surf. Interface Anal.*, **2017**, *49* (7), 640–646. https://doi.org/10.1002/sia.6203.

[47] James, S. P.; Oldinski, R. K.; Zhang, M.; Schwartz, H. *UHMWPE/Hyaluronan Microcomposite Biomaterials*, Third Edit.; Elsevier Inc., 2009. https://doi.org/10.1016/B978-0-12-374721-1.00018-3.

[48] Kane, S. R.; Ashby, P. D.; Pruitt, L. A. Characterization and Tribology of PEG-like Coatings on UHMWPE for Total Hip Replacements. *J. Biomed. Mater. Res. - Part A*, **2010**, *92* (4), 1500–1509. https://doi.org/10.1002/jbm.a.32484.

[49] Liu, R.; Liu, S.; Yu, J.; Zhang, W.; Dai, J.; Zhang, Y.; Zhang, G. The Construction of a Hydrophilic Inorganic Layer Enables Mechanochemically Robust Super Antifouling UHMWPE Composite Membrane Surfaces. *Polymers (Basel).*, **2020**, *12* (3). https://doi.org/10.3390/polym12030569.

[50] Denes, F.; Young, R. A.; Sarmadi, M. Surface Functionalization of Polymers under Cold Plasma Conditions-A Mechanistic Approach. *J. Photopolym. Sci. Technol.*, **2008**, *10* (1), 91–112. https://doi.org/10.2494/photopolymer.10.91.

[51] Dufay, M.; Jimenez, M.; Degoutin, S. Effect of Cold Plasma Treatment on Electrospun Nanofibers Properties: A Review. *ACS Appl. Bio Mater.*, **2020**. https://doi.org/10.1021/acsabm.0c00154.

[52] Bočková, J.; Vojtová, L.; Přikryl, R.; Čechal, J.; Jančář, J. Collagen-Grafted Ultra-High Molecular Weight Polyethylene for Biomedical Applications. *Chem. Pap.*, **2008**, *62* (6), 580–588. https://doi.org/10.2478/s11696-008-0076-1.

[53] Ren, Y.; Ding, Z.; Wang, C.; Zang, C.; Zhang, Y.; Xu, L. Influence of DBD Plasma Pretreatment on the Deposition of Chitosan onto UHMWPE Fiber Surfaces for Improvement of Adhesion and Dyeing Properties. *Appl. Surf. Sci.*, **2017**, *396*, 1571–1579. https://doi.org/10.1016/j.apsusc.2016.11.215.

[54] Cools, P.; Van Vrekhem, S.; De Geyter, N.; Morent, R. The Use of DBD Plasma Treatment and Polymerization for the Enhancement of Biomedical UHMWPE. *Thin Solid Films*, **2014**, *572*, 251–259. https://doi.org/10.1016/j.tsf.2014.08.033.

[55] Wang, A.; Sun, D. C.; Yau, S.; Edwards, B.; Sokol, M.; Essner, A.; Polineni, V. K.; Stark, C.; Dumbleton, J. H. Softetring In. *Wear*, **1997**, *204*, 230–241.

[56] Huot, J. C.; Van Citters, D. W.; Currier, J. H.; Collier, J. P. The Effect of Radiation Dose on the Tensile and Impact Toughness of Highly Cross-Linked and Remelted Ultrahigh-Molecular Weight Polyethylenes. *J. Biomed. Mater. Res. - Part B Appl. Biomater.*, **2011**, *97 B* (2), 327–333. https://doi.org/10.1002/jbm.b.31818.

[57] Cho, E. H.; Lee, S. G.; Kim, J. K. Surface Modification of UHMWPE with γ-Ray Radiation for Improving Interfacial Bonding Strength with Bone Cement (II). *Curr. Appl.*

Phys., **2005**, *5* (5), 475–479. https://doi.org/10.1016/j.cap.2005.01.013.

[58] Xia, B.; Xie, M.; Yang, B. Surface Modification of Ultrahigh Molecular Weight Polyethylene by the Poly(Ethylene Glycol)-Grafted Method and Its Effect on the Adsorption of Proteins and the Adhesion of Blood Platelets. *J. Biomed. Mater. Res. - Part A*, **2013**, *101 A* (1), 54–63. https://doi.org/10.1002/jbm.a.34301.

[59] Puppulin, L.; Leto, A.; Hasegawa, M.; Pezzotti, G. A Comparative Microstructural Study of Vitamin-E Blended and Infused Highly Crosslinked UHMWPE for Total Knee Arthroplasty. *J. Mech. Behav. Biomed. Mater.*, **2014**, *39*, 247–256. https://doi.org/10.1016/j.jmbbm.2014.07.029.

[60] Shi, W.; Li, X. Y.; Dong, H. Improved Wear Resistance of Ultra-High Molecular Weight Polyethylene by Plasma Immersion Ion Implantation. *Wear*, **2001**, *250–251* (PART 1), 544–552. https://doi.org/10.1016/S0043-1648(01)00636-6.

[61] Rossi, J. O.; Ueda, M.; Silva, A. R.; Neto, L. P. S. Improvement on UHMWPE and PMMA Surface Flashover Under Atmospheric Pressure Using PIII Processing. *IEEE Trans. Plasma Sci.*, **2020**, 1–6. https://doi.org/10.1109/tps.2020.3007735.

[62] Gan, B. K.; Kondyurin, A.; Bilek, M. M. M. Comparison of Protein Surface Attachment on Untreated and Plasma Immersion Ion Implantation Treated Polystyrene: Protein Islands and Carpet. *Langmuir*, **2007**, *23* (5), 2741–2746. https://doi.org/10.1021/la062722v.

[63] Kondyurin, A.; Nosworthy, N. J.; Bilek, M. M. M. Effect of Low Molecular Weight Additives on Immobilization Strength, Activity, and Conformation of Protein Immobilized on PVC AndUHMWPE. *Langmuir*, **2011**, *27* (10), 6138–6148. https://doi.org/10.1021/la200376f.

[64] García, A.; Domínguez-Díaz, M.; Paniagua, R.; Hernández-Pérez, J. A.; Martínez, H. Microhardness Modification of Ultrahigh-Molecular-Weight Polyethylene by Oxygen Plasma: Effect of the Polymer Crosslinking. *Nucl. Instruments Methods Phys. Res. Sect. B Beam Interact. with Mater. Atoms*, **2019**, *445* (February), 8–12. https://doi.org/10.1016/j.nimb.2019.02.020.

[65] Kurtz, S. M. *4 The Origins of UHMWPE in Total Hip Arthroplasty*, Third Edit.; Elsevier Inc., 1982. https://doi.org/10.1016/B978-0-323-35401-1/00004-1.

[66] Sobieraj, M. C.; Rimnac, C. M. Ultra High Molecular Weight Polyethylene: Mechanics, Morphology, and Clinical Behavior. *J. Mech. Behav. Biomed. Mater.*, **2009**, *2* (5), 433–443. https://doi.org/10.1016/j.jmbbm.2008.12.006.

[67] Patel, K.; Chikkali, S. H.; Sivaram, S. Ultrahigh Molecular Weight Polyethylene: Catalysis, Structure, Properties, Processing and Applications. *Prog. Polym. Sci.*, **2020**, 101290. https://doi.org/10.1016/j.progpolymsci.2020.101290.

[68] Hussain, M.; Naqvi, R. A.; Abbas, N.; Khan, S. M.; Nawaz, S.; Hussain, A.; Zahra, N.; Khalid, M. W. Ultra-High-Molecular-Weight-Polyethylene (UHMWPE) as a Promising Polymer Material for Biomedical Applications: A Concise Review. *Polymers (Basel).*, **2020**, *12* (2), 1–28. https://doi.org/10.3390/polym12020323.

[69] Sobieraj, M.; Marwin, S. Ultra-High-Molecular-Weight Polyethylene (UHMWPE) in

Total Joint Arthroplasty. **2018**, *76* (1), 38–46.

[70] Kopova, I.; Kronek, J.; Bacakova, L.; Fencl, J. A Cytotoxicity and Wear Analysis of Trapeziometacarpal Total Joint Replacement Implant Consisting of DLC-Coated Co-Cr-Mo Alloy with the Use of Titanium Gradient Interlayer. *Diam. Relat. Mater.*, **2019**, *97* (March), 107456. https://doi.org/10.1016/j.diamond.2019.107456.

[71] Macuvele, D. L. P.; Nones, J.; Matsinhe, J. V.; Lima, M. M.; Soares, C.; Fiori, M. A.; Riella, H. G. Advances in Ultra High Molecular Weight Polyethylene/Hydroxyapatite Composites for Biomedical Applications: A Brief Review. *Mater. Sci. Eng. C*, **2017**, *76*, 1248–1262. https://doi.org/10.1016/j.msec.2017.02.070.

[72] Avinash Patil, N.; Njuguna, J.; Kandasubramanian, B. UHMWPE for Biomedical Applications: Performance and Functionalization. *Eur. Polym. J.*, **2020**, *125* (January), 109529. https://doi.org/10.1016/j.eurpolymj.2020.109529.

[73] Gomez-Barrena, E.; Puertolas, J. A.; Munuera, L.; Konttinen, Y. T. Update on UHMWPE Research: From the Bench to the Bedside. *Acta Orthop.*, **2008**, *79* (6), 832–840. https://doi.org/10.1080/17453670810016939.

[74] Jiang, J. H.; Zhu, L. P.; Li, X. L.; Xu, Y. Y.; Zhu, B. K. Surface Modification of PE Porous Membranes Based on the Strong Adhesion of Polydopamine and Covalent Immobilization of Heparin. *J. Memb. Sci.*, **2010**, *364* (1–2), 194–202. https://doi.org/10.1016/j.memsci.2010.08.017.

[75] Shanmugam, L.; Kazemi, M. E.; Li, Z.; Luo, W.; Xiang, Y.; Yang, L.; Yang, J. Low-Velocity Impact Behavior of UHMWPE Fabric/Thermoplastic Laminates with Combined Surface Treatments of Polydopamine and Functionalized Carbon Nanotubes. *Compos. Commun.*, **2020**, *22* (September), 100527. https://doi.org/10.1016/j.coco.2020.100527.

[76] Nomura, K.; Terwilliger, P. Self-Dual Leonard Pairs Modifications on the Properties and Their Composites. **2019**, 40–49.

[77] Silverstein, M. S.; Breuer, O.; Dodiuk, H. Surface Modification of UHMWPE Fibers. *J. Appl. Polym. Sci.*, **1994**, *52* (12), 1785–1795. https://doi.org/10.1002/app.1994.070521213.

[78] Chhetri, S.; Bougherara, H. A Comprehensive Review on Surface Modification of UHMWPE Fiber and Interfacial Properties. *Compos. Part A Appl. Sci. Manuf.*, **2021**, *140* (October 2020), 106146. https://doi.org/10.1016/j.compositesa.2020.106146.

[79] Firouzi, D.; Youssef, A.; Amer, M.; Srouji, R.; Amleh, A.; Foucher, D. A.; Bougherara, H. A New Technique to Improve the Mechanical and Biological Performance of Ultra High Molecular Weight Polyethylene Using a Nylon Coating. *J. Mech. Behav. Biomed. Mater.*, **2014**, *32*, 198–209. https://doi.org/10.1016/j.jmbbm.2014.01.001.

[80] Kang, K.; Choi, I. S.; Nam, Y. A Biofunctionalization Scheme for Neural Interfaces Using Polydopamine Polymer. *Biomaterials*, **2011**, *32* (27), 6374–6380. https://doi.org/10.1016/j.biomaterials.2011.05.028.

[81] Liu, R.; Wang, X.; Yu, J.; Wang, Y.; Zhu, J.; Hu, Z. Surface Modification of UHMWPE/Fabric Composite Membrane via Self-Polymerized Polydopamine Followed

by MPEG-NH2 Immobilization. *J. Appl. Polym. Sci.*, **2018**, *135* (26), 1–11. https://doi.org/10.1002/app.46428.

[82] Amirgoulova, E. V.; Groll, J.; Heyes, C. D.; Ameringer, T.; Röcker, C.; Möller, M.; Nienhaus, G. U. Biofunctionalized Polymer Surfaces Exhibiting Minimal Interaction towards Immobilized Proteins. *ChemPhysChem*, **2004**, *5* (4), 552–555. https://doi.org/10.1002/cphc.200400024.

[83] Smolko, E.; Romero, G. Studies on Crosslinked Hydroxyapatite-Polyethylene Composite as a Bone-Analogue Material. *Radiat. Phys. Chem.*, **2007**, *76* (8–9), 1414–1418. https://doi.org/10.1016/j.radphyschem.2007.02.043.

[84] Chen, S.; Fu, P.; Wu, H.; Pei, M. Meniscus, Articular Cartilage and Nucleus Pulposus: A Comparative Review of Cartilage-like Tissues in Anatomy, Development and Function. *Cell Tissue Res.*, **2017**, *370* (1), 53–70. https://doi.org/10.1007/s00441-017-2613-0.

[85] Cheng, X.; Kondyurin, A.; Bao, S.; Bilek, M. M. M.; Ye, L. Plasma Immersion Ion Implantation of Polyurethane Shape Memory Polymer: Surface Properties and Protein Immobilization. *Appl. Surf. Sci.*, **2017**, *416*, 686–695. https://doi.org/10.1016/j.apsusc.2017.04.179.

[86] Nichols, S. P.; Koh, A.; Storm, W. L.; Shin, J. H.; Schoenfisch, M. H. Biocompatible Materials for Continuous Glucose Monitoring Devices. *Chem. Rev.*, **2013**, *113* (4), 2528–2549. https://doi.org/10.1021/cr300387j.

[87] Gu, X.; Zheng, Y.; Cheng, Y.; Zhong, S.; Xi, T. In Vitro Corrosion and Biocompatibility of Binary Magnesium Alloys. *Biomaterials*, **2009**, *30* (4), 484–498. https://doi.org/10.1016/j.biomaterials.2008.10.021.

[88] Yoshida, S.; Hagiwara, K.; Hasebe, T.; Hotta, A. Surface Modification of Polymers by Plasma Treatments for the Enhancement of Biocompatibility and Controlled Drug Release. *Surf. Coatings Technol.*, **2013**, *233*, 99–107. https://doi.org/10.1016/j.surfcoat.2013.02.042.

[89] Schoonen, L.; Van Hest, J. C. M. Functionalization of Protein-Based Nanocages for Drug Delivery Applications. *Nanoscale*, **2014**, *6* (13), 7124–7141. https://doi.org/10.1039/c4nr00915k.

[90] Poncin-Epaillard, F.; Legeay, G. Surface Engineering of Biomaterials with Plasma Techniques. *J. Biomater. Sci. Polym. Ed.*, **2003**, *14* (10), 1005–1028. https://doi.org/10.1163/156856203769231538.

[91] Stewart, C. A. C.; Akhavan, B.; Hung, J.; Bao, S.; Jang, J. H.; Wise, S. G.; Bilek, M. M. M. Multifunctional Protein-Immobilized Plasma Polymer Films for Orthopedic Applications. *ACS Biomater. Sci. Eng.*, **2018**, *4* (12), 4084–4094. https://doi.org/10.1021/acsbiomaterials.8b00954.

[92] Tang, L.; Wang, Y.; Li, J. The Graphene/Nucleic Acid Nanobiointerface. *Chem. Soc. Rev.*, **2015**, *44* (19), 6954–6980. https://doi.org/10.1039/c4cs00519h.

[93] Nedela, O.; Slepicka, P.; Švorcík, V. Surface Modification of Polymer Substrates for Biomedical Applications. *Materials (Basel).*, **2017**, *10* (10).

https://doi.org/10.3390/ma10101115.

[94] Ratner, B. D. The Engineering of Biomaterials Exhibiting Recognition and Specificity. *J. Mol. Recognit.*, **1996**, *9* (5–6), 617–625. https://doi.org/10.1002/(SICI)1099-1352(199634/12)9:5/6<617::AID-JMR310>3.0.CO;2-D.

[95] Hegemann, D.; Brunner, H.; Oehr, C. Plasma Treatment of Polymers for Surface and Adhesion Improvement. *Nucl. Instruments Methods Phys. Res. Sect. B Beam Interact. with Mater. Atoms*, **2003**, *208* (1–4), 281–286. https://doi.org/10.1016/S0168-583X(03)00644-X.

[96] Riveiro, A.; Soto, R.; Del Val, J.; Comesaña, R.; Boutinguiza, M.; Quintero, F.; Lusquiños, F.; Pou, J. Laser Surface Modification of Ultra-High-Molecular-Weight Polyethylene (UHMWPE) for Biomedical Applications. *Appl. Surf. Sci.*, **2014**, *302*, 236–242. https://doi.org/10.1016/j.apsusc.2014.02.130.

[97] Tan, F.; Fang, Y.; Zhu, L.; Al-rubeai, M. Critical Reviews in Biotechnology Cold Atmospheric Plasma as an Interface Biotechnology for Enhancing Surgical Implants. *Crit. Rev. Biotechnol.*, **2021**, *41* (3), 425–440. https://doi.org/10.1080/07388551.2020.1853671.

[98] Perni, S.; Kong, M. G.; Prokopovich, P. Cold Atmospheric Pressure Gas Plasma Enhances the Wear Performance of Ultra-High Molecular Weight Polyethylene. *Acta Biomater.*, **2012**, *8* (3), 1357–1365. https://doi.org/10.1016/j.actbio.2011.12.007.

[99] Van Vrekhem, S.; Vloebergh, K.; Asadian, M.; Vercruysse, C.; Declercq, H.; Van Tongel, A.; De Wilde, L.; De Geyter, N.; Morent, R. Improving the Surface Properties of an UHMWPE Shoulder Implant with an Atmospheric Pressure Plasma Jet. *Sci. Rep.*, **2018**, *8* (1), 1–11. https://doi.org/10.1038/s41598-018-22921-6.

[100] Asadian, M.; Chan, K. V.; Norouzi, M.; Grande, S.; Cools, P.; Morent, R.; De Geyter, N. Fabrication and Plasma Modification of Nanofibrous Tissue Engineering Scaffolds. *Nanomaterials*, **2020**, *10* (1). https://doi.org/10.3390/nano10010119.

[101] Rodrigues, M. M.; Fontoura, C. P.; Garcia, C. S. C.; Martins, S. T.; Henriques, J. A. P.; Figueroa, C. A.; Roesch-Ely, M.; Aguzzoli, C. Investigation of Plasma Treatment on UHMWPE Surfaces: Impact on Physicochemical Properties, Sterilization and Fibroblastic Adhesion. *Mater. Sci. Eng. C*, **2019**, *102* (March), 264–275. https://doi.org/10.1016/j.msec.2019.04.048.

[102] Liang, H.; Shi, B.; Fairchild, A.; Cale, T. Applications of Plasma Coatings in Artificial Joints: An Overview. *Vacuum*, **2004**, *73* (3–4), 317–326. https://doi.org/10.1016/j.vacuum.2003.12.160.

[103] Cvrček, L.; Horáková, M. *Plasma Modified Polymeric Materials for Implant Applications*; 2019. https://doi.org/10.1016/b978-0-12-813152-7.00014-7.

[104] Das, S.; Jana, S.; De, D.; Gangopadhyay, U.; Mondal, A. Low Temperature Growth of Diamond-like Nanocomposite Films Prepared by PACVD from Ar Diluted Siloxane Plasma. *Mater. Res. Express*, **2019**, *6* (11). https://doi.org/10.1088/2053-1591/ab4d80.

[105] Buchkremer-Hermanns, H.; Long, C.; Weiss, H. ECR Plasma Polishing of CVD Diamond Films. *Diam. Relat. Mater.*, **1996**, *5* (6–8), 845–849. https://doi.org/10.1016/0925-

9635(95)00484-x.

[106] Mwale, F.; Wang, H. T.; Nelea, V.; Luo, L.; Antoniou, J.; Wertheimer, M. R. The Effect of Glow Discharge Plasma Surface Modification of Polymers on the Osteogenic Differentiation of Committed Human Mesenchymal Stem Cells. *Biomaterials*, **2006**, *27* (10), 2258–2264. https://doi.org/10.1016/j.biomaterials.2005.11.006.

[107] Activity, A. Characterization of Biopolymer and Chitosan -Based Nanocomposites with Antimicrobial Activity. **2013**.

[108] Yang, Z.; Peng, H.; Wang, W.; Liu, T. Crystallization Behavior of Poly(ε-Caprolactone)/Layered Double Hydroxide Nanocomposites. *J. Appl. Polym. Sci.*, **2010**, *116* (5), 2658–2667. https://doi.org/10.1002/app.

[109] Ma, Y.; Liu, L.; Yang, W. Photo-Induced Living/Controlled Surface Radical Grafting Polymerization and Its Application in Fabricating 3-D Micro-Architectures on the Surface of Flat/Particulate Organic Substrates. *Polymer (Guildf).*, **2011**, *52* (19), 4159–4173. https://doi.org/10.1016/j.polymer.2011.07.027.

[110] Hu, J.; Gao, Q.; Xu, L.; Zhang, M.; Xing, Z.; Guo, X.; Zhang, K.; Wu, G. Significant Improvement in Thermal and UV Resistances of UHMWPE Fabric through in Situ Formation of Polysiloxane-TiO2 Hybrid Layers. *ACS Appl. Mater. Interfaces*, **2016**, *8* (35), 23311–23320. https://doi.org/10.1021/acsami.6b04914.

[111] Koseki, H.; Yonekura, A.; Shida, T.; Yoda, I.; Horiuchi, H.; Morinaga, Y.; Yanagihara, K.; Sakoda, H.; Osaki, M.; Tomita, M. Early Staphylococcal Biofilm Formation on Solid Orthopaedic Implant Materials: In Vitro Study. *PLoS One*, **2014**, *9* (10), 1–8. https://doi.org/10.1371/journal.pone.0107588.

[112] Shen, J.; Costa, L.; Xu, Y.; Cong, Y.; Cheng, Y.; Liu, X.; Fu, J. Stabilization of Highly Crosslinked Ultra High Molecular Weight Polyethylene with Natural Polyphenols. *Polym. Degrad. Stab.*, **2014**, *105* (1), 197–205. https://doi.org/10.1016/j.polymdegradstab.2014.04.018.

[113] Meng, C.; Chen, Y.; Xie, M.; Yu, Z.; Yang, B. Surface Modification of Ultrahigh Molecular Weight Polyethylene by Plasma-Induced in-Situ Grafting with Vinyl Triethoxysilane. *J. Biomed. Mater. Res. - Part A*, **2018**, *106* (2), 321–332. https://doi.org/10.1002/jbm.a.36241.

[114] Aziz, G.; De Geyter, N.; Declercq, H.; Cornelissen, R.; Morent, R. Incorporation of Amine Moieties onto Ultra-High Molecular Weight Polyethylene (UHMWPE) Surface via Plasma and UV Polymerization of Allylamine. *Surf. Coatings Technol.*, **2015**, *271*, 39–47. https://doi.org/10.1016/j.surfcoat.2015.01.027.

[115] John R. Conrad. Method and Apparatus for Plasma Source Ion Implantation. **1987**, *252* (3), 102–113.

[116] Conrad, J. R.; Radtke, J. L.; Dodd, R. A.; Worzala, F. J.; Tran, N. C. Plasma Source Ion-Implantation Technique for Surface Modification of Materials. *J. Appl. Phys.*, **1987**, *62* (11), 4591–4596. https://doi.org/10.1063/1.339055.

[117] Biederman, H. Polymer Films Prepared by Plasma Polymerization and Their Potential

Application. *Vacuum*, **1987**, *37* (3–4), 367–373. https://doi.org/10.1016/0042-207X(87)90027-3.

[118] Gutensohn, K.; Beythien, C.; Bau, J.; Fenner, T.; Grewe, P.; Koester, R.; Padmanaban, K.; Kuehnl, P. In Vitro Analyses of Diamond-like Carbon Coated Stents: Reduction of Metal Ion Release, Platelet Activation, and Thrombogenicity. *Thromb. Res.*, **2000**, *99* (6), 577–585. https://doi.org/10.1016/S0049-3848(00)00295-4.

[119] Kaur, G.; Pandey, O. P.; Singh, K.; Homa, D.; Scott, B.; Pickrell, G. A Review of Bioactive Glasses: Their Structure, Properties, Fabrication, and Apatite Formation. *J. Biomed. Mater. Res. A*, **2013**, 254–274. https://doi.org/10.1002/jbm.a.34690.

[120] Mahapatro, A. Bio-Functional Nano-Coatings on Metallic Biomaterials. *Mater. Sci. Eng. C*, **2015**, *55*, 227–251. https://doi.org/10.1016/j.msec.2015.05.018.

[121] Kosobrodova, E.; Kondyurin, A.; McKenzie, D. R.; Bilek, M. M. M. Kinetics of Post-Treatment Structural Transformations of Nitrogen Plasma Ion Immersion Implanted Polystyrene. *Nucl. Instruments Methods Phys. Res. Sect. B Beam Interact. with Mater. Atoms*, **2013**, *304*, 57–66. https://doi.org/10.1016/j.nimb.2013.03.038.

[122] Huang, N.; Yang, P.; Leng, Y. X.; Wang, J.; Sun, H.; Chen, J. Y.; Wan, G. J. Surface Modification of Biomaterials by Plasma Immersion Ion Implantation. *Surf. Coatings Technol.*, **2004**, *186* (1-2 SPEC. ISS.), 218–226. https://doi.org/10.1016/j.surfcoat.2004.04.041.

[123] Chen, J. S.; Sun, Z.; Guo, P. S.; Zhang, Z. B.; Zhu, D. Z.; Xu, H. J. Effect of Ion Implantation on Surface Energy of Ultrahigh Molecular Weight Polyethylene. *J. Appl. Phys.*, **2003**, *93* (9), 5103–5108. https://doi.org/10.1063/1.1559943.

[124] Farm, D. F.; Brain, A. A. The Microstructure of Ultra-High Molecular Weight Polyethylene Used in Total Joint Replacements. **1998**, *18* (24), 1677–1685.

[125] An, Y. H.; Alvi, F. I.; Kang, Q.; Laberge, M.; Drews, M. J.; Zhang, J.; Matthews, M. A.; Arciola, C. R. Effects of Sterilization on Implant Mechanical Property and Biocompatibility. *Int. J. Artif. Organs*, **2005**, *28* (11), 1126–1137. https://doi.org/10.1177/039139880502801110.

[126] Baranowska, J. Plasma Nitriding and Plasma Immersion Ion Implantation. **2008**.

[127] Day, J. S.; MacDonald, D. W.; Ramsey, M. L.; Abboud, J. A.; Kurtz, S. M. Quantitative Ultrahigh-Molecular-Weight Polyethylene Wear in Total Elbow Retrievals. *J. Shoulder Elb. Surg.*, **2020**, 1–11. https://doi.org/10.1016/j.jse.2020.03.026.

[128] Liu, R.; Dai, J.; Ma, L.; Chen, J.; Shi, X.; Du, Y.; Li, Z.; Deng, H. Low-Temperature Plasma Treatment-Assisted Layer-by-Layer Self-Assembly for the Modification of Nanofibrous Mats. *J. Colloid Interface Sci.*, **2019**, *540*, 535–543. https://doi.org/10.1016/j.jcis.2019.01.054.

[129] Puliyalil, H.; Filipič, G.; Cvelbar, U. Selective Plasma Etching of Polymers and Polymer Matrix Composites. *Non-Thermal Plasma Technol. Polym. Mater.*, **2019**, 241–259. https://doi.org/10.1016/b978-0-12-813152-7.00009-3.

[130] Mohammadalipour, M.; Masoomi, M.; Ahmadi, M.; Safi, S. Interfacial Shear Strength Characterization of GMA-Grafted UHMWPE Fiber/Epoxy/Nano Clay Hybrid Nanocomposite Materials. *RSC Adv.*, **2016**, *6* (48), 41793–41799. https://doi.org/10.1039/c6ra05027a.

[131] Mamidi, N.; Leija, H. M.; Diabb, J. M.; Lopez Romo, I.; Hernandez, D.; Castrejón, J. V.; Martinez Romero, O.; Barrera, E. V.; Elias Zúñiga, A. Cytotoxicity Evaluation of Unfunctionalized Multiwall Carbon Nanotubes-Ultrahigh Molecular Weight Polyethylene Nanocomposites. *J. Biomed. Mater. Res. - Part A*, **2017**, *105* (11), 3042–3049. https://doi.org/10.1002/jbm.a.36168.

[132] Manoj Kumar, R.; Rajesh, K.; Haldar, S.; Gupta, P.; Murali, K.; Roy, P.; Lahiri, D. Surface Modification of CNT Reinforced UHMWPE Composite for Sustained Drug Delivery. *J. Drug Deliv. Sci. Technol.*, **2019**, *52* (May), 748–759. https://doi.org/10.1016/j.jddst.2019.05.044.

[133] Dyachkova, T.; Gutnik, I.; Nagdaev, V.; Maksimkin, A.; Burakova, E.; Galunin, E.; Memetov, N.; Khan, Y.; Dayyoub, T. Studying the Surface of UHMWPE Films Modified with Graphene Nanoplatelets Using a Raman Mapping Method. *Fullerenes Nanotub. Carbon Nanostructures*, **2020**, *28* (7), 561–564. https://doi.org/10.1080/1536383X.2020.1724103.

[134] Liu, C. Y.; Ishigami, A.; Kurose, T.; Ito, H. Wear Resistance of Graphene Reinforced Ultra-High Molecular Weight Polyethylene Nanocomposites Prepared by Octa-Screw Extrusion Process. *Compos. Part B Eng.*, **2021**, *215* (January), 108810. https://doi.org/10.1016/j.compositesb.2021.108810.

[135] Ahmadi, M.; Zabihi, O.; Masoomi, M.; Naebe, M. Synergistic Effect of MWCNTs Functionalization on Interfacial and Mechanical Properties of Multi-Scale UHMWPE Fibre Reinforced Epoxy Composites. *Compos. Sci. Technol.*, **2016**, *134*, 1–11. https://doi.org/10.1016/j.compscitech.2016.07.026.

[136] Aghvami-Panah, M.; Panahi-Sarmad, M.; Seraji, A. A.; Jamalpour, S.; Ghaffarian, S. R.; Park, C. B. LDPE/MWCNT and LDPE/MWCNT/UHMWPE Self-Reinforced Fiber-Composite Foams Prepared via Supercritical CO2: A Microstructure-Engineering Property Perspective. *J. Supercrit. Fluids*, **2021**, *174* (January), 105248. https://doi.org/10.1016/j.supflu.2021.105248.

[137] Azam, M. U.; Samad, M. A. Tribological Evaluation of a UHMWPE Hybrid Nanocomposite Coating Reinforced with Nanoclay and Carbon Nanotubes under Dry Conditions. *J. Tribol.*, **2018**, *140* (5), 26–28. https://doi.org/10.1115/1.4039956.

[138] Xin, X.; Wang, Y.; Meng, Z.; Yan, F. Improving Mechanical Properties and Fretting Wear Resistance of Ultra-High-Molecular-Weight-Polyethylene via Incorporation of Zeolitic Imidazolate Frameworks-Carbon Nano-Fiber. *Polym. Adv. Technol.*, **2021**, *32* (6), 2622–2632. https://doi.org/10.1002/pat.5294.

[139] Chen, X.; Zhang, S.; Zhang, L.; Zhu, P.; Zhang, G. Design and Characterization of the Surface Porous Uhmwpe Composite Reinforced by Graphene Oxide. *Polymers (Basel).*, **2021**, *13* (4), 1–14. https://doi.org/10.3390/polym13040482.

[140] Fang, Z.; Tu, Q.; Shen, X.; Yang, X.; Liang, K.; Pan, M.; Chen, Z. Biomimetic Surface Modification of UHMWPE Fibers to Enhance Interfacial Adhesion with Rubber Matrix via Constructing Polydopamine Functionalization Platform and Then Depositing Zinc Oxide Nanoparticles. *Surfaces and Interfaces*, **2022**, *29* (January), 101728. https://doi.org/10.1016/j.surfin.2022.101728.

[141] Rusmini, F.; Zhong, Z.; Feijen, J. Protein Immobilization Strategies for Protein Biochips. *Biomacromolecules*, **2007**, *8* (6), 1775–1789. https://doi.org/10.1021/bm061197b.

[142] Puertas, S.; de Gracia Villa, M.; Mendoza, E.; Jiménez-Jorquera, C.; de la Fuente, J. M.; Fernández-Sánchez, C.; Grazú, V. Improving Immunosensor Performance through Oriented Immobilization of Antibodies on Carbon Nanotube Composite Surfaces. *Biosens. Bioelectron.*, **2013**, *43*, 274–280. https://doi.org/10.1016/j.bios.2012.12.010.

[143] Yang, Z.; Wang, J.; Luo, R.; Maitz, M. F.; Jing, F.; Sun, H.; Huang, N. The Covalent Immobilization of Heparin to Pulsed-Plasma Polymeric Allylamine Films on 316L Stainless Steel and the Resulting Effects on Hemocompatibility. *Biomaterials*, **2010**, *31* (8), 2072–2083. https://doi.org/10.1016/j.biomaterials.2009.11.091.

[144] Bilek, M. M. M. Biofunctionalization of Surfaces by Energetic Ion Implantation: Review of Progress on Applications in Implantable Biomedical Devices and Antibody Microarrays. *Appl. Surf. Sci.*, **2014**, *310*, 3–10. https://doi.org/10.1016/j.apsusc.2014.03.097.

[145] Cruz, G. J.; Gómez, L. M.; Gonzalez-Torres, M.; Gonzalez-Salgado, F.; Basurto, R.; Colín, E.; Palacios, J. C.; Olayo, M. G. Polymerization Mechanisms in Plasma Polyallylamine. *J. Mater. Sci.*, **2017**, *52* (2), 1005–1013. https://doi.org/10.1007/s10853-016-0396-4.

[146] Pfeiffer, Ã. The Hydrolysis = Condensation Behaviour of Methacryloyloxyalkylfunctional Alkoxysilanes : Structure-Reactivity Relations. **2003**, *1092*, 1081–1092. https://doi.org/10.1007/s00706-003-0615-y.

[147] Voggenreiter, G.; Hartl, K.; Assenmacher, S. Assesment of the Biological Activity of Chemically Immobilized RhBMP-2 on Titanium Surfaces in Vivo. **2001**, *948*.

[148] Widmer, M. R.; Heuberger, M.; Vörös, J.; Spencer, N. D. Influence of Polymer Surface Chemistry on Frictional Properties under Protein-Lubrication Conditions: Implications for Hip-Implant Design. *Tribol. Lett.*, **2001**, *10* (1–2), 111–116. https://doi.org/10.1023/A:1009074228662.

[149] Lu, T.; Qiao, Y.; Liu, X. Surface Modification of Biomaterials Using Plasma Immersion Ion Implantation and Deposition. *Interface Focus*, **2012**, *2* (3), 325–336. https://doi.org/10.1098/rsfs.2012.0003.

[150] Kwok, D. T. K.; Tong, L.; Yeung, C. Y.; Remedios, C. G. do.; Chu, P. K. Hybrid Plasma Surface Modification and Ion Implantation of Biopolymers. *Surf. Coatings Technol.*, **2010**, *204* (18–19), 2892–2897. https://doi.org/10.1016/j.surfcoat.2010.02.043.

[151] Kan, Y.; Cvjetinovic, J.; Statnik, E. S.; Ryazantsev, S. V.; Anisimova, N. Y.; Kiselevskiy, M. V.; Salimon, A. I.; Maksimkin, A. V.; Korsunsky, A. M. The Fabrication and

Characterization of Bioengineered Ultra-High Molecular Weight Polyethylene-Collagen-Hap Hybrid Bone-Cartilage Patch. *Mater. Today Commun.*, **2020**, *24* (January), 101052. https://doi.org/10.1016/j.mtcomm.2020.101052.

[152] Teodoru, S.; Kusano, Y.; Rozlosnik, N.; Michelsen, P. K. Continuous Plasma Treatment of Ultra-High-Molecular-Weight Polyethylene (UHMWPE) Fibres for Adhesion Improvement. *Plasma Process. Polym.*, **2009**, *6* (SUPPL. 1), 375–381. https://doi.org/10.1002/ppap.200930906.

[153] Ho, J. P. Y.; Nosworthy, N. J.; Bilek, M. M. M.; Gan, B. K.; McKenzie, D. R.; Chu, P. K.; dos Remedios, C. G. Plasma-Treated Polyethylene Surfaces for Improved Binding of Active Protein. *Plasma Process. Polym.*, **2007**, *4* (5), 583–590. https://doi.org/10.1002/ppap.200600182.

[154] Gan, B. K.; Bilek, M. M. M.; Kondyurin, A.; Mizuno, K.; McKenzie, D. R. Etching and Structural Changes in Nitrogen Plasma Immersion Ion Implanted Polystyrene Films. *Nucl. Instruments Methods Phys. Res. Sect. B Beam Interact. with Mater. Atoms*, **2006**, *247* (2), 254–260. https://doi.org/10.1016/j.nimb.2006.01.063.

[155] Gan, B. K.; Nosworthy, N. J.; McKenzie, D. R.; Dos Remedios, C. G.; Bilek, M. M. M. Plasma Immersion Ion Implantation Treatment of Polyethylene for Enhanced Binding of Active Horseradish Peroxidase. *J. Biomed. Mater. Res. - Part A*, **2008**, *85* (3), 605–610. https://doi.org/10.1002/jbm.a.31612.

[156] Hassanein, N.; Bougherara, H.; Amleh, A. In- Vitro Evaluation of the Bioactivity and the Biocompatibility of a Novel Coated UHMWPE Biomaterial for Biomedical Applications. *J. Mech. Behav. Biomed. Mater.*, **2020**, *101* (April 2019), 103409. https://doi.org/10.1016/j.jmbbm.2019.103409.

[157] Zolotarevová, E.; Hudeček, J.; Špundová, M.; Entlicher, G. Binding of Proteins to Ultra High Molecular Weight Polyethylene Wear Particles as a Possible Mechanism of Macrophage and Lymphocyte Activation. *J. Biomed. Mater. Res. - Part A*, **2010**, *95* (3 A), 950–955. https://doi.org/10.1002/jbm.a.32924.

[158] Nečas, D.; Sawae, Y.; Fujisawa, T.; Nakashima, K.; Morita, T.; Yamaguchi, T.; Vrbka, M.; Křupka, I.; Hartl, M. The Influence of Proteins and Speed on Friction and Adsorption of Metal/UHMWPE Contact Pair. *Biotribology*, **2017**, *11* (May), 51–59. https://doi.org/10.1016/j.biotri.2017.03.003.

[159] Nečas, D.; Sawae, Y.; Fujisawa, T.; Nakashima, K.; Morita, T.; Yamaguchi, T.; Vrbka, M.; Křupka, I.; Hartl, M. The Influence of Proteins and Speed on Friction and Adsorption of Metal/UHMWPE Contact Pair. *Biotribology*, **2017**, *11* (November 2016), 51–59. https://doi.org/10.1016/j.biotri.2017.03.003.

[160] Anindyajati, A.; Boughton, P.; Ruys, A. J. Mechanical and Cytocompatibility Evaluation of UHMWPE/PCL/Bioglass® Fibrous Composite for Acetabular Labrum Implant. *Materials (Basel).*, **2019**, *16* (6). https://doi.org/10.3390/ma12060916.

[161] Roseti, L.; Buda, R.; Cavallo, C.; Desando, G.; Facchini, A.; Grigolo, B.; Barbiano, V. Ligament Repair : A Molecular and Immunohistological Characterization. **2007**. https://doi.org/10.1002/jbm.a.

[162] Vermeijden, H. D.; Jonkergouw, A.; van der List, J. P.; DiFelice, G. S. The Multiple Ligament-Injured Knee: When Is Primary Repair an Option? *Knee*, **2020**, *27* (1), 173–182. https://doi.org/10.1016/j.knee.2019.11.013.

[163] Iwamatsu-Kobayashi, Y.; Nishihara, D.; Hirata, M.; Kindaichi, K.; Komatsu, M. Effects of Biomaterials on Cell Adhesion of Human Periodontal Ligament Fibroblasts and Fibronectin Adsorption. *Int. Congr. Ser.*, **2005**, *1284*, 334–335. https://doi.org/10.1016/j.ics.2005.06.055.

[164] Murray, M. M.; Spindler, K. P.; Abreu, E.; Muller, J. A.; Nedder, A.; Kelly, M.; Frino, J.; Zurakowski, D.; Valenza, M.; Snyder, B. D.; et al. Collagen-Platelet Rich Plasma Hydrogel Enhances Primary Repair of the Porcine Anterior Cruciate Ligament. **2007**, No. January, 81–91. https://doi.org/10.1002/jor.

[165] Ma, T.; Gao, X.; Dong, H.; He, H.; Cao, X. High-Throughput Generation of Hyaluronic Acid Microgels via Microfluidics-Assisted Enzymatic Crosslinking and/or Diels–Alder Click Chemistry for Cell Encapsulation and Delivery. *Appl. Mater. Today*, **2017**, *9*, 49–59. https://doi.org/10.1016/j.apmt.2017.01.007.

[166] Halder, A. M.; Ludwig, S.; Neumann, W. Arthroscopic Anterior Cruciate Ligament Reconstruction Using the Double Press- Fit Technique: An Alternative to Interference Screw Fixation. *Arthrosc. J. Arthrosc. Relat. Surg. Off. Publ. Arthrosc. Assoc. North Am. Int. Arthrosc. Assoc.*, **2002**, *18* (9), 974–982. https://doi.org/10.1053/jars.2002.36107.

[167] Chen, S.; Wu, Y.; Mi, F.; Lin, Y.; Yu, L.; Sung, H. A Novel PH-Sensitive Hydrogel Composed of N , O -Carboxymethyl Chitosan and Alginate Cross-Linked by Genipin for Protein Drug Delivery. **2004**, *96*, 285–300. https://doi.org/10.1016/j.jconrel.2004.02.002.

[168] Sorsa, T.; Noponen, J.; Kelloma, M.; Juuti, H.; Lindqvist, C.; Asikainen, A. J.; Hagstro, J. Soft Tissue Reactions to Bioactive Glass 13-93 Combined with Chitosan. No. iii. https://doi.org/10.1002/jbm.a.

[169] Mourya, V. K.; Inamdar, N. N.; Tiwari, A. Carboxymethyl Chitosan and Its Applications. *Adv. Mater. Lett.*, **2010**, *1* (1), 11–33. https://doi.org/10.5185/amlett.2010.3108.

[170] Pok, S.; Myers, J. D.; Madihally, S. V.; Jacot, J. G. A Multilayered Scaffold of a Chitosan and Gelatin Hydrogel Supported by a PCL Core for Cardiac Tissue Engineering. *Acta Biomater.*, **2013**, *9* (3), 5630–5642. https://doi.org/10.1016/j.actbio.2012.10.032.

[171] Stähelin, A. C.; Weiler, A.; Rüfenacht, H.; Hoffmann, R.; Geissmann, A.; Feinstein, R. Clinical Degradation and Biocompatibility of Different Bioabsorbable Interference Screws: A Report of Six Cases. *Arthroscopy*, **1997**, *13* (2), 238–244. https://doi.org/10.1016/S0749-8063(97)90162-6.

[172] Dürselen, L.; Dauner, M.; Hierlemann, H.; Planck, H.; Claes, L. E.; Ignatius, a. Resorbable Polymer Fibers for Ligament Augmentation. *J. Biomed. Mater. Res.*, **2001**, *58* (6), 666–672.

[173] Li, M.; Mondrinos, M. J.; Chen, X.; Gandhi, M. R.; Ko, F. K.; Lelkes, P. I. Elastin Blends for Tissue Engineering Scaffolds. *J. Biomed. Mater. Res. Part A*, **2006**, *79* (4), 963–973. https://doi.org/10.1002/jbm.a.

[174] Margheritini, F.; Rihn, J. a.; Mauro, C. S.; Stabile, K. J.; Woo, S. L. Y.; Harner, C. D. Biomechanics of Initial Tibial Fixation in Posterior Cruciate Ligament Reconstruction. *Arthrosc. - J. Arthrosc. Relat. Surg.*, **2005**, *21* (10), 1164–1171. https://doi.org/10.1016/j.arthro.2005.06.017.

[175] Zhang, P.; Han, F.; Chen, T.; Wu, Z.; Chen, S. "Swiss Roll"-Like Bioactive Hybrid Scaffolds for Promoting Bone Tissue Ingrowth and Tendon-Bone Healing After Anterior Cruciate Ligament Reconstruction. *Biomater. Sci.*, **2020**, *8* (3), 871–883. https://doi.org/10.1039/c9bm01703h.

[176] McDonald, L. K.; Cosic, F.; Joseph, S. The Use of the Ligament Augmentation and Reconstruction System for Posterior Cruciate Ligament Reconstruction in Isolated and Multiligament Knee Injuries: A Systematic Review. *Knee*, **2021**, *30*, 322–336. https://doi.org/10.1016/j.knee.2021.04.008.

[177] Kanitkar, M.; Jaiswal, A.; Deshpande, R.; Bellare, J.; Kale, V. P. Enhanced Growth of Endothelial Precursor Cells on PCG-Matrix Facilitates Accelerated, Fibrosis-Free, Wound Healing: A Diabetic Mouse Model. *PLoS One*, **2013**, *8* (7). https://doi.org/10.1371/journal.pone.0069960.

[178] Tovar, N.; Bourke, S.; Jaffe, M.; Murthy, N. S.; Kohn, J.; Gatt, C.; Dunn, M. G. A Comparison of Degradable Synthetic Polymer Fibers for Anterior Cruciate Ligament Reconstruction. *J. Biomed. Mater. Res. A*, **2010**, *93* (2), 738–747. https://doi.org/10.1002/jbm.a.32567.

[179] Goldberg, J. a; Viglione, W.; Cumming, W. J.; Waddell, F. S.; Ruz, P. a. Review of Coracoclavicular Ligament Reconstruction Using Dacron Graft Material. *Aust. N. Z. J. Surg.*, **1987**, *57* (7), 441–445.

[180] Sharp, J. W.; Kani, K. K.; Gee, A.; Mulcahy, H.; Chew, F. S.; Porrino, J. Anterior Cruciate Ligament Fixation Devices: Expected Imaging Appearance and Common Complications. *Eur. J. Radiol.*, **2018**, *99* (December 2017), 17–27. https://doi.org/10.1016/j.ejrad.2017.12.006.

[181] Hertel, P.; Behrend, H.; Cierpinski, T.; Musahl, V.; Widjaja, G. ACL Reconstruction Using Bone-Patellar Tendon-Bone Press-Fit Fixation: 10-Year Clinical Results. *Knee Surgery, Sport. Traumatol. Arthrosc.*, **2005**, *13*, 248–255. https://doi.org/10.1007/s00167-004-0606-5.

[182] Lo, I. K. Y.; Ou, Y.; Rattner, J.; Hart, D. A.; Marchuk, L. L.; Frank, C. B.; Rattner, J. B. The Cellular Networks of Normal Ovine Medial Collateral and Anterior Cruciate Ligaments Are Not Accurately Recapitulated in Scar Tissue. **2002**, No. January, 283–296.

[183] S.L.Y.Woo,J.Adams, in:Daniel et al. Knee Ligaments : Structure , Function , Injury , and Repair. **2015**, No. JANUARY 1991.

[184] Zantop, T.; Petersen, W.; Sekiya, J. K.; Musahl, V.; Fu, F. H. Anterior Cruciate Ligament Anatomy and Function Relating to Anatomical Reconstruction. *Knee Surg. Sports Traumatol. Arthrosc.*, **2006**, *14* (10), 982–992. https://doi.org/10.1007/s00167-006-0076-z.

[185] Vieira, A. C.; Guedes, R. M.; Marques, A. T. Development of Ligament Tissue Biodegradable Devices : A Review.

[186] Chehab, E. L.; Flik, K. R.; Vidal, A. F.; Levinson, M.; Gallo, R. a; Altchek, D. W.; Warren, R. F. Anterior Cruciate Ligament Reconstruction Using Achilles Tendon Allograft: An Assessment of Outcome for Patients Age 30 Years and Older. *HSS J.*, **2011**, *7*, 44–51. https://doi.org/10.1007/s11420-010-9183-y.

[187] Legnani, C.; Ventura, A.; Terzaghi, C.; Borgo, E.; Albisetti, W. Anterior Cruciate Ligament Reconstruction with Synthetic Grafts. A Review of Literature. *Int. Orthop.*, **2010**, *34* (4), 465–471. https://doi.org/10.1007/s00264-010-0963-2.

[188] Murray, A. W.; MacNicol, M. F. 10-16 Year Results of Leeds-Keio Anterior Cruciate Ligament Reconstruction. *Knee*, **2004**, *11* (1), 9–14. https://doi.org/10.1016/S0968-0160(03)00076-0.

[189] Esposito, I. J.; Beard, D. J.; Dodd, C. A. F.; Shafighian, B. Rehabilitation Following Patellar Tendon or ABC Prosthetic Ligament Reconstruction for Chronic Anterior Cruciate Ligament Deficient Knees. *Knee*, **1997**, *4* (2), 81–86. https://doi.org/10.1016/S0968-0160(96)00242-6.

[190] Johnson, D. Gore-Tex Synthetic Ligament. *Oper. Tech. Sports Med.*, **1995**, *3* (3), 173–176. https://doi.org/10.1016/S1060-1872(95)80006-9.

[191] Glousman, R.; Shields, C.; Kerlan, R.; Jobe, F.; Lombardo, S.; Yocum, L.; Tibone, J.; Gambardella, R. Gore-Tex Prosthetic Ligament in Anterior Cruciate Deficient Knees. *Am. J. Sports Med.*, **1988**, *16* (4), 321–326. https://doi.org/10.1177/036354658801600402.

[192] Mulford, J. S.; Chen, D. Anterior Cruciate Ligament Reconstruction: A Systematic Review of Polyethylene Terephthalate Grafts. *ANZ J. Surg.*, **2011**, *81* (11), 785–789. https://doi.org/10.1111/j.1445-2197.2011.05884.x.

[193] Guidoin, M. F.; Marois, Y.; Bejui, J.; Poddevin, N.; King, M. W.; Guidoin, R. Analysis of Retrieved Polymer Fiber Based Replacements for the ACL. *Biomaterials*, **2000**, *21* (23), 2461–2474. https://doi.org/10.1016/S0142-9612(00)00114-9.

[194] Lewis, J. L.; Lew, W. D.; Engebretsen, L.; Hunter, R. E.; Kowalczyk, C. Factors Affecting Graft Force in Surgical Reconstruction of the Anterior Cruciate Ligament. *J. Orthop. Res.*, **1990**, *8*, 514–521. https://doi.org/10.1002/jor.1100080407.

[195] Illingworth, K. D.; Musahl, V.; Lorenz, S. G. F.; Fu, F. H. Use of Fibrin Clot in the Knee. *Oper. Tech. Orthop.*, **2010**, *20* (2), 90–97. https://doi.org/10.1053/j.oto.2009.11.002.

[196] Ventura, A.; Terzaghi, C.; Legnani, C.; Borgo, E.; Albisetti, W. Synthetic Grafts for Anterior Cruciate Ligament Rupture: 19-Year Outcome Study. *Knee*, **2010**, *17* (2), 108–113. https://doi.org/10.1016/j.knee.2009.07.013.

[197] Chen, K.; Liu, J.; Yang, X.; Zhang, D. Preparation , Optimization and Property of PVA-HA / PAA Composite Hydrogel. *Mater. Sci. Eng. C*, **2017**, *78*, 520–529. https://doi.org/10.1016/j.msec.2017.04.117.

[198] Marois, Y.; Roy, R.; Vidovszky, T.; King, M. W.; Bélanger, A. Y.; Chaput, C.; Guidoin,

R. Histopathological and Immunological Investigations of Synthetic Fibres and Structures Used in Three Prosthetic Anterior Cruciate Ligaments: In Vivo Study in the Rat. *Biomaterials*, **1993**, *14* (4), 255–262. https://doi.org/10.1016/0142-9612(93)90115-I.

[199] Farè, S.; Torricelli, P.; Giavaresi, G.; Bertoldi, S.; Alessandrino, A.; Villa, T.; Fini, M.; Tanzi, M. C.; Freddi, G. In Vitro Study on Silk Fibroin Textile Structure for Anterior Cruciate Ligament Regeneration. *Mater. Sci. Eng. C. Mater. Biol. Appl.*, **2013**, *33* (7), 3601–3608. https://doi.org/10.1016/j.msec.2013.04.027.

[200] Van Oeveren, W.; Tielliu, I. F.; De Hart, J. Comparison of Modified Chandler, Roller Pump, and Ball Valve Circulation Models for in Vitro Testing in High Blood Flow Conditions: Application in Thrombogenicity Testing of Different Materials for Vascular Applications. *Int. J. Biomater.*, **2012**, *2012*. https://doi.org/10.1155/2012/673163.

[201] Poulsson, A. H. C.; Mitchell, S. A.; Davidson, M. R.; Johnstone, A. J.; Emmison, N.; Bradley, R. H. Attachment of Human Primary Osteoblast Cells to Modified Polyethylene Surfaces. *Langmuir*, **2009**, *25* (6), 3718–3727. https://doi.org/10.1021/la801820s.

[202] Park, J. H.; Han, C. M.; Lee, E. J.; Kim, H. W. Preparation of Highly Monodispersed Porous-Channeled Poly(Caprolactone) Microspheres by a Microfluidic System. *Mater. Lett.*, **2016**, *181*, 92–98. https://doi.org/10.1016/j.matlet.2016.06.020.

[203] Gerhardt, L.-C.; Boccaccini, A. R. Bioactive Glass and Glass-Ceramic Scaffolds for Bone Tissue Engineering. *Materials (Basel).*, **2010**, *3* (7), 3867–3910. https://doi.org/10.3390/ma3073867.

[204] Varanasi, V. G.; Velten, M. F.; Odatsu, T.; Ilyas, A.; Iqbal, S. M.; Aswath, P. B. *Surface Modifications and Surface Characterization of Biomaterials Used in Bone Healing*; Elsevier Inc., 2016. https://doi.org/10.1016/B978-0-12-802792-9.00009-4.

[205] Vaquette, C.; Kahn, C.; Frochot, C.; Nouvel, C.; Six, J.-L.; De Isla, N.; Luo, L.-H.; Cooper-White, J.; Rahouadj, R.; Wang, X. Aligned Poly(L-Lactic-Co-e-Caprolactone) Electrospun Microfibers and Knitted Structure: A Novel Composite Scaffold for Ligament Tissue Engineering. *J. Biomed. Mater. Res. A*, **2010**, *94* (4), 1270–1282. https://doi.org/10.1002/jbm.a.32801.

[206] Vaish. 基因的改变NIH Public Access. *Bone*, **2012**, *23* (1), 1–7. https://doi.org/10.1038/jid.2014.371.

[207] Day, R. M. Bioactive Glass Stimulates the Secretion of Angiogenic Growth Factors and Angiogenesis in Vitro. *Tissue Eng.*, **2005**, *11* (5), 768–777. https://doi.org/10.1089/ten.2005.11.768.

[208] Oréfice, R.; Hench, L.; Brennan, A. Evaluation of the Interactions between Collagen and the Surface of a Bioactive Glass during in Vitro Test. *J. Biomed. Mater. Res. A*, **2009**, *90* (1), 114–120. https://doi.org/10.1002/jbm.a.32080.

[209] Hench, L. L.; Greenspan, D. Interactions between Bioactive Glass and Collagen : A Review and New Perspectives. *J. Aust. Ceram. Soc.*, **2013**, *49* (2), 1–40.

[210] Rawlings, R. D. Bioactive Glasses and Glass-Ceramics. *Clin. Mater.*, **1993**, *14* (2), 155–

179.

[211] Yunos, D. M.; Ahmad, Z.; Boccaccini, a. R. Fabrication and Characterization of Electrospun Poly-DL-Lactide (PDLLA) Fibrous Coatings on 45S5 Bioglass® Substrates for Bone Tissue Engineering Applications. *J. Chem. Technol. Biotechnol.*, **2009**, *85* (6), 768–774. https://doi.org/10.1002/jctb.2283.

[212] Bi, L.; Jung, S.; Day, D.; Neidig, K.; Dusevich, V.; Eick, D.; Bonewald, L. Evaluation of Bone Regeneration, Angiogenesis, and Hydroxyapatite Conversion in Critical-Sized Rat Calvarial Defects Implanted with Bioactive Glass Scaffolds. *J. Biomed. Mater. Res. A*, **2012**, *100* (12), 3267–3275. https://doi.org/10.1002/jbm.a.34272.

[213] Sepulveda, P.; Jones, J. R.; Hench, L. L. Bioactive Sol-Gel Foams for Tissue Repair. *J. Biomed. Mater. Res.*, **2002**, *59* (2), 340–348.

[214] Rahaman, M. N.; Day, D. E.; Sonny Bal, B.; Fu, Q.; Jung, S. B.; Bonewald, L. F.; Tomsia, A. P. Bioactive Glass in Tissue Engineering. *Acta Biomater.*, **2011**, *7* (6), 2355–2373. https://doi.org/10.1016/j.actbio.2011.03.016.

[215] Liu, H.; Fan, H.; Wang, Y.; Toh, S. L.; Goh, J. C. H. The Interaction between a Combined Knitted Silk Scaffold and Microporous Silk Sponge with Human Mesenchymal Stem Cells for Ligament Tissue Engineering. *Biomaterials*, **2008**, *29* (6), 662–674. https://doi.org/10.1016/j.biomaterials.2007.10.035.

[216] Laflamme, M.; Lamontagne, J.; Guidoin, R. * - *Anterior Cruciate Ligament Prostheses Using Biotextiles*; Elsevier Ltd., 2015. https://doi.org/10.1016/B978-1-78242-017-0.00007-6.

[217] Zhang, Q.; Li, C.; Luan, J.; Guan, G.; Lin, J.; Wang, F.; Wang, L. Polycaprolactone / Ultra-High Molecular Weight Polyethylene Partially Absorbable Suture with Improved Mechanical Performances for Tendon and Ligament Repair. **2020**. https://doi.org/10.1177/0040517520912478.

[218] Tong, S. Y.; Wang, Z.; Lim, P. N.; Wang, W.; Thian, E. S. Uniformly-Dispersed Nanohydroxapatite-Reinforced Poly(ε-Caprolactone) Composite Films for Tendon Tissue Engineering Application. *Mater. Sci. Eng. C*, **2017**, *70*, 1149–1155. https://doi.org/10.1016/j.msec.2016.03.051.

[219] Schmidt, C. C.; Georgescu, H. I.; Kwoh, C. K.; Blomstrom, G. L.; Engle, C. P.; Larkin, L. A.; Evans, C. H.; Woo, S. L. Effect of Growth Factors on the Proliferation of Fibroblasts from the Medial Collateral and Anterior Cruciate Ligaments. *J. Orthop. Res.*, **1995**, *13* (2), 184–190. https://doi.org/10.1002/jor.1100130206.

[220] T., M.; Y., W.; G.A.C., M. The Roles of Growth Factors in Tendon and Ligament Healing. *Sport. Med.*, **2003**, *33* (5), 381–394. https://doi.org/10.2165/00007256-200333050-00004.

[221] Pierce, G. F.; Mustoe, T. A.; Lingelbach, J.; Masakowski, V. R.; Griffin, G. L.; Senior, R. M.; Deuel, T. F. Platelet-Derived Growth Factor and Transforming Growth Factor-β Enhance Tissue Repair Activities by Unique Mechanisms. *J. Cell Biol.*, **1989**, *109* (1), 429–440. https://doi.org/10.1083/jcb.109.1.429.

[222] Jones, J. I. Insulin-like Growth Factors and Their Binding Proteins: Biological Actions. *Endocr. Rev.*, **2004**, *16* (1), 3–34. https://doi.org/10.1210/er.16.1.3.

[223] Marui, T.; Niyibizi, C.; Georgescu, H. I.; Cao, M.; Kavalkovich, K. W.; Levine, R. E.; Woo, S. L. Y. Effect of Growth Factors on Matrix Synthesis by Ligament Fibroblasts. *J. Orthop. Res.*, **1997**, *15* (1), 18–23. https://doi.org/10.1002/jor.1100150104.

[224] Nau, T.; Teuschl, A. Regeneration of the Anterior Cruciate Ligament: Current Strategies in Tissue Engineering. *World J. Orthop.*, **2015**, *6* (1), 127–136. https://doi.org/10.5312/wjo.v6.i1.127.

[225] Hirukawa, M.; Katayama, S.; Sato, T.; Yamada, M.; Kageyama, S.; Unno, H.; Suzuki, Y.; Miura, Y.; Shiratsuchi, E.; Hasegawa, M.; et al. Development of Tissue-Engineered Ligaments: Elastin Promotes Regeneration of the Rabbit Medial Collateral Ligament. *Artif. Organs*, **2018**, *42* (6), E102–E113. https://doi.org/10.1111/aor.13066.

[226] Leong, N. L.; Arshi, A.; Kabir, N.; Nazemi, A.; Petrigliano, F. A.; Wu, B. M.; McAllister, D. R. In Vitro and in Vivo Evaluation of Heparin Mediated Growth Factor Release from Tissue-Engineered Constructs for Anterior Cruciate Ligament Reconstruction. *J. Orthop. Res.*, **2015**, *33* (2), 229–236. https://doi.org/10.1002/jor.22757.

[227] Cheng, M.; Johnson, V. M.; Murray, M. M. Effects of Age and Platelet-Rich Plasma on ACL Cell Viability and Collagen Gene Expression. *J. Orthop. Res.*, **2012**, *30* (1), 79–85. https://doi.org/10.1002/jor.21496.

[228] Stegen, S.; Carmeliet, G. *Vascular Endothelial Growth Factor and Bone–Vascular Interactions*; Elsevier Inc., 2020. https://doi.org/10.1016/b978-0-12-814841-9.00046-4.

[229] Mifune, Y.; Matsumoto, T.; Ota, S.; Nishimori, M.; Usas, A.; Kopf, S.; Kuroda, R.; Kurosaka, M.; Fu, F. H.; Huard, J. Therapeutic Potential of Anterior Cruciate Ligament-Derived Stem Cells for Anterior Cruciate Ligament Reconstruction. *Cell Transplant.*, **2012**, *21* (8), 1651–1665. https://doi.org/10.3727/096368912X647234.

[230] Mifune, Y.; Matsumoto, T.; Takayama, K.; Terada, S.; Sekiya, N.; Kuroda, R.; Kurosaka, M.; Fu, F. H.; Huard, J. Tendon Graft Revitalization Using Adult Anterior Cruciate Ligament (ACL)-Derived CD34+ Cell Sheets for ACL Reconstruction. *Biomaterials*, **2013**, *34* (22), 5476–5487. https://doi.org/10.1016/j.biomaterials.2013.04.013.

[231] Anderson, A. F.; Snyder, R. B.; Lipscomb, A. B. Anterior Cruciate Ligament Reconstruction A Prospective Randomized Study of Three Surgical Methods. **2001**, *29* (3), 272–279.

[232] Weetall, H. H. Preparation of Immobilized Proteins Covalently Coupled through Silane Coupling Agents to Inorganic Supports. *Appl. Biochem. Biotechnol.*, **1993**, *41* (3), 157–188. https://doi.org/10.1007/BF02916421.

[233] Akhavan, B.; Michl, T. D.; Giles, C.; Ho, K.; Martin, L.; Sharifahmadian, O.; Wise, S. G.; Coad, B. R.; Kumar, N.; Griesser, H. J.; et al. Plasma Activated Coatings with Dual Action against Fungi and Bacteria. *Appl. Mater. Today*, **2018**, *12*, 72–84. https://doi.org/10.1016/j.apmt.2018.04.003.

[234] Marcondes, A. R.; Ueda, M.; Kostov, K. G.; Beloto, A. F.; Leite, N. F.; Gomes, G. F.;

Lepienski, C. M. Improvements of Ultra-High Molecular Weight Polyethylene Mechanical Properties by Nitrogen Plasma Immersion Ion Implantation. **2004**, *34* (4), 1667–1672.

[235] Valenza, A.; Visco, A. M.; Torrisi, L.; Campo, N. Characterization of Ultra-High-Molecular-Weight Polyethylene (UHMWPE) Modified by Ion Implantation. *Polymer (Guildf).*, **2004**, *45* (5), 1707–1715. https://doi.org/10.1016/j.polymer.2003.12.056.

[236] Ulery, B. D.; Nair, L. S.; Laurencin, C. T. Biomedical Applications of Biodegradable Polymers. *J. Polym. Sci. Part B Polym. Phys.*, **2011**, *49* (12), 832–864. https://doi.org/10.1002/polb.22259.

[237] Avg, W. "24.1% 1. **1957**, 1952–1954.

[238] Laffir, R.; Mellot, N. P.; Ay, X. LECTRON S PECTROSC COPY : **2022**, No. 2010, 8–11.

[239] SHEILA MARIA BELGIS PUTRI AFFIZA. *No Title*; *הכי קשה לראות את מה שבאמת לנגד העינים* 2022.

[240] Time, F.; Hm, Y.; Cranfield University; Executive, H. & S.; Thermo Fisher Scientific; Kingdom, U.; Office, I.; Street, W.; Kingdom, U.; Service, C. A.; et al. *No 主観的健康感を中心とした在宅高齢者における 健康関連指標に関する共分散構造分析Title*; 2022; Vol. 33.

[241] Schweiger, B. A. Pulsed Electron Spin Resonance Spectroscopy: Basic Principles, Techniques, and Examples of Applications. **1991**.

[242] Wilmshurst, T. H. *Electron Spin Resonance*.

[243] Akhavan, B.; Jarvis, K.; Majewski, P. Development of Negatively Charged Particulate Surfaces through a Dry Plasma-Assisted Approach. *RSC Adv.*, **2015**, *5* (17), 12910–12921. https://doi.org/10.1039/c4ra13767a.

[244] Lau, K.; Akhavan, B.; Lord, M. S.; Bilek, M. M.; Rnjak-Kovacina, J. Dry Surface Treatments of Silk Biomaterials and Their Utility in Biomedical Applications. *ACS Biomater. Sci. Eng.*, **2020**, *6* (10), 5431–5452. https://doi.org/10.1021/acsbiomaterials.0c00888.

[245] Kosobrodova, E.; Kondyurin, A.; Chrzanowski, W.; McCulloch, D. G.; McKenzie, D. R.; Bilek, M. M. M. Optical Properties and Oxidation of Carbonized and Cross-Linked Structures Formed in Polycarbonate by Plasma Immersion Ion Implantation. *Nucl. Instruments Methods Phys. Res. Sect. B Beam Interact. with Mater. Atoms*, **2014**, *329*, 52–63. https://doi.org/10.1016/j.nimb.2014.03.010.

[246] Chen, Y.; Xu, C.; Bilek, M. M. M.; Cheng, X.; Wang, C. H. An Effective Method to Optimise Plasma Immersion Ion Implantation: Sensitivity Analysis and Design Based on Low-Density Polyethylene. *Plasma Process. Polym.*, **2022**, No. November 2021. https://doi.org/10.1002/ppap.202100199.

[247] Bilek, M. M.; McKenzie, D. R. Plasma Modified Surfaces for Covalent Immobilization of Functional Biomolecules in the Absence of Chemical Linkers: Towards Better Biosensors and a New Generation of Medical Implants. *Biophys. Rev.*, **2010**, *2* (2), 55–65.

https://doi.org/10.1007/s12551-010-0028-1.

[248] Kondyurin, A.; Naseri, P.; Fisher, K.; McKenzie, D. R.; Bilek, M. M. M. Mechanisms for Surface Energy Changes Observed in Plasma Immersion Ion Implanted Polyethylene: The Roles of Free Radicals and Oxygen-Containing Groups. *Polym. Degrad. Stab.*, **2009**, *94* (4), 638–646. https://doi.org/10.1016/j.polymdegradstab.2009.01.004.

[249] Bilek, M. M. M.; Bax, D. V.; Kondyurin, A.; Yin, Y.; Nosworthy, N. J.; Fisher, K.; Waterhouse, A.; Weiss, A. S.; Dos Remedios, C. G.; McKenzie, D. R. Free Radical Functionalization of Surfaces to Prevent Adverse Responses to Biomedical Devices. *Proc. Natl. Acad. Sci. U. S. A.*, **2011**, *108* (35), 14405–14410. https://doi.org/10.1073/pnas.1103277108.

[250] Shetty, A.; Prabhath, S.; Alappatt, K.; Krishna KN, L.; Bhat, N.; Sumalatha, S. Lateral Collateral Ligament and Anterolateral Ligament of the Knee – A Morphological Analysis with Orthopedic Significance. *Knee*, **2021**, *28*, 202–206. https://doi.org/10.1016/j.knee.2020.12.002.

[251] Frank, C. B. Ligament Structure, Physiology and Function. *J. Musculoskelet. Neuronal Interact.*, **2004**, *4* (2), 199–201.

[252] Chan, Y. S.; Wang, C. J. Femoral Interference Screw Placement Through the Tibial Tunnel: A Novel Method Without Graft Damage. *Arthrosc. - J. Arthrosc. Relat. Surg.*, **2006**, *22* (11), 4–7. https://doi.org/10.1016/j.arthro.2006.05.025.

[253] Bach, J. S.; Ku, D. N. Design and Evaluation of a Prosthetic Anterior Cruciate Ligament Replacement Medical Device. *ProQuest Diss. Theses*, **2012**, No. May, 159.

[254] Cohen, S. B.; Sekiya, J. K. Allograft Safety in Anterior Cruciate Ligament Reconstruction. *Clin. Sports Med.*, **2007**, *26*, 597–605. https://doi.org/10.1016/j.csm.2007.06.003.

[255] Tovar, N.; Murthy, N. S.; Kohn, J.; Gatt, C.; Dunn, M. ACL Reconstruction Using a Novel Hybrid Scaffold Composed of Polyarylate Fibers and Collagen Fibers. *J. Biomed. Mater. Res. A*, **2012**, *100* (11), 2913–2920. https://doi.org/10.1002/jbm.a.34229.

[256] Lu, H. H.; Cooper, J. a.; Manuel, S.; Freeman, J. W.; Attawia, M. a.; Ko, F. K.; Laurencin, C. T. Anterior Cruciate Ligament Regeneration Using Braided Biodegradable Scaffolds: In Vitro Optimization Studies. *Biomaterials*, **2005**, *26* (23), 4805–4816. https://doi.org/10.1016/j.biomaterials.2004.11.050.

[257] Leong, N. L.; Petrigliano, F. a; McAllister, D. R. Current Tissue Engineering Strategies in Anterior Cruciate Ligament Reconstruction. *J. Biomed. Mater. Res. A*, **2014**, *102* (5), 1614–1624. https://doi.org/10.1002/jbm.a.34820.

[258] Ozdil, D.; Aydin, H. M. Polymers for Medical and Tissue Engineering Applications. *J. Chem. Technol. Biotechnol.*, **2014**, *89* (12), 1793–1810. https://doi.org/10.1002/jctb.4505.

[259] Binte Wahed, S. Synthetic Anterior Cruciate Ligament Implants Utilising UHMWPE-Polyethylene Fibre Doped with Bioactivity Enhancing Additives. **2016**, No. February.

[260] Jackson, D. W.; Gasser, S. I. Tibial Tunnel Placement in ACL Reconstruction.

Arthroscopy, **1994**, *10* (2), 124–131. https://doi.org/10.1016/S0749-8063(05)80079-9.

[261] Boniello, M. R.; Schwingler, P. M.; Bonner, J. M.; Robinson, S. P.; Cotter, A.; Bonner, K. F. Impact of Hamstring Graft Diameter on Tendon Strength: A Biomechanical Study. *Arthrosc. - J. Arthrosc. Relat. Surg.*, **2015**, *31* (6), 1084–1090. https://doi.org/10.1016/j.arthro.2014.12.023.

[262] Miller, K.; Hsu, J. E.; Soslowsky, L. J. *Materials in Tendon and Ligament Repair*; Elsevier Ltd., 2011; Vol. 6. https://doi.org/10.1016/b978-0-08-055294-1.00218-x.

[263] Jedda, H.; Ben Abessalem, S.; Sakli, F. The Effect of Cyclic Loading on the Mechanical Properties of Artificial Ligaments. *J. Text. Inst.*, **2011**, *102* (4), 332–342. https://doi.org/10.1080/00405001003771218.

[264] Beynnon, B. D.; Amis, a a. In Vitro Testing Protocols for the Cruciate Ligaments and Ligament Reconstructions. *Knee Surg. Sports Traumatol. Arthrosc.*, **1998**, *6 Suppl 1*, S70–S76. https://doi.org/10.1007/s001670050226.

[265] Beynnon, B. D.; Meriam, C. M.; Ryder, S. H.; Fleming, B. C.; Johnson, R. J. The Effect of Screw Insertion Torque on Tendons Fixed with Spiked Washers. *Am. J. Sports Med.*, **1998**, *26* (4), 536–539.

[266] Vieira, A. C.; Guedes, R. M.; Marques, A. T. Development of Ligament Tissue Biodegradable Devices: A Review. *J. Biomech.*, **2009**, *42* (15), 2421–2430. https://doi.org/10.1016/j.jbiomech.2009.07.019.

[267] Sahoo, S.; Ouyang, H.; James, C. H.; Tay, T. E.; Toh, S. L. Characterization of a Novel Polymeric Scaffold for Potential Application in Tendon/Ligament Tissue Engineering. *Tissue Eng.*, **2006**, *12* (1), 91–99. https://doi.org/10.1089/ten.2006.12.91.

[268] Wang, C.; Hou, W.; Yan, M.; Guo, Z.; Wu, Q.; Bi, L.; Han, Y. Effects of Artificial Ligaments with Different Porous Structures on the Migration of BMSCs. **2015**, *2015*. https://doi.org/10.1155/2015/702381.

[269] Rowden, N. J.; Sher, D.; Rogers, G. J.; Schindhelm, K. Anterior Cruciate Ligament Graft Fixation: Initial Comparison of Patellar Tendon and Semitendinosus Autografts in Young Fresh Cadavers. *Am. J. Sports Med.*, **1997**, *25*, 472–478. https://doi.org/10.1177/036354659702500409.

[270] Li, X.; He, J.; Bian, W.; Li, Z.; Zhang, W.; Li, D.; Snedeker, J. G. A Novel Silk-Based Artificial Ligament and Tricalcium Phosphate/Polyether Ether Ketone Anchor for Anterior Cruciate Ligament Reconstruction - Safety and Efficacy in a Porcine Model. *Acta Biomater.*, **2014**, *10* (8), 3696–3704. https://doi.org/10.1016/j.actbio.2014.05.015.

[271] Ogura, Y.; Parsons, W. H.; Kamat, S. S.; Cravatt, B. F. 乳鼠心肌提取 HHS Public Access. *Physiol. Behav.*, **2017**, *176* (10), 139–148. https://doi.org/10.1021/acsbiomaterials.9b01584.Micropatterned.

[272] Salminen, A. T.; Zhang, J.; Madejski, G. R.; Khire, T. S.; Waugh, R. E.; McGrath, J. L.; Gaborski, T. R. Ultrathin Dual-Scale Nano- and Microporous Membranes for Vascular Transmigration Models. *Small*, **2019**, *15* (6), 1–11.

https://doi.org/10.1002/smll.201804111.

[273] Moya, M. L.; Huang, J.; Francis-sedlak, M.; Kao, S.; Opara, E. C.; Cheng, M.-H.; Brey, E. M. The Effect of FGF-1 Loaded Alginate Microbeads on Neovascularization and Adipogenesis in a Vascular Pedicle Model of Adipose Tissue Engineering. *Biomaterials*, **2010**, *31* (10), 2816–2826. https://doi.org/10.1016/j.biomaterials.2009.12.053.The.

[274] Eton & Lepore. 基因的改变NIH Public Access. *Bone*, **2008**, *23* (1), 1–7. https://doi.org/10.1016/j.biomaterials.2010.01.144.The.

[275] Shen, W.; Chen, X.; Chen, J.; Yin, Z.; Heng, B. C.; Chen, W.; Ouyang, H. W. The Effect of Incorporation of Exogenous Stromal Cell-Derived Factor-1 Alpha within a Knitted Silk-Collagen Sponge Scaffold on Tendon Regeneration. *Biomaterials*, **2010**, *31* (28), 7239–7249. https://doi.org/10.1016/j.biomaterials.2010.05.040.

[276] Liu, H.; Yang, L.; Zhang, E.; Zhang, R.; Cai, D.; Zhu, S.; Ran, J.; Bunpetch, V.; Cai, Y.; Heng, B. C.; et al. Biomimetic Tendon Extracellular Matrix Composite Gradient Scaffold Enhances Ligament-to-Bone Junction Reconstruction. *Acta Biomater.*, **2017**, *56*, 129–140. https://doi.org/10.1016/j.actbio.2017.05.027.

[277] Chen, X.; Qi, Y.-Y.; Wang, L.-L.; Yin, Z.; Yin, G.-L.; Zou, X.-H.; Ouyang, H.-W. Ligament Regeneration Using a Knitted Silk Scaffold Combined with Collagen Matrix. *Biomaterials*, **2008**, *29* (27), 3683–3692. https://doi.org/10.1016/j.biomaterials.2008.05.017.

[278] Gresham, R. C. H.; Bahney, C. S.; Leach, J. K. Growth Factor Delivery Using Extracellular Matrix-Mimicking Substrates for Musculoskeletal Tissue Engineering and Repair. *Bioact. Mater.*, **2021**, *6* (7), 1945–1956. https://doi.org/10.1016/j.bioactmat.2020.12.012.

[279] Lee, Y.; Han, S.; Lim, H.; Kim, Y.; Kim, H. Surface Analysis of Polymers Electrically Improved by Plasma-Source Ion-Implantation. *Anal. Bioanal. Chem.*, **2002**, *373* (7), 595–600. https://doi.org/10.1007/s00216-002-1374-z.

[280] Yu, H.; Perni, S.; Shi, J. J.; Wang, D. Z.; Kong, M. G.; Shama, G. Effects of Cell Surface Loading and Phase of Growth in Cold Atmospheric Gas Plasma Inactivation of Escherichia Coli K12. *J. Appl. Microbiol.*, **2006**, *101* (6), 1323–1330. https://doi.org/10.1111/j.1365-2672.2006.03033.x.

[281] Stewart, C. A. C.; Akhavan, B.; Santos, M.; Hung, J. C.; Hawkins, C. L.; Bao, S.; Wise, S. G.; Bilek, M. M. M. Cellular Responses to Radical Propagation from Ion-Implanted Plasma Polymer Surfaces. *Appl. Surf. Sci.*, **2018**, *456* (June), 701–710. https://doi.org/10.1016/j.apsusc.2018.06.111.

[282] Kleinman, H. K.; Klebe, R. J.; Martin, G. R. Role of Collagenous Matrices in the Adhesion and Growth of Cells. *J. Cell Biol.*, **1981**, *88* (3), 473–485. https://doi.org/10.1083/jcb.88.3.473.

[283] Henriksen, K.; Karsdal, M. A. *Type I Collagen*, Second Edi.; Elsevier Inc., 2019; Vol. 2. https://doi.org/10.1016/B978-0-12-817068-7.00001-X.

[284] Shoulders, M. D.; Raines, R. T. Collagen Structure and Stability. *Annu. Rev. Biochem.*, **2009**, *78*, 929–958. https://doi.org/10.1146/annurev.biochem.77.032207.120833.

[285] *No Title*.

[286] Zhu, J.; Li, Z.; Zou, Y.; Lu, G.; Ronca, A.; D'Amora, U.; Liang, J.; Fan, Y.; Zhang, X.; Sun, Y. Advanced Application of Collagen-Based Biomaterials in Tissue Repair and Restoration. *J. Leather Sci. Eng.*, **2022**, *4* (1). https://doi.org/10.1186/s42825-022-00102-6.

[287] Sahoo, S.; Toh, S. L.; Goh, J. C. H. A BFGF-Releasing Silk/PLGA-Based Biohybrid Scaffold for Ligament/Tendon Tissue Engineering Using Mesenchymal Progenitor Cells. *Biomaterials*, **2010**, *31* (11), 2990–2998. https://doi.org/10.1016/j.biomaterials.2010.01.004.

[288] Czaplewski, S. K.; Tsai, T. L.; Duenwald-Kuehl, S. E.; Vanderby, R.; Li, W. J. Tenogenic Differentiation of Human Induced Pluripotent Stem Cell-Derived Mesenchymal Stem Cells Dictated by Properties of Braided Submicron Fibrous Scaffolds. *Biomaterials*, **2014**, *35* (25), 6907–6917. https://doi.org/10.1016/j.biomaterials.2014.05.006.

[289] Stanco, D.; Caprara, C.; Ciardelli, G.; Mariotta, L.; Gola, M.; Minonzio, G.; Soldati, G. Tenogenic Differentiation Protocol in Xenogenic-Free Media Enhances Tendon-Related Marker Expression in ASCs. *PLoS One*, **2019**, *14* (2), 1–21. https://doi.org/10.1371/journal.pone.0212192.

[290] Ruoslahti, E. Fibronectin in Cell Adhesion and Invasion. *Cancer Metastasis Rev.*, **1984**, *3* (1), 43–51. https://doi.org/10.1007/BF00047692.

[291] Gestrelius, S.; Andersson, C.; Lidstrom, D.; Hammarstrom, L.; Somerman, M. In Vitro Studies on Periodontal Ligament Cells and Enamel Matrix Derivative. *J. Clin. Periodontol.*, **2005**, *24* (9), 685–692. https://doi.org/10.1111/j.1600-051x.1997.tb00250.x.

[292] Caballé-Serrano, J.; Abdeslam-Mohamed, Y.; Munar-Frau, A.; Fujioka-Kobayashi, M.; Hernández-Alfaro, F.; Miron, R. Adsorption and Release Kinetics of Growth Factors on Barrier Membranes for Guided Tissue/Bone Regeneration: A Systematic Review. *Arch. Oral Biol.*, **2019**, *100* (February), 57–68. https://doi.org/10.1016/j.archoralbio.2019.02.006.

[293] Su, C. Y.; Kuo, Y. P.; Nieh, H. L.; Tseng, Y. H.; Burnouf, T. Quantitative Assessment of the Kinetics of Growth Factors Release from Platelet Gel. *Transfusion*, **2008**, *48* (11), 2414–2420. https://doi.org/10.1111/j.1537-2995.2008.01862.x.

[294] Ma, Z.; Mao, Z.; Gao, C. Surface Modification and Property Analysis of Biomedical Polymers Used for Tissue Engineering. *Colloids Surfaces B Biointerfaces*, **2007**, *60* (2), 137–157. https://doi.org/10.1016/j.colsurfb.2007.06.019.

[295] Vandencasteele, N.; Reniers, F. Plasma-Modified Polymer Surfaces: Characterization Using XPS. *J. Electron Spectros. Relat. Phenomena*, **2010**, *178–179* (C), 394–408. https://doi.org/10.1016/j.elspec.2009.12.003.

[296] ج. غ, الوزير ;.ف .إ ,الشعراني. *No Title* □ □□□□□□□ □□□□□□□□ □□□□□□□□□ 2006; □□□□□□□ □□□□□□ □□□□□□□□□; Vol. 1999.

[297] Nosworthy, N. J.; Ho, J. P. Y.; Kondyurin, A.; McKenzie, D. R.; Bilek, M. M. M. The Attachment of Catalase and Poly-l-Lysine to Plasma Immersion Ion Implantation-Treated Polyethylene. *Acta Biomater.*, **2007**, *3* (5), 695–704. https://doi.org/10.1016/j.actbio.2007.02.005.

[298] Yu, F.; Cui, Y.; Zhou, X.; Zhang, X.; Han, J. Osteogenic Differentiation of Human Ligament Fibroblasts Induced by Conditioned Medium of Osteoclast-like Cells. *Biosci. Trends*, **2011**, *5* (2), 46–51. https://doi.org/10.5582/bst.2011.v5.2.46.

[299] Font Tellado, S.; Balmayor, E. R.; Van Griensven, M. Strategies to Engineer Tendon/Ligament-to-Bone Interface: Biomaterials, Cells and Growth Factors. *Adv. Drug Deliv. Rev.*, **2015**, *94*, 126–140. https://doi.org/10.1016/j.addr.2015.03.004.

[300] Cardona-Ramirez, S.; Stoker, A. M.; Cook, J. L.; Ma, R. Fibroblasts From Common Anterior Cruciate Ligament Tendon Grafts Exhibit Different Biologic Responses to Mechanical Strain. *Am. J. Sports Med.*, **2021**, *49* (1), 215–225. https://doi.org/10.1177/0363546520971852.

[301] Kew, S. J.; Gwynne, J. H.; Enea, D.; Abu-Rub, M.; Pandit, A.; Zeugolis, D.; Brooks, R. A.; Rushton, N.; Best, S. M.; Cameron, R. E. Regeneration and Repair of Tendon and Ligament Tissue Using Collagen Fibre Biomaterials. *Acta Biomater.*, **2011**, *7* (9), 3237–3247. https://doi.org/10.1016/j.actbio.2011.06.002.

[302] Proffen, B. L.; Haslauer, C. M.; Harris, C. E.; Murray, M. M. Mesenchymal Stem Cells from the Retropatellar Fat Pad and Peripheral Blood Stimulate ACL Fibroblast Migration, Proliferation, and Collagen Gene Expression. *Connect. Tissue Res.*, **2013**, *54* (1), 14–21. https://doi.org/10.3109/03008207.2012.715701.

[303] Yates, E. W.; Rupani, A.; Foley, G. T.; Khan, W. S.; Cartmell, S.; Anand, S. J. Ligament Tissue Engineering and Its Potential Role in Anterior Cruciate Ligament Reconstruction. *Stem Cells Int.*, **2012**, *2012*, 11–14. https://doi.org/10.1155/2012/438125.

[304] Zhang, X.; Ma, Y.; Fu, X.; Liu, Q.; Shao, Z.; Dai, L.; Pi, Y.; Hu, X.; Zhang, J.; Duan, X.; et al. Runx2-Modified Adipose-Derived Stem Cells Promote Tendon Graft Integration in Anterior Cruciate Ligament Reconstruction. *Sci. Rep.*, **2016**, *6* (January), 1–15. https://doi.org/10.1038/srep19073.

[305] Humphries, M. J. Cell Adhesion Assays. **2001**, *18*, 9–13.

[306] Cai, L.; Qin, X.; Xu, Z.; Song, Y.; Jiang, H.; Wu, Y.; Ruan, H.; Chen, J. Comparison of Cytotoxicity Evaluation of Anticancer Drugs between Real-Time Cell Analysis and CCK - 8 Method. **2019**, 4–10. https://doi.org/10.1021/acsomega.9b01142.

[307] An, S.; Ling, J.; Gao, Y.; Xiao, Y. Effects of Varied Ionic Calcium and Phosphate on the Proliferation, Osteogenic Differentiation and Mineralization of Human Periodontal Ligament Cells in Vitro. *J. Periodontal Res.*, **2012**, *47* (3), 374–382. https://doi.org/10.1111/j.1600-0765.2011.01443.x.

[308] Renson, W. H.; Stackhouse, R. A. Evaluation of a New Approach to the Safety Assessment of Biomaterials. *Drug Chem. Toxicol.*, **1986**, *9* (3–4), 275–283. https://doi.org/10.3109/01480548608998280.

[309] Kaklamani, G.; Mehrban, N.; Chen, J.; Bowen, J.; Dong, H.; Grover, L.; Stamboulis, A. Effect of Plasma Surface Modification on the Biocompatibility of UHMWPE. *Biomed. Mater.*, **2010**, *5* (5). https://doi.org/10.1088/1748-6041/5/5/054102.

[310] Zhang, P.; Han, F.; Li, Y.; Chen, J.; Chen, T.; Zhi, Y.; Jiang, J.; Lin, C.; Chen, S.; Zhao, P. Local Delivery of Controlled-Release Simvastatin to Improve the Biocompatibility of Polyethylene Terephthalate Artificial Ligaments for Reconstruction of the Anterior Cruciate Ligament. *Int. J. Nanomedicine*, **2016**, *11*, 465–478. https://doi.org/10.2147/IJN.S95032.

[311] Piattelli, A.; Scarano, A.; Corigliano, M.; Piattelli, M. Effects of Alkaline Phosphatase on Bone Healing around Plasma-Sprayed Titanium Implants : A Pilot Study in Rabbits. **1996**, *17* (14), 1443–1449.

[312] Shojaee, A.; Parham, A. Strategies of Tenogenic Differentiation of Equine Stem Cells for Tendon Repair: Current Status and Challenges. *Stem Cell Res. Ther.*, **2019**, *10* (1), 1–13. https://doi.org/10.1186/s13287-019-1291-0.

[313] Bayrak, E.; Yilgor Huri, P. Engineering Musculoskeletal Tissue Interfaces. *Front. Mater.*, **2018**, *5* (April), 1–8. https://doi.org/10.3389/fmats.2018.00024.

[314] Bax, D. V.; McKenzie, D. R.; Weiss, A. S.; Bilek, M. M. M. Linker-Free Covalent Attachment of the Extracellular Matrix Protein Tropoelastin to a Polymer Surface for Directed Cell Spreading. *Acta Biomater.*, **2009**, *5* (9), 3371–3381. https://doi.org/10.1016/j.actbio.2009.05.016.

[315] Mizutani, N.; Kageyama, S.; Yamada, M.; Hasegawa, M.; Miyamoto, K.; Horiuchi, T. The Behavior of Ligament Cells Cultured on Elastin and Collagen Scaffolds. *J. Artif. Organs*, **2014**, *17* (1), 50–59. https://doi.org/10.1007/s10047-013-0736-y.

[316] Dunn, M. G.; Avasarala, P. N.; Zawadsky, J. P.; Al, D. E. T. Optimization of Extruded Collagen Fibers for ACL Reconstruction. **1993**, *27*, 1545–1552.

[317] Chen, Z.; Zhang, N.; Chu, H. Y.; Yu, Y.; Zhang, Z. K.; Zhang, G.; Zhang, B. T. Connective Tissue Growth Factor: From Molecular Understandings to Drug Discovery. *Front. Cell Dev. Biol.*, **2020**, *8* (October), 1–17. https://doi.org/10.3389/fcell.2020.593269.

[318] Chen, C. H.; Cao, Y.; Wu, Y. F.; Bais, A. J.; Gao, J. S.; Tang, J. B. Tendon Healing In Vivo: Gene Expression and Production of Multiple Growth Factors in Early Tendon Healing Period. *J. Hand Surg. Am.*, **2008**, *33* (10), 1834–1842. https://doi.org/10.1016/j.jhsa.2008.07.003.

[319] Olvera, D.; Schipani, R.; Sathy, B. N.; Kelly, D. J. Electrospinning of Highly Porous yet Mechanically Functional Microfibrillar Scaffolds at the Human Scale for Ligament and Tendon Tissue Engineering. *Biomed. Mater.*, **2019**, *14* (3). https://doi.org/10.1088/1748-605X/ab0de1.

[320] Li, X.; Pongkitwitoon, S.; Lu, H.; Lee, C.; Gelberman, R.; Thomopoulos, S. CTGF Induces Tenogenic Differentiation and Proliferation of Adipose-Derived Stromal Cells. *J. Orthop. Res.*, **2019**, *37* (3), 574–582. https://doi.org/10.1002/jor.24248.

[321] Liu, H.; Pei, Y.; Xie, D.; Deng, X.; Leng, Y. X.; Jin, Y.; Huang, N. Surface Modification

of Ultra-High Molecular Weight Polyethylene (UHMWPE) by Argon Plasma. *Appl. Surf. Sci.*, **2010**, *256* (12), 3941–3945. https://doi.org/10.1016/j.apsusc.2010.01.054.

[322] Tamada, Y.; Ikada, Y. Effect of Preadsorbed Proteins on Cell Adhesion to Polymer Surfaces. *Journal of Colloid And Interface Science*. 1993, pp 334–339. https://doi.org/10.1006/jcis.1993.1044.

[323] Tamada, Y.; Ikada, Y. Cell Adhesion to Plasma-Treated Polymer Surfaces. *Polymer (Guildf).*, **1993**, *34* (10), 2208–2212. https://doi.org/10.1016/0032-3861(93)90752-V.

[324] Bilek, M. M. M.; Bax, D. V.; Kondyurin, A.; Yin, Y.; Nosworthy, N. J.; Fisher, K.; Waterhouse, A.; Weiss, A. S.; Dos Remedios, C. G.; McKenzie, D. R. Free Radical Functionalization of Surfaces to Prevent Adverse Responses to Biomedical Devices. *Proc. Natl. Acad. Sci. U. S. A.*, **2011**, *108* (35), 14405–14410. https://doi.org/10.1073/pnas.1103277108.